CIRCULAR-ECONOMY DRIVEN RECOVERY OF CRITICAL RAW MATERIALS FROM END-OF-LIFE LITHIUM-ION BATTERIES VIA ELECTROCHEMICAL- AND ASSISTED LEACHING

Lappeenranta–Lahti University of Technology LUT

Master's Programme in Chemical Engineering, Master's Thesis

2025

Juhani Ilonen

Examiner(s): (Professor) Eveliina Repo and (Associate Professor) Ekaterina Laakso

Supervisor: (Professor) Eveliina Repo

ABSTRACT

Lappeenranta–Lahti University of Technology LUT

LUT School of Engineering Sciences

Chemical Engineering

Juhani Ilonen

Circular-economy driven recovery of critical raw materials from End-of-Life lithium-ion batteries via electrochemical- and assisted leaching

Master's thesis

2025

279 pages, 40 figures, 66 tables and 1 appendix

Examiner(s): (Professor) Eveliina Repo and (Associate Professor) Ekaterina Laakso

Keywords: Lithium-ion battery, recycling, recovery, hydrometallurgy, SEM-EDS, ICP-MS, electrochemical leaching, black mass, prototype flow-reactor

This thesis investigates the structural composition and recycling potential of lithium-ion batteries (LIBs), with a particular focus on the electrochemical leaching (ECL) of critical raw materials (CRMs) from end-of-life (EoL) LIBs. The work is divided into two main sections: the theoretical section offers a comprehensive review of LIB chemistry (e.g., $LiCoO_2$, $LiFePO_4$, $LiMn_2O_4$, NMC), component architecture, and operational mechanisms, emphasising the roles of cathode, anode, electrolyte, separator, and binder materials. It highlights the European Union's circular economy (CE) framework, including targets and sector-specific challenges, and discusses the current status of LIB recycling, incentives, and risks associated with CRMs. The thesis also summarizes existing LIB recycling techniques and commercial processes worldwide, detailing their underlying principles.

The experimental section focuses on disassembly, characterisation, and leaching of the active materials black mass (BM) derived from end-of-life laptop spent LIBs. The BM was milled and sieved into five particle fractions, and ICP-MS and SEM-EDS analysis identified that the <75 μm fraction had the highest cobalt (38.9 wt%) and lithium (5.77 wt%). Three chemical leaching (CL) and two ECL tests were performed. CL achieved up to 89.3% Li and 37.3% Co leaching efficiencies, whereas ECL yielded 72.3% Li and 33.0% Co. These results indicate that higher acid concentrations and temperatures predominantly enhance Li and Co dissolution, whereas electrochemically-assisted leaching (EAL) improves Mn and Ni extraction. Overall, the findings underscore the promise of small-scale ECL reactors for selective CRM recovery and highlight the need for design optimization — alternative electrode materials, flow configurations, and pre-treatments — to enhance efficiency and scalability for sustainable LIB recycling.

TIIVISTELMÄ

Lappeenrannan–Lahden teknillinen yliopisto LUT

LUTin insinööritieteiden tiedekunta

Kemiantekniikka

Juhani Ilonen

Kiertotalouden lähtöinen kriittisten raaka-aineiden talteenotto käytetystä litiumioniakuista sähkökemiallisella- ja avustetulla liuotuksella

Kemiatekniikan diplomityö

2025

279 sivua, 40 kuvaa, 66 taulukkoa ja 1 liite

Tarkastaja(t): (Professori) Eveliina Repo ja (Tutkijaopettaja) Ekaterina Laakso

Avainsanat: Litiumioniakku, kierrätys, talteenotto, hydrometallurgia, SEM-EDS, ICP-MS, sähkökemiallinen liuotus, musta massa, prototyyppivirtausreaktori

Tämä diplomityö tutkii litiumioniakkujen (LIB) rakenteellista koostumusta ja kierrätyspotentiaalia, erityisesti elinkaarensa päässä olevista (EoL) poistuvista litiumioniakuista peräisin olevien kriittisten raaka-aineiden (CRM) sähkökemiallista liuotusta (ECL). Työ on jaettu kahteen pääosaan: teoreettisessa osiossa tarjotaan kattava katsaus litiumioniakkujen kemiaan (esim. $LiCoO_2$, $LiFePO_4$, $LiMn_2O_4$, NMC), komponenttien arkkitehtuuriin ja toimintamekanismeihin, korostaen katodin, anodin, elektrolyytin, erotuskalvon ja sideaineiden rooleja. Siinä tuodaan esiin Euroopan unionin kiertotalouskehyksen (CE) rakenne, mukaan lukien tavoitteet ja toimialakohtaiset haasteet, sekä käsitellään litiumioniakkujen kierrätyksen nykytilaa, kannustimia ja CRM liittyviä riskejä. Diplomityö tiivistää myös olemassa olevat litiumioniakkujen kierrätystekniikat ja kaupalliset prosessit maailmanlaajuisesti, kuvaillen niiden taustalla olevia periaatteita.

Kokeellisessa osassa keskitytään litiumioniakkujen aktiivimateriaalien mustan massan (BM) purkamiseen, karakterisointiin ja liuotukseen. BM on peräisin käytöstä poistuneista kannettavien tietokoneiden litiumioniakuista. BM jauhettiin ja seulottiin viiteen raekokojaksoon. ICP-MS- ja SEM-EDS-analyysien perusteella havaittiin, että alle 75 µm:n fraktiossa havaittiin korkein Co pitoisuus (38,9 painoprosenttia) ja Li (5,77 painoprosenttia) pitoisuudet. Kokeellisessa työssä suoritettiin kolme kemiallista liuotuskokeilua (CL) ja kaksi ECL. CL kokeissa Li liotustehokkuus ylsi enimmillään 89,3 %:iin ja Co 37,3 %:iin, kun taas ECL:ssä vastaavat luvut olivat 72,3 % Li:lle ja 33,0 % Co:lle. Tulokset osoittavat, että korkeammat happopitoisuudet ja lämpötilat edistävät erityisesti Li ja Co liukenemista, kun taas sähkökemiallisesti avustettu liotus (EAL) tehostaa Mn ja Ni talteenottoa. Kaiken kaikkiaan tulokset korostavat pienten ECL-reaktoreiden lupaavuutta CRM selektiivisessä talteenotossa ja osoittavat tarpeen optimoida reaktorin suunnittelua — hyödyntämällä vaihtoehtoisia elektrodimateriaaleja, erilaisia virtausasetelmia ja esikäsittelyjä — litiumioniakkujen kierrätyksen tehokkuuden ja skaalautuvuuden parantamiseksi.

ACKNOWLEDGEMENTS

Foremost, I would like to show my gratitude and appreciation to my supervisor, Eveliina Repo, for this amazing opportunity and currently an important topic for the moment. In addition to support and assistance during the thesis. I am also grateful to Mohammad Reza Bilesan and Iryna Makarava for this project, and to Reza Bilesan foremost for the help with the laboratory part, with the reactor especially. I would also like to express my appreciation to Liisa Puro for all of the ICP-MS help I needed, to Mari Raitavuo for the help microwave digestion system, and their vast expertise in helping with the initial sample analysis and preparation in the initial stages of the thesis. Additionally, I would like to show my gratitude to Daria Givirovskaia for the help with the SEM-EDS and BM's sample characterisation. I am also grateful for your support given by Mari Trinidad when it was needed.

LIST OF ABBREVIATIONS AND SYMBOLS

Roman Characters (35)

C_1	Concentration of the stock acid	[mol/L or M]
C_2	Concentration of desired acid	[mol/L or M]
C_s	Concentration of the metal	[$mg \cdot kg^{-1}$]
C_{LIX}	Metal ion concentration in lixiviant	[mg/L]
DF	Diffusion factor	[-]
E	Electrical energy	[kWh]
e^-	Electron particle	[-]
E_g	Electrochemically stable potential window	[eV]
E_{HOMO}	Highest occupied molecular orbital electron-volt	[eV]
E_{LUMO}	Lowest unoccupied molecular orbital electron-volt	[eV]
E_{rxn}	Electrochemical potential	[V or J/C]
E_{TS}	Thermodynamic stability	[-]
I	Current	[A]
j	Current density	[A/m^2 or A/cm^2]
k_1	Reaction constant (1)	[min^{-1}]
k_2	Reaction constant (2)	[min^{-1}]
M	Transition metal	[-]
M_{mass}	Molar mass	[g/mol]
m_s	Mass of the solid material	[kg]
P	Power	[W]
PA	Projected surface area	[cm^2]
P_P	Electrochemical discharge of electrical power	[W/kg or W/L]
Q	Capacity	[Ah]
q	Capacity of an electric charge	[Ah]
R	Resistance	[Ω (ohms)]
t	Time	[min]
U	Energy density	[Wh/kg or Wh/L]

V	Voltage	[V or $kg \cdot m^2 \cdot s^{-3} \cdot A^{-1}$]
V'	Redox potential	[-]
V_V	Volume	[L]
V_1	Desired final volume (1)	[L]
V_2	Desired final volume (2)	[L]
V_{LIX}	Recovered volume of lixiviant	[L]
W_s	Sample weight	[gram]
X	Leaching rate of a specific metal	[-]

Greek Characters (8)

α	Insertion material	[-]
Δα	Thermal coefficient difference	[-]
ΔG	Gibbs free energy change	[J or J/mol]
Δt	Time to achieve complete discharge by LIBs	[min]
μ_A	Anode's chemical potentials	[-]
μ_C	Cathode's chemical potentials	[-]
σ	Conductivity	[S/m]
ρ	Density	[g/mL]

States of Matter and Units (11)

l	Liquid	[-]
g	Gas	[-]
s	Solid	[-]
aq	Aqua	[-]
ppb	Parts per billion	[μg/L]
Eff.%	Leaching efficiency	[-]
Wt.%	Weight percentage	[-]
M	Molarity of solution	[M]
A	Ampere	[-]
eV	Electron-volt	[-]
kWh	Kilowatt-hour	[-]

Abbreviations (182)

3Rs model	Reduce, Reuse and Recycle model
AB	Acetylene black
AEM	Anion exchange membrane
Al	Aluminium
Ap	Projected surface area
AQUA regia	HCl/HNO_3 3:1 ratio acid solution
ASM	Artisanal mining
BMS	Battery management system
BPM	Bipolar membrane
C	Carbon
$C_2H_2O_4$	Oxalic acid
$C_4H_6O_5$	Malic acid
$C_4H_6O_6$	Tartaric acid
$C_4H_7NO_4$	Aspartic acid
$C_6H_8O_6$	Ascorbic acid
$C_6H_8O_7$	Citric acid
$C_6H_{12}O_6$	Glucose
CAM	Cathode active material
CCZ	Clarion-Clipperton Zone
CE	Circular Economy
CEM	Cation exchange membranes
Ce	Colloidal electrolyte
CEI	Cathode electrolyte interface
CH_3COOH	Acetic acid
CHNS	elemental analysis
CL	Chemical leaching
CMC	Carboxymethyl cellulose
CNY	Chinese Yuan Renminbi [¥]
Co	Cobalt
CO_2	Carbon dioxide
CO_3^{2-}	Carbonate ion

CPSC	Consumer Product Safety Commission
CRM	Critical raw materials
CRM Act	Critical Raw Material Act
CS	Corporate sustainability
CTR	Carbothermic reduction
Cu	Copper
Cyanex 272	Bis(2,4,4-trimethylpentyl) phosphinic acid
D2EHPA	Phosphoric acid
DC	Direct current
DES	Deep eutectic solvent
DI	Deionised water
DMF	Dimethylformamide
DOE	Department of Energy
DOT	Department of Transport
DRC	Democratic Republic of Congo
EAL	Electrochemically-Assisted-Leaching
EAOP	Electrochemical advanced oxidation processes
EBA	European Battery Alliance
EBRA	European Battery Recycling Association
EC	European Commission
ECL	Electrochemical leaching
EDS	Energy Dispersive X-ray Spectroscopy
EERs	Rare earth elements
EIA	Environmental impact assessments
eLi	European Lithium Institute
EMF	Ellen MacArthur Foundation
EMM	Electrolytic Mn metal
EP	European Parliament
EPA	Environmental Protection Agency
EoL	End-of-Life
EoLC	End-of-Life-Cycle
EU	European Union
EUROBAT	Association of European Automotive and Industrial Battery

	Manufacturers	
EV	Electric vehicle	
F	Fluorine	
FKM	Fluoroelastomer	
FOT	Frontier orbital theory	
GA	Geometric area	[cm^2]
Ge	Germanium	
GDP	Gross domestic product	
GPE	Gel polymer electrolyte	
Gr	Graphite	
H2	Half of a year	
H^+	Hydrogen ion	
$H_2C_2O_4$	Oxalic acid	
H_2O	Water	
H_2O_2	Hydrogen peroxide	
H_2SO_4	Sulfuric acid	
H_3PO_4	Phosphoric acid	
HBTA	Benzoyl trifluoroacetone	
HCl	Hydrochloric acid	
HF	Hydrogen fluoride	
HFP	Hexafluoropropylene	
HNO_3	Nitric acid	
HOMO	Highest occupied molecular orbital	
IA	Immersed surface area	[cm^2]
IEA	International Energy Agency	
IEM	Ion-exchange membrane	
ISRI	Institute of Scrap Recycling Industries	
K	Potassium	
LCA	Life Cycle Assessments	
LE	Linear Economy	
LIB	Lithium-ion battery / Li-ion battery	
LIBS	Laser-induced breakdown spectroscopy	
Li	Lithium	

Li^+	Lithium ion	
Li_2CO_3	Lithium carbonate	
Li_2SO_4	Lithium sulfate	
$LiCoO_2$ or LCO	Lithium cobalt oxide	
$LiFePO_4$ or LFP	Lithium iron phosphate	
$LiMn_2O_4$ or LMO	Lithium manganese oxide	
$LiNiMnCoO_2$ or NMC	Lithium nickel manganese cobalt oxide	
LiOH	Lithium hydroxide	
$LiPF_6$	Lithium hexafluorophosphate	
Li_xGr_6	Lithium-graphite	
LUMO	Lowest unoccupied molecular orbital	
$MgSO_4$	Magnesium sulfate	
MHP	Nickel cobalt hydroxide	
Mn	Manganese	
MO	Metal oxide	
MOF	Metal-organic framework	
Mts	Metric tons	[-]
Mtu	Metric ton unit	[-]
N	Nitrogen	
NA	North America	
NAATBatt	The Trade Association for Advanced Battery Technology in North America	
Na^+	Sodium ion	
Na_2CO_3	Sodium carbonate	
Na_2SO_4	Sodium sulphate	
Na_3PO_4	Sodium phosphate	
NaCl	Sodium Chloride	
$NaHCO_3$	Sodium bicarbonate	
NaOH	Sodium hydroxide	
NCA	Lithium nickel cobalt aluminium oxide	

NCM	Lithium nickel cobalt manganese oxide	
NEV	New energy vehicle	
NGO	Non-governmental organization	
Ni	Nickel	
NiMH	Nickel metal-hydride	
NMC	Lithium nickel manganese cobalt oxide	
NMP	N-methyl pyrrolidone	
O	Oxygen	
O/A	Organic-to-aqueous ratio	
OEM	Original equipment manufacturer	
OSHA	Occupational Safety and Health Administration	
P	Phosphorus	
PAA	Polyacrylic acid	
Pb	Lead (element)	
PC-88A	2-ethylhexyl phosphoric acid mono-2-ethylhexyl ester	
PCM	Polymer composite membrane	
PE	Polyethylene	
PFAS	Per- and polyfluoroalkyl substances	
PP	Polypropylene	
PPE	Personal protective equipment	
PTFE	Polytetrafluoroethylene	
PVA	Polyvinyl alcohol	
PVDF	Polyvinylidene fluoride	
Q	Quarter of the year	
R&D	Research and development	
ROS	Reactive oxygen species	
RSD	Relative standard deviation	[-]
S	Sulfur	
S/L	Solid-to-liquid ratio	[-]
SBR	Styrene-butadiene rubber	
SE	Solid electrolytes	
Se	Secondary electron detection	
SEI	Solid-electrolyte interface	

SEM	Scanning Electron Microscopy	
SEM-EDS	Scanning Electron Microscopy with Energy Dispersive X-ray Spectroscopy	
Si	Silicone	
Sn	Tin	
SOAM	South America	
SOC	State of charge	
SS	Stainless steel	
SWANA	Solid Waste Association of North America	
SWM	Sustainable Waste Management	
TEM	Transmission electron microscopy	
Ti	Titanium	
TiO_2	Titanium dioxide	
TMO	Transition metal oxide	
TOPO	Trioctyl phosphine oxide	
UNK	Unknown	
US	United States	
USA	United States of America	
USD	United States Dollar	[$]
Vol.	Volume	[-]
WFD	Waste Framework Directive	
WH	Waste Hierarchy	
WM	Waste Management	
XRD	X-ray diffraction	

TABLE OF CONTENTS

ABSTRACT....2
TIIVISTELMÄ....3
ACKNOWLEDGEMENTS....4
LIST OF ABBREVIATIONS AND SYMBOLS....5
TABLE OF CONTENTS....13
LIST OF FIGURES AND TABLES....16
1. Introduction....25
2. Lithium-ion Battery....29
2.1. Lithium-ion battery history....29
2.2. The Structure of Lithium-ion Battery....30
2.2.1. The Cathode....32
2.2.2. The Anode....34
2.2.3. The Electrolyte....36
2.2.4. The Separator....38
2.2.5. The Binder....39
2.2.6. The Solid Electrolyte Interface (SEI)....43
2.3. Concept of LIB principles....46
3. Recycling....51
3.1. Recycling definition....51
3.2. Recycling concept/methods and models....54
3.2.1. The Waste Hierarchy....54
3.2.2. Circular economy....57
3.2.2.1. Critique and obscurity of the CE's....63
3.3. Recycling degree of the LIB....69
3.4. Incentives of the LIBs recycling....73
3.4.1. Cobalt....74
3.4.2. Lithium....81
3.4.3. Nickel & Manganese....86
3.4.4. Graphite....90
3.4.5. Geopolitics and Prospects of Raw Materials....94
4. Recycling Processes of the LIBs....99

4.1. Pre-Treatment Processes & Methods for the LIBs Waste 105
4.1.1. Sorting, discharging, disassembly and separation 108
4.1.1.1. The Physical and Mechanical Separation 111
4.1.1.2. The Chemical & Mechano-Chemical Separation 116
4.1.1.3. The Thermal Separation 118
4.2. The Hydrometallurgical process of LIB recycling 121
4.2.1. Leaching Processes with the Reducing Agents 123
4.2.1.1. The Organic Acid Leaching 124
4.2.1.2. The Inorganic Acid Leaching 127
4.2.1.3. The Alkaline- and Ammonia-Based Leaching 129
4.2.1.4. The Bio-metallurgy & Bioleaching 131
4.2.2. Treatment and Purification of Valuable Metals from the Leaching Process 133
4.2.2.1. Chemical Precipitation 133
4.2.2.2. Solvent Extraction 136
4.2.2.3. Ion-Exchange and Ion-Exchange Resin 137
4.3. The Pyrometallurgical process of LIB recycling 138
4.3.1. Extraction of the LIBs valuables by the Pyrometallurgy Process 141
4.3.1.1. Roasting 141
4.3.1.2. Smelting 143
4.4. Direct Recycling of the LIBs 144
4.5. Comparison of current Recycling Processes for the LIBs 146
4.6. The Electrochemistry 149
4.6.1. Electrochemical-Leaching 150
4.6.1.1. The Direct Leaching and Indirect Leaching 152
4.6.2. Electrochemically-Assisted Leaching 154
5. Methodology 156
5.1. Research & Experimentation Purpose 156
5.2. Preparation of Lithium-Ion Battery 157
5.2.1. Spent-LIBs battery packs 158
5.2.2. Disassembly of LIB battery packs 159
5.2.2.1. Discharge method of single Cell 161
5.2.2.2. Dismantling method of a single LIB cell 163
5.2.3. Creation of the Black Mass 164
5.2.4. Characterisation of the LIB cells and Black Mass 167
5.2.4.1. Characterisation of BM by ICP-MS analysis 169

5.2.4.2. Characterisation of BM by SEM-EDS Analysis 176
5.3. Experimental Reactor and Other Equipment for it 184
5.4. Literature review & Selection of aspects 187
5.4.1. Chemical Leaching of BM Literature 188
5.4.2. Electrochemical Leaching of BM Literature 194
5.5. Experiment & Test methods 200
5.5.1. Chemical Leaching 201
5.5.1.1. Experimental conditions 201
5.5.1.2. H_2SO_4 lixiviant preparation 202
5.5.1.3. Testing setup 203
5.5.1.4. Sampling & Parameter collection CL 204
5.5.2. Electrochemical Leaching 206
5.5.2.1. Experimental conditions 206
5.5.2.2. Reagent preparation 207
5.5.2.3. Testing setup 208
5.5.2.4. Sampling & Parameter collection ECL 210
5.6. Filtering and BM collection 212
5.7. Data Calculation and Leaching Efficiency 215
5.8. Safety Operations in Thesis 217
5.9. Theoretical Reactions 220
6. Results 224
6.1. Chemical Leaching Results 224
6.2. Electrochemical Leaching Results 232
6.3. Comparison of CL and ECL results 237
7. Discussion 241
8. Conclusion 247
References 251
Appendices 280
Appendix 1 Parameters for the experimental setups of ECL-T-1 and ECL-T-3 280

LIST OF FIGURES AND TABLES

FIGURES

Figure 1. Structure of LIB (a) (cylindrical). Structure in the current figure: anode of copper foil and cathode of aluminium foil, which are used as current collectors [14]. Structure of LIB (b) in the layered form: 1/5 current collectors, 2/4 anode and cathode, 3 separators and 6 casing (outside) [20]. 31

Figure 2. Crystal structures of three lithium-insertion compounds from left to right: Lithium Cobalt Oxide, Lithium Manganese Oxide, and Lithium Iron Phosphate [33]. 34

Figure 3. Schematic illustration of the main ageing mechanisms of commercial LIBs with the composition and formation of SEI and CEI films [61]. 44

Figure 4. Schematic of electrolyte stability limits (positive/negative potentials) vs. HOMO/LUMO energy levels. Red arrow: Stability window, violet/purple arrow: LUMO-HOMO gap, and blue arrow: Cathode-anode electrochemical potential difference [52], [54], [59], [60], [62]. 45

Figure 5. Schematic illustration of the basic components and working principle of a Li^{+}-Ion battery during charge, consisting of a graphite anode on a Cu current collector and a cathode an Al current collector, an organic electrolyte, and a transition metal, throughout the discharge and charge of LIBs [63]. 49

Figure 6. Waste Hierarchy, the tier/layer model as in EU Waste Hierarchy WFD 2008 implementation on the left (a) and the 3R's model concept on the right (b). Source of (a), Ref. [77]. 55

Figure 7. Schematic presentation of principles of the Circular Economy, which corresponds to that provided and accepted by the EU Parliament and its Research Service/Division [90]. 61

Figure 8. Data on Sales and collection of portable batteries and accumulators, European Union, 2009–2022 (tonnes) [97]. 71

Figure 9. Secondary Co supply from batteries in volume terms (left) and as a percentage of total supply (right) [124]. 79

Figure 10. Cobalt annual prices from 2010 through 2025 in (US$ / Mt). Data exported (02.06.2025) from the Ref. [135]. 80

Figure 11. Lithium annual prices from 2017 H2 through 2025 in (US$ / Mt). Data exported (02.06.2025) from the Ref. [146]. 85

Figure 12. Geographical distribution of planned additional lithium chemical for the Lithium carbonate on the left (a) and Lithium hydroxide on the right (b) projects, 2024–

2035. Note: CSAM = Central and South America — figure reproduced with the data from [147]. 86

Figure 13. Nickel on the right (a) and Manganese on the left (b) prices from 2015–2025 in the case of Ni as (USD / Metric Ton) and for Manganese as (CNY / mtu), (mtu = Metric Ton Unit). Data exported (02.06.2025) from the Refs. [154], [155]. 89

Figure 14. Short-term 2020–2025 on the right (a) criticality matrix for the CRMs, and on the left, medium-term 2025–2035 (b) criticality matrix for the same CRMs, based on the importance to energy as Y-axis and supply risk as X-axis, by U.S. Department of Energy [169]. 95

Figure 15. Graphs for the (a) Publication trends and (b) geographical distribution of publications in the field of LIB recycling between 2004–2024 years by countries and regions, *Data for 2024 is partial and encompasses January to September — figure reproduced with the data by CAS from Ref. [187]. 100

Figure 16. Graphs for the Publication trends for the most common and commercialised recycling methods/processes: hydrometallurgy, pyrometallurgy and direct recycling between 2004–2024 years, data by CAS and *Data for 2024 is partial and encompasses January to September — figure reproduced with the data by CAS from Ref. [187]..... 103

Figure 17. Graphs for the (a) trends of three major recycling methods-hydrometallurgy, pyrometallurgy and direct recycling with respect to various parts of LIB recycled (cathode, anode, electrolyte, separator, and current collector) and (b) major recycling respect to various types of LIBs (LFP, NMC, NCA, LMO and LCO) utilized in various applications between 2004–2024 years — figure reproduced with the data by CAS from Ref. [187]..... 104

Figure 18. Pre-treatment approaches for the industry-scale pre-treatment processes (left, red) and laboratory-scale processes (right, blue). Both methods require disassembling packs into modules (centre, yellow), Figure/Schematic property of Ref. [189]..... 107

Figure 19. Difference between Direct and Indirect Electrochemical Leaching and their principles. 153

Figure 20.Some of the battery packs used in the research and disassembled in later stages. 159

Figure 21. One of the tested LIBs and disassembled in the thesis, TYPE PC764 DELL battery pack on the right (a), and on the left, disassembled the same battery inside of battery cells 6x of LGDB118650 (cylindrical) and the BMS unit of the battery (b) that was tested subsequently..... 161

Figure 22. Use of the Fluke 189 True RMS multimeter to check the charge and capacity of energy inside the individual cells on the left (a), and schematic of the discharging method done for the individual LIB cells on the right (b). 163

Figure 23. Image of the (5x5 mm) sized cathode/anode sheets in the upper left corner (a), 76x of (⌀ 1 cm) stainless-steel balls inside the planetary ball mill drum, with the cathode/anode sheets (partially shredded) in the upper right corner (b), biggest particles what

is left of cathode/anode sheets BM material (particle size >250 μm) in the bottom left corner (c) and BM material of the finest size (<75 μm) in the bottom right corner (d).....165

Figure 24. BM sample preparation for the SEM-EDS, with the six different samples, out of which No.5 and No.6 are the same samples of (<75 μm) particle size and the rest were sampled and used only once. 177

Figure 25. SEM images done at LUT, for the different CM particle size distributions, are as follows: (a) <75, (b) 90–75, (c) 125–90, (d) 250–125 and (e) >250. 178

Figure 26. SEM images of (<75) μm particle size BM in (a1) and (b1), with two separate point analyses selected for the EDS (c1) and (d1) samples. (*Note! Samples (a1) and (c1) are that of No.5, and samples (b1) and (d1) are that of No.6 from* (**Figure 24**)).....180

Figure 27. SEM image of the samples in (**Figure 25**) without the (d1) sample and their corresponding EDS elemental mapping on the (<75) μm particle size BM samples. (*Note! (d1) sampling was not done or lost in the data exchange*). Additionally, (*Note! Sample (a2) and (c2) are that of No.5, and sample (b2) is that of No.6 from* (**Figure 24**)).....181

Figure 28. EDS spectrum and quantitative results for all the samples (**Figure 25**), all the samples with corresponding counts, atomic percentages and elemental Wt.% in the samples, as (a3) and (b3) for the whole sample, while (c3) and (d3) for the corresponding point analyses. (*Note! Samples (a3) and (c3) are that of No.5, and samples (b3) and (d3) are that of No.6 from* (**Figure 24**)).....181

Figure 29. EDS spectrum and quantitative results for the separate sample of (<75) μm particle size BM, after it was stored to see the effect of moisture/air and other factors that can affect the sample morphology, as it is waiting to be tested.....184

Figure 30. 3D printed and used in the thesis, reactor taken from the 3D printer in its raw form with filaments/residue plastics (a), reactor just used in experimentation from an angled view with electrode still in it (b), reactor from an angled view where the channels inside of the reactor can be seen (c) and view of reactor from the top with electrode inside after experimentation (d).....185

Figure 31. Two electrodes used in the reactor with their parameters: a cathode made of SS in a 4-rod mesh style per rod on the left (a) and an anode made of Ti in an 8-rod mesh style per rod on the right (b).....186

Figure 32. Visual images of the anode's Ti 8 rod surface structure on the left (a) and the cathode's SS 4 rod surface structure on the right (b). Images/photos were captured by the Olympus DF PL 2x Stereo Microscope Objective and captured by the Leica Microsystems. 187

Figure 33. Operation parameters, pulp density vs. acid concentration from the LIBs by (Diaz et al. [6]). (*Note! Solid points represent reported pulp densities at the corresponding acid concentration, and regional colours are operational ranges (yellow is of electrochemical leaching, while blue/red are of chemical leaching)*) [6].....193

Figure 34. Experimental setup for the chemical leaching Tests 1/2/3 for the BM. 204

Figure 35. Electrochemical leaching TESTs 1–3, with their setup photos, and additional modifications for the reactor. ELC-T-1 testing setup in the photo of (a), ELC-T-2 testing setup in the photo of (b), ELC-T-3 testing setup in the photo of (c), an addition of the gasket between the two parts that hold electrodes so that the membrane has a tight sealing in the reactor separating electrode compartments (d), use of silicone based sealant base to minimise leakage from the reactor when testing (e), and connection of electrode to that of DC, via alligator clips (f).....209

Figure 36. The filtration system of BM from the lixiviate (in the picture of 2 M H_2SO_4) using Whatman 50 grade filter paper, BM in lixiviate from the testing after cooling black colour in H_2SO_4 on the left (a) and filtered H_2SO_4 with some residue from the BM, which colours its colour into pinkish on the right (b).....213

Figure 37. Results of the (Vieceli et al. [5]) reconstructed, for elements with their respective Leaching Eff.% from the BM in correlation to time (min) for the 0.5/1.0/1.5/2.5 M concentration of H_2SO_4 at a temperature of 50°C, Lithium (Li) Eff.% in (a), Manganese (Mn) Eff.% in (b), Cobalt (Co) Eff.% in (c), and Nickel (Ni) Eff.% in (d).....225

Figure 38. Results of Chemical Leaching (CL) for the TEST's 1–3, where the x-axis is time (min) and the y-axis of Leaching Eff.%. Results for CL-T-1 are in red, CL-T-2 in blue, and CL-T-3 in green. Additionally, results for the corresponding times per TEST are in solid line that of in Eff.% per sampling, while the dotted line is the result for the whole TEST's average value of the Eff.%. Results for the Lithium (Li) are in (a), Manganese (Mn) are in (b), Cobalt (Co) are in (c), and Nickel (Ni) are in (d), respectively. 226

Figure 39. Investigation of the temperature and concentration on the leaching, when comparing 30- and 60-minute leaching results of the reference material to those of the CL-T-1 and CL-T-2. Temperature investigation using 50°C temperature on 0.5 M concentration results at 25°C temperatures on the left (a), and concentration investigation using 0.5 M concentration in 2.5 M concentration result at 50°C temperatures on the right (b). (*Note! Reference BM has been thermally pre-treated, so the investigation of 50°C and 0.5 M is optimal*). 229

Figure 40. Result of the ECL-T-1 and ECL-T-3 for the Eff.% values of the Li, Mn, Co and Ni in straight graph line and their averages respectively in the same colour as dotted graph lines, in a time frame of 0 to 180 minutes. Test 1 or ECL-T-1 for the one-compartment cell type of reactor results on the left (a) and Test 3 or ECL-T-3 for the three-compartment cell type of reactor results on the right (a).....232

TABLES

Table 1. Chemical composition of some typical LIBs using the Wt.% and Cost fraction of LIB's components in % fraction. (*Note! Data values are calculated as min. & max. values*). Data is a collection of Refs. [22], [23], [24], [25], [26], [27]. 32

Table 2. Three different categories for LIBs are based on reaction mechanisms with typical materials and elements used in them [34], [36]. 35

Table 3. The most used and available electrolytes in LIBs are up to date on the market and in manufacturing, with their type, material, and linear formula. 37

Table 4. Polymers used as polymer binders in typical applied LIB electrodes, with their properties, adapted from Refs [49], [50], [51]. 41

Table 5. Information regarding the recycling and requirements for the efficiency and material recovery of the 2006 years (Directive 2006/66/EC) and 2023 (Regulation (EU) 2023/1542) comparison of Batteries Directives. 53

Table 6. Mining of the Cobalt (Co) globally, between 2022–2024 with the total global reserves as of 2024, reserves in (Mt), with [e]Estimated values for 2024, based on 2024 data for the mined Co amount for 2024 year, with Total Cal. Calculated data for the countries in the table in comparison to the World total from the available data. 77

Table 7. Mining Share of global refined production by country, % years 2022–2024, with *Calculated values for 2022–2024 refined in (Mt). 77

Table 8. Mining of the Lithium (Li) globally, between 2022–2024 with the total global reserves as of 2024, reserves in (Mt), with estimated values for 2024, based on 2024 data for the mined Co amount for 2024 year, with [e]Estimated values from 2023 for the lithium carbonate (data is not taken into account in Total Cal. or World Total), with Total Cal. Calculated data for the countries in the table in comparison to the World total, from the available data. 82

Table 9. Mining of Nickel (Ni) globally, between 2022 and 2024, with total global reserves as of 2024, in metric tons (Mt), with [e]Estimated values for 2024, based on 2024 data for the mined Ni amount for the 2024 year, with Total Cal reserves. Calculated data for the countries in the table in comparison to the World total from the available data. 87

Table 10. Mining of Manganese (Mn) globally, between 2022 and 2024, with total global reserves as of 2024, in metric tons (Mt), [e]Estimated values for 2024, based on 2024 data for the mined Mn amount for the 2024 year, with Total Cal reserves. Calculated data for the countries in the table in comparison to the World total from the available data. 88

Table 11. Mining of the Natural Graphite (Gr) globally, between 2022–2024 with the total global reserves as of 2024, reserves in (Mt), with [e]Estimated values for 2024, based on 2024 data for the mined Mn amount for 2024 year, with Total Cal. Calculated data for the countries in the table in comparison to the World total from the available data. 91

Table 12. Prices for the US, China, and Germany for natural Graphite in US$/Mts for the 2024 yearly Quarters 1–4. 91

Table 13. Reasons for Europe's natural Graphite's 2024 yearly quarters 1–4 price fluctuations explained. 92

Table 14. Reasons for North America's natural Graphite's 2024 yearly quarters 1–4 price fluctuations explained. 93

Table 15. Reasons for the Asia's natural Graphite's 2024 yearly quarters 1–4 price fluctuations explained. 93

Table 16. Pre-treatment of LIB battery recycling is categorised into three different segments from the start to the end, before the main recycling process. 106

Table 17. Physical and Mechanical separation pre-treatment processes/methods in LIB Recycling. Table reproduced by Refs. [27], [94], [98], [186], [190], [192], [193]. 112

Table 18. Chemical and Mechano-chemical separations of the pre-treatment processes/methods in LIB recycling. Table reproduced by Refs. [27], [94], [190], [192]. 117

Table 19. Thermal separations of the pre-treatment processes/methods in LIBs recycling with details of the methods, to advantages, and disadvantages. Table reproduced by Refs. [40], [94], [98], [192]. 119

Table 20. Summary of some research results for the leaching of spent LIBs in inorganic acids based on the reference materials. 127

Table 21. Summary of some research results for the leaching of spent LIBs in inorganic acids based on the reference materials. 129

Table 22. Summary of some research results for the Alkaline- and Ammonia-based leaching of spent LIBs in organic acids based on the reference materials. 130

Table 23. Summary of some research results for the Bio-Hydrometallurgy leaching of spent LIBs in organic acids based on the reference materials. 132

Table 24. Summary of some research results for the precipitation methods of spent LIBs in organic acids based on the reference materials. 135

Table 25. Summary on advantages and disadvantages of Hydrometallurgy, Pyrometallurgy and Direct Recycling processes, in different aspects, reproduced by Reference. [27], [40], [93], [94], [142], [188], [189], [190], [192], [193], [194], [195], [196], [197], [198], [239], [241], [242], [246]. 147

Table 26. Summary on current commercialised/industrial companies, with their locations, methods of processing and capacities, for the Hydrometallurgy, Pyrometallurgy and Direct Recycling processes, in different aspects, reproduced by Reference. [27], [40], [93], [94], [142], [188], [189], [190], [192], [193], [194], [195], [196], [197], [198], [239], [241], [242], [246]. 148

Table 27. LIBs used in thesis with manufacturers and corresponding models, based on the (**Figure 20**) data for some of them. 159

Table 28. Process of milling BM into finer particles for the thesis. 166

Table 29. Distribution of 358.17 grams of BM material throughout different particle sizes. 166

Table 30. LIB cells tested in the thesis, with their information based on plastic wraps and using the tool (https://batterybro.com/pages/18650-date-code-lookup-tool) for deciphering Date codes [270]. 168

Table 31. Typical measurements of the 18650 cell type battery components compared to one another, from minimal to maximal data for different manufacturers. (*Note! Data for Matsushita cells was taken separately due to too great of a difference from other manufacturers' cells*). Table reproduced from the Ref. [271]. 168

Table 32. Sampling and dissolving of the BM via AQUA regia by microwave digestion system for the different particle size distribution of BM, as per (**Table 29**). 171

Table 33. Wt.% for the samples calculated from the ICP-MS concentration in parts per billion (ppb). 172

Table 34. BM Elemental Detection & Reliability of the CPS-values/Concentrations of the Elements for the (<75 µm by AQUA regia). 173

Table 35. Results of the CPS-value for samples and the minimal CPS-value of elemental detection by the ICP-MS for (<75 µm by AQUA regia) samples. (*Note! Elements in detection/reliability order, based on the* (**Table 34**) *100% → 50/50% → 0%*). 174

Table 36. Results of the initial BM characterisation for the (<75 µm by AQUA regia), by the ICP-MS in the form of Wt.% & corresponding Concentration (ppb). (*Note! Elements in detection/reliability order, based on* (**Table 34**) *100% → 50/50% → 0%. Values for the C and Gr cannot be seen via ICP-MS, values for the Reference material can be*). 175

Table 37. CHNS analysis results for the (<75 µm) particle size of BM. 176

Table 38. Chemical leaching of BM method/settings/parameters/leaching Efficiency.% from the Ref. [273]. (*Note! Table of 1/5 set of chemical leaching collection*). 188

Table 39. Chemical leaching of BM method/settings/parameters/leaching Efficiency.% from the Ref. [2], [3], [4], [230]. (*Note! Table of 2/5 set of chemical leaching collection*). 189

Table 40. Chemical leaching of BM method/settings/parameters/leaching Efficiency.% from the Ref. [279]. (*Note! Table of 3/5 set of chemical leaching collection*). 189

Table 41. Chemical leaching of BM method/settings/parameters/leaching Efficiency.% from the Ref. [272]. (*Note! Table of 4/5 set of chemical leaching collection*). 190

Table 42. Chemical leaching of BM method/settings/parameters/leaching Efficiency.% from the Ref. [280]. (*Note! Table of 5/5 set pf chemical leaching collection*).....192

Table 43. Electrochemical Leaching data/parameters based on the literature/research review references, for the LIB and/or BM. (Geometric area (GA) and immersed surface area (IA)). (*Note! Table of a 1/4 set of electrochemical leaching collection*).....194

Table 44. Electrochemical Leaching data/parameters based on the literature/research review references, for the LIB and/or BM. (*Note! Table of a 2/4 set of electrochemical leaching collection*).....195

Table 45. Electrochemical Leaching data/parameters based on the literature/research review references, for the LIB and/or BM. (*Note! Table of a 3/4 set of electrochemical leaching collection*).....196

Table 46. Electrochemical Leaching data/parameters based on the literature/research review references, for the LIB and/or BM. (*Note! Table of a 4/4 set of electrochemical leaching collection*).....198

Table 47. Experimental tests of theoretical and actual conditions based on the literature reviews, mainly influenced by (Petranikova et al. [1]), (Vieceli et al. [5]) and (Klimko et al. [279]). 202

Table 48. Addition of BM material at 0 minutes, but the sample was taken before the addition of BM, a total of 14 samplings of three per No. A total of 42 samples were taken in 180 minutes, BM added at * mark. 205

Table 49. Elemental Detection & Reliability by the ICP-MS from the samples for the CL-Ts 1–3. 205

Table 50. Experimental tests of theoretical and actual conditions based on the literature reviews and compromises between their parameters. 206

Table 51. Solution preparation for the initial and desired parameters for the ECL-T-1/2/3, with all the needed information for the calculations to be done using the correct Equations. To create 200 mL volume of solutions for tests. 207

Table 52. The necessary equipment amounts in different ELC tests performed in addition to the reactor. 210

Table 53. Elemental Detection & Reliability by the ICP-MS from the samples for the ECL-T-1 and ECL-T-3. 212

Table 54. Collected values of the Whatman grade 50 filter paper and BM before the chemical leaching (CL) tests 1 & 2, and after the tests, to calculate/get undissolved BM and leached BM total mass/weight in grams. 214

Table 55. This resulted in values for the 90 minutes of the CL-T-1, out of which the average value was taken for later use. Steps for the (Eq. (**32.1**)) with the conversion of the units for the calculations as shown in (Eq. (**32.2**)). 216

Table 56. Safety procedures and mitigations during Battery packs → BM creation. ...217

Table 57. Safety precautions and operational steps in the experimental part of the laboratory, when dealing with chemical substances (e.g., acids and BM). 219

Table 58. Difference between the reference values/data, and comparison with the values for the CL-T-1 and CL-T-2.....230

Table 59. Difference between the reference values/data, and comparison with the values for the CL-T-2 and CL-T-3.....231

Table 60. Values of the Eff.% in cases of different experimentations and their comparisons with one another. (*Note! Values with the * maximum values of the Eff.% for the metals and consist of the maximum value X Eff.% and time mark Y minutes data in → X/Y*). 231

Table 61. Result for the ECL-T-1 and ECL-T-3 in comparison to one another's metals at their corresponding times, in addition to their average values, all of the results are in Eff.%. 232

Table 62. Difference of Eff.% between 5 and 180 minutes in a percentage-wise wise for the ECL-T-1 and ECL-T-3 results. 234

Table 63. Data for the leaching efficiencies Eff.% and other parameters used to achieve them based on the literature review studies by (Lei et al. [7]), (Meng et al. [8]) and (Li et al. [12]). 236

Table 64. Investigation of the reference materials from (**Table 63**) in comparison to ECL-T-1 and ECL-T-3, Eff.% and percentage differences of their values. 237

Table 65. Comparison of the highest values based on the reference materials for the metals Li, Mn, Co, and Ni, in Eff.% value, with the addition of the average value (Avg.) for three ECL methodology references. 238

Table 66. Comparison between CL and ECL tests at times of 5/90/180 minutes to one another in Eff.% and in average (Avg.) Eff.%.....239

1. Introduction

This thesis examines the potential of recovering lithium, cobalt, nickel, and manganese, classified as critical raw materials (CRMs) by the European Union (EU), through efficient and sustainable methods to recover and reuse these critical materials. As the increasing global demand for advanced energy storage technologies, particularly lithium-ion batteries (LIBs), has surged over the past decade due to green transition technologies, subsequent electrification, and digitalisation. As such, there is an urgent need to explore alternative sources beyond traditional primary extraction, such as the industrial transition toward circular economy (CE) models that have already begun. The use of recycled or end-of-life (EoL) materials as feedstock to support and alter current raw-material routes presents an opportunity to reduce environmental impacts, improve resource efficiency, and secure a more resilient material supply chain to meet this global need, as it is increasingly critical to reduce resource dependency. Ensuring access to strategic materials through circular strategies is not only vital for technological development but also for environmental and economic resilience. This thesis investigates the chemical recovery of selected battery metals on a laboratory scale, specifically the spent LIBs, via electrochemistry from secondary sources. The aim is to assess their technical feasibility, improve material efficiency, and support sustainable battery value chains, including environmental potential and CE initiatives. The topic is particularly timely given the accelerating scale of battery production, environmental regulations, and pressure to reduce reliance on primary raw material extraction. Although the current recycling capacity can be seen lagging substantially behind that of circulating and EoL LIBs, which in the future and a close timeline will pose a significant risk to the supply/demand of that capacity load of recycling and reuse. As such, the efficient recovery is further accelerated by both the industry and research sectors, which are actively seeking alternative sources of materials due to supply chain uncertainties, geopolitical risks, and sustainability challenges that are associated with metals such as cobalt and manganese. This thesis contributes to the field by combining theoretical insights with practical laboratory work to investigate and improve the recovery of electrochemical leaching (ECL) via a flow reactor.

Previous studies have explored a wide range of different mechanical, hydrometallurgical, and pyrometallurgical methods, including leaching, precipitation, and solvent extraction for recovering selective metals from spent LIBs, industrial residues, slags, and other EoL products. These conventional and commercialised recovery/recycling methods can and do achieve high recovery rates and material purity, particularly when combined into hybrid processes. Out of these, the most commonly used hydrometallurgy methods are chemical leaching (CL) in Western global regions. Utilising complex steps like solvent extraction and precipitation, offering selectivity and moderate operating conditions, not only under controlled laboratory conditions. For instance, in CL, sulphuric acid-based leaching combined with reductants, most commonly (e.g., hydrogen peroxide (H_2O_2)) has been widely examined for various battery and industrial waste streams, yielding a of 85–100% recovery or efficiency rate for the selected CRMs using different parameter configurations [1], [2], [3], [4], [5]. New studies and research also indicate progress being made in ECL recovery technologies. While they are all done exclusively on small laboratory scales, currently their recovery rates and purities are on par with those commercially and under laboratory-tested conditions of CLs. ECL results in the literature vary widely, but they do show 66–100% leaching recovery rates, a stark contrast to the more stable recovery rates in the literature for CL results [6], [7], [8], [9], [10], [11], [12]. The literature also underlines the influence and importance of variables such as pH, temperature, reaction time, reagent concentrations, solid-to-liquid (S/L) ratios, oxidising agents, and reagent selection on process efficiency, metal recovery/selectivity rates, and purity. It also highlights the effects of pre-treating the cathode/anode materials in LIBs or the black mass (BM) and how this influences metal recovery during leaching [1], [5]. Studies into the use of other acidic solutions, more eco-friendly, not only inorganic acids, but also organic acids (e.g., citric acid ($C_6H_8O_7$), gluconic acid ($C_6H_{12}O_7$), and oxalic acid ($H_2C_2O_4$)) are gaining momentum. These investigations have laid a strong foundation for understanding the chemical behaviour of valuable elements in different matrices and guided the development of industrial-scale processes. As such, the literature highlights the importance of process optimization, reagent selection, and the role of impurities, as well as the environmental implications of recovery strategies. These have been further strengthened by advancements in automation and selective separation technologies, pushing the boundaries of what is technically and economically viable. Highlighting clear progression from basic feasibility studies to the potential for integrating such processes into industrial recycling flows.

Despite many advantages in LIBs recycling and material recovery, many gaps persist in the current research on material recovery processes. Much of the existing literature focuses narrowly on isolated process steps, idealised inputs, or specific material systems, often neglecting comprehensive evaluations of whole process chains under realistic and varied conditions. This is notable not only in ECL but also in EC, particularly when examining the development of integration and hybrid systems. These are then further hinged by the notable lack of systematic comparisons between different recovery techniques using consistent experimental frameworks, which limits the broader applicability of findings to complex or heterogeneous waste streams. As all the research and studies have different consistencies in BM and operational parameters, not to mention the pre-treatment methods, beforehand. Furthermore, critical factors such as the influence of key process parameters, the trade-offs between recovery efficiency, purity, and operational simplicity, as well as industrial feasibility, are often overlooked. Experimental validation of theoretical models is also limited, particularly under real-world conditions. In response to these deficiencies, this thesis combines a thorough literature review with controlled laboratory experiments for the CL and ECL, utilizing selected parameters from the literature and relevant studies. To assess multiple recovery methods using representative materials and operational conditions, in an attempt to deliver a more holistic and applicable understanding of recovery performance across diverse scenarios of LIB metal recovery from the BM.

The objective of this thesis is to investigate and compare selected material recovery methods through a combined approach of laboratory-scale experiments and comprehensive literature analysis. Hence, drawing on current scientific and technical literature. This study will focus on extracting valuable metals from the EoL spent LIB laptop batteries, as the primary source, utilising ECL and a new prototype flow-reactor. The research problem centres on how recovery efficiency, selectivity, and process viability vary across different treatment conditions, and which parameters have the most significant impact on these outcomes. The central research questions are: *How do different process parameters affect recovery efficiency, material purity, and selectivity? How do key process parameters — such as reagent concentration, temperature, and time — influence the outcomes?* The methodology consists of a literature-based review followed by limited small-scale laboratory work involving leaching and separation techniques of BM. The thesis does not include full-scale industrial trials or any sort of comprehensive life cycle assessments. The structure of

the thesis includes a literature review of the LIB's internal structure and working principle, led by the current CE and the LIB recycling state, that goes into aspects that over the last decade have affected LIBs demand/pricing, fast-forwarding its metals classification as CRMs. Review of the current LIB recycling technologies, and what process steps they have. Followed by the research/laboratory methods, results, analysis, and conclusions based on the results.

2. Lithium-ion Battery

This chapter provides a comprehensive overview of lithium-ion batteries, beginning with their history, tracing their evolution from early primary batteries to today's sophisticated power-house rechargeable systems. Without which, the current energy development would not be possible. The chapter as such delves into the structure of lithium-ion batteries, detailing their five key components: anode, cathode, separator, electrolyte, and current collectors, and classifying battery types by shape and casing they share all together. This will also lead to the introduction of the, maybe most important, aspects solid electrolyte interface explaining its formation, function, and critical impact on battery stability, performance, and degradation, which is one of many causes for the need of recycling methods/processes and development of a new type of batteries. Finally, the principles of lithium-ion battery operation is going to be explained, including the mechanisms of charging and discharging, energy flow, and the electrochemical reactions governing performance, with mathematical formulations and practical examples using common materials like lithium cobalt oxide and lithium nickel manganese cobalt oxides, in addition to graphite as non-conductive material.

2.1. Lithium-ion battery history

Lithium-ion batteries, or Li-ion batteries (abbreviated as LIBs), are efficient energy storage devices that can be categorised into two different battery types: primary and secondary batteries [13], [14]. Primary batteries are those that cannot be recharged after use and were the first type of LIBs when they were introduced in 1962 [13]. While secondary batteries are those that can be recharged repeatedly [13]. Such batteries were already developed by many companies, including Exxon and Duracell, in 1978 and 1981 [15]. However, the true commercial LIBs, as we know them today, are still credited to Sony, which did not introduce them to the market until 1991, when they were commercialised as we know them today [13], [14], [15].

2.2. The Structure of Lithium-ion Battery

There are many kinds of LIBs on the market and in development, but they all share similarities with one another, which makes them perfect and reliable energy storage systems. Even if one may not look alike like the others, they all have the five major structural components in them, without which they would simply put just not feasibly be able to work as they do: separator, anode (-), cathode (+), electrolyte, and current collectors [16], [17]. There are many different applications for LIBs, as such, they can also be categorized into two different types based on the geometric shape of the batteries and their outer housings. Based on their configurations, they are cylindrical and prismatic in shape. These two can then further be divided into housing stabilities: cylindrical into hard-case and coin/button, while the prismatic can be divided into hard-case, pouch, and thin film [18], [19]. When talking about LIBs in these three different housing styles, these LIBs are typically referred to as cells due to the following factors:

1. Do they consist of single or multiple Lithium-ion cells?
2. Do they have or are they fitted with some sort of protective circuit board inside or outside of the cell/cells?

When both criteria above are met, the electrochemical cells are then referred to as batteries or, in some cases, battery systems. All three of these housing stabilities share the same five structural components, as mentioned earlier, but the key factor is how these are layered/connected within the housing to one another. Many of the commercially available LIBs do share standardised components with one another, as they are manufactured by different companies, such as electrolytes, separators, and casings (cylindrical), which are made of steel, aluminium, or plastics, but typically of Ni-Fe-coated alloy material [18], [20]. However, what differentiates them from one another is the concentration of metals, more specifically, in anodes and cathodes, as well as lithiated metal oxides for the cathodes [18]. (**Figure 1 (a)**) shows a typical cylindrical structure of a single LIB, in which anode, cathode, separator, and current collectors are visualised, with the addition of a simplified and layered view of the LIB (**Figure 1 (b)**), while electrolyte solution in aqueous phase between the layers cannot be visualised.

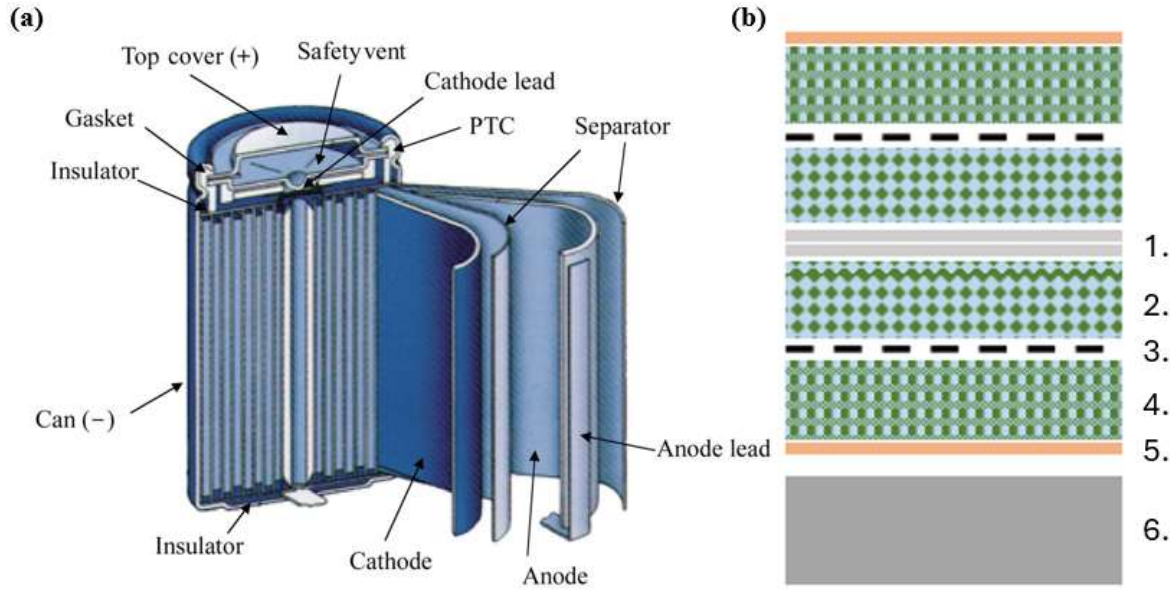

Figure 1. Structure of LIB (a) (cylindrical). Structure in the current figure: anode of copper foil and cathode of aluminium foil, which are used as current collectors [14]. Structure of LIB (b) in the layered form: 1/5 current collectors, 2/4 anode and cathode, 3 separators and 6 casing (outside) [20].

There is a new type of LIBs also under development, called tertiary batteries. These are relatively new types of batteries, utilizing the principle of thermal energy harvesting, and based on available information that can be found, they are not rechargeable, making secondary batteries the only rechargeable ones in the LIBs category thus far [18], [21]. A key principle of this battery type is in how it is charged thermally, which utilizes the principle of the thermal coefficient difference $\Delta\alpha$ by using the redox potential V^1 [21].

The LIBs are the dominant energy storage technology for portable electronics, electric vehicles (EVs), and grid storage. While all LIBs share a similar fundamental structure, their performance characteristics, such as energy density, power output, cycle life, and safety, vary significantly due to differences in electrode materials and electrolyte compositions, as represented in (**Table 1**).

Table 1. Chemical composition of some typical LIBs using the Wt.% and Cost fraction of LIB's components in % fraction. (*Note! Data values are calculated as min. & max. values*). Data is a collection of Refs. [22], [23], [24], [25], [26], [27].

	Different types of LIB metal oxides					
LIB components	**LCO**	**LFP**	**LMO**	**NMC**	**NCA**	**Cost**
Cathode active material	33.00–37.00	30.00–44.40	12.20–39.00	25.00–31.68	16.40–29.00	26.00
Anode active material	15.00–31.00	28.50	32.00	16.00–28.68	24.72	13.00
Cathode (-) foil Al	5.20–20.00	6.50–9.00	7.00–21.70	8.00–22.72	9.00–21.90	8.00
Anode (+) foil Cu	7.00–16.00	7.00–14.00	8.00–14.00	6.93–16.60	6.93–16.00	1.00
Conductive salts & electrolytes	11.00–15.00	14.90–31.00	11.80–15.00	11.66–16.83	11.70–19.80	9.00
Graphite	16.00–23.10	13.00–18.00	14.00–16.30	16.83–19.00	16.50–28.71	–
Carbon Black	3.00	2.00	3.00	2.00	2.00	–
Binder	2.00–2.40	0.90–2.00	3.00–3.70	1.39–4.00	3.00–3.80	8–9
Conductive additive	1.00	2.00	1.00	0.99	0.99	–
Plastic	3.00–5.00	3.00–4.40	3.00–5.00	3.00–5.94	3.00–4.20	–
Separator	3.00–4.00	3.00–4.00	3.00–4.00	3.00–4.00	3.00–4.00	12.00
Other	3.00	4.00	3.00	2.97	0.99	–
	Wt.%	Wt.%	Wt.%	Wt.%	Wt.%	%

As shown in (**Table 1**), different LIBs in metal oxide compositions typically have and commercially a different amount of the material in them. Overall, the majority of the costs in any type of LIBs metal oxides seem to be those of the cathode active materials (CAMs), followed by those of the anode active materials, while the least being those of the anode foils, typically made of Cu. Information for certain materials cost fractions was also subsequently hard to come by, which may lead to variations and also, and which are affected by shifting market prices, or information just was not readily available.

2.2.1. The Cathode

One of the most important components, if not the most important component, of any type of LIB. The cathode, the positive electrode, determines the most essential things of any LIB electrochemical performance. Performance in LIBs as such is measured in terms of capacity Q, which can be reached with specific power, aka operating/output voltage V, and conductivity σ [28], [29]. These, in turn, lead to the energy density U, which in return affects stability, cyclability, and, most importantly, the safety of the entire LIBs when different structures and materials are combined and in contact with each other [19], [29]. All of the above aspects, when taken into account and researched, determine the chemical composition

of the cathode material, which leads to its development, which in turn is affected by the variety of different aspects these days [29]. For instance, countries/tech companies and the world overall are moving towards and embracing renewable energy and its solutions. The scarcity and availability of certain important components, such as metals like cobalt (Co) and lithium (Li), on the market and demand create a real supply risk, which is one of the many risks at this level. These, in turn, lead to the development of new batteries and technologies related to them, such as sodium-ion batteries or (Na^+)-batteries, in a positive way [22].

As cathode has such an important part in the LIBs, it is no surprise that the key component in the cathode is Li, which then is bonded with other different metals, such as Co, manganese (Mn), and nickel (Ni), in addition to other essential elements bonded to them, to create chemical compounds, which can be known as lithium transition metal compounds. These are referred to as CAMs, which result from the reaction of metal cations and oxide anions, creating metal oxides (MOs). The most commonly used and encountered in LIBs and CAMs alike are lithium cobalt oxide ($LiCoO_2$ or LCO), lithium manganese oxide ($LiMn_2O_4$ or LMO), lithium iron phosphate ($LiFePO_4$ or LFP), and lithium nickel manganese cobalt oxide ($LiNiMnCoO_2$ or NMC) formats. All four are lithium-bearing metallic oxides, and for a reason, as MOs are, for the moment dominant and widely used for the LIBs industry, a new type of compound, called polyanionic is paving a replacement for certain aspects of LIBs, due to them being more ecological/safer and being as stable if not more stable, under different environments LIBs are put through [29], [30].

When discussing structures, one cannot overemphasize the importance of morphology and microstructure over other variables mentioned earlier. When looking at CAMs and cathode materials overall, they consist of layers upon layers, which can be separated into different dimensions, ranging from zero to three [31]. While there are four different dimensions in the cathode structures, they are categorized into three different hierarchical structures: layered, spinel, and olivine, which essentially define the cathodes and CAMs what they are [28], [29]. To put into perspective, typically LCO is layered, while LMO is spinel and LFP olivine, or also known as a polyanion-type compound, as seen in (**Figure 2**) [28]. The ability to influence and understand these dimensions, based on the hierarchical structures, enables LIB development to improve and undergo architectural modifications, such as surface modification and doping different elements to change/modify

lithium excess layers, which are the three different hierarchical structures [31], [32]. All these factors contribute to LIB electrochemical performance on multiple levels.

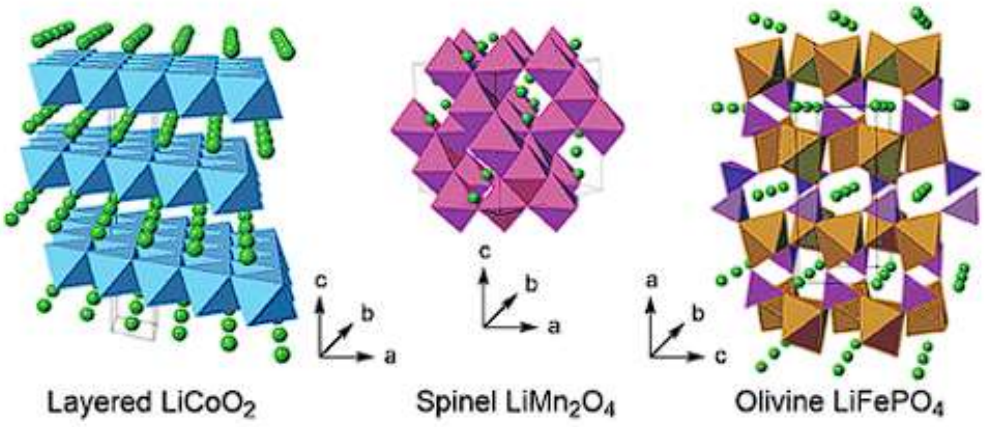

Figure 2. Crystal structures of three lithium-insertion compounds from left to right: Lithium Cobalt Oxide, Lithium Manganese Oxide, and Lithium Iron Phosphate [33].

As (**Figure 2**) illustrates, the clear differences in the structures and layers of those layered, spinel, and olivine in the most commonly found metal oxides can be observed in comparison to one another. Most noticeable differences between the layered and olivine, for instance, are that of a clear difference in organised pattern, which then starts to differ as seen in spinel, and as subsequent in olivine is that of a more chaotic nature. All of these structures are critical in understanding the LIB's architectural concept and how different layer concepts of the LIB work and affect one another.

2.2.2. The Anode

Anodes, the negative electrodes of any given LIBs, play an important role as cathodes in LIB battery performance. These affect the working principles of LIBs on both physical and chemical levels, like the properties of energy/storage capacity [28], [31]. Like in cathodes, the Li metal is best suited for anode material in LIBs like the high specific capacity of (3,860 mAh/g) with the addition of negative potential, but due to safety factors such as cells self-discharging or internal chain reaction and practicality overall, different type of elements is

used in the development of high-performance and high-capacity cells [13], [34]. Graphite (Gr) is one of the most commonly used elements in the anode, with the combination of different carbons from hard to soft or so-called amorphous carbons [13], [23], [28]. These are the number one choice for current industry and commercial use due to the high availability, cycle of life, and, importantly, extremely low costs, with the combination of industry modifying the structural level of materials to enhance their capabilities [23], [29], [35]. Even if Li is more effective in terms of capacity, its high-rate consumption of Li, which is over two or three times, has led to the usage of C, disregarding the drawbacks of not meeting the rapidly rising demand for high-performance LIBs [13], [34].

The difficulties in coming up with effective and high-performance/capacity LIBs, in addition to the need to fill high demand from an economic perspective, have led to some peculiar types of anodes, as mentioned amorphous carbons throughout their development because carbon (C) in anodes cannot meet the demands currently based on the market and features that are needed from the cells/LIBs currently [13], [34]. Anodes themselves can be separated into three different categories. These are purely based on their reaction mechanism, which takes place in the LIBs when discharge and charging occur, basically the way how Li-ions are stored inside the LIBs as per (**Table 2**) [34].

Table 2. Three different categories for LIBs are based on reaction mechanisms with typical materials and elements used in them [34], [36].

Reaction mechanism	Anode Materials & Elements
Insertion reaction mechanism	Carbon materials & Titanium dioxide (TiO_2)
Alloying reaction mechanism	Silicone (Si), Germanium (Ge), Tin (Sn) & Alloy materials of IV & V groups
Conversion reaction mechanism	Transition metal oxides (TMOs), Metal-organic frameworks (MOFs) & Sulfides (S^{2-})

Based on (**Table 2**), it is noticeable that there are multiple different materials in comparison to one another that are being used in the LIBs anode developments. There are currently four material groups, out of which three are in (**Table 2**): carbon-based materials, alloys of Sn and Si, TOMs, and lithium TiO_2 materials, with the addition of different composites [30]. These are all significant and promising materials in the development of high-performance LIBs. However, there is a limit to what can be achieved only by the

selection of materials. Consequently, the importance of structure cannot be neglected. The structure of the anode and its materials, whether they are of amorphous or crystalline structure, will dictate the size, shape, and state of the components used in the LIB anodes. Because of this, like in the cathode, the architectural arrangement is of importance and poses, to some extent, challenges for the future development of the anode [30], [32], [34], [36].

2.2.3. The Electrolyte

Electrolytes are typically in a liquid and colourless form in an organic solvent in the LIBs between two electrodes to allow control and promote the ions flow and traverse between these two while functioning as a medium when the LIB/cell is charging or discharging in reverse. While essentially at the same time electrically insulating, avoiding electrical conduction or so-called short circuits from happening [19], [24], [37], [38], [39]. Electrolytes, although only one of the five LIBs structural components, are of high-purity, and multi-component systems themselves, which keep the chemical reaction in the cells going smoothly in close hands with separators [39].

There are five types of electrolytes on the market for LIBs: solid polymer electrolyte (SPE), gel polymer electrolyte (GPE), colloidal electrolyte (Ce), liquid or aqueous electrolyte, and ceramic electrolyte, in addition to different combinations of these five types [40], [41]. These can then be further divided into weak and strong electrolytes, which are based on their conductivity aspect, specifically the ion concentration within themselves [41]. What makes these five electrolytes viable options is the three criteria classes they meet: conducting salt, organic aprotic solvent or “partly polymers”, and additives. Electrolytes are primarily responsible for the cell’s stability, primarily by allowing ion movement between cells, but also for the performance, which they boost by enhancing. [39] The importance of electrolytes is also imperative in LIBs, as the cells' operating temperature range cannot exceed certain levels, depending on the three other LIBs' structural material choices/combinations, as well as the specific capacity the LIBs are rated for. These requirements have zero tolerance for flexibility in LIBs and cells alike, in correlation with the high demand of consumers/users, which just cannot affect their safety and cycle efficiency. [24] To achieve these primary and desired functions, electrolytes must be

thermally, chemically, and electrochemically stable while having high ionic conductivity with various other different properties [24], [37].

While all the electrolytes used in LIBs share basic functionality and goals, they are designed to achieve high standards depending on the compound used in them. There is quite a wide variety of different electrolytes available on the market and subsequently used in the LIBs, but their key features are high permittivity and low viscosity [24]. The development of solid electrolytes (SE) not just in LIBs but other types of batteries/cells has been on the rise, as these enable the development of solid-state batteries, which provide advantages in thermal stability, lower flammability, durability and design simplicity of LIBs/cells alike, in retro perspective to current electrolytes, which are primarily aqueous type [42]. While development and technical solutions are being researched and tested, the (**Table 3**) electrolytes are being used in most of the commercially available LIBs.

Table 3. The most used and available electrolytes in LIBs are up to date on the market and in manufacturing, with their type, material, and linear formula.

Electrolyte type	Electrolyte material/synonym	Linear formula	Ref.
Lithium salts	Lithium hexafluorophosphate	$LiPF_6$	[23]
	Lithium tetrafluoroborate	$LiBF_4$	[23]
	Lithium perchlorate	$LiClO_4$	[23]
	Lithium hexafluoroarsenate	$LiAsF_6$	[43]
	Lithium hexafluorophosphate	$LiPF_6$	[24]
	Lithium triflate (LiOTf)	$Li(CF_3SO_3)$	[24]
	Lithium trifluoro methanesulfonamide (LiTFSI)	$Li[N(CF_3SO_2)_2]$	[24]
	bis(trifluoromethane sulfonyl)imide (LiTFSI)	$LiC_2F_6NO_4S_2$	[43]
Organic solvent	Ethylene carbonate (EC)	$C_3H_4O_3$	[23]
	Propylene carbonate (PC)	$C_4H_6O_3$	[23]
	Dimethyl sulfoxide (DMSO)	$(CH_3)_2SO$	[23]
	Diethylene carbon (DEC)	$C_5H_{10}O_3$	[24]
PEs	Poly(acrylonitrile) (PAN)	$(C_3H_3N)_n$	[24]
	Poly(methyl methacrylate) (PMMA)	$[CH_2C(CH_3)(CO_2CH_3)]_n$	[24]
	Poly(Propylene Oxide) (PPO)	$H[OCH(CH_3)CH_2]_nOH$	[24]
GPEs	poly (vinyl alcohol)-lithium nitrate (PVA-$LiNO_3$)	PVA-$LiNO_3$	[41]
	polyethylene oxide (PEO)	$H(OCH_2CH_2)_nOH$	[24]
	1-ethyl-3-methylimidazolium bis(trifluoromethyl sulfonyl)imide (EMIMTFSI)	$C_8H_{11}F_6N3O_4S_2$	[41]
SEs	Lithium phosphorus sulfur chloride (LPSCl)	$Li_6PS_5C_l$	[41]
	Lithium lanthanum zirconate oxide (LLZO)	$Li_7La_3Zr_2O_{12}$	[41]

Use and development of different electrolytes on the market and manufacturing, as in that of the (**Table 3**), can be observed. As there are other types of electrolytes also available, the list of (**Table 3**) is that of a mere fraction, while having the majority of the commercially used electrolytes. Highlighting the vast electrolyte development and availability, not only commercially or manufactured, but also overall, what is available at different stages of LIB's development and manufacturing/commercialisation alike.

2.2.4. The Separator

The Separator's key structure of any kind of LIB performs the critical role of separating anode and cathode from one another physically, while the mass of the cell may only be that of 4–5 wt.%, its role may not be undermined [30]. The separator is the only one out of five LIB structures not to participate in any way in the LIB electrochemical reactions. Their role is specifically to be the inactive part of the cells, thereby separating and keeping all the other three in check in the LIBs, while being sandwiched between both electrodes and keeping them away from the electronic contact of one another [30], [37]. While the separator may not be directly involved in the reaction of LIBs, its fundamental role is to hold the electrolyte within itself, much like a reservoir, enabling important ion transportation via the electrolyte and between both electrodes through its structurally interconnected porous structure [30], [37], [44].

There are many types of separators in use and still in development, which can be categorized into six different categories or types of membranes: GPEs, polymer composite membranes (PCMs), nonwoven mats/webs, electrospun membranes, membranes with external surface modification and microporous membranes, or a combination of these all [37], [44], [45]. These six classifications are, at the moment, a cornerstone for the separators, but due to the shift in the "green" products and trends around LIBs has led to a shifting of research/manufacturing priorities are shifting from obtaining a specific membrane morphology in favour of new desired properties. There is an immense number of properties that could be attributed here, but the most common these days are the safety, longevity, and environmental impact of materials. This has led to the suggestion that classification be based on the number of layers, ceramic addition, and any type of surface modifications. The

importance of all of the structural changes in separators is that they can be related in a direct way to LIBs' interfacial characteristics, such as internal resistance, capacity, cycling, and safety [37], [44], [45], [46]. Nevertheless, all of the separators in the LIBs fall under one of the main categories, that being the porous type separators, which are different polymer matrices, if not combinations, and soaked in with different electrolyte solutions [37].

When it comes to the factors that either improve or hinder the characteristics of the separators, they come most commonly to the twelve different factors: wettability, tortuosity, pore structure and geometry, porosity, ionic conductivity, thermal dimensional stability, mechanical properties, shutdown temperature, melt integrity, chemical stability, dimensional stability and most importantly thickness of the separator itself [46]. As per the suggestion of classification change, thickness plays a significant role due to the single- or multilayer possibility. Most commercial separators are around (<25 μm), and when going higher/thicker than that, for example, of (>50 μm), then the areal power density of LIBs decreases [44]. The material that is typically applied in these is a polyolefin monolayer microporous, while other fluorinated or aromatic polymers also are/have been used, such as polyvinylidene fluoride (PVDF) and hexafluoropropylene (HFP), which is typically deposited directly on the PVDF, thus creating a PVDF-HFP separator. When charting into multilayer separators, the most commonly used separators are either dual-layered poly(ethylene)/poly(propylene) (PE/PP) or tri-layered poly(propylene)/poly(ethylene)/poly(propylene) (PP/PE/PP) [16], [37], [38], [44], [45]. What all of these commonly used separators have in common is their remarkable chemical stability, cost-effectiveness, mechanical strength, and thermal shutdown properties [37], [38].

2.2.5. The Binder

For the battery and its components working principle, the anode and cathode active material particles are adhered to their respective current collectors (Cu and Al) using an inert organic binder, such as PVDF or polytetrafluoroethylene (PTFE), as an adhesive agent [23], [24], [35], [37]. For PVDF to form and make sufficient adhesion to the current collector, it forms hair-like structures that efficiently keep the coating together so that active materials do not fall off during the charge/discharge processes of LIB [47]. These are then typically mixed or

added in with the conductive high-surface-area carbon (acetylene black) or (AB) to ensure electron conduction to the current collectors [37], [40]. Because of the role of binders in LIBs, they are required to have good mechanical and chemical strength to bind the cells effectively [40]. The typical amount of PVDF in LIB's cathode materials is 10 wt.%, and that of AB is 5 wt.%, in contrast to the rest of the metal oxide powder, which is 80–85 wt.%, depending on the type used [24]. Binder's role in structurally consolidating electrodes inside the LIBs chemically has been found to contribute to solid-electrolyte interface (SEI) formation, making its role as important as any other part in LIBs [48].

While the use of AB appears to be a simple solution in battery manufacturing, the addition of PVDF to electrodes is not as simple. For the PVDF to stick, it requires the use of an organic dipolar aprotic solvent, N-methyl pyrrolidone (NMP), due to PVDF not being soluble in water, or the use of a polar aprotic solvent, dimethylformamide (DMF) [47], [49], [50]. The use of NMP itself is harmful to the environment and causes safety and health hazards due to its volatility and flammability. While the process of making LIBs may use NMP, the NMP is evaporated during electrode drying, leaving none in the finished cell [47]. The application of NMP production is made by the slurry preparation, which contains active materials, conductive agents, and binders, which are then mixed in with the NMP and coated on the current collector's surface, by which they then are evaporated, thus allowing the PVDF to create hair-like structure [47], [49]. Because LIBs do not have NMP in them, after production, it is typically either burned or recycled, thus elevating the risks/exposure associated with its use, which has led to the current industry utilizing other types of most commonly found polymer binders in LIBs, in addition to PVDF, such as styrene-butadiene rubber/carboxymethyl cellulose (SBR/CMC), polyacrylic acid (PAA), and polytetrafluoroethylene/polyvinyl alcohol (PTFE/PVA) [47], [49]. The difference in these binders to PVDF is in the manufacturing of the electors, as they do not require NMP, as the processing solvent is water (H_2O), leading to two different soluble binders on the market, those of oil-soluble binders and water-soluble binders, out of which PVDF is oil-based and has the most significant share out of other binders used in cathodes [17], [49]. Although PVDF is toxic and leads to difficulties and risks associated with recycling, its properties are similar to those of other binders, making it a more desirable choice in both cathodes and anodes, as per (**Table 4**), binders used in LIBs [47], [49]. When recycling LIBs, the use of thermal pre-treatment has been found to decompose organic binders at 300°C, while the AB

decomposes at 600°C, meaning that when thermal treating the PVDF containing LIBs, at the ranges of 300–650°C, the risk of its degradation can be observed [40]. One common risk associated with the thermal treatment of LIBs containing PVDF is the release of highly toxic gases such as hydrogen fluoride (HF), which is not helped by the fact that PVDF's chemical inertness resists common recycling solvents, necessitating aggressive and often hazardous chemicals for its removal and breaking the bind between electrodes. For these reasons, the use of organic solvents in dissolving PVDF has been utilized to mitigate risks, but on larger scales, risks of high volatility and high toxicity [17]. Additionally, the EU and the US Environmental Protection Agency (EPA) proposed a ban on all per- and polyfluoroalkyl substances (PFAS), which would have also included PVDF, under the REACH regulation. What REACH does is regulate the use of NMP on an industrial scale due to its toxicity [50].

Table 4. Polymers used as polymer binders in typical applied LIB electrodes, with their properties, adapted from Refs [49], [50], [51].

Binders	Binder Type	Processing Solvent	Properties
PVDF	Synthetic polymer	NMP	- Good absorbing, solubility & electrolyte capability - Bond ability - Good mechanical properties - Good electrochemical stability - Excellent weather resistance - High adhesion strength
PAN	Synthetic polymer	Toluene + NMP	- Good chemistry stability - Strong adhesion - High conductivity & flame resistance - Lowest occupied molecular level & antioxidant properties
SBR/CMC	Synthetic polymer & natural polymer	Water	- High adhesion strength - Good mechanical properties - Better elastomer & higher temperature resistance of (PVDF) - Prevents the formation of Li dendrites - Low cost - Environmentally friendly - Easy processability
PTFE/PAA	Synthetic polymer	Water + NMP	- Good mechanical properties - Chemically inert - High hydrophobicity - Wide temperature range - Excellent weather resistance - Low cost - Environmentally friendly - No health risk/hazards

(*Continued on next page*)

Table 4. (*Continued*)

Binders	Binder Type	Processing Solvent	Properties
PTFE/PAA	Synthetic polymer	Water + NMP	- Without the co-intercalation and decomposition of propylene carbonate (PC) molecules - Functional groups - Improve reversibility of lithium intercalation
PAmA	Synthetic polymer	DMAc	- Highly adhesive - Good binding, - Good mechanical properties
PEI	Synthetic polymer	DMF	- Strong adhesion - Dispersion ability - Robust network structure - Chemical interaction with the electrolyte - Strong affinity with the electrolyte - Hyperbranched network structures
PMMA	Synthetic polymer	Toluene	- Good mechanical properties - High thermal stability - High ionic conductivity - Good electrochemical stability - Good adhesion
Chitosan	Natural polymer	Water	- Chemical stability - High discharge capacity - Good capacity retention ratio - Positive amine groups - Water-soluble - Strong chemical bonding - Low-cost fabrication
PAAm	Biopolymer	Water	- Fast penetration of electrolyte - Improved Li^+ conductivity - High thermal stability - Formation of a more conductive (SEI) - Strong adhesion
PAH	Biopolymer	Water	- Reduces expansion damage - Chemical interaction - Strong adhesion
SA	Natural polymer	Water	- Good battery stability - Mechanical stability (50x the stiffness of PVDF) - Forms strong interactions (hydrogen or covalent bonds)

PVDF is one of the most commonly used binders in LIBs, as shown in (**Table 4**), and offers relatively good, often excellent, properties that are essential for binder performance. However, among various binders, there are also options like PTFE/PAA and PEI, which possess comparable or even superior properties to PVDF. Overall, most binders are water-based or use water as a processing solvent, while some employ other solvents that

are increasingly less researched or used in current LIB development as the industry progresses.

2.2.6. The Solid Electrolyte Interface (SEI)

The operational integrity of LIBs depends on the coordinated performance of three key elements: (1) electrode pair, (2) separator, and (3) electrolyte – all essential for electrochemical energy storage. To achieve stable and high-performance LIBs at high energy densities, their electrodes are designed to function at extreme potentials [52]. This is achieved by a phenomenon called the SEI, which is an organic/inorganic composite mosaic structure that is a film described as a complex heterogeneous, structurally disordered passivation layer that is ionically conductive but electronically insulating [52], [53], [54], [55], [56]. SEI's role in LIB's performance is essential, as it ensures and allows the electrolytes' operation beyond their thermodynamic stability limits [52]. SEI's formation in LIB happens in-situ on the negative electrode's Gr particles and its surface within the Helmholtz double layer that of an inner and outer layer, creating the solid interphase as the reductive products build up on it, as illustrated in (**Figure 3)** [52], [56], [57], [58]. This formation is triggered instantaneously by the reduction of lithium salt and the electrolyte by Li metal, meaning that when the electrode (metal) comes in contact with the electrolyte, the electrochemical instability of the electrolyte inside the LIB leads to the development of reactive decomposition inside the anode, hence the formation of SEI [52], [54], [55], [56], [59]. As this formation occurs, SEI controls the battery performance by the electrode and electrolyte, leading to kinetic electrochemical stability and its window of operation range, which in turn attracts dendrite growth, and allows the electrolyte mutations inside LIBs [52], [60]. SEI's principle is to passivate the electrode surface, thus preventing further reactions between the alkali metal, which Li is, and the electrolyte. As the SEI reaches the thickness, electronic tunneling is suppressed, thereby preventing excessive electrolyte decomposition. This protective layer not only enhances the cycling stability and lifespan of LIBs but also regulates ion transport between the electrode and electrolyte, leading to a reduction in the amount of undesirable electron transfers. While the SEI is essential for performance, its inherent resistance to Li^+ diffusion, which impacts battery kinetics [48], [53], [54], [55].

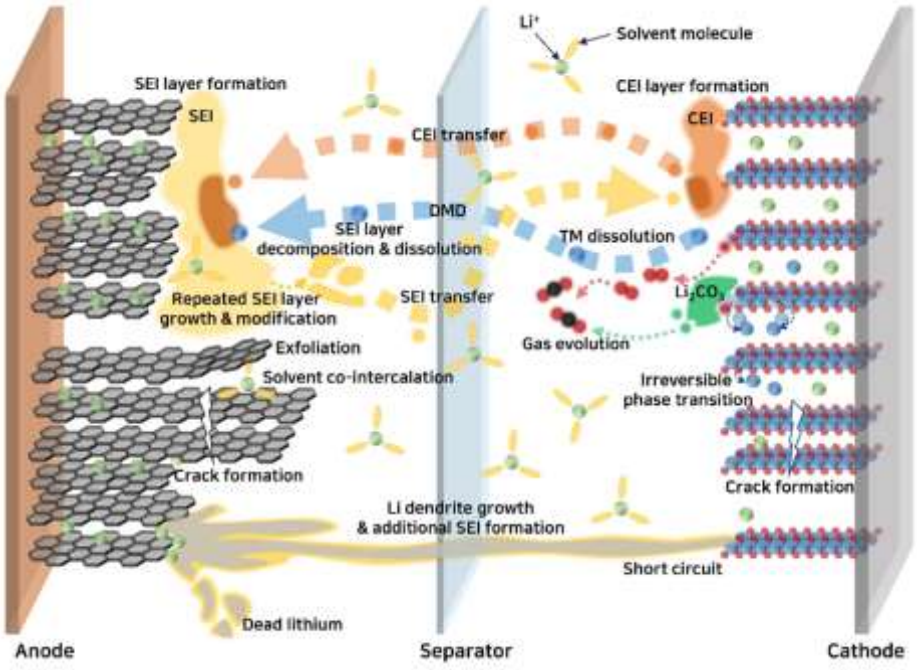

Figure 3. Schematic illustration of the main ageing mechanisms of commercial LIBs with the composition and formation of SEI and CEI films [61].

To explain and understand how SEI in LIBs works, the concept devised by Goodenough and Kim is widely accepted in showing and explaining the electrode/electrolyte interface, which derives from the thermodynamic analyses of electrolyte redox reactivity at extreme potentials, lies outside of the electrolyte electrochemical window, leading to SEI layer formation in LIB's [52], [54]. This theorem of frontier orbital theory (FOT) describes the nature of the anode and cathode, as the energy band diagram of electrolyte shown in (**Figure 4**), by chemical potentials of the anode and cathode or their energy difference between the highest occupied molecular orbital (HOMO) and lowest unoccupied molecular orbital (LUMO) of the solvent molecules [54], [55], [60]. This window in between LUMO and HOMO orbits represents hence the electrochemically stable potential window "stability window" or the E_g, which is the difference between the E_{LUMO} and E_{HOMO} electron-volt (eV) as per (Eq. (**1**)) and is extended by surface films, denoted as the cathode electrolyte interface (CEI) and SEI on the electrodes as per (**Figure 4**) [54], [59], [60], [62].

$$E_g = E_{LUMO} - E_{HOMO} \tag{1}$$

LUMO's and HOMO's importance lies in explaining LIB's stability of electrolyte solution from thermodynamic perspective is determined by the energy difference between the Fermi level, by anode's μ_A and cathode's μ_C chemical potentials [55], [60]. Using the differences in the anode's and cathode's potentials, one can express the LIB's thermodynamic stability E_{TS} as per (Eq. (**2**)), which must be within the E_g region [54], [55], [60].

$$E_{TS} = \mu_A - \mu_C \tag{2}$$

By this, if the electrolyte's LUMO is lower (more negative) than the μ_A or the Fermi level → ($\mu_A > E_{LUMO}$), then the electrolyte is thermodynamically unstable [55], [59], [60]. This leads to the electrolyte solution gaining electrons from the anode, and the solvent-electrolyte reduction reaction occurs, resulting in the formation of the SEI film on the anode's surface. [52], [59], [60] On the contrary, if the electrolyte's HOMO is that of higher (more positive) than the μ_C → ($\mu_C < E_{HOMO}$), leading to oxidation of the solvent-electrolyte and formation of that CEI film on the surface of the cathode, as the electrolyte tends to transfer to the cathode [52], [54], [59].

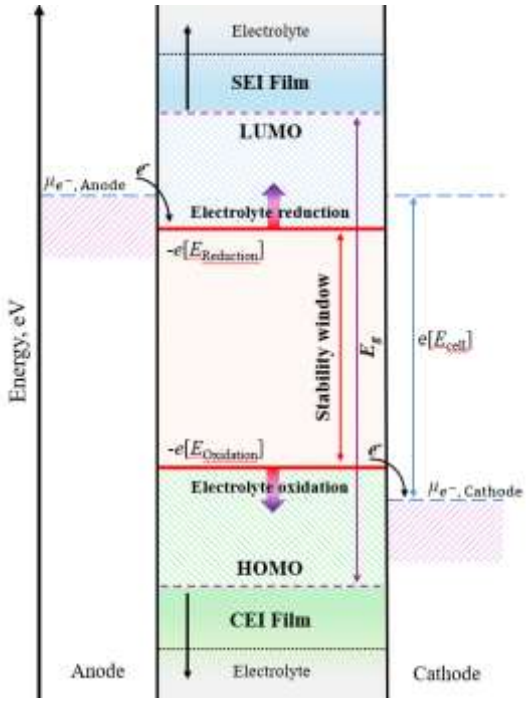

Figure 4. Schematic of electrolyte stability limits (positive/negative potentials) vs. HOMO/LUMO energy levels. Red arrow: Stability window, violet/purple arrow: LUMO-HOMO gap, and blue arrow: Cathode-anode electrochemical potential difference [52], [54], [59], [60], [62].

Aspects that affect the properties of the SEI formation in LIB are the electrolyte composition, current, voltage, temperature, and electrode substrate. For instance, the weak solvent-graphite interactions may hinder effective intercalation and exfoliation, preserving Gr stability [59]. General use of different organic solvents, like that of lithium ion (Li^+) or any type of high electronegativity atoms "complexant" in LIBs, by increasing the lithium salt concentration in the electrolyte leads to interactions and influences on Gr stability and battery performance, weakening the Li^+ solvation sheath and shielding of the Gr against exfoliation [54], [59]. SEI's stability in LIBs is an important factor in limiting the lifetime, performance, and safety [54]. These attributes are in correlation to those of the SEI film, as it reduces resistance, polarization, and maintains a strong discharge plateau, which is then enhanced by the thin and lightweight SEI film, leading to minimization of power fading, an increase in initial capacity, and extends cycle life of LIB [55]. The operation of LIB at high current rates thickens the SEI, increasing capacity loss attributed to lithium consumption in LIB, while higher current density may mitigate this [59]. The overcharging and high state of charge (SOC) lead to degradation of the SEI structure, while elevated temperatures promote SEI growth and thermal decomposition, which in turn may lead to LIB's thermal runaway [54], [55]. Dendrite growth on the SEI may also be attributed to the porosity of the SEI structure, as well as the non-uniform Li deposition and acceleration [55], [59]. Overall, the repeated cycle of charge and discharge of LIB leads to the development of SEI and its uncontrolled growth, thus leading to the degradation of LIB [55].

2.3. Concept of LIB principles

LIBs, as an energy source and rechargeable batteries for many common appliances, have to store energy but also be able to convert this energy into a form of electricity, which happens by discharging the energy when needed [19], [36]. This energy, so-called electrochemical energy, is a reaction and result of the interaction between the five primal structures of LIBs and cells alike, as per (**Figure 1**) shown [19]. The movement inside LIBs is part of the Li+ transition between opposite-polarity electrodes, known as anode and cathode, utilizing a separator in between them. This separator typically has embedded within it an aqueous electrolyte due to its material porosity. These ions, in the case of discharge, move towards the cathode and are absorbed, while during charging, the same process occurs, and vice

versa, into the anode [30], [36]. Discharge occurs in two forms, current I in Amps (A) and V ($kg{\cdot}m^2{\cdot}s^{-3}{\cdot}A^{-1}$) electric potential, which results in electrochemical discharge of electrical power P_P, which can be written simply by (Eq. (**3**))).

$$P_P = I \times V \tag{3}$$

This LIB power can be expressed either as above or either by gravimetric power (W/kg) and gravimetric volumetric power density (W/L). It has been mentioned in (***2.2.1. The Cathode***) that battery capacity Q is one of the most important values when it comes to comparing and developing LIBs. This variable can be expressed as (Eq. (**4**)).

$$Q = I \times \Delta t \tag{4}$$

Where capacity or the total charge is the result of I over the set of certain time Δt to achieve the complete discharge by LIBs. This can then be represented in a Q/weight ratio (Ah/kg or mAh/g) as to battery capacity in an electric charge q with respect to the time t itself or simply put rate of change of electric charge q over the course of time, which is the I itself. As such, the Q can be expressed as (Eq. (**5**)) below, Q charge transported by I over to set of Δt.

$$Q = \int_0^{\Delta t} I \times dt = \int_0^{Q} \left(\frac{dq}{dt}\right) \times dt \tag{5}$$

Q, as such, can further be expressed in the weight or volume per battery unit as to gravimetric energy density of (Wh/kg) or volumetric energy density of (Wh/L). This is all thanks to the electrical energy E, which is typically referred to in electricity output/consumption as kilowatts per hour (kW·h), which is the result of Q and V as per (Eq. (**6**)).

$$E = Q \times V \tag{6}$$

LIBs have two modes: discharging and charging. Both happen similarly, but vice versa. When charging and discharging any type of LIBs, it is essential to understand that the cathode and anode roles change, with the cathode becoming negative and the anode becoming positive. During the discharging process, the cathode works as a (+) electrode, while the anode works as a (-) electrode. During the charging process, roles are swapped, with the cathode acting as (-) and the anode acting as (+). This allows deintercalation and

intercalation of Li^+ between these two LIB modes to occur, while simultaneously, electrons are moved in between some sort of cable or outside bridge in between the anode and cathode using the two collectors connected to two electrodes separately. The movement of electrons occurs simultaneously with the migration of the Li^+, utilizing the electrolyte as a medium while using the separator as an assisting bridge due to the materials' porosity [13], [34], [47]. Electron movement and interaction within any LIB anode and cathode can simply be written off as (Eq. (**7**)), where α is the insertion material (anode or cathode), e^- is the electron particle, and α - Li^+ is the lithium-ion being inserted into the material of α.

$$Li^+ + e^- + \alpha \leftrightarrow Li - \alpha \tag{7}$$

Discharging occurs when the lithium is being deintercalated, and Li^+ from the negatively (-) charged electrode anode starts to migrate, which means electrons are being released from the current collector that is made of copper (Cu). The movement of the Li^+ and electrons is possible by the fact that the opposite side electrode, positively (+) charged cathode materials are primarily oxides -CAMs per (***2.2.1. The Cathode***) section, and those of anode materials, such as graphite and amorphous carbon compounds -CAMs. Due to the CAMs' properties in both the anode and cathode, Li^+ migration is possible effortlessly from negative to positive. Due to the CAMs' properties in both the anode and cathode, Li^+ migration is possible effortlessly from the negative to the positive. Meanwhile, electrons, thanks to the connection bridge between two collectors, can migrate from the negative Cu to a positive collector made of Al, using the electricity being generated. When it comes to charging mode, the roles of the electrodes are changed, and Li^+ moves from the cathode to the anode and electrons in between Al to Cu [13], [17], [34], [36], [47]. The concept of LIBs and understanding the two modes in them is fascinating and important, as small changes in materials and their structures may impact working principles, as illustrated in (**Figure 5**) LIBs, to some extent, if not wholly.

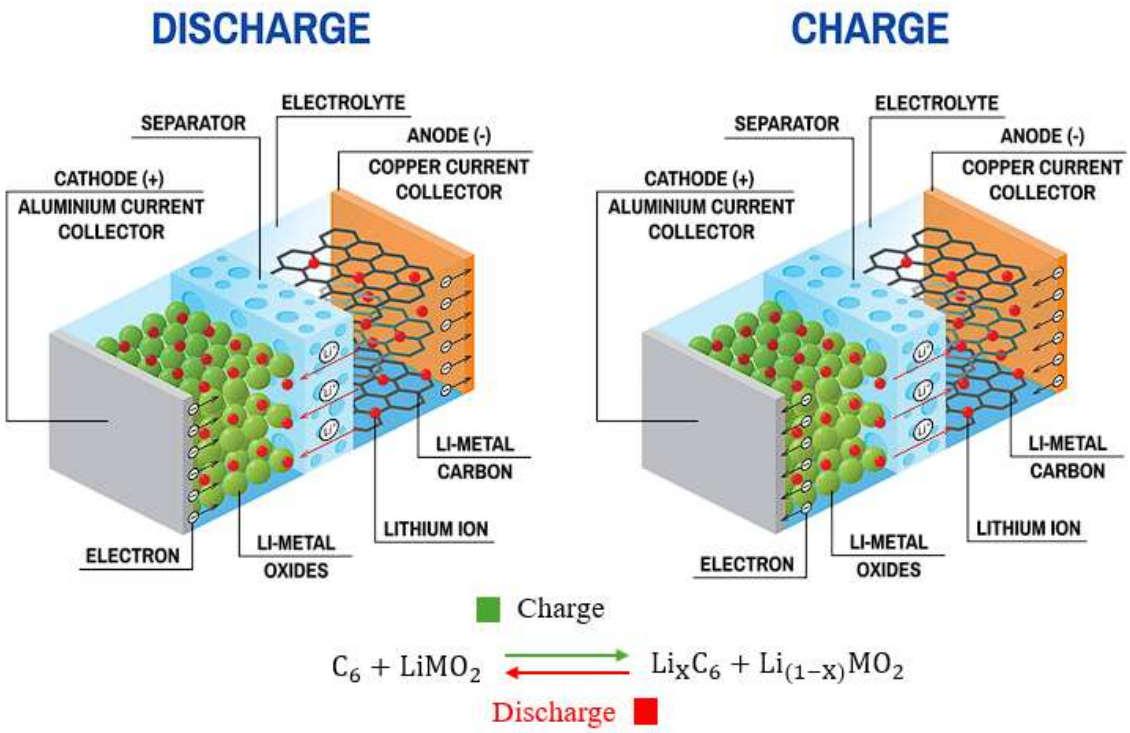

Figure 5. Schematic illustration of the basic components and working principle of a Li^+-Ion battery during charge, consisting of a graphite anode on a Cu current collector and a cathode an Al current collector, an organic electrolyte, and a transition metal, throughout the discharge and charge of LIBs [63].

Reactions that occur in the LIBs between the charging and discharging of the Li^+ are not as simple as one might think. The movement of Li^+, to some extent, is not free and can be attributed to the SEI. As discussed earlier, SEI's main role is to limit further electrolyte decomposition by insulating the electron flow inside of the LIBs by passivating the electrodes and thus preventing reactions with electrolyte, which in return then improves the overall performance cycle of life for the LIBs and performance itself of the LIBs [48], [53]. The reaction that occurs in LIBs is fully attributed to the factors as to which material anode, cathode, and electrolyte are made of, or more specifically, what compound/elemental mixes/combinations they are made of. As such, SEI's formation is intrinsically linked to battery cycling, where during charging Li^+ migrates from cathode to anode through the electrolyte (increasing cell voltage), while discharging returns Li^+ to the cathode (decreasing cell voltage) [54]. The most practical way of looking at reactions can be as follows: $LiMO_2$, where *M* stands for a transition metal, like the (Co, Ni, Mn, etc.), and Gr stands for graphite.

We can then, for instance, look at the full reaction for the LCO, the most common CAM for anode, which would go as follows [64].

Cathode $$\mathrm{Li}M\mathrm{O}_2 \leftrightarrow \mathrm{Li}_{1-x}M\mathrm{O}_2 + x\mathrm{Li}^+ + xe^- \quad (8.1)$$

Anode $$x\mathrm{Li}^+ + xe^- + 6\mathrm{Gr} \underset{\text{discharge}}{\overset{\text{charge}}{\rightleftharpoons}} \mathrm{Li}_x\mathrm{Gr}_6 \quad (8.2)$$

Total $$\mathrm{Li}M\mathrm{O}_2 + 6\mathrm{Gr} \leftrightarrow \mathrm{Li}_x\mathrm{Gr}_6 + \mathrm{Li}_{1-x}M\mathrm{O}_2 \quad (8.3)$$

During the discharge of the cathode as (Eq. (**8.1**)) of LIB, the cathode ($\mathrm{Li}M\mathrm{O}_2$, where M is a metal like Co, Ni, Mn) releases Li^+ and leads to oxidation, hence loss of electrons (e^-). (Eq. (**8.2**)) represents the anode reaction during the LIB's discharge, in which the Li^+ ions and electrons (e^-) are inserted into graphite (Gr), leading to a reduction reaction, which we see as ions and electrons intercalate into graphite, forming the lithium-graphite ($\mathrm{Li}_x\mathrm{Gr}_6$). (Eq. (**8.2**)) summarises the overall reaction of the LIB as it discharges, as the Li migrates from the anode to the cathode, by utilising the electrolyte as a medium. Another reaction of the LCO, Co oxide metal LIB reaction during discharge.

Cathode $$\mathrm{LiCoO}_2 \leftrightarrow \mathrm{Li}_{1-x}\mathrm{CoO}_2 + x\mathrm{Li}^+ + xe^- \quad (9.1)$$

Anode $$x\mathrm{Li}^+ + xe^- + 6\mathrm{Gr} \underset{\text{discharge}}{\overset{\text{charge}}{\rightleftharpoons}} \mathrm{Li}_x\mathrm{Gr}_6 \quad (9.2)$$

LCO total $$\mathrm{LiCoO}_2 + 6\mathrm{Gr} \leftrightarrow \mathrm{Li}_x\mathrm{Gr}_6 + \mathrm{Li}_{1-x}\mathrm{CoO}_2 \quad (9.3)$$

Like in the general LIB discharge reaction process, (Eqs. (**8.1**), (**8.2**) and (**8.2**)), the LCO specific reaction of (Eq. (**9.1**)) of the cathode reaction, where (LiCoO_2) releases Li^+ and e^-, so that oxidation and cathode discharge occur. (Eq. (**9.2**)) is the same as that of (Eq. (**8.2**)) but with the LCO leads to a reduction reaction. (Eq. (**9.3**)) then represents the overall discharge of an LCO battery as per (Eq. (**8.3**)). These are reactions that happen in LIBs during their charging and discharge sequences. In these sequences, Li^+ are reversibly inserted or intercalated into the Gr layers, meaning that during discharge, Li^+ are removed from the Gr and, in charge, vice versa. This is what happens in the (Eq. (**8.2**)) and (Eq. (**9.2**)), as shown above, note that x is generally between 0 and 1 in all reactions [65].

3. Recycling

This chapter explores the evolving landscape of recycling in the context of battery technology, in particular that of LIBs, and its critical role in enabling the current sustainable development and its further progress/trend. The chapter as a whole is separated into four sections and further divided into an additional seven sub-sections, which are part of the bigger picture in a highly complex and still developing drivers leading the recycling principles. The section (***3.1. Recycling definition***) defines the current recycling through legal and technical lenses, contrasting historical and current EU regulations (e.g., 2006 Batteries Directive with the updated 2023 Regulation) to highlight how definitions, targets, and expectations have shifted over the course of time, as battery technology has and does evolve further. Section (***3.2. Recycling concept/methods and models***) then examines various recycling methods and models, focusing on the foundational two sub-sections and their concepts, such as the Waste Hierarchy and the Circular Economy frameworks, both of which guide modern sustainable waste management strategies. By promoting resource efficiency and environmental responsibility, which is attached to them, or is being legislated by the EU legislative body, in addition to different sectoral levels inside the EU. In section (***3.3. Recycling degree of the LIB***), the discussion turns to the actual degree of LIB recycling, shedding light on data inconsistencies, regulatory shortcomings, and geographic disparities in recycling practices across the EU, North America, and Asia. Finally, section (***3.4. Incentives of the LIBs recycling***) outlines five of the sub-sections, with the addition of the economic, political, environmental, and technological incentives driving LIB recycling. While emphasising the global dependence on critical raw materials like cobalt and lithium and the geopolitical implications of their supply chains, with the risk associated with their supply/demand. Leading to implications that do incentivise the need for recycling of LIBs and their needed technological development advancements.

3.1. Recycling definition

Recycling is a process by which a material or waste, in this instance, is reused by converting this material back into reusable material. The EU parliament and its Batteries Directive,

known as (Directive 2006/66/EC), published in 2006 on 6th September, is going to be repealed at some point in 2025 by the new Batteries Regulation. In accordance with Article 3(8) (Directive 2006/66/EC), the recycling term is defined as follows: "*reprocessing in a production process of waste materials for their original purpose or other purposes, but excluding energy recovery*" [66]. The understanding of recycling is simple and straightforward, but the addition of the process into with "recycling process" is the one that should be used and understood. Recycling is a process a whole concept, which starts from the waste batteries themselves as they are received as they are/were. After collecting and subsequently sorting out. Whatever final fraction is left out of this is then used for the battery's original purpose or some other, not specified by Article 3(10) (Directive 2006/66/EC), but without any further treatment, which is defined as: "*means any activity carried out on waste batteries and accumulators after they have been handed over to a facility for sorting, preparation for recycling or preparation for disposal*" [66], [67]. What is interesting in (Directive 2006/66/EC) of 2006, is that the EU Parliament did not define or take into account in recycling or the recycling process the energy consumption, and in what form the energy comes in. Meaning that they did not define whether the materials being recycled in the battery recycling process could be utilized in some way to produce energy during the recycling process. Simply put, energy consumption and generation by using existing materials in the recycling process were not regarded as recycling in any format or way. This may be the reason why (Directive 2006/66/EC) it was stated that the minimum target recycling efficiencies for batteries in (Annexe III, Part B: Recycling), at that time, batteries, with the avoidance of excessive costs. 2006 years requirements were the first type of guidance on the EU level and have ever since been updated once in 2023 by (Regulation (EU) 2023/1542), which amends (The Waste Framework Directive 2008/98/EC and Regulation (EU) 2019/1020) in addition to repealing (Directive 2006/66/EC). In (Regulation (EU) 2023/1542) targets for recycling and efficiencies are updated to new target levels, and an acknowledgment in regards to LIBs is made of form by adding them to the list in comparison to 2006, as their commercialization/need/use in comparison to other type of batteries has skyrocketed ever since. It is noticeable that in the 2023 regulation, the EU is more lenient on the recycling efficiency when it comes to different types of batteries in comparison to that of 2006, as from the requirements, "*recycling of the X content to the highest degree that is technically feasible while avoiding excessive costs*" was removed, where *X* is the primary element of batteries, as Li, lead (Pb), or Ni [66], [68]. Why there is

such an apparent explanatory change is unclear, but it may be due to challenges and recent developments in the recycling of the battery industry. The new target levels are projected to be 2025, 2027, 2030, and 2031, at the end of calendar years, for materials/recycling efficiencies for different types of batteries and the materials used in them [68]. Values and differences in (Directive 2006/66/EC) and (Regulation (EU) 2023/1542) can be seen in (**Table 5**) where the clear importance of lithium in the battery industry can be seen as a rising element/mineral/component on a global level since addition in 2023 and what targets are given for it.

Table 5. Information regarding the recycling and requirements for the efficiency and material recovery of the 2006 years (Directive 2006/66/EC) and 2023 (Regulation (EU) 2023/1542) comparison of Batteries Directives.

Directive & Parameter	Type of battery/mineral	Info	Info	Ref.
Directive 2006/66/EC				
Recycling efficiency		by N/S	–	
	Lead-acid batteries	65 wt.%	–	[66]
	Nickel-Cadmium-based batteries	75 wt.%	–	[66]
	Other waste batteries	50 wt.%	–	[66]
Regulation (EU) 2023/1542				
Recycling efficiency		by 31/12/2025	by 31/12/2030	
	Nickle-based batteries	80 wt.%	N/S	[68]
	Lead-acid batteries	75 wt.%	80 wt.%	[68]
	Lithium-based batteries	65 wt.%	70 wt.%	[68]
	Other waste batteries	50 wt.%	N/S	[68]
Material recovery				
		by 31/12/2027	by 31/12/2031	
	Cobalt (Co)	90%	95%	[68]
	Copper (Cu)	90%	95%	[68]
	Lead (Pb)	90%	95%	[68]
	Nickel (Ni)	90%	95%	[68]
	Lithium (Li)	50%	80%	[68]

The development of the directives and regulations is all the time ongoing process, and as seen from (**Table 5**), when comparing the 2006 and 2023 directives/regulations. The key difference is that of the addition of the material recovery values, with the addition of a clear new type of battery, Li-based batteries or LIBs, with their respective values for recycling efficiency and material recovery values. In comparison to other metals previously being in the 2006 directive, the addition of Li in 2023 shows a clear difference in target or expected values, as those of Li are less than those of Ni or Pb, as they have had more time for their recycling development technologies and strategies alike, having those of ranging

from 80–95 and 75–95, wt.% and % for the Ni and Pb batteries respectively, while values of Li are expected or set currently for those of 50–80 wt.% and %, based on available information of that presented in (**Table 5**).

3.2. Recycling concept/methods and models

The recycling process in LIBs and all types of batteries originates from the reprocessing of waste materials or spent batteries, as described previously. While the (Directive 2006/66/EC) may be of 2006 origin, its roots are older than that. In the directive itself, there is mention of 30th July 1996 on the "*Review of the Community Strategy for Waste Management*", where the guidelines for that time and future Community waste policies were established [67]. From this, it is possible to deduce that the (Directive 2006/66/EC) comes from some sort of Waste Management (WM) order or hierarchy typically associated with it. On 15th July 1975, the first type of directive or framework regarding all types of waste was established (Council Directive 75/442/EEC), which paved the way for the Waste Framework Directive (WFD) as we know it these days. The current WFD in the EU used is (Directive 2008/98/EC) of 2008 and has been updated to the 2024 standards on the 18th of February 2024 [69]. WFD is only one of the many so-called Waste Hierarchy principles and/or models that are crucial in LIBs and battery recycling, with the concept of the Circular Economy (CE), which has been getting traction since 2013 by the Ellen MacArthur Foundation (EMF).

3.2.1. The Waste Hierarchy

The Waste Hierarchy is a method or view to manage and develop Sustainable Waste Management (SWM) strategies as if a philosophy in the EU with a firm foundation since the first introduction in 1975 by utilizing it as a waste policy guidance principle in terms of how to prioritize methods for waste treatment and disposal alike [70], [71]. The simple way to describe this hierarchy is to think of it as consisting of two different entities: 1) the order of priority for WM options, where three are at the minimum needed to be, and 2) their assumed impact on the environment. The origin of this hierarchy started from prioritizing the reduction, recycling, and reuse of all kinds of hazardous waste over any type of disposal or

treatment of theirs [72]. Simply put, the Waste Hierarchy is a method/model to manage End-of-Life (EoL) products and their reduction of getting wasted on landfills across EU territory by defining a rank among the WM actions based on environmental impacts in safeguarding its citizens, which is the issue being of great concern at some point in history [72], [73]. In 2008, with the introduction and implementation of WFD into EU legislation, the true and strict priority order for the Waste Hierarchy was acknowledged and put into use [72]. In 2016, the Waste Hierarchy was also taken for the first time on the topic in the United Nations of ”Agenda 2030” [73]. It is widely acknowledged that the privately owned 3M Company was the first one to adapt and come forth with the Waste Hierarchy in the United States of America (USA) proposed by a Dutch politician, Ad Lansink in 1979 from the EU side, which originated from the Ladder of Lansink and is the cornerstone of waste policy worldwide and strategic pillar of the European WM legislation [73], [74], [75]. The model for the Waste Hierarchy is quite simple, consisting of levels or tiers and multiple steps. The most well-known and acknowledged model is that of the official WFD introduced in 2008, consisting of five different level hierarchies as in (**Figure 6** (**a**)), consisting of ”Prevention”, then ”Preparing for re-use ”Recycling”, ”Recovery” and lastly ”Disposal”. The other hierarchy, even if not used by the EU, is as important and known as the (3Rs) model, consisting of ”Reduce”, then ”Reuse” and ”Recycle” as in (**Figure 6** (**b**)) illustrated. Even if these two models look different from one another, they are both widely used and accepted in situations where they are deemed appropriate [72], [73], [76].

Figure 6. Waste Hierarchy, the tier/layer model as in EU Waste Hierarchy WFD 2008 implementation on the left (a) and the 3R’s model concept on the right (b). Source of (a), Ref. [77].

In the EU WM hierarchy, the desirability, as in (**Figure 6** (**a**)), goes from top to bottom, while in 3R's model, the whole concept revolves around the circular approach when it comes to singular waste, product, or a thing in WM itself. In the Waste Hierarchy, certain levels can and could be interpreted as follows: prevention as reduction, recovery as energy, and disposal as landfill, as in (**Figure 6** (**a**)), illustration on the right side of the hierarchy levels. The importance of all these five levels is evident as they are targets for the EU in WM; as such, the prevention/reduction of waste is one of the most important steps in the hierarchy. The reduction as prevention is driven by demand, but this demand for certain products and materials consists of, and can consist of, either primary materials, known as virgin extraction, and/or secondary materials, known as recycling, reuse, and recovery materials [72]. The reduction of products and materials should be the first step in waste production and management. This is typically achieved by increasing product lifetime by repairing and maintaining the product. In the case of any battery, this is possible and quite feasible on many levels, but concerning their metals and other materials out of which they consist and are combined in the production process, it is well known that bulk materials are generally the most energy-intensive in any form of material conversion processes [76]. The extensive investment into the product design initially can significantly affect any of the Waste Hierarchy levels, as such, but greatly the first three ones [75], [76]. Reuse is a secondary level and a strategy in the WM hierarchy, similar to the 3Rs, in which energy intensity is entirely avoided by implementing a long recycling chain of supply. The product of the material in question is hence used as it is/was intended without any modification, as in the original state when received at the WM start. This implies to the use of products/elements/components as they are not waste but rather as new products/elements/components for the purpose they were made/conceived for initially. [75], [76] After the first two levels and their methods/ideas have been depleted and used up to their maximum/reasonable capacity, the utilization of the recycling level is implemented. Recycling any type of product/elements/components needs and uses an outside source of energy, which needs to be put into the system to recycle somewhere, and at some point, of course, on that level. There are many factors as to when and what can be recycled, but it eventually comes down to multiple factors, such as EoL conditions, the function of materials, and marketing for this non-virgin secondary aspect. All of these are important, but without a cost-effective treatment process itself, all of these factors are as wasted as there are limits to what is acceptable in terms/levels for each one of the factors. [75] When all of the above

levels and their options have been utilized, the least optimal two levels are being implemented, in which the products/elements/components are used as an energy source, from which, if something, then little can be utilized/used for further use and cycle of theirs original or any other purpose. This, of course, is a better option than the last one, where the products/elements/components are just lost to time and are stored as they are, after nothing can be made or they can be used up.

While WM hierarchy and many variations of it in some form, as WFD has shown us that they, are meant to help minimize environmental impacts and natural resource use on a global scale, the perfect framework for WM has never been achieved, as its evolution has been evident and is ongoing as from the (Directive 75/442/EEC) to the (Directive 92/156/EEC) till the current (Directive 2008/98/EC). Whatever the WM hierarchy is and will be in the future, it will all have something in common with the three mentioned above, while it may have one or even a dozen other layers or levels added to it, depending on the need and the usefulness they will provide. If there is one thing that should and needs to be taken into consideration in any type of Waste Hierarchy, it should be the efficiency of the resources [75]. In (Directive 2006/66/EC), the efficiency recovery for certain things is clarified, as they should align with the targets of waste recovery as such. However, with the changing world and values, the efficiency of resources should also be taken into consideration, not just in waste recovery but also in other assets and needs along the long supply chain of waste, such as money, personnel, time, and many others. These all would make and supplement the current and, in many cases, use management hierarchies by viewing them from many different levels.

3.2.2. Circular economy

In the last two decades, the CE concept has gotten traction and been aimed at designing methods/models to perform reductional and subsequently cutting waste and minimizing inputs non-renewable resource use, in contrast to the fundamentals of the LE when comparing CE vs LE, by utilizing the 3R's rule/principles [73], [75], [78]. Much of the current enthusiasm regarding CE looks to be in its approach and promotion of economic growth in line with a sustainable approach in environmental direction, those being the

benefits of Sustainable Development, while imposing and yielding economic development [79], [80]. The need to challenge rising social challenges and the creation of new economies are only part of the driving force behind the current human-driven natural phenomena or necessity, more likely orchestrated by population growth, higher living standards, and automation-enabled mass consumption [81]. Although CE has gained traction for the past two decades, its core ideas already emerged in the 1960s and were further refined and discussed throughout the 1970s [80]. Its roots throughout history have been deeply embedded in ideas that were before the CE concept as we know it these days, and focused primarily on the WM. Over time, this led to a response of depletion and highlighting the diversity of activities and definitions that are within the concept nowadays [78].

While China was the first ones to implement CE as a law, Sweden has been since 1990's forthcoming in green growth-based welfare as a state and implementing legislative means and solving issues coming, by making the state more involved in aiding when it came to environmental problems and navigating the structural concepts those of CE, by structuring consumer markets [78]. These lessons and cases not only in Sweden but also in other places were almost exclusively developed and led by practitioners i.e., policymakers, businesses, business consultants, business associations, and business foundations, which just shows further how CE has been formulated to put that of more emphasis on economics than its other aspects, one could say [79]. Hence, these developments and cases with the studies and practitioners were one of the stepping stones of CE, as in 2008 CE was projected and further precipitated by China implementing first in the World 'Circular Economy Promotion Law of the People's Republic of China), passed on 15th August 2008 and implemented 1st January 2009, and further followed by EU's (First Circular Economy Action Plan), where the 54 actions were implemented and mapped by EU and its EU Member States (MSs) across the EU territory and then were adopted or implemented by the end of 2019. On 11th March 2020, the EU took and approved the newest Circular Economy Action Plan (CEAP), by the (A new Circular Economy Action Plan) or (Document 52020DC0098), that implements 35 action plans for the 2050 year's EU goals and led same year to implementation and revision of landfill tax under the EU Taxonomy Regulation [75], [78], [82], [83].

An incremental twist for a new and more refined energy flow model in a more modern economic system was needed over the years in comparison to that of a Linear Economy (LE) model [79], [84]. Where the model's flow principle is linear extract-produce-

use-dump material and energy or simply “take, make, dispose”, compared to that of CE’s cyclical [79]. LE has pushed the Earth's systems with resource/waste imbalances to resource scarcity and waste crises over the decades [75]. CE’s prioritization of the energy recovery over the landfill option to maximize resource value and energy efficiency throughout the product lifecycle is a core hierarchy of WM, which CE is preserving while adding many other features [79]. What WM lacks in the “end-of-cycle” solution approach, or the CE has been meticulously engineered to do, is incentivizing the circularity and valorizing EoL of the materials, WH’s that of (**Figure 6** (**a**)) the pyramid’s last/bottom stage [81]. These issues plagued LE and WM, with many needs, promises, and results delivered by CE to sustainability, in contrast to the latter, which emphasized resource efficiency policies and business actions at different sector levels (e.g., Eco-Design or Extended Producer Responsibility) to outcompete LE in the socio-economic system. What makes CE different is its portrayal as a powerful metaphor that breaks the barriers and limits of silo thinking, engages companies, and provides economic benefits to various stakeholders and parties, being engaged in CE at different levels [85].

The road of the CE has been framed as a novel circular flow and economic system based on the business model that focuses on emphasizing increasing employment and sustaining business competitiveness via the technological and environmental aspects of cleaner design, business models, and industrial symbiosis [78], [80]. These are then further emphasized by product, component, and material reuse while their maximization, remanufacturing, refurbishment, repair, cascading, and upgrading while increasing and putting emphasis on the integration of renewable and more sustainable energy sources throughout the product value chain and cradle-to-cradle life cycle of the material utilization and life cycle’s maximization [79], [81], [86], [87]. These are CE’s strong points in addition to the concept's capability to adapt to unlimited possibilities in R-based principal forms of recycling, ranging from the 3Rs, 4Rs, up to 9Rs (ii) [75]. Similar to that of the Waste Hierarchy philosophy, CE improves the resource effectiveness of its production to reduce and averse the generational impact of the waste [75]. This, in part, is the primary core of the CE, to implement secondary production while stimulating economic growth and outperforming the mentality of the primary production of the older LE model in the long term. The model that stimulates economic growth while minimizing environmental harm and damage has led to the “Win-Win” catchphrase or narrative within the CE and those who

use it [86], [87]. On paper, these things look amazing, but one cannot help but remember that while CE thrives and societies are seeing unprecedented economic growth, it comes with the cost of finite resources dwindling in quantity, quality, and accessibility, with mounting waste, and worsening emissions and environmental impacts [81]. CE does not only bring help in the progression and development of sustainability and WM alike, but it brings tools while being itself a tool like or strategy**,** which can and is to integrate Life Cycle Assessments (LCA) and business models into discussions on social inequality, policy harmonization, and global trade to advance Sustainable Development through surrounding the three pillars of environmental, economic and social development's [85], [86]. As traction behind CE ramps up, it could be argued that instead of being a tool or strategy, CE works more like an "economic system" and replaces the "EoL" concept while promoting what CE stands for [86]. But on the other hand, CE works also as a condition for reaching sustainability, and hence these two work and can be seen as a relationship that is necessary for them to work [84].

CE's pre-existing narrative, in comparison to that of LE, is balancing between prioritization of the global market competitiveness while being within planetary ecological boundaries and as stated, "*protecting human health*" [73], [78]. CE seeks to minimize and put stress on the virgin resource extraction by closing material loops, by reducing waste, extending product lifespans by reusing and recycling materials in production/distribution and consumption processes as to allow turning wastes into valuable resources, increasing renewable energy sources to achieve and fulfil Sustainable Development, which implies creating environmental quality, economic prosperity and social equity, while preserving the core strategy of "loop-closing" and resource efficiency that of the CE, benefitting current and future generations alike [75], [79], [80], [81], [86]. This core foundational idea of the CE, based on its circularity, is rooted in the belief that a closed-loop system can be achieved by perpetually reusing, repairing, remanufacturing, refurbishing, repurposing, recycling, and/or recovering all materials produced throughout the product's lifespan [73], [88], [89]. Leading to the elimination of waste and keeping resources in continuous use or closed loop, as we know it now, has been illustrated by the EU and EMF as of (**Figure 7**) schematic [88], [89]. CE's schematic also highlights the goal of efficient use of natural resources by binding it to the importance of technology and design of CE. This mentality has led to the development of various innovations in designs and technologies, resulting in improved

efficiency in multiple ways. These different technological concepts then led to the creation and materialization of the blockchains, which then led to CE business model developments and extended material lifetimes, such as Industry 4.0 and technologies alike [89].

Figure 7. Schematic presentation of principles of the Circular Economy, which corresponds to that provided and accepted by the EU Parliament and its Research Service/Division [90].

The CE has become one of the most inspirational and widely embraced sustainability concepts, capturing the interest and dedication of academics, businesses, non-governmental organizations (NGOs), and governments globally over the course it is of its time, but most notably since 2015 [85]. Unlike many other sustainability ideas, CE has uniquely motivated collective action and innovation across different sectors, ranging from the Macro (e.g., policy changes on national, legal systems and regional levels, referring to ones like EU, nations, cities and beyond them), Meso (e.g., industrial networks and symbiosis between

companies), and Micro (e.g., companies, products and citizens as consumers, referring to them and their impact on one another and other sectors) [81], [85], [86], [91]. CE's fundamental purpose, consequently, is in the creation of environmental quality, economic prosperity, and social equity. Because of CE's nature, its primary focus is to benefit the current generation in the short or long term, while also emphasizing the future generation, which is core and fundamental to CE [86]. As CE needs the multisector collaboration, it reshapes how they interact with each other, as they then influence barriers in them like those of culture → regulation, → markets, → technology, which in turn shape the next and one another as new solutions and implementations are adopted [80]. Out of these four barriers, culture has been identified by literature and studies as being the most significant constraint for the CE [81]. Hence, the transition to a CE depends on collaboration among diverse stakeholders, including employees (especially managers), customers, governments, supply chain partners, and innovative ecosystems. Some scholars emphasize the consumer's role in driving bottom-up change by adopting circular innovations and pro-environmental behaviors. Others highlight the state's importance in regulating standards, introducing certifications and eco-labels, and creating market incentives to guide business and technological development [89].

The economic growth and opportunities provided by CE were and are immense, while the narrative of "Win-Win", in light of the promise of environmental sustainability, led to development and more preferred business model approaches, such as those of Corporate Sustainability (CS). CS's position, in relation to that of CE, is its business-friendly strategy, which is aligned with profit motives connected to sustainability (e.g., preserving material value and lowering costs through recycling). This "business case" has framed and encouraged corporate adoption by emphasizing the efficiency and competitiveness of CE by the CS, which is further highlighted by business and economics studies/papers [89]. CS allows and supports CE by providing stakeholders, both internal and external, with a description of their sustainability strategies and practices through meetings and reports. The role of the CS is detrimental for the companies currently, as CS reports play an important legitimacy role as communication tools, to justify and show their operational legitimacy by aligning practices with stakeholder sustainability expectations [84].

What enables and helps CE to thrive and develop even further is the crucial role of social processes and stakeholder participation in advancing sustainable CE development.

This development is fueled by the inclusion of the diverse local stakeholders, primarily by the Macro and Miso level stakeholders, to ensure comprehensive, equitable, and contextually relevant solutions for the CE and its aspects that come in addition to it. This, in turn, leads to the Meso level of collaboration and co-creation of the CE by strengthening its sustainability, social acceptance, and practices coming from CE for the long term [85]. EU's funded projects and collaborations (e.g., HORIZON 2020 and LIFE 2014-2020) as in (Document 52017DC0033), between different sectors one of the important stepping stones in CE's development and advancement further and bringing innovation to the table for all stakeholders to use and future generations [75], [81]. The (Document 52020DC0098) underlines the well-written points above by its commitment to accelerating the green transition, and hence CE's by financing and integrating CE into the EU Taxonomy Regulation.

Despite the optimistic narrative's focus on policies, many lessons still highlight the need for new business models, data, and technology to deploy sustainable models and practices via CE and tools alike [85]. While CE as a concept is not a new one and has been in various forms and come from different approaches, it has also led to its critique and obscurity, as the concept needs and must be deployed equally by stakeholders and sectors, using or discussing the CE context.

3.2.2.1. Critique and obscurity of the CE's

While CE is characterized by many papers and scholars as something to be used as/a tool for sustainability and WM. In many cases, it is not, but as a "one-size-fits-all" solution to systemic challenges (e.g., climate change, biodiversity loss). While CE is great at offering tools for monitoring and characterizing resource efficiency, it may not address deeper issues, such as overconsumption, social inequity, or the need for systemic regulatory/policy shifts. [89] Although many accounts of CE are mainly positive, there is room for criticism, which challenges its core assumptions, social equity implications, and actual environmental benefits. These are the results of the arguments that stem from the question of what if the CE does not deliver on its promises without addressing systemic issues, which derive from the CE's foundational principles of socio-economic equity and ecological effectiveness [78],

[89]. Systemic challenges that are present in many of the systems into which CE can be incorporated, coming from the WM, Research, and Development (R&D), and the resource extraction processes are scalability, resource constraints, and unintended consequences, which may entail accidentally from these [78]. Nevertheless, the CE's potential is immeasurable in many sectors and likewise in the LIBs industry from a development and recycling standpoint.

The circular economy offers significant benefits and has enhanced many business models by providing better process characterization. However, the transition to a CE cannot be approached solely from a firm-centric perspective. This means that the CE should be placed under systemic governance, thereby making business model innovation one of the many levers. This is important, as the putting emphasis and then even overemphasis on the business model transformation as the primary driver of systemic change may/will lead to more of prevalent in prognostic framing, which in contrast will affect how the solution is proposed, with addition to risks overlooking the multi-actor, multi-level nature of economic systems. [89]

Because of the CE's nature and complexity, its terminology and content in different contexts have led to sharply divided opinions among scholars primarily, but also between ordinary businessmen and companies alike, through trials and errors, which have led to the questioning of the CE's regarding its feasibility and impacts [85]. Across many dimensions/sectors, there are, in addition to the obstacle of creating policy-relevant CE knowledge, creating a real paradigm. The assessments vary widely across technical, socio-economic, environmental, and regulatory dimensions, reflecting both their promise and potential pitfalls [84], [85]. Due to these technicalities and interpretations of the CE, depending on who asked, there appears to be an existing consensus and ambiguity on the topic of CE, which therefore leads to either a transformative solution or an overly ambitious challenge [85]. These ambiguities present a problem when one tries to promote the CE idea or ideas as a tool in achieving Sustainable Development, which in the process itself as a concept has conceptual vagueness, while myriads of definitions [86]. While this ambiguity of the CE leads to several interpretations, it results in differing assessments of the terminology and a lack of shared direction among stakeholders, while simultaneously helping to explain the widely diverging perspectives on its potential and challenges within academia, businesses, and policies alike. These interpretations and diverse perspectives from

different stakeholders lead in the end CE's to fragmented research agendas, inconsistent implementations, a lack of unified direction, and conflicting assessments, while at the same time reversing these effects, bringing both challenges and an opportunity alike inside the concept. This has been somewhat helpful and opportunistic for individuals who have served as "issue entrepreneurs", driving the CE from the concept's inception to the present day. Thanks to the complexity and factors driving assessments, which can lead to the misinterpretation of core concepts, resulting in differential results and factors in the data and research questions, as well as policy implementations from both legislative and scholarly perspectives. [85]

Some scholars and papers argue that business case thinking and assumption views have a high degree of dominance in CE cases, which may hinder optimal yield outcomes for the environment or a company alike. This has led to less discussion and disclosure within the business case regarding potential trade-offs, tensions, and paradoxical situations. [89] Things like these then have and do lead to uncertainty and varying inside of the companies and business models to implement changes due to "lack of data, (e.g., of impacts)", which leads to a learning curve inside them, and hence to sort of chain reaction of, "first invest and learn, while losing time, money and precious resources, while others watch, and earn a fortune, from the lessons of others" → leading to waiting game in between actors and stakeholders as described by research, "*hesitant company culture*" [80]. Things like these and mentality have led to studies and cases showing that approaches like these and CE initiatives inside of the companies would and will yield negative economic benefits and, on the contrary, increase the costs and exposure to the trade-offs, which CE as a tool initially was made to decrease and avoid [89]. Furthermore, this just shows that CE research lacks cohesive direction, with studies often siloed in narrow domains, such as industrial processes, business models, or policy governance, rather than being integrated into a holistic framework or some bigger picture encased in CE. Because of findings and real-life case studies, the CE's fragmentation underscores the need for more systematic and interdisciplinary approaches to address the complexities and trade-offs of CE [85]. These, then, as research has noted, can be attributed to the lack of "*smart regulation*" and "*supportive policy frameworks*" leading to a lack of policies that support CE transition [80]. Hence, the role of business models or of any sort, business case thinking, stakeholder relationships, and the CS in between the CE, as a whole, should be better characterized and taken into consideration when making changes to any sort of process or business model. Hence, there should be more

elaborate mediators and moderators between the CS and CE relationship to minimize and lower the tension in these two [89].

What has been concluded over time of CE via analyses, lessons, and research is the emphasis on the need for stronger policy steering of the CE by requiring stronger policy intervention and prioritizing political action over purely economic or technical solutions. These were more and still are somewhat in contrast with the EU's prevailing narrative, which frames CE advancement as primarily driven by market forces and economic incentives, as some studies have also shown to do [82], [85]. Nonetheless, for the past years, the EU has changed and put more emphasis on the prioritization of resource efficiency, reuse, and recycling [85]. This shows somewhat the EU's policy versus market-driven views and the EU's institutional stance, which then leads and results in unnecessary tensions. Hence, the CE's success, in contrast, hinges on recognizing governance as a core driver, not just as an enabler, which leads to the EU's ambitious circularity goals, which may be disappointing. Many of these are then related to those of the EU's Waste Hierarchy priority order, where the minimum and maximum levels for recycling rates and landfilling threshold are presented and monitored by the European Environment Agency and other subsidiary actors to ensure CE's smooth transition and course correctness [73].

Over time, CE has shown not only in scholars, academics, politicians, business holders, and other stakeholders, is that of clear debate in the literature between the idealistic visions of full loop-closure, where CE's ability to achieve this gap over time is envisioned to that of pragmatic approaches, where the CE is nothing more than a more sustainable model to that of LE, with optimal (rather than maximal) circularity of loop closing [86]. These have been noted and, in many instances, incorporated into CE, which is fundamental thinking that CE can and could be used as a "closed loop" and then brought into context to the root metaphor assumption, which includes circularity and industrial relationships resembling biological metabolisms. These are then further reinforced by the belief that the loop is perfect and would lead to not needing anything outside of the loop, such as a significant reduction in the need for virgin materials. [89] This would hence lead to CE as a concept being thermodynamically naïve or, more precisely, its 2nd Law, with rebound effects often undermining its environmental benefits [78]. Naiveness is even further demonstrated by CE's definition and its closed loop, as alternatively the energy simply cannot transcend and be recycled but only cascaded, hence CE will always create waste and side-products due to

increasing entropy, as per the 2nd Law [79], [86], [92]. Therefore, closed material loops are practically and theoretically impossible, which can mislead and ultimately lead to the simplification of the CE terminology known [79]. What may not be discussed, studied, or cased is that the balance of the CE across what it stands for may ultimately be its worst nightmare when it comes to a closed loop, as the global economy's physical scale can and/or cause unsustainable depletion, pollution, and waste. At the same time, CE enjoys its "unchecked growth". CE, therefore, would not differ from the LE, which it was made to combat and replace, as the same problems/impacts of LE would only be delayed and postponed for the future and its generations, in contrast to that what the current stakeholder would/will yield from the CE at its implementation date if done. [86]

While CE is credited for improving the economy through sustainability, the criticism and gaps in its long-term "after-effects" on material flows are not well studied, and these gaps are relatively extensive. By prolonging the lifespans of materials and products, CE may also inadvertently create unsustainable systems and jeopardize long-term sustainability. Effects of CE for that reason may subsequently affect future decision-making and models that may come forth, as they will inherit the problems left by the CE as degradation, albeit at a slower temporal rate [86]. This begs two questions: (1) *What evidence proves CE's superiority to current linear models?* (2) *How can rebound effects be conclusively avoided?*

Flexibility is one of the many aspects that make CE a valuable tool in various models and cases alike when serving as a convening narrative, yet it is also so vague that it risks political capture, potentially undermining its normative value [78]. Furthermore, it has been criticized for not achieving a comprehensive CE research agenda or for not being close to it. CE research and agendas need to link technical, environmental, and managerial types of research, emphasizing the social costs alongside the benefits, socio-economic disparities, and interdependencies, as well as policy design and harmonization. Only then can the CE research and results achieve what has been characterized as "*systemic*," "*holistic*", or "*cross-sectoral*" in searching and completing the complex challenges effectively under the CE. [85] Because the narrative and focus of CE is more on economics, the advancements in social equity have been minimal when compared to other aspects that CE stands for and was intended to deliver to its stakeholders. Human rights and social justice are two important concepts within the "social dimensions". But for some reason, studies, literature, and case studies do show a limited focus on this. Of course, CE's promises contribute to the

development of the “job creation”, which is one of its cornerstone promises behind the CE. Job creation as one of the social equities is not enough, as inequality and equity between the global North and South are evident [86]. Hence, one could argue whether the CE is a suitable tool for addressing social equity questions and providing answers to them as actions are being implemented, or indicators to monitor these, such as the Gross Domestic Product (GDP), while at the same time being a tool for Sustainable Development. *Thus, how can a CE measure the social benefits it is meant to produce?* Adding to these problems, it has been noted that there is a clear lack of reviews that explicitly analyze how the CE can advance Sustainable Development [86].

While corporations and corporate actors may embrace circularity, if aligned with their market interests and global economic demand, it has simultaneously been used to deceive and mislead various sectors' stakeholders from Macro to Meso, as a “greenwashing tool” [78], [84]. This tool enables actors to maintain a green image globally, despite local controversies and conflicts (e.g., Shell Greenwashing Scandal), which have been uncovered in recent years regarding their “carbon credit” scheme. Cases like this suggest that CE should be seen as systemic innovation, not merely as a tweak to the status quo [80]. Instances like the above are among the reasons for criticism of CE, as the concept itself distracts from “key” and “more” important issues like equity, neglects social implications, and depoliticises sustainability. Others contend it is an illusion that fails to address economic growth itself. Hence, there is a noticeable gap that remains in financing the circular transition, which is often overlooked by simplistic claims that waste reduction alone will yield savings and new market opportunities. [80] However, to achieve such outcomes, CE would require all stakeholders to be integrated fairly and close to their optimal value needed to realize CE. Nevertheless, there appear to be issues and weaknesses with the current CE when implementing Sustainable Development and pursuing similar models of understanding. Thus, advancements in CE necessitate full collaboration among key fields like ecological economics, industrial ecology, and cleaner production, alongside newer disciplines like “behavioural economics”. What emerges from this is a clear need for cross-disciplinary teamwork amongst all actors to develop CE whilst simultaneously meeting the Sustainable Development criteria. [86] These would lead to improved relationship management and implementation between various actions and their respective target values [73].

3.3. Recycling degree of the LIB

As the world moves towards cleaner energy sourcing, the demand for renewable energy storage systems and the heavy transition towards electrical transportation electrification will further increase the need for LIBs and battery technology in the future [93]. All of these lead to the importance of reorganization actions that need to be implemented, which CE has been tasked with. The increasing demand for LIBs needed materials has led to waste streams of unprecedented levels, but at the same time highlights the need for LCA, when it comes to the disposal of these hazardous wastes in landfills, for the single most important commodity of this decade [86], [93]. Globally, the amount of discharged spent LIBs currently being recycled is only 5%, meaning that an astonishing 95% are being landfilled, which CE, Waste Hierarchy, WM, and Sustainable Development have categorized as the "last resort" [94]. This means that over the past decade, although technology and awareness of the need to go greener and support/stay within Earth's boundaries throughout countless directives and agreements ranging from Macro to Micro levels, LIBs' recycling values are stuck at those of the year 2016 values [95]. *However, are the values of 5% and 95% actually correct, given that they have remained unchanged for almost the entire decade?* Hans Eric Melin, as the 2025 Managing Director at Circular Energy Storage, has conducted research and reached conclusions, along with other researchers, that the actual value for 2019 could have been as high as 59% for LIBs recycling [95]. The rate of 59% in 2019 appears to be a number in the correct direction, but while one study reports such values, there are many more studies before and after 2019 that also report similar values of 5% and 95%. Even media outlets such as The Guardian and The BBC have circulated those values. As to where these values come from, it is also a bit greyish, as (Heelan et al. [95]) "*95% of Li-ion batteries are landfilled*", which was calculated. However, the paper does mention that in the EU, the LIB recycling rate is 9%, but the mention of 5% is not found, which is often cited in many papers and even credible outlets [95]. Due to these, the actual "recycling % value" is honestly more like that of unknown (UNK) origin.

But has the damage already been done, as the source for projects and research heavily relies on other research and findings, and the values that have been circulated for the past decade show a somewhat blind and not-to-question validity approach? The spread of false or that known to be at least questionable information for so long. This aligns with

the critique of that CE, as it could have led to prioritizing multiple sector levels incorrectly and further influenced those at the Macro to Micro levels. Examples of what this could look like could be those delays in the development of policies supporting EVs, and then consumers' hesitation in supporting/change from fuel-fed engines that are more affordable as the value to eco-friendly so-called is not achieved or the impact to sustainability is minimal if at all, in light of values.

On the European continent, the organizations or entities that govern the LIBs industry throughout its EoL, from the start to end, consist of the European Commission (EC), European Battery Alliance (EBA), Association of European Automotive and Industrial Battery Manufacturers (EUROBAT), European Parliament (EP), The European Battery Recycling Association (EBRA), Batteries Europe and European Lithium Institute (eLi). As to EP's briefing for the EU Legislation in Progress in September 2024, which acknowledges that the global battery demand is to increase 14-fold by the end of 2023, and out of this, 17% is expected to happen on EU soil and the battery market could be of 250 billion euros worth "a year" by 2025. [96] As per (**Table 4**), the EU has set over the course of the year different values for material as recycling efficiencies for the batteries, as well as for LIBs. By (**Table 5**) the current set of values given for recycling efficiency for Li-based batteries would be 65% by the end of 2025, while for the material recovery, 50% by the end of 2027. Although these values are given, it is unclear whether they are being achieved or are achievable, as they may be too ambitious, as CE has been attributed to. In 2022, Eurostat published data on the EU website indicating that around 46.38% of all the portable batteries and accumulators sold in the EU were collected for recycling. Out of the EU27 countries and Norway represented, Croatia had the highest rate at 68.3%, while Finland had the lowest rate at 51.5%. [97] This type of data, although important, is somewhat complex and also misleading, as it takes into account how many batteries were sold and how many of those were then collected for recycling. This does not even mean that they were recycled, as what is being said is "for recycling", meaning that those were collected, but whether they were recycled is not clarified, which leads to further ambiguity in this case. This type of ambiguity is then even further shown by their explanation of how data was calculated in by (European Commission., [97]): "*Collection rates are calculated based on the sales data in Table 1a and the collection data in Table 1b, as a ratio of the weight of the collected batteries in a reference year divided by the average of the weight of the batteries sold during the reference*

year and the previous two years.", where no mention of recycling is found at all. What is clear from the Eurostat data is that compared to the 2009 collection per (tonne) and sales per (tonne) in comparison to those of 2022 had increased 2.22 times and 1.38 representatively, which can be seen from (**Figure 8**) Eurostat's data. While the report of Eurostat is comprehensive, it does show lots of questions about how specific data is being collected and then shown, but what is even further questionable is the complete lack of mention of LIBs or Li at all. The report covers lead- and nickel-based batteries, as well as other types of batteries, while overlooking the current state of the economy, which requires LIBs and their recycling data. The importance of understanding more data and how it is collected and presented increases, as Europe's current LIB recycling capacity ranges from ~54,200 to 81,500 tonnes annually, as presented in September 2021. [98] Although in paper capacity was presented to that of LIBs, the technology and battery consumption/need in the EU are rapidly increasing, does shows that the EU is not ready for the capacity of batteries that will need to be recycled, which is also quite evident from the collection and sales differences of batteries based on (**Figure 8**). As a matter of fact, the EoL of LIBs will also play a crucial role in the next 10 or 15 years, the need for larger recycling plants and optimized processes will be seen, as the life span of a typical LIB is around 2 to 10 years, depending on their battery type [98]. Whether the EU is ready for this remains to be quite an interesting aspect.

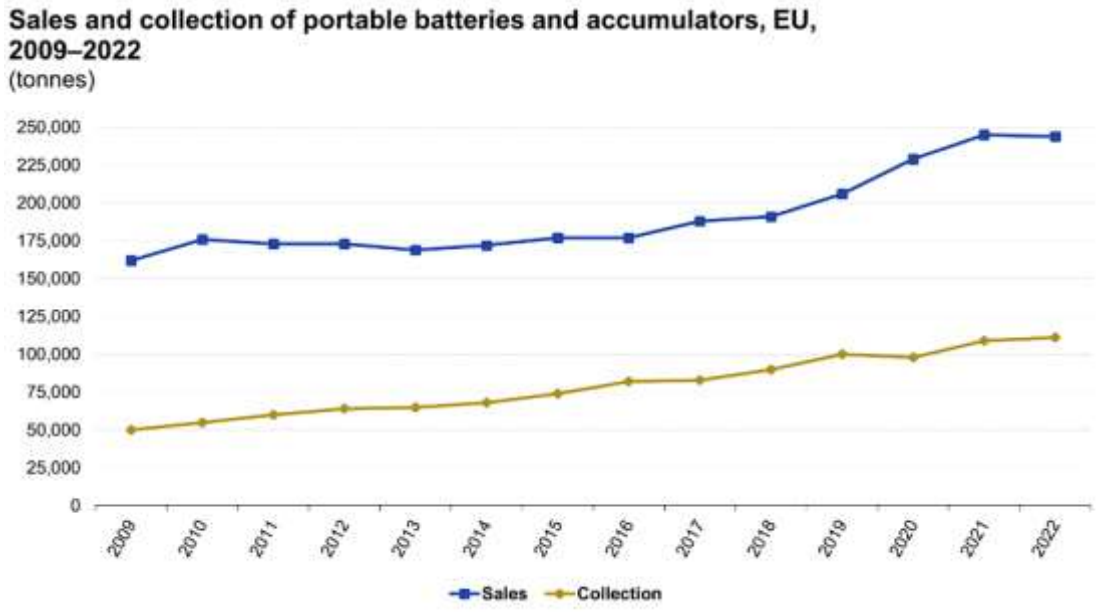

Figure 8. Data on Sales and collection of portable batteries and accumulators, European Union, 2009–2022 (tonnes) [97].

On the other side of the continent, the North American (NA) organizations or entities that govern the LIBs industry throughout its EoL, from start to the end, consist of governmental and/or federal agencies such as the Department of Energy (DOE), Department of Transportation (DOT), Occupational Safety and Health Administration (OSHA), Consumer Product Safety Commission (CPSC) and EPA in addition to those of Trade Associations and Industry Groups, and other organizations, like Call2Recycle, Institute of Scrap Recycling Industries (ISRI), Solid Waste Association of North America (SWANA), The Trade Association for Advanced Battery Technology in North America (NAATBatt) and, etc. The difference between the EU and NA is that although NA has more agencies and organizations, which are relatively easy to find. The EU comprises 27 separate countries, collectively referred to as EU27, which all have their own agencies and organizations in addition to those united under the EU. NAATBatt's informational collection of "lithium recycling laws" brings clarity to consumers in navigating these complex regulations in NA, using the link to the Call2Recycle website's recycling laws by states shows an apparent disparity in regulations for batteries and LIBs recycling alike on the state and producer level, and shows somewhat issues in enforcement and obligatory, compared that on EU. [99], [100] Of 50 states in the United States (US), only 21 (Puerto Rico is not a state, but is accounted as one) have some sort of state battery recycling requirements, while 12 (Washington DC is not a state, but is accounted as one) have producers offer or fund battery recycling directly, while the other 19 states have no requirements, based on the data [99]. It has been estimated that by 2025, the capacity of battery recycling will increase to 17,650 tonnes in North America alone, which would account for 4.5% of the World's capacity at that time [101]. In 2023, the US Pb battery industry alone employed 28,350 jobs directly, out of which 3,040 were in Pb battery recycling, accounting for only 10.7% of the Pb industry [102]. As in the EU's LIBs recycling, the lack of information and data is evident on the part of NA and US alike, which is further strengthened by the same data of only ~5% LIBs being recycled in the US, but while lead-based batteries do achieve a 99% recycling rate, which then yields over 80% mass of the new Pb battery when used in their manufacturing [102], [103].

In 2024, China held a total market share of 55% in LIBs in the Asia-Pacific region, followed by other countries such as Japan, South Korea, and India [104]. Approximately 70% of LIBs in Asia are collected, which is a result of the high concentration of the LIBs manufacturing industry, which, over time, has led to the promotion and high development

of the recycling industry [25]. In 2018, China and South Korea had recycling volumes of over 69% and 19%, respectively, totalling 88% of the global recycling volume, compared to the rest of the World at that time [105]. An estimated 250,000 tonnes of LIB waste were generated in 2020 by China, highlighting the disparity between production and recycling capacity, as also observed in the EU [106]. In 2023, statistics by China's Ministry of Public Security and the China Charging Alliance showed the registration and sale of new energy vehicles (NEVs) that year at 20.41 million units, which shows the rapid expansion and increase in NEVs in China, but also shows the trend across the World alike [107]. By 2020, it was estimated that around 80% of EV batteries on the Chinese market were those of LIBs. By increasing the EoL of EVs in China, which, by estimates, suggested that almost 70% of EVs on the Chinese market would have been second-hand, leading to 70% of LIBs flowing into the informal recycling route as of today. [108]

3.4. Incentives of the LIBs recycling

The rapid demand for LIBs, fueled by the insane growth of EVs, consumer electronics, and the need for new energy storage solutions, in the renewable sector, has led to intense production of LIBs globally alike. However, the increasing volume of spent LIBs poses environmental and economic challenges, as the recycling/processing capacity lags behind that of production, as the first wave of LIBs at the EoL starts to flood this capacity. This chapter explores in different ways that are the key incentives for LIB recycling, including:

- Economic,
- Political,
- Environmental,
- Technological [109].

All these four incentives are only part of many others that exist, but they are all intertwined with one another, some more and less than others. LIB recycling not only needs incentives but is also fueled with opportunities from across Macro to the Miso level. LIBs consist of a wide array of elements or metals to speak of, which need to be unearthed and often occur on the borders of countries and continents, leading to political involvement. The dispersion and concentration of these then even further affect the LIB industry, as they need

to be transported to countries that have the technology and capital to refine them and subsequently assemble them into LIBs. As CE's part in shaping the EU's LIB industry and recycling develops. So do the LIBs and spent LIBs' impact on the environment continue being shaped, as more of them are being recycled annually, so do their hazardous waste risks also diminish.

As the demand for lithium to fuel greener energy increases, the usage of Li-metal surged to 87% of the total Li-metal demand in batteries globally in 2023 [110]. This has led Li to be categorized into Critical Raw Materials (CRM) as of 2020 in the fourth list of CRMs by EU (Document 52020DC0474) as one of the critical minerals or "critical metals" defined as metals essential for clean energy infrastructure and technologies, to ensure nation's or region's economic stability, with acknowledged vulnerable supply chains, due geological scarcity and/or geopolitical tensions [111], [112]. The EU and other countries have noted that the need for these CRMs is essential for the future energy sector. Consequently, on 23rd May 2024, the EU enacted its Critical Raw Materials Act (CRM Act). LIBs' most important metal elements are Gr, Co, Li, Ni, Mn, and Al [113]. All of these elements are listed in the new 2024 CRM Act (ANNEX I & II) (Document 32024R1252), which contains 17 strategic raw materials and 34 critical raw materials, respectively [114]. Currently, critical metals enabling the energy transition face supply constraints and their limits, lack viable substitutes in industrial applications, and remain economically unrecyclable at scale [112].

3.4.1. Cobalt

Cobalt is one of the most important components of the LIBs, having an estimated 25 million metric tons (Mts) globally resources (estimated values for the minerals/metals, these are called "resources") estimated by the US Geological Survey and that of 11 million Mts reserves (minerals/metals that can be technologically and economically mined are called "reserves") in different countries where mining operations are happening currently, Co ranks as 32nd abundant metal globally [115]. Although Co is important in the sense of the LIB essential working principle in enhancing the energy density of those cathodes, but Li essentiality is what makes the LIB working principle possible by allowing Li^+ to move between the electrodes. Around 68 vol.% of all the Co reserves are geolocated in the

Democratic Republic of Congo (DRC) on its central African ”copper belt” and the other 7.3 vol.% in Indonesia, based on that (**Table 6**), making DRC one of the heavy and sought-after mining regions in the world and from the mining companies' perspective alike. While Co demand has increased over the past decade, the mining of Co itself is not a primary product but rather a by-product of Cu and Ni mining, resulting in the mining of cobalt-oxidized rich ore [116]. Around 35% of Co is mined as a result of Ni mining, and 55% of Cu mining, resulting in ~90% of Co mined as a by-product, but some papers do put values as high as 95% due to Co’s low concentration in Ni and Cu ores alike [117], [118]. As a by-product of Ni and Cu mining, the production of Co remains vulnerable to output reductions due to these primary metals, meaning that the global supply chain could be at risk. In the DRC, mainly international companies of Western and Chinese origin operate and are responsible for the mining [119]. As a matter of fact, the Chinese ”Going Out Strategy” since 1999 has aimed to attract and increase foreign investment and secure critical minerals, with a focus on African and Asian sources [120]. This has led to 15 out of 19 cobalt-producing mines in the DRC being under the control of either private or state-owned Chinese companies, with alarming numbers, including around 70% Cu and 50% Co, of all mines operated by them [119]. The majority of the mined Co in the DRC is then primarily imported to mainland China, with some additional supply coming from Indonesia, which exports its main supply to China; these two supply streams are then further refined [115], [120]. Indonesia, as a secondary supply partner of China, is important, as due to the DRC country’s instability and volatility necessitate a secondary supply. This enables China to remain a leading country in co-refining, which includes battery-grade Co [115], [119],]120]. While the Swiss-owned Glencore mining company may have been a major miner in DRC, its presence to this day is significant with the addition of the 2021 Canadian Ivanhoe Mines company in Kamoa-Kakula, as Chinese investors pour money by buying or financing mines as Tenke Furungume, Kinsenda, and Sicomines alike and other infrastructure [120], [121]. Mining Co in CDR but also in Africa overall has been under heavy scrutiny due to the ethics behind mining, as known cases of child labor, and political instability (as in 2024–2025, Rwanda-backed rebel M23 captured and initiated havoc in several cities across CDR regions) with unsafe mining practices have led to outrageous environmental issues and impacts that are in some cases irreversible by large already, which are fueled by multinational investments and international mining companies violating international law not to mention CDR’s, strengthened by corruption and allowing straight exploitation of CDR and its people [119],

[120], [122], [123], [124]. These are pressing matters, as indicated in the 2024 estimation (**Table 6**), which showed that while CDR and Indonesia combined account for 75.3 vol.% of all Co reserves, CDR's mining operations alone yielded 83.1% of the Co mined globally, with Indonesia accounting for 10.6%. This means that their mining operations accounted for 93.7% of the Co mined globally in 2024 alone. Mining for Co is clearly under the energy-intensive and sustainable supply chain risk, as almost the entirety of mining operations is carried out by two countries [122], [123]. This is even further displayed by the data comparison of Cu mining operations globally, as CDR mining constitutes ~14.3% of total Cu mined globally, lagging behind Chile's ~23%, indicating the reliance of Co mining operations in DRC, as ~83.1% Co is mined in there, and thus showing its strategic importance globally as Co availability lies on the political stability of CDR [115], [123]. As electrification and energy storage capacity grow, the reliance on this element becomes increasingly important as supply chain risks are inevitable at some point and cannot be ignored, which has been concluded even by leading countries, such as the US and EU member states [113]. Ways to combat this reliance are remanufacturing, repurposing, and recycling of EoL EV batteries, with the reuse of batteries in EoL EVs, as China has been doing already, and then the reduction of those LIBs, with Co content as lithium nickel cobalt manganese oxide (NCM)'s, nickel cobalt aluminium oxide (NCA)'s and LCO's alike [108], [123]. To combat the reliance and risk posed by the Chinese monopoly on DRC's Co importation and then its refined Co exportation, from 2021 to 2023, Western countries have tried to make deals and support DRC financially to break this supply chain bottleneck and help CDR to achieve its Co-processing and a 3% supply chain of batteries and EVs [125]. However, these investments are dwarfed by China's US$155 billion investments in Sub-Saharan Africa and US$100 billion in CDR alone, with the latest deal of US$7 billion in 2023, leading to what some call high undervaluing of DRC resources in contrast to what is being invested and overtime leading to that of well documented and known China's "debt trap" not only in CDR [125], [126], [127].

Table 6. Mining of the Cobalt (Co) globally, between 2022–2024 with the total global reserves as of 2024, reserves in (Mt), with [e]Estimated values for 2024, based on 2024 data for the mined Co amount for 2024 year, with Total Cal. Calculated data for the countries in the table in comparison to the World total from the available data.

	Mine production			Data of 2024		Ref.
Region	**2022**	**2023**	**2024[e]**	**Reserves**	**Resources**	
Australia	5,790	5,220	3,600	1,700,000	N/S	[115], [128]
Canada	3,060	4,220	4,500	230,000	N/S	[115], [128]
Congo	144,000	175,000	220,000	6,000,000	N/S	[115], [128]
Indonesia	9,600	19,000	28,000	500,000	N/S	[115], [128]
Russia	9,200	8,700	8,700	250,000	N/S	[115], [128]
Total Cal.	171,650	212,140	264,800	8,680,000	N/A	
World total	197,000	238,000	290,000	11,000,000	25,000,000	[115], [128]

As China finances the majority of mining operations, one could say that China is becoming one of the largest Co miners globally. However, while this may be the case, China is renowned for being the largest DRC's Co importers and then the biggest Co refiners in the world [115], [123], [129]. In 2022, some estimates put the Chinese Co refinery yield at 76–77% in comparison to other global Co refined, followed by Finland at 10% and 1% by other major producing countries, fueled by its hunger for the battery industry, which uses up to 80% of all Co refined globally [118], [125], [130]. As Co mining ramps back up, so does its refining, but while China's refining capacity had grown from 2022 to 2024 by 2.5%, other countries like Finland, Australia and Canada have had a trend of slowing down by 0.4–2.7%, some less than others on year-over-year (y/y) basis, in percentage wise, due to Chinas ramp up, but when looking from (tonne) perspective, the number of refined Co has increased, as per (**Table 7**) nonetheless [124], [131].

Table 7. Mining Share of global refined production by country, % years 2022–2024, with *Calculated values for 2022–2024 refined in (Mt).

	Percentage			Metric Tonnes			Ref.
Region	**2022**	**2023**	**2024**	**2022***	**2023***	**2024***	
Australia	2.0	1.6	1.6	3,300	2,864	3,552	[124], [131]
Canada	4.0	2.9	2.7	6,600	5,191	5,994	[124], [131]
China	76.1	78.6	78.6	125,565	140,694	174,492	[124], [131]
Finland	9.9	8.3	7.2	16,335	14,857	15,984	[124], [131]
Norway	1.9	1.6	1.4	3,135	2,864	3,108	[124], [131]
Total Cal.	93.9	93	91.5	154,935	166,470	203,130	
World total	100	100	100	165,000	179,000	222,000	[124], [131]

Sustainability, EV makers, and other stakeholders have somewhat had an impact on these numbers, and CE highlighted its position in LIBs and EVs comes to light. EU's regulatory framework, with consumer and producer requirements and procurements, is being influenced by (e.g., EU Batteries Regulation, original equipment manufacturer (OEM), and LCA), not to mention carbon dioxide (CO_2) emission values, which have the highest values out of other industries when it comes to mining and refining of metals. As the main supply chain of Co is dominated by DRC mining and China's refining capacity, the secondary supply of Co has a future and a need if the West and the EU want to break this supply chain risk and dependence. As already mentioned, reliance on Co in batteries is one way, but recycling LIBs and then extracting their Co for utilization in new LIBs is another, more holistic method. China has already been doing this by using the EoL EVs batteries in the process, while the EU has implemented 2023 Batteries Regulation (EU) 2023/1542 or (Document 32023R1542), known giving recovery rates for CRMs and metals as by (**Table 6**) per for Co 90% and 95% by end of 2027 and 2031 years respectively, from the recycling [68], [108], [124], [131]. Co refining from the EoLs and batteries is a massive opportunity for West and EU, as refining of Co and battery manufacturing is sourced currently by China, meaning that as EoL comes closer globally, due to battery life nearing the end from the start of the 2015–2017 "green energy hype", this should happen in close years before 2030. As such, the Co supply will come in a waste form for many West and EU regions, as per CE availability, with increased collection rate targets and business and consumer incentives [124], [131]. These, in turn, affect and drive the Co supply from the batteries and enhance the secondary supply in return, which has been seen from 2020–2024 increase in tonnes y/y as per (**Figure 9**) [124]. If this trend and technological advances continue y/y with technological recovery rates of 95% for Co and Ni alike, then the recovery/recycling rates from the secondary supply rate for the Co annual primary demand of 83.4% and total annual demand of 45.1% with values of 45.1–59.3% with or without the closed-loop recycling by the end of 2039 [132], [133].

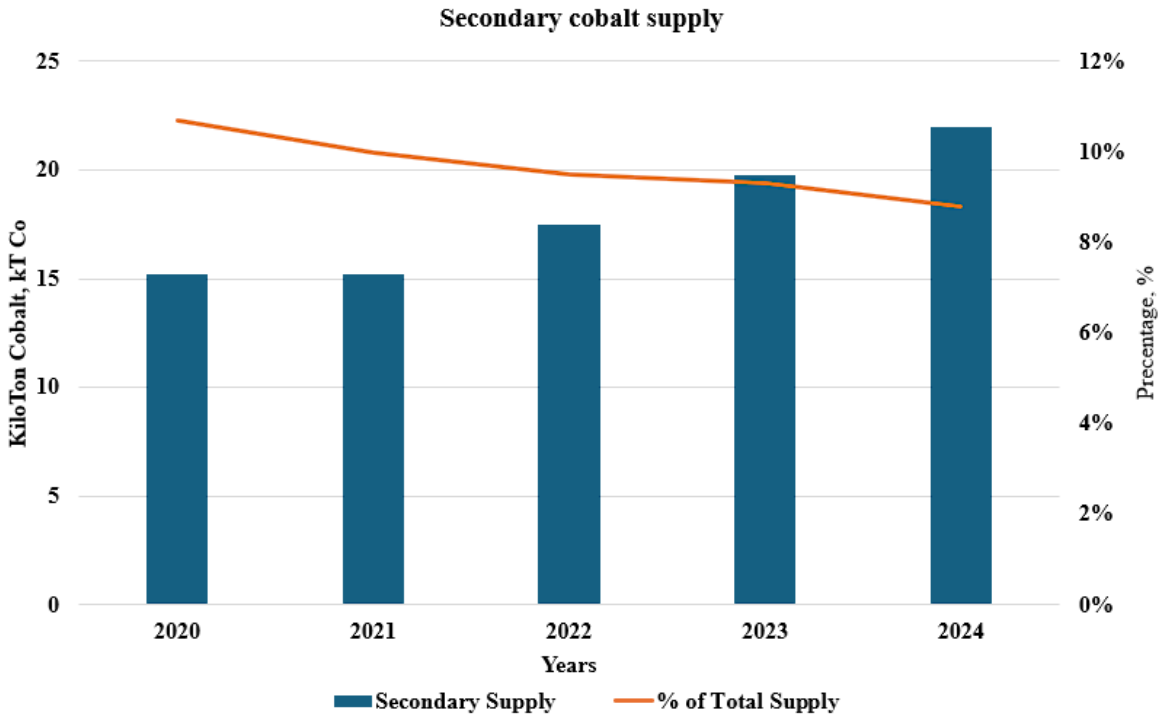

Figure 9. Secondary Co supply from batteries in volume terms (left) and as a percentage of total supply (right) [124].

Like any commodity, the price is the main factor in sourcing and enabling development. For the past three consecutive years, the Co stocks have been in market surplus, but as the market balance is balanced between demand and supply capacity, the price of the Co keeps declining as total supply growth has outpaced Co demand, which has also led to somewhat some smaller producers in the DRC to cut output, as artisanal mining (ASM), has long roots in DRC [124], [130]. As the price of Co started to dwindle, the CDR government enacted for the first time a significant policy intervention by banning the exportation and sales of Co out of the country until further notice for the next 4 months on 22nd February 2025, which promptly resulted in immediate price support as seen in (**Figure 10**) by spike [124], [134]. As the history of Co prices has shown, they are quite volatile and have been affected by recessions/depressions in 2010–2016 and 2019–2021, as well as economic expansions and recoveries in 2016–2019 and 2021–2023.

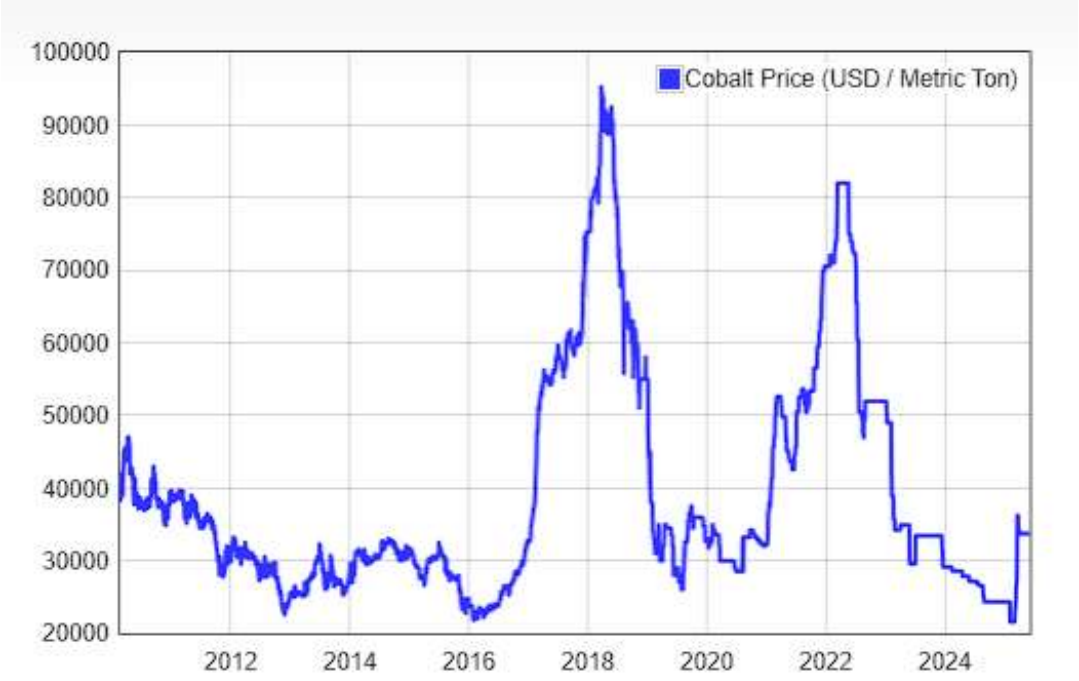

Figure 10. Cobalt annual prices from 2010 through 2025 in (US$ / Mt). Data exported (02.06.2025) from the Ref. [135].

Throughout 2010–2016, Co prices have been relatively stable, with an average. 26,000–31,000 US$/Mt between 2014 and 2016. However, between 2016 and 2019, prices of Co surged to 56,000 US$/Mt and kept climbing, peaking in the second quarter (Q2), in March of 2018 at 95,000 US$/Mt, a record high in a ten-year high for the Co price history, while maintaining the annual average. 73,000 US$/Mt of that year [136], [137], [138]. This was then promptly responded to by recession as oversupply by then DRC and sluggish demand by China stockpiling cobalt chemicals led to a sharp drop in the second half of a year (H2) 2018 and early 2019 [137], [138]. The price surge between 2016–2019 was a direct result of the lithium-ion battery demand and global net-zero policies being enacted globally, like the ”Agenda 2030” and as CE attracted traction in 2015 and ”Circular Economy Action Plan” adoption into the EU’s waste policies, in addition to corners regarding supply and its chains [137]. As COVID-19 rampaged across the globe throughout 2019–2020, the Co price further dropped due to weakened demand and a hit to the average. 31,000 US$/Mt in the 2020 quarter. However, after COVID-19, the market rebounded which was seen in Co prices going back up between 2021–2022 and capping at 64,000 US$/Mt 2022 Q1, as a result of the surging EV sector demand, until it declined to 35,000 US$/Mt 2023, which effect we can

see even now 2025 [124], [131], [137]. Co price as such can be defined as volatile due to its demand, and Co mined as to the amount of refined Co, which both flood the market and break the price down.

3.4.2. Lithium

As the global energy transition is expected to drive a surge in lithium demand, further increasing its importance and the need for mining operations. Although Li may not be the rarest of all the CRMs, being the 25th most abundant element in the Earth's crust and estimated to have 115 million Mts resources globally by the US Geological Survey, and out of that, 30 million (Mt) are reserves, and currently being mined in different countries [115], [128], [139]. Li as itself does not occur in its native metallic form in nature due to its high reactivity, but is found primarily in hard rock pegmatite ores, sedimentary formations, and brines pumped from beneath arid basins [139]. The concentration of Li is mainly in three South American (SOAM) countries, Chile, Argentina, and Bolivia, with resources of 11, 23, and 23 of million Mts, respectively, making up 49.6 vol.% of all the global resources combined. Out of these resources, those of 13.3% in Argentina and 31% in Chile are reserves being mined at a combined of 44.3 vol.% of global reserves. Although 44.3 vol.% of global Li reserves are being mined, Argentina's and Chile's mines' output of Li has been 7.5% and 20.4%, respectively, of all mined Li globally, totaling 27.9% by 2024. Although Bolivia does have a vast amount of Li deposits, its mining operations remain largely untapped due to remote locations and underdeveloped transport infrastructure when compared to those of Argentina and Chile alike, which is then further pushed back by the communities as the environmental impact assessments (EIA) are lacking and environmental pollution, with the clear lack of long-term effect, are understudied, as the Bolivian Li-deposits are unique and biodiverse ecosystems themselves [140]. While the SOAM countries may have the largest resources and mine that of 27.9% reserves all altogether, their risk on the Li supply chain is not as bad as that of the two other countries, Australia and China. As they have the other two largest reserves of 7 and 3 million Mts respectively, making up 33.3 vol.% of Li reserves. However, while the reserves of these two countries may seem less than those of the SOAM countries and appear dwarfed in comparison to the resources of SOAM, at 49.6 vol.%, as theirs is 13.7 vol.%. They make up for this by sheer mining operations and Li exportation as

Australia alone mined 36.7% of all Li and China 17.1%, flooding the market of Li with 53.8% mined goods in 2024 in comparison to those of SOAM's 28%, which was that of double the amount by two countries as per (**Table 8**) values. These numbers, in terms of sheer reserves and mining capacity in 2024, on opposite sides of the globe, are a clear indication of supply chain risks for other countries that are heavily invested in the green energy transition and have a high demand for Li for LIBs and EVs alike. While this may be the case in other parts of the Earth, there are also Li deposits and resources to be found, but their mining operations and extractions have either been slow or minimal due to various factors, such as costs, viability, and environmental concerns. In Europe alone, the Li deposit sources are estimated to be of Germany 4, Czechia 1.3, Serbia 1.2, Portugal 0.27, Spain 0.32, Austria 0.06, and Finland 0.055 million Mts, making a total of 7,205,000 Mts, while in NA, US and Canadas are calculated to be of 19 and 5.7 million Mts, making that of 24.7 million Mts. From the available data, it is possible to conclude that if a need for Li demand arises in the future, it could be met by mining in Europe or by investing now in SOAM by building infrastructure and ramping up their capacity. This would mean mitigating the supply risk posed by Australia and China, as they account for 53.8% of Li market suppliers and miners.

Table 8. Mining of the Lithium (Li) globally, between 2022–2024 with the total global reserves as of 2024, reserves in (Mt), with estimated values for 2024, based on 2024 data for the mined Co amount for 2024 year, with [e]Estimated values from 2023 for the lithium carbonate (data is not taken into account in Total Cal. or World Total), with Total Cal. Calculated data for the countries in the table in comparison to the World total, from the available data.

	Mine production			Data of 2024		Ref.
Region	**2022**	**2023**	**2024[e]**	**Reserves**	**Resources**	
Argentina	6,590	8,630	18,000	4,000,000	23,000,000	[115], [128]
Australia	74,700	91,700	88,000	7,000,000	8,900,000	[115], [128]
Bolivia	N/S	N/S	N/S	948,000*	23,000,000	[115], [128], [141]
Canada	520	3,240	4,300	1,200,000	5,700,000	[115], [128]
Chile	38,000	41,400	49,000	9,300,000	11,000,000	[115], [128]
China	22,600	35,700	41,000	3,000,000	6,800,000	[115], [128]
Total Cal.	142,410	180,670	200,300	24,500,000	78,400,000	
World total	146,000	204,000	240,000	30,000,000	115,000,000	[115], [128]

As already mentioned, over 87% of the Li is being used in batteries, which enables the EV and fuels the growing demand for LIBs [110]. As the LIBs demand keeps rising, so does the old and spent LIBs increase, which are either coming to EoL or are already off their

EoL. This source of Li metal is one of the many methods to provide support and mitigate the risks of Li as discussed above, by recycling and opening up the secondary supply chain for Li. In 2019, the LIBs waste generated by EVs alone was approximately 500,000 metric tons, which is expected to rise to 8 million metric tons by the end of 2040 [94]. Some estimates by the International Energy Agency (IEA) suggest that if recycling scaling can be done successfully and implemented into CE, then the need for mining activities can be reduced by 25–40% by 2050 and generate US$ 200 billion, which could mean reduction in need of 25% Li total need alone [142]. Additionally, the recycling impact on mineral scarcity can be reduced by 75%, meaning that by recycling cells, their normalized and weighted environmental impact would decrease by 75%, according to some estimations and calculations [143]. At the current stage, China has the most competitive edge in Li recycling, while it may not technologically implement the best of the best methods, because of the lower labor costs, combined with greater recycling economies of scale and increased vertical integration, drive significantly lower recycling costs all together combined, which means of greater edge on recycling market in comparison to that of Na and Europe, leading to development and building of larger capacity recovery/recycling facilities, being those of five times larger [142]. While recycling is the look of the future and encouraged by different initiatives, as in Co discussion, the consensus on feasibility for the moment is not promising in NA and Europe, as the typical price of scrap metal is 50–80% of that of primary material and that the recycling's impact on CO_2 emissions is relatively small, in comparison to that of recycling and manufacturing costs of batteries [142], [143]. Another way of recycling batteries and materials in them is Li and Co. For instance, it would be repurposing them. Battery repurposing would offer a viable EoL solution, with retired batteries retaining 70–80% of their original capacity. Then, batteries that would need to be retired from EoL, that could be used in smaller storage systems, thus significantly reducing battery production. However, the limited compatibility needs to be taken into account [94], [144]. This method would also then reshape the principles of CE, as currently, CE does not look beyond recycling when it comes to repurposing. To implement more traction, new standards and evaluations would need to be implemented. Currently (ISO 59014:2024 and UL 1974 Standard for Evaluation for Repurposing Batteries), do have somewhat criteria and methods to solve issues with repurposing [142]. However, as time progresses, the current battery technology moves forward, and in the future, battery composition and chemistry may be different altogether or the same but with multiple times less material than today, which will

affect the demand and price of Li drastically. As such, it is important to understand what drives and has driven Li prices over the past years, as currently, the risk of physical supply shortage is impossible, but a short disruption can and has already happened, as a Chinese company in 2025 has halted lithium tech exports, in a direct move orchestrated by the Chinese government [145]. While Li may not be as volatile as Co, it has clear 2018–2021(H2) / 2023–2025 recessions/depressions and then 2017(H2)–2018 and in 2021(H2) till the beginning of 2023 economic expansions/recoveries as per (**Figure 11**). Rising prices in 2017 were affected by the demand from electronics, EVs, and renewable storage in addition to two new mines being taken effect in Australia, which saw the Li price go as high as 24,000 US$/mt. This was then followed by recessions and, leading prices to drop as low as 12,000 US$/Mt in 2018, led by the oversupply and development of five new mines in Australia alone. As oversupply and demand increased by the end of 2019, Li prices fell as low as 7,300 US$/Mt and, by 2020, as low as 5,000 US$/Mt as a consequence. By the 2021 Q4, prices reached as high as 26,200 US$/Mt as lithium carbonate (Li_2CO_3) prices surged, which was then followed by a further increase in EV demand and led to a high of 67,000 US$/Mt in 2022. This was then followed by the lithium hydroxide (LiOH), which saw a price surge of 35,300 to 78,000 US$/Mt during 2022. As the demand and supply have fluctuated as much as they have, this inevitably led to oversupply and led to the price falling on average of 32% on y/y since the start of 2023, when the average price was that of 46,000 US$/Mt [110].

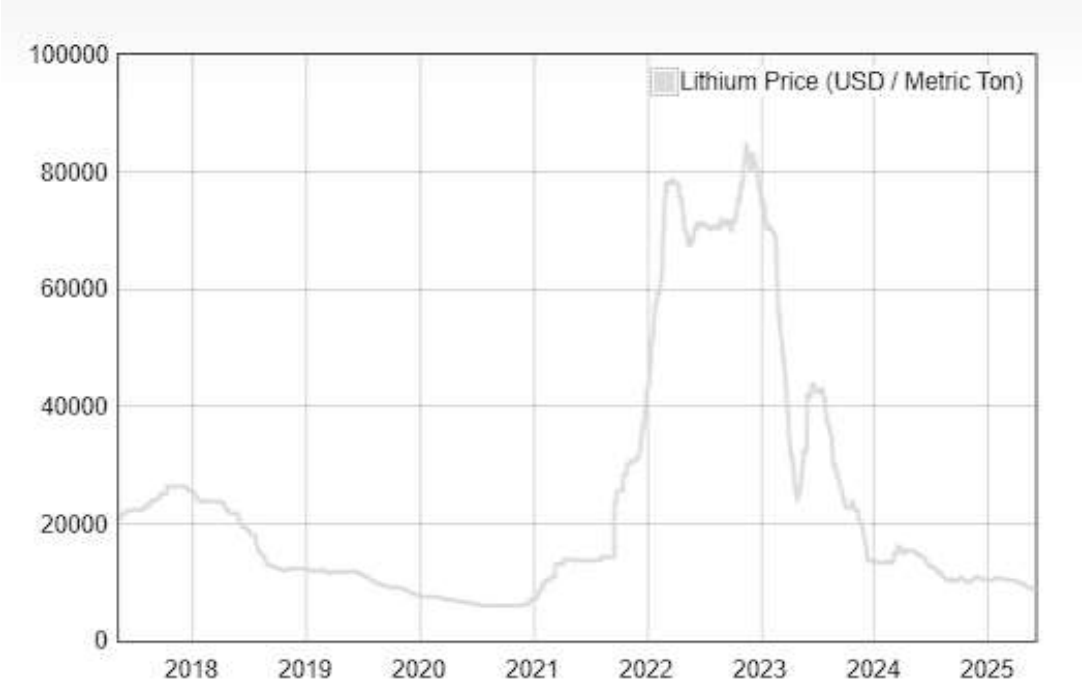

Figure 11. Lithium annual prices from 2017 H2 through 2025 in (US$ / Mt). Data exported (02.06.2025) from the Ref. [146].

As the Chinese EV market requires a vast amount of raw Li, so does the demand for refined Li increase, even when Li prices are dropping, and refining costs become less profitable. As of 2024, China has a share of 70% of all Li refined globally by producing Li chemicals of (Li_2CO_3) and (LiOH). By 2024–2035, this number will change as other countries are investing and in need of Li refining, which would lead, in the case of (Li_2CO_3), to the following number: China ~61%, Argentina ~25%, Chile ~9%, and NA ~5%, while in case of (LiOH): China ~41%, Australia ~23%, NA ~19%, Korea ~11%, and Europe ~6% as per (**Figure 12**).

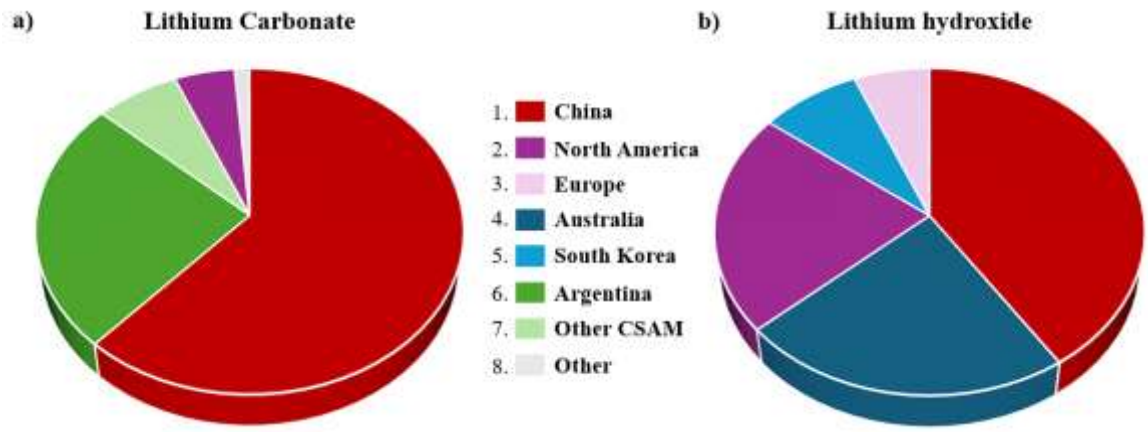

Figure 12. Geographical distribution of planned additional lithium chemical for the Lithium carbonate on the left (a) and Lithium hydroxide on the right (b) projects, 2024–2035. Note: CSAM = Central and South America — figure reproduced with the data from [147].

This shows how a raw supply of Li is not at risk in the long term, while its refined form of chemicals is, due to the demand and need for LIBs and EVs, may not be met by production capacity globally, maybe under short-term and temporary demand/supply risk as consumption-production imbalance playing a part [147].

3.4.3. Nickel & Manganese

Nickel and manganese, two other important metals in the battery industry, are essential for the production of LIBs. These two are key elements in the production of electrode cathode materials for NCM (NCM 111, NCM 523, NCM 622, and NCM 811), NCA, and LMO [107], [148]. Total reserves of these metals put Ni at 130 million Mts and Mn at 1.7 billion Mts, making Mn the 12th most abundant element, while for resources, Ni is at 350 million Mts and Mn estimation are those of UNK, but some estimations put its resource values on African continent to that of 916 billion Mt, out of which South Africa and Gabon would have of 96.6% total resources and respectively of 75.9% and 19.7% as the countries [149]. Ni is most commonly found in laterites and magmatic sulphide deposits, with concentrations of 54% and 35%, respectively. Additional amounts are found in seafloor nodules (10%) and tailings (1%) [115]. Out of all mined Ni in 2020 globally, 75.5% of Ni came from the laterite type of deposits and 29.5% from the sulphide [150]. Over 70% of the world's Mn resources are

found in South Africa, according to the U.S. Geological Survey. Mn, when found and mined in nature, is typically found in 35–54% Mn concentrations per ore as (low-manganese-grade of mamatwan-type ore), but in ferromanganese (high-manganese-grade wessels-type ore), with content is 74–95% [115], [149]. Both Ni and Mn are clear supply risks, as certain countries have larger reserves than others and then mine and export more, leading to a bottleneck and potential monopoly. Ni mining is currently dominated by Indonesia, which mines 59.5% of all Ni mined, followed by Russia and Canada at 5.7% and 5.1%, respectively, as per (**Table 9**) 2024 data. Mn mining, in comparison, is more diverse, as the largest miner and exporter of Mn was Gabon in 2024 at 23%, followed then by Australia, South Africa, and China, all at 14%, 6.5%, and 3.9%, respectively, as per (**Table 10**) 2024 data. From these data, it is mining operations.

Table 9. Mining of Nickel (Ni) globally, between 2022 and 2024, with total global reserves as of 2024, in metric tons (Mt), with [e]Estimated values for 2024, based on 2024 data for the mined Ni amount for the 2024 year, with Total Cal reserves. Calculated data for the countries in the table in comparison to the World total from the available data.

	Mine production			Data of 2024		Ref.
Region	**2022**	**2023**	**2024[e]**	**Reserves**	**Resources**	
Australia	155,000	149,000	110,000	24,000,000	N/S	[115], [128]
Brazil	88,500	82,700	77,000	16,000,000	N/S	[115], [128]
Canada	143,000	159,000	190,000	2,200,000	N/S	[115], [128]
Indonesia	1,580,000	2,030,000	2,200,000	55,000,000	N/S	[115], [128]
Russia	222,000	210,000	210,000	8,300,000	N/S	[115], [128]
Total Cal.	2,188,500	2,630,700	2,787,000	105,500,000	N/A	
World total	3,270,000	3,750,000	3,700,000	130,000,000	350,000,000	[115], [128]

Table 10. Mining of Manganese (Mn) globally, between 2022 and 2024, with total global reserves as of 2024, in metric tons (Mt), [e]Estimated values for 2024, based on 2024 data for the mined Mn amount for the 2024 year, with Total Cal reserves. Calculated data for the countries in the table in comparison to the World total from the available data.

	Mine production			Data of 2024		Ref.
Region	**2022**	**2023**	**2024[e]**	**Reserves**	**Resources**	
Australia	3,040,000	2,860,000	2,800,000	500,000,000	N/S	[115], [128]
Brazil	624,000	580,000	590,000	270,000,000	N/S	[115], [128]
China	743,000	767,000	770,000	280,000,000	N/S	[115], [128]
Gabon	4,670,000	4,490,000	4,600,000	61,000,000	179,974,050	[115], [128]
South Africa	7,300,000	1,230,000	1,300,000	560,000,000	695,463,420	[115], [128], [149]
Ukraine	323,000	N/S	N/S	N/S	N/S	[115], [128]
Total Cal.	16,700,000	9,927,000	10,060,000	1,671,000,000	875,437,470	
World total	19,800,000	19,600,000	20,000,000	1,700,000,000	N/S	[115], [128]

The majority of the Ni in 2023 was used in the metal and, in particular, the steel industry, accounting for 72%, of which 64% was stainless steel. The other major use for Ni was 16% of the overall battery market [151]. Similarly to Ni, around 85–90% of Mn is also used in the steel industry and is a crucial element in steel production, as it is important in alloys and superalloys, enhancing their strength and hardenability, which makes them suitable for high-strength steels [152]. An assessment by the European Commission in 2022 revealed that Ni is refined in China at a rate of over 64%, Indonesia at 27%, and the rest of the world at 37%, indicating an apparent disparity in global Ni refining [150]. The same assessments for Mn were more dispersed, as refining occurred in India, Norway, Australia, and Ukraine at rates of 16%, 14%, 12%, and 11%, respectively. At the same time, the majority of all the Mn imported was done by China. In contrast, India was the leading exporter of refined products, followed by China, which showed its growing appetite for industrial products, including batteries, automotive components, and others [153]. In 2022, European Commission estimations ranked China as the top refiner of Ni-based salts, oxides, and Ni-class 1 at 23.3 vol.%, followed by ferronickel and nickel pig iron at 50.7 vol.%. Additionally, China refined Ni into 63.3% of nickel sulfate, which is a key ingredient in battery manufacturing, including that of Ni-class 1 products [150]. The same data for the Mn showed that China was the leader in Mn refined product, as Mn ferroalloys, ferromanganese, silicomanganese, and electrolytic Mn metal (EMM) productions were at 67.7%, 39.2%, 74.9%, and 96,6% of all global manufacturing, out of which EMM importance not only in steel industry but in battery especially that of LIB manufacturing [153]. As prices of Ni and

Mn continue to fluctuate, due to their volatile nature, Ni prices are affected by almost the same factors as Co and Li, as seen from (**Figures 10** and **11**), when compared to (**Figure 13** (**a**)), where apparent effect of COVID-19 can be seen as the Ni price plummeted from 17,657 US$/Mt of 2019 September to that of near 12,000 US$/Mts 2020 Q1. In 2022, as the EV and LIB boom happened and demand was needed, the prices peaked as high of 49,000 US$/Mt, which was then subsequently met with the surplus of Ni from Indonesia in the form of nickel-cobalt-hydroxide (MHP), which was additionally led by the stainless-steel demand, which effect is seen into the 2025 year [151].

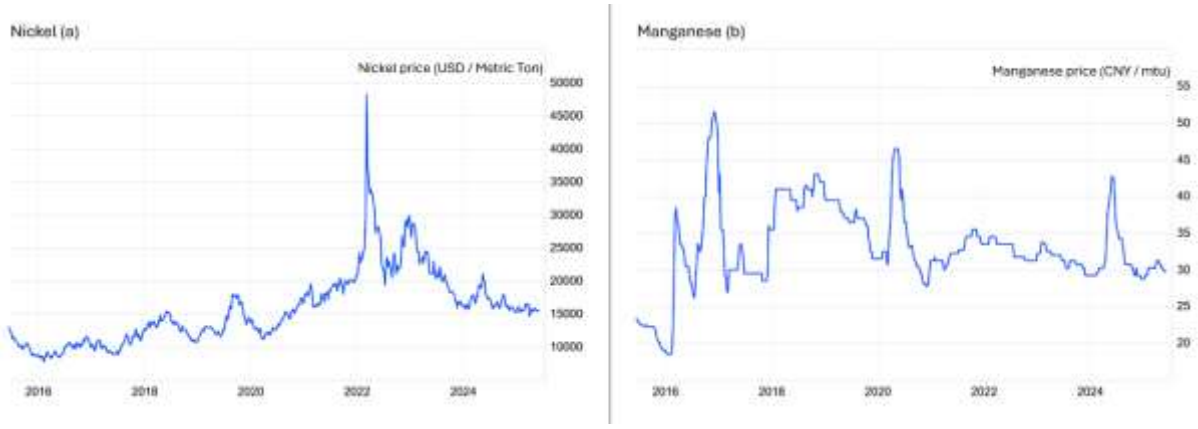

Figure 13. Nickel on the right (a) and Manganese on the left (b) prices from 2015–2025 in the case of Ni as (USD / Metric Ton) and for Manganese as (CNY / mtu), (mtu = Metric Ton Unit). Data exported (02.06.2025) from the Refs. [154], [155].

Out of all four elements discussed above, the volatility of Mn is on another level when compared (**Figure 13** (**b**)) to the others, as its price charts for the past 10 years have fluctuated significantly in comparison to the others. Reasons for this are the understanding of lower- and higher-grade ore demand, as well as the applications for which they are used. In 2024, prices fell due to low buying power, led by the panic of 2024 H2 steel demand and the lack of sufficient high-grade material, resulting in a high level of oversupply. In 2019, COVID-19 emerged, and it can be seen that prices surged due to China's strict enforcement to contain it, which led to a supply deficit and a buying power, which then was followed by a price surge due to the need for production rates. The years 2016–2018, on the other hand, were compared to others as stable, as the need for battery and energy storage systems started gaining traction with a steady supply and a new market that they opened. These are a few of

many reasons for the Mn price fluctuation and, as such, supply chain risks globally, which are further realized as Gabon is planning on banning Mn ore exportation out of the country by 2029, which has led to a French company Eramet shares falling, who are the shareholders in Gabon-Based largest mining company Comilog [156]. This move, if it were to happen, would pose a significant risk to the World's Mn supply. However, at the same time, it would. enable Gabon to attract more investment from other countries and bring the refining industry closer to ore sourcing, thereby reducing its dependence on Chinese refining of Mn.

3.4.4. Graphite

Graphite, either in its natural or synthetic form, in 2023 made a total of Gr by 34% and 66%, respectively [157], [158]. Gr is used in a multitude of different applications, from lubricant and friction material to those of batteries, which is Gr's primary application or where the most significant supply goes, as Gr has a 98% market share in anodes as of 2021 [159]. Demand is primarily driven by battery and energy storage systems, which were seen in 2023, by demand for natural and synthetic Gr at 87% and 84% respectively into Asia, out of which China had the biggest share [157]. This is not surprising, as China has the most significant need for other CRMs, but this is also evident from (**Table 11**), as China has the largest reserves globally, and whose mines produce the most natural Gr. It has been estimated by the U.S. Geological Survey that global reserves of natural Gr are 800 million Mts, which are also recoverable. China has a clear monopoly in mining, as it mines 79.4% of all natural Gr and holds 27.9% of all reserves [115]. Other countries, such as Brazil, Gabon, and South Africa, have rates of 4.3%, 5.6%, and 4.7%, respectively. Natural Gr's mining may be monopolized, but its reserves can be found from different corners of the globe, as from SOAM's Brazil, NA's Canada (the African continent's Madagascar and Mozambique), and Europe's Russia, at reserve percentages of 25.5%, 2.0%, (27.9% and 9.3%), 8.6%, and 4.8%, showing that each continent has reserves if needed for the future, as China is extracting their reserves, due to high demand.

Table 11. Mining of the Natural Graphite (Gr) globally, between 2022–2024 with the total global reserves as of 2024, reserves in (Mt), with [e]Estimated values for 2024, based on 2024 data for the mined Mn amount for 2024 year, with Total Cal. Calculated data for the countries in the table in comparison to the World total from the available data.

	Mine production			Data of 2024		Ref.
Region	**2022**	**2023**	**2024[e]**	**Reserves**	**Resources**	
Brazil	72,000	66,300	68,000	74,000,000	N/S	[115], [128]
Canada	13,000	5,470	20,000	5,900,000	N/S	[115], [128]
China	1,210,000	1,210,000	1,270,000	81,000,000	N/S	[115], [128]
Madagascar	130,000	63,000	89,000	27,000,000	N/S	[115], [128]
Mozambique	166,000	98,000	75,000	25,000,000	N/S	[115], [128]
Russia	6,000	15,000	20,000	14,000,000	N/S	[115], [128]
Total Cal.	1,597,000	1,457,770	1,542,000	226,900,000	N/A	
World total	1,680,000	1,530,000	1,600,000	290,000,000	800,000,000	[115], [128]

While China may be dominant in natural Gr production, it can be seen that other countries are also increasing their capacity in extraction operations. The market for natural and synthetic Gr alike is stabilizing and is being shaped by the automotive industry and battery manufacturers. What needs to be understood when looking at the Gr market is that natural Gr does not have standard pricing or an active spot/futures market; as such, the transactions are primarily negotiated directly between buyers and sellers, leading to misleading prices on the internet or that they are hidden behind a paid wall, and given for the payment by companies that research and trade. In (**Table 12**), prices for natural Gr can be seen for Germany, the US, and China alike to show how prices go, but what needs to be reminded is that pricing is also done by the type of natural Gr sized flake is being sold, as they are typically traded in flake sizes.

Table 12. Prices for the US, China, and Germany for natural Graphite in US$/Mts for the 2024 yearly Quarters 1–4.

	Yearly Quarters of 2024					Ref.
Region	**Q1**	**Q2**	**Q3**	**Q4**	**Avg. price**	
United States	1157	1109	1030	1114	1102.5	[160]
China	879	804	665	721	767.25	[160]
Germany	872	858	815	876	855.25	[160]
Avg. Price per Q	969.3	923.7	836.7	903.7	908.3	

In 2024, Gr's market size was estimated to be 7.8 billion US$ globally, and Asia's share alone was 4.37 billion US$, accounting for 56% of the global market size. Additionally, estimates predict that 2025 will be 8.32 billion US$, but by the end of 2032, it is expected to reach 13.5 billion US$ [161]. Meaning an increase of 0.52 billion US$ between 2024–2025 and by 2025–2032 a 5.18 billion US$, meaning the y/y increase of 0.74 billion US$ for 7 years. As the importance of CRMs is being realized, it inevitably leads to their strain for the countries that depend on them; reasons like these are the factors that led to (**Table 12**) prices 2024, and further analysis can be found under (**Tables 13 – 15**), further showcasing somewhat volatile prices of natural Gr, even though it may not seem for the moment.

Table 13. Reasons for Europe's natural Graphite's 2024 yearly quarters 1–4 price fluctuations explained.

Quarter	Price Trend	Key Drivers	Ref
Q1 2024	Mixed fluctuations	- Automotive growth vs. construction slump - Lower power costs reduced production expenses - EU's support for East and Central Europe	[160], [161], [162], [163]
Q2 2024	Sharp decline	- The EU's Raw Materials Act caused the surplus - Inflation led to manufacturing costs and energy price rise - Geopolitical & shipping disruptions	[160], [161], [162], [163]
Q3 2024	Continued drop	- Weak steel & auto demand - Oversupply of Gr on the market - Germany's economy took the hardest hit	[160], [161], [162], [163]
Q4 2024	Further slump	- Synthetic Gr substitution increased competition - Further decline in natural Gr - Oversupply from Madagascar - Declined BEV registration 5% y/y	[160], [161], [162], [163]

Table 14. Reasons for North America's natural Graphite's 2024 yearly quarters 1–4 price fluctuations explained.

Quarter	Price Trend	Key Drivers	Ref
Q1 2024	Stable & slight rise	- Balanced supply and demand - Winter was relatively easy - Construction and automotive	[159], [160], [161], [162]
Q2 2024	Sharp decline	- Supply vs demand (oversupply) - Geopolitical & shipping disruptions - Automotive & construction demand declined - Weak manufacturing and vehicle sales	[159], [160], [161], [162]
Q3 2024	Continued drop	- Import influx (oversupply) - Manufacturing & construction slowdown - Slowed logistics & low freight rates	[159], [160], [161], [162]
Q4 2024	Moderate decline	- Geopolitical risks - EV demand volatility - Supply chain strain	[159], [160], [161], [162]

Table 15. Reasons for the Asia's natural Graphite's 2024 yearly quarters 1–4 price fluctuations explained.

Quarter	Price Trend	Key Drivers	Ref
Q1 2024	High volatility	- Weak Chinese demand in the auto & construction sectors - Weak domestic consumption - Challenging market - High inventories	[160], [161], [162], [163]
Q2 2024	Sharp decline	- Oversupply (mining output + Chinese production) - Trading restrictions (bans & tariffs) - EV & electronic demand	[160], [161], [162], [163]
Q3 2024	Steep drop	- Oversupply by China - Weak industrial demand - Low consumer confidence	[160], [161], [162], [163]
Q4 2024	Moderate fall	- Low demand & evolving supply trends - Economic uncertainty - China's reduced production - Geopolitical risks	[160], [161], [162], [163]

What all of the (**Tables 13 – 15**), do showcase is a clear reasoning of geopolitical and shipping disruptions in Q2 of 2024 year, globally, as seen from Europe, NA, and Asia, as the Gr price declines sharply, due to this primary reason, with some other factors in different regions, with one most notably of that oversupply in NA and Asia alike. This oversupply then continued across all three of the regions in the Q3 of that year 2024, seen as a weakened price trend of the Gr. The Q4 in 2024 across all of the regions did not seem to do better by much, as a decline in the Gr price continued, which led to that concluding the 2024 year of

Gr price being in a declining or negative trend overall, with exception of that Q1 across them all. Showcasing the high volatility of the Gr prices in LIB development, manufacturing, and recycling alike.

3.4.5. Geopolitics and Prospects of Raw Materials

As shown, LIBs hold a high amount of critically important metals and elements in them, those being (Co, Li, Ni, Mn, and Gr), which are also under different pressures, as their demand, importation, and exportation are highly volatile in battery and storage systems, like those of LIBs. Nonetheless, this has not discouraged China 2024 from producing even more and cheaper EV batteries, which supply 80% of the global EV battery cells [164]. According to the IEA's 2023 analysis, China held nearly 90% of the global cathode and over 97% of the anode material production capacity alone [165]. These numbers are a reality that highlights the dependence of other countries on Chinese battery, cathode, and anode manufacturing, as well as the raw materials required for their production, which are imported and exported in equal measure, resulting in a geographic concentration of production [164], [165]. These allowed China 2024 to directly manufacture battery electric vehicles (BEVs) and hence keep manufacturing costs for battery cells for BEVs lower than in the US and EU by 44.7% [165]. Over the last two years, from 2023 to 2024, NEV sales in China increased by 36%. This trend is projected to continue, with a 25% increase from 2024 to 2025. Additionally, NEV sales are expected to rise globally by 26% and 18%, respectively [166]. This is all possible by the Chinese competitive nature, as low labor costs, automation, and a vast market, which are fueled by low energy costs in China compared to those of the EU and US, while the raw materials/materials for industries to manufacture are almost of the same price [167], [168]. If these trends continue at the current rate and the prognosis done by different institutes, then the assessment done by the US Department of Energy in 2023 (**Figure 14**) would put Co and Gr into the short term based on anticipated market response and emergence/availability of viable substitutes or a dramatic increase in demand for the materials, when it comes to their importance in energy infrastructure [169].

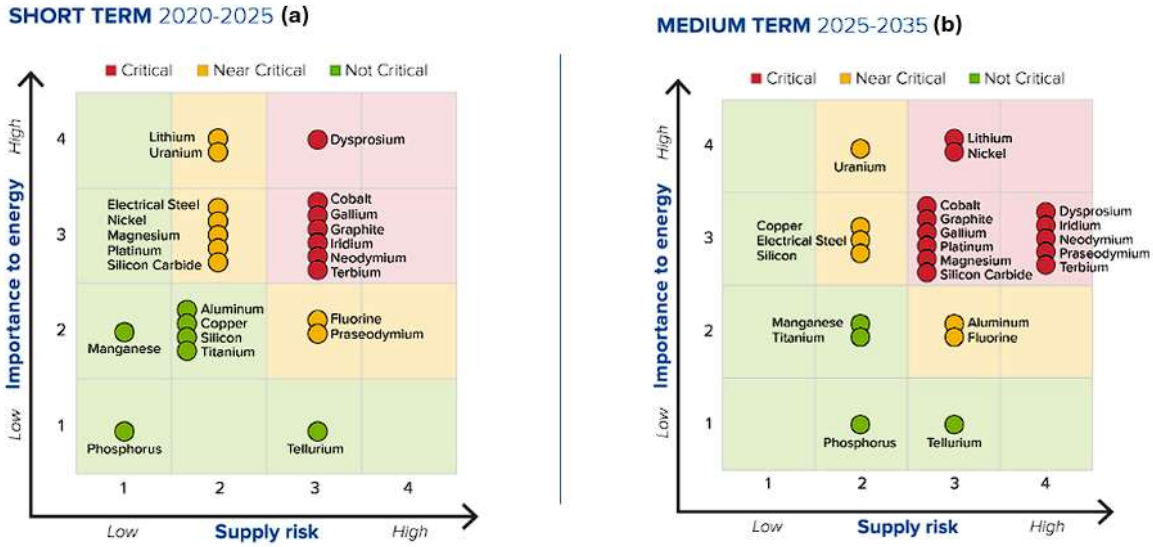

Figure 14. Short-term 2020–2025 on the right (a) criticality matrix for the CRMs, and on the left, medium-term 2025–2035 (b) criticality matrix for the same CRMs, based on the importance to energy as Y-axis and supply risk as X-axis, by U.S. Department of Energy [169].

From a short-term perspective, Co and Gr are categorized as critical materials, while Li, Ni, and Mn are near-critical materials [169]. However, as their importance and need increase in the medium term, so does their risk matrix value change in the case of Li and Ni, as they even surpass the Co and Gr, the increasing matrix values for the Li, Gr, and Mn are driven by high material intensities of LIBs, nickel-metal-hydride (NiMH) batteries, fuel cells, and electrolyzers, needed all for the growing demand of EVs, leading to that of 41% in 2025–2035 of Mn for battery industry, instead of current 94% in lightweight alloys [169], [170], [171]. Due to the criticality of certain CRMs, some exporters and importers have been imposing limitations on availability and supply, as stated earlier. This is important for the countries that are doing business with each other and supporting each other's economies via this, but what if you are a country with high sanctions, like that of Russia, and need key CRMs and metals, which are essential for the current market and technological advancement, wellbeing of country's citizens and development. Russia is not alone in this situation, as it explores new grounds and participates in a larger global gameplay on the world stage. While other countries, such as China, invest heavily in other countries through subsidiaries and investment companies to secure resources, including those of Chile and

Bolivia [125], [126], [140], [172]. In Bolivia, for instance, Russian-backed Uranium One Group invested in a Li plant in 2024, as it requires Li as a raw material for its industry [172]. One way Russia has also achieved its hunger for CRMs is by exploiting the Ukrainian territories, which it currently controls, although these territories may not contain much of the CRMs needed for the battery and EV industry. However, they do have other sources. Ukraine is one of the richest CRM countries in Europe, as it has 22 out of the 34 materials identified as critical by the EU [173]. As (**Table 10**) shows, Ukraine mined 323,000 Mts, or 1.6% of 2022 mined Mn, before the start of the war, impacting its economy sharply and the World supply, with impact on its Mn refining capability, as it refined that of 11% of worlds Mn, not to mention Russian share of Co, Ni, and Gr [115], [173]. As discussed, the various factors affected the prices of Co, Li, Ni, Mn, and Gr. However, the start of the conflict in 2022 also increased the prices of Co by 2%, Li by 14.97%, and Ni by 36%, demonstrating that the Russia-Ukraine conflict substantially affected their prices, and hence the battery industry as a whole [174]. What history has shown across many types of conflicts, from the 2018 China-US trade conflict to that of the 2022 Russia-Ukraine and another 2025 China-US trade/tariff war, is that Europe and countries participating in conflicts lead to geopolitical uncertainty, have an effect on future projects and progress done, with the shipments of raw materials and products alike on supply/demand [173], [174], [175], [176]. What all these conflicts have in common is their underscoring the critical role of key national resources in global health and economic stability, which also reinforces the need for international collaboration even stronger by using investments in vital sectors and the protection of trade routes to ensure supply and demand alike, which in return then lays the groundwork for long-term global security [174], [175]. The Russia-Ukraine war has also demonstrated how regional military-political instability can trigger global economic disruptions and discussions alike [175]. To combat reliance and secure the strategic interests of the US and its allies, the US has done so in 2025 after long negotiations with Ukraine on the" mineral agreement or deal", which aims to invest in Ukraine's natural resources, including those of keen interest to CRMs for [177]. This agreement aims to support Ukraine in the long run. However, it has also been criticized for exploiting Ukraine's natural resources to a certain level, which is why the EU should ensure this by implementing EU environmental directives and community benefit-sharing mechanisms if the EU and US want and must to diversify critical mineral sources by cutting cut reliance on Russian and Chinese suppliers [178]. If the EU wants to become self-sufficient from the rest of the world, as the Paris Agreement targets, it may raise electric

storage mineral demand by 450% by the end of 2050 [174]. Another source of CRMs could be that of a highly lucrative but environmentally unfriendly and invasively aggressive method of deep-sea mining, which has, over the last few years, also seen considerable talk and traction [179], [180]. There are multiple places that have been studied and mapped by countries and companies, which have led to estimations of 300 billion Mts worth of metal and element resources [181]. A zone alone called Clarion-Clipperton Zone (CCZ) in the north-central Pacific Ocean could hold that of high-rich nodules of 21 billion Mts, which would disrupt the markets as we know them today, as the 6000 million Mts of Mn, 270 million Mts of Ni, and 44 million tonnes of Co, could be extracted from the ocean bottom [181], [182]. These Mn nodules are highly rich in CRMs and other elements, such as Mn, Cu, Co, Ni, Ti, Li, Mo, Te, V, Zr, Nb, Ta, rare earth elements (EERs), and platinum group [181]. As such, deep-sea mining could be a lucrative opportunity; however, we will not delve into this in this Thesis, as it is a complex theme due to the lack of regulation surrounding mining, permits, and international laws, which also fall outside the scope of the thesis.

As shown, demand and supply are driving forces of how fast and how the future greener energy trend happens. One way would be to intensify the mining operations, or another could be to find a solution in the EoL of LIBs. Mining impacts on society, economics, and the environment throughout the mining process, from exploration to operation and closure, can have a complex impact in various ways, both directly and indirectly, with both negative and positive effects [183], [184]. The most noticeable mining operations in the case of the CRMs discussed in the chapter are those which are typically mined in open-pit style mines, leading to deforestation, erosion, contamination and alteration of soil profiles, contamination of local streams, and CO_2 emissions [184]. To reduce the burden of mining and refining, given the growing demand and supply, which necessitates transportation, as most battery components are either assembled or their raw materials originate from Asia or China, it is more likely. As discussed, the recycling itself might not be the solution. However, the repurposing of LIBs and batteries alike could be the solution, which could be incentivized by general policies, targeted regulations, or voluntary frameworks, along with new standards that are currently in short supply and high demand, to ensure safe handling and ensure the CE principles [142]. By upscaling the processes, like with the large-scale refiners, end users own the material and contract manufacturers to recycle it, this collaboration between parties enables collection/recycling rates exceeding

90%, maximizing recovered material for mutual benefit, enabling that of closed-loop recycling of industrial catalysts, which would be on par with CE [142].

For these reasons, lots of research and studies are needed, and help and collaborations between different sectors and levels from different fields are a necessity if one could put emphasis on it. Goals of CE are relatively straightforward, but how to achieve them in relatively optimized manners and in manners that also bring economic gain on some level, as the fluctuating markets have been shown to have a detrimental affect on the whole CRM and LIB demand/supply chains, with addition to theirs recycling and/or manufacturing from the component to whole systems alike, into technologies enabling the current trend and transition. Highlighting the importance of stability, which can be achieved by the utilisation of CE as a concept in this field.

4. Recycling Processes of the LIBs

As the need for increasing LIBs and batteries demand alike for the use of NEVs, EVs, and energy storage. It has been established previously that China and Asia are the predominant sources of raw materials and components for LIBs and LIB manufacturers alike, not to mention the NEV and EV markets worldwide. These have been enabled and enabled advancements in LIBs and batteries alike to produce and develop high-voltage and/or high-capacity capability batteries. The most common commercialised methods for LIB recycling to date require logistics, pre-treatment, and metal recovery, typically through some form of metallurgical processing, which involves recycling LIB waste via thermal, chemical, or physical processing [93]. Overall, the recycling cycle of LIBs can be categorised into two stages:

1. Mechanical recycling process (Pre-treatment)
    1. disassembling,
    2. crushing,
    3. screening,
    4. and separation.
2. Recycling process (Recycling)
    1. recycling precious metals,
    2. and raw materials from the spent battery [23].

Currently, the primary components of LIBs required for recycling or that come with them are a plastic and metallic shell, a cathode, an anode, a separator, and an organic electrolyte. As the first wave of EV batteries is reaching retirement, the curiosity and need for better, more efficient, and higher-capacity recycling processes are growing as the battery demand growth strains lithium and cobalt supplies and is under high supply risk [27]. These and many other different factors are a leading cause of the interest, research, innovation, and recycling implementation globally, which is evident in the spike in journals and patents since 2014, as shown by (**Figure 15** (**a**)), where the patent-to-journal publication ratio of 2:1 compared to the typical ratio of 1:5 means that commercialization and industrial players are key players in developing LIB recycling. This is then further backed by the geographical

distribution (**Figure 15** (**b**)), which is clearly influenced by the LIBs industry/manufacturing distribution in Asia, in comparison globally, as per China, as they are the biggest manufacturer of the LIBs and their components, which has logically also led to recycling industry developing the highest in comparison to other World countries, leading to publications and research aligning with the trend [185]. These have also been fueled and fueled alike, the battery manufacturing/development industry from 2005–2018, as the patent activity for battery and energy storage technology did grow by a 14% y/y rate globally, in comparison, this was four times faster than the average across all technology fields, resulting in 90% of all patents in field of energy storage, are those of battery [186].

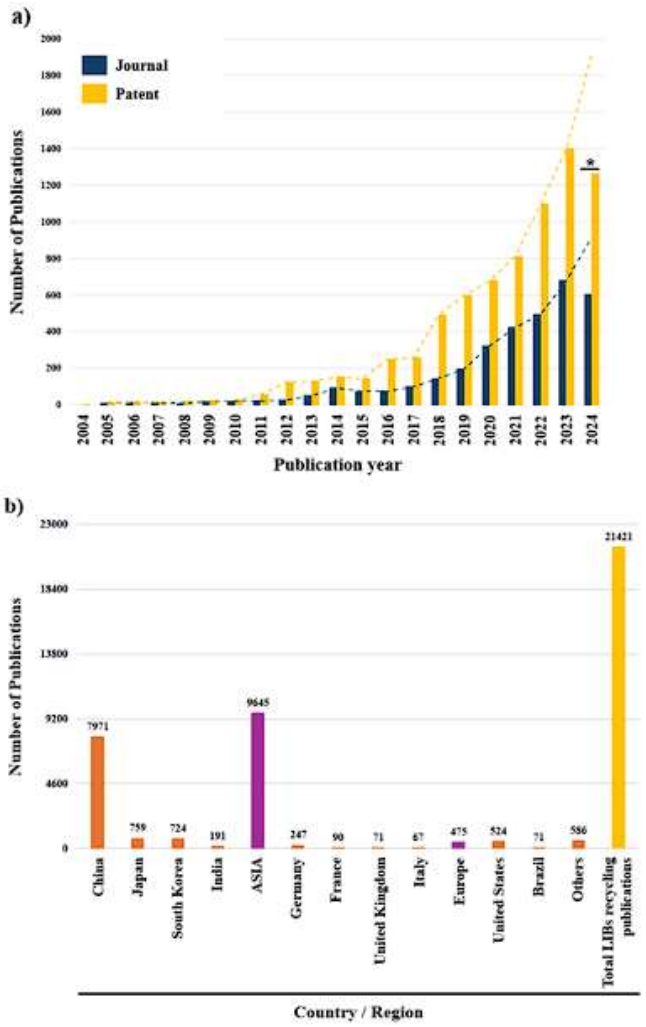

Figure 15. Graphs for the (a) Publication trends and (b) geographical distribution of publications in the field of LIB recycling between 2004–2024 years by countries and regions, *Data for 2024 is partial and encompasses January to September — figure reproduced with the data by CAS from Ref. [187].

Market and commercialised LIB recycling processes are currently dominated by three major methods of recycling LIBs, which are effective and differ from one another quite drastically in the approach they implement in recovering and recycling the metals and other particles from LIBs by breaking down the battery components into different forms that can be used to resynthesize new material [94], [103], [187].

1. Chemical processes
    - Pyrometallurgical,
    - Hydrometallurgical.
2. Physical process
    - Direct recycling.

Pyrometallurgy uses high-temperature heat treatment followed by separation. It is one of the most ubiquitous metal recycling technologies used and methods commercialised today in LIB recycling, which/can operate at large industrial scales (e.g., the steel industry), where conventional pyrometallurgical knowledge and industrial practicality can be partly applied to that of LIB recycling [26], [98], [187]. The concept of pyrometallurgy is the recovery of valuable LIB metals by decomposing the components of spent LIBs and converting metal oxides used in battery materials to metals or metal compounds, using high and elevated temperatures, which are then followed by purification through physical and chemical transformations, from the whole LIBs or their black mass (BM) [23], [40], [187], [188], [189]. These are achieved by processes such as smelting, pyrolysis, incineration, or torrefaction/calcination [93]. Out of this, calcination is one of the most used methods in pyrolysis for LIB recycling, which thermally treats materials in oxygen-deficient atmospheres to remove volatiles, inducing phase changes or decomposition. For LIB waste, it decomposes lithium metal oxides (e.g., $LiCoO_2$) into metal oxides and (Li_2CO_3), releasing oxygen in the process, which can be utilized [98].

Hydrometallurgy dissolves LIB components in aqueous solutions for recovery through concentration/purification, which is achieved via a series of chemical methods, most commonly by dissolution, precipitation, extraction, and crystallization [94], [98], [190]. Recycling concepts that utilize this method are known for their leaching of metal from the CAMs into ions in a solution using lixiviant solvents/chemical reagents as acids of organic or inorganic, alkalis, or reducing agents, which is then followed by metal recovery from the

leachate, leading to the metal purifying concept as recycling of hydrometallurgy, as the metals are recovered via precipitation, solvent extraction and electrolytic deposition [25], [190], [191], [192].

Direct recycling or functional recycling recovers components intact and happens without breaking down the cathode crystal structures of LIB components without the chemicals, aiming to keep their chemical structure, as they are manually disassembled and separated into different parts, and reconditioned [94], [187], [189]. The typical commercial purpose of this process is to re-lithiate and reincorporate electrode coating into a new cell, this can be done by electrochemical, mechanical, cathode-to-cathode, and cathode-healing [25], [26]. Allowing the maximization of material retention of constituent materials to their greatest extent [25]. The direct recycling strong points are that it offers low energy use, high recovery rates, short processing, eco-friendliness, and low cost, as the method recovers nearly all battery materials for reuse, thereby reducing both cycle time and material/energy needed [94]. Although direct recycling involves the direct recycling of batteries, it still requires pre-treatment methods, such as those used in hydrometallurgy, to isolate cathodic BM by removing Al foils and organic binders, which impede both leaching and leachate processing [94].

Out of these three predominant methods on an industrial scale, hydrometallurgy is the most used and researched topic due to the method's high and pure recovery rate of metals from the LIBs [185]. This has led to its mainstream technical route in the industry and the primary recycling process used in Asian countries [191]. The data by Chemical Abstracts Service (CAS) (**Figure 16**), shows that hydrometallurgy leads in publications over pyrometallurgy, while direct recycling trails, which indicates a stronger research focus on efficient, green chemical processes, which then further are elaborated by the data of these recycling methods in different LIB components and LIBs active battery metal oxides, as per (**Figure 17**) where hydrometallurgy and pyrometallurgy are close to one another, as their innovations, technological and recycling recovery rates increase for the metals, like those of CRMs [187].

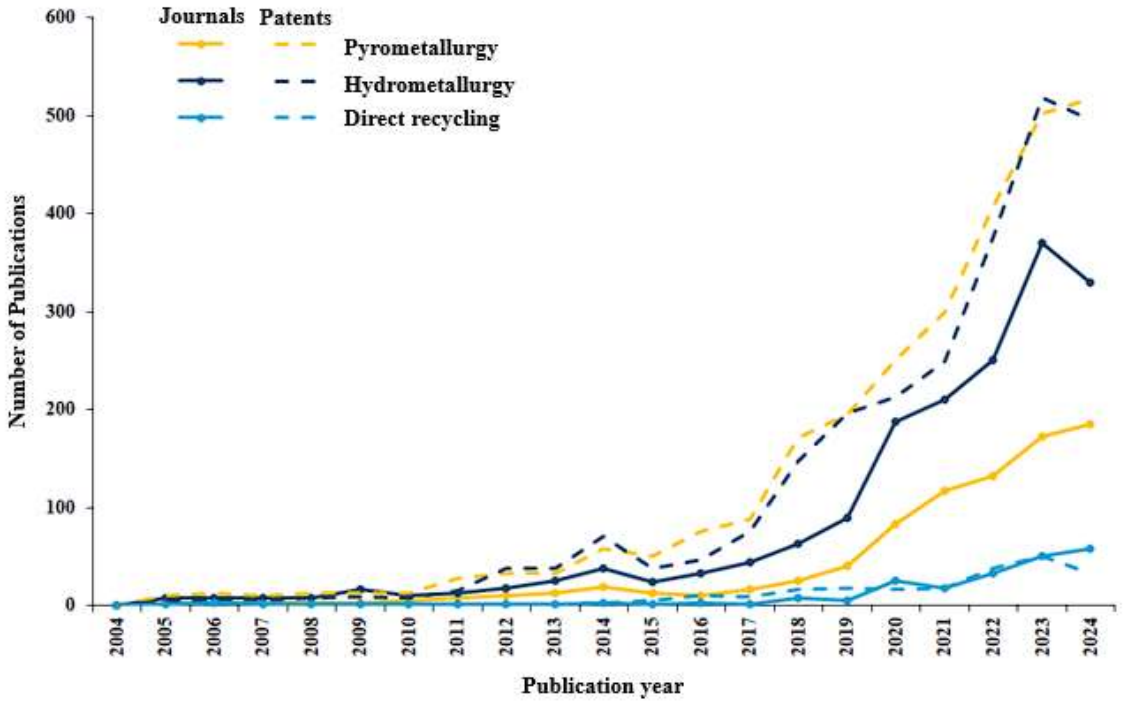

Figure 16. Graphs for the Publication trends for the most common and commercialised recycling methods/processes: hydrometallurgy, pyrometallurgy and direct recycling between 2004–2024 years, data by CAS and *Data for 2024 is partial and encompasses January to September — figure reproduced with the data by CAS from Ref. [187].

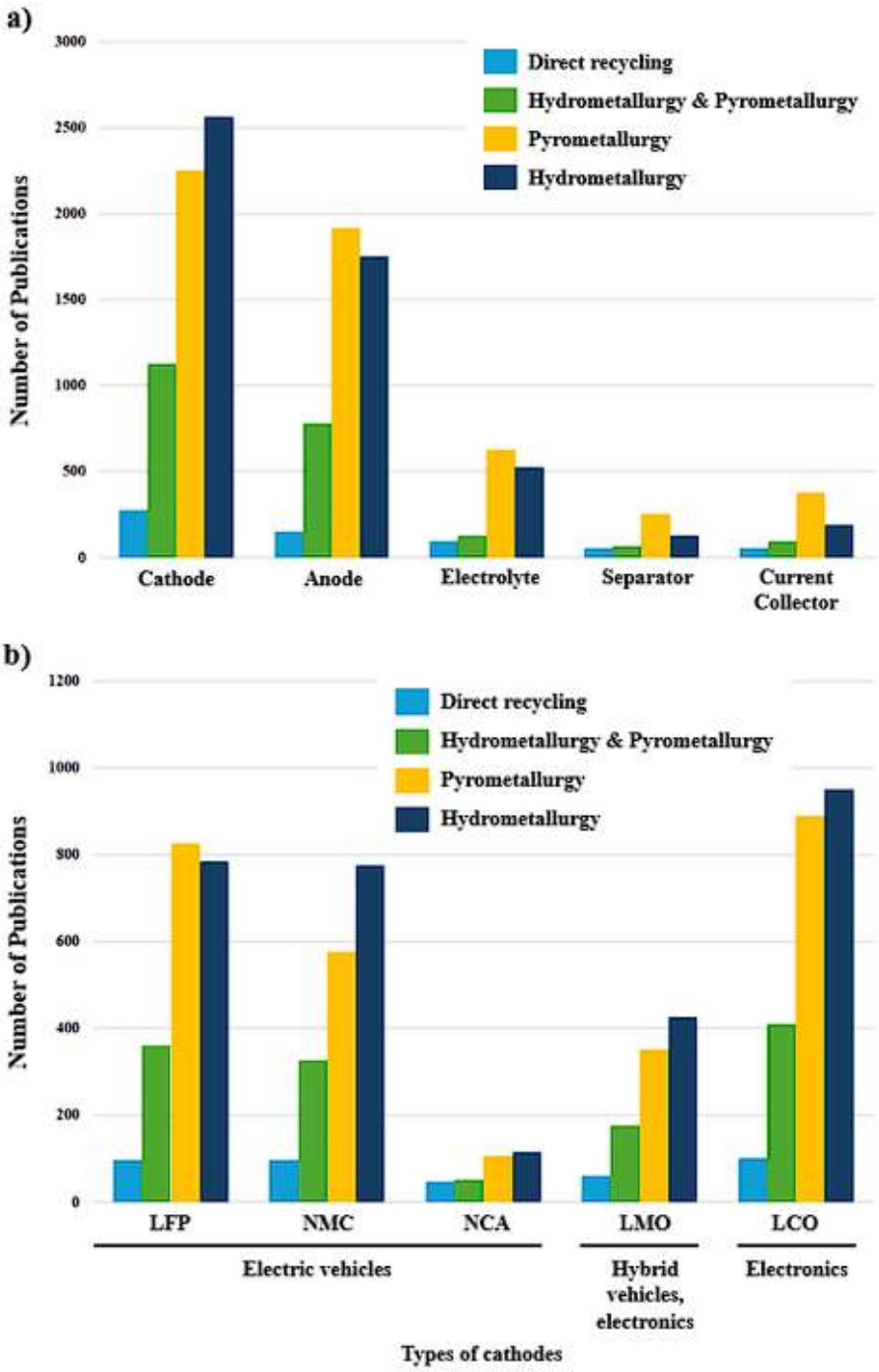

Figure 17. Graphs for the (a) trends of three major recycling methods-hydrometallurgy, pyrometallurgy and direct recycling with respect to various parts of LIB recycled (cathode, anode, electrolyte, separator, and current collector) and (b) major recycling respect to various types of LIBs (LFP, NMC, NCA, LMO and LCO) utilized in various applications between 2004–2024 years — figure reproduced with the data by CAS from Ref. [187].

As one may see the current trends and market projects those of what methods are more beneficial and widely used on an industrial scale when it comes to LIBs recycling, as

well as to what battery types are more commonly used in what applications, as the transition from more Co free batteries has begun, which also is contrasted by what battery types are more stable and optimized for the particular use.

4.1. Pre-Treatment Processes & Methods for the LIBs Waste

Before any pre-treatment may occur, the first stage of LIB recycling is the safe collection and sorting of EoL LIBs, which requires strict thermal runaway prevention measures during transportation [93], [98]. As a result, certain precautions have been implemented, such as the EU Battery Directive 2006/66/EC and the International Carriage of Dangerous Goods by Road (ADR) agreement, which govern international safety standards for the transportation, storage, and packaging of LIBs. According to this definition, the batteries of any type must be protected against extreme weather conditions, mechanical damage, and short circuits. The addition of resistant foils/sacks or marked drums, with packaging approved by ADR-compliant authorities, is required for portable batteries [93]. Afterward, only next may the pre-treatment step separate active cathode materials from other cell components (e.g., housings, current collectors, electrolytes, binders, separators) and convert LIB feed waste into BM, alloy, or matte. Subsequent metallurgical processing refines these materials into battery metal intermediates or precursors, while specialized recovery technologies further separate organic compounds (plastics, adhesives) from metallic fractions for refining [93], [98], [189]. LIBs have a complex structure comprising key components such as the cathode, anode, electrolyte, separator, and protective casing [190]. For these reasons, the pre-treatment separates the battery case from valuable materials, enabling subsequent pyrometallurgical, hydrometallurgical, or direct recycling processes [193]. The importance of pre-treatment is one of the requirements for other recycling methods, including the extraction of cathodic BM and the removal of Al foils and organic binders, which hinder leaching and further complicate the leachate downstream in the recycling line [94]. Because of this, the importance of pre-treatment at the initial stages is important, as the intermediates produced during pre-treatment impact the recovery efficiency and downstream conversion into battery-grade materials [189]. These are key elements in safety as the pre-treatment process is essential to: (1) safely dismantle batteries, (2) efficiently separate active materials and recover valuable components, (3) reduce impurities, and (4) enable downstream

recovery by leveraging the distinct chemical and physical properties of LIB components [190], [192]. This step is critical for safety, as it prevents hazards during disassembly while also concentrating valuables and minimizing waste through the recycling process [27], [191]. Typically, pre-treatments employ a wide array of methods for treatment, but industrially/commercially, they are divided into thermal or physical/mechanical methods employed in pre-treatment, though laboratory-scale processes often differ from industrial approaches due to varying operational priorities and research objectives [93], [188], [193]. As such, the pre-treatment process comprises multiple steps and varies based on different classification systems proposed by researchers and how the industrial/commercial ones are designed and operated [194]. For this reason, a different array of pre-treatment processes can be done as per commercial/industrial or laboratory scale, and in order of importance and ability to help the next process step to sufficiently contribute to the pre-treatment process as per (**Table 16**).

Table 16. Pre-treatment of LIB battery recycling is categorised into three different segments from the start to the end, before the main recycling process.

Phase	Key Processes	Ref.
1. Stabilisation / preliminary	- Discharging, - Sorting, - Dismantling, - Separation.	[27], [93], [98], [191]
2. Segregation	- Thermal: pyrolysis, evaporation, - Mechanical: crushing, shredding, sieving, pneumatic separation, - Physical: flotation, magnetic separation, gravity, separation, Eddy current separation, - Chemical: current collector foils dissolution - mechano-chemical processes (separation).	[94], [190], [192], [186]
3. Concentration	- Metal-rich fraction preparation for leaching/smelting	[40], [192], [194]

The better way to showcase the vast, but not so complex, pre-treatment process of LIB battery from the start to its appearance in pre-treatment to the end product of different raw materials for the recycling process, based on the (**Table 16**), can be illustrated by the (**Figure 18**) as seen below.

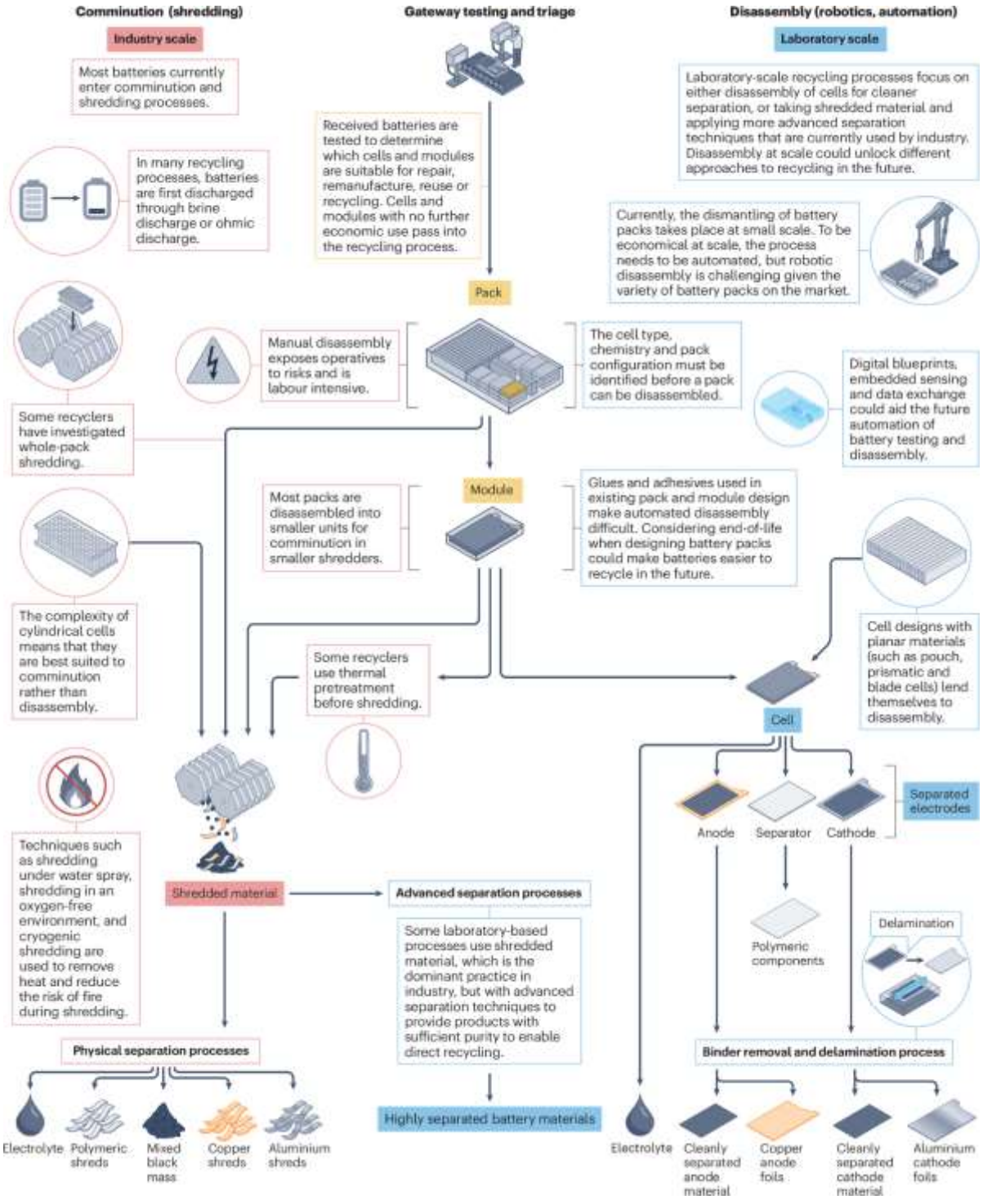

Figure 18. Pre-treatment approaches for the industry-scale pre-treatment processes (left, red) and laboratory-scale processes (right, blue). Both methods require disassembling packs into modules (centre, yellow), Figure/Schematic property of Ref. [189].

What (**Figure 18**) shows is the complex and transparent schematic of the pre-treatment approaches of three different ways how pre-treatment can be done. From this, we can see that while the approaches are different, they can be enhanced and supported by each other as they interconnect to yield better pre-treatment efficiency.

4.1.1. Sorting, discharging, disassembly and separation

Sorting the LIBs is a mandatory task for the LIB recycling process, as they have different chemistries and compositions of materials, which may make them hazardous, or they will yield bad recovery rates if done wrong in later stages. For this reason, the sorting method for spent LIBs is categorising them according to the battery chemistry. Because of this importance, the revised EU Battery Directive 2006/66/EC's “battery passport” in the future is supposed to enhance pre-sorting/deactivation safety through detailed battery chemistry documentation, as it comes into force on February 18, 2027 [98]. For this moment, Visual-manual sorting remains the EU standard (~50% of Germany's portable batteries), despite being labor-intensive, it yields remarkably high material recovery of (≥80% LIB mass) when disassembled manually [98], [189]. However, this labor intensity then leads to the current limitations of industrial scalability for specific cell types, such as planar cells, due to their complexity [94]. These constraints underscore how battery architecture dictates recycling efficiency, necessitating design-for-recyclability approaches [94], [189]. For these reasons, the most common separation processes at the sorting stage are those from handpicking to magnetic separation, X-ray, electromagnetic, and UV-based sorting [98]. Challenges and barriers that the recycling industry faces due to their size, weight, and non-standard designs make manual sorting/disassembly the only viable but costly option, as industrial-scale automation struggles with non-standardization and vast commercial market battery selection. This underscores the need for better labelling and automated sorting, as they are urgently needed [98]. The use of smart systems or AI-assisted alike in EV batteries can help to optimize component tracing and pre-treatment sorting, which then would allow intelligent visual recognition, enabling precise electrode separation for efficient recycling, as already has been tested on a laboratory scale, with the commercially available/deployed X-ray fluorescence and automated sorting technologies [94], [142], [191]. Sorting is not only used in the starting process of pre-treatment or recycling but also in its various stages throughout,

as the sieving/screening isolates metal-rich fractions in battery preprocessing and allows better separation at the end [193].

Discharging is an important risk management, which in (**Figure 18**) can be relied on for safety as well as hazardous materials in both of the routes presented [189]. For safe handling, LIBs are required to be stabilized, which is typically done industrially via discharge (e.g., salt solutions or Ohmic methods), to mitigate or subsequently remove the risk of thermal or gaseous reaction, as the residual energy stored in LIBs, that may lead to explosions, short circuits, and toxic emissions to those of HF or lithium hexafluorophosphate ($LiPF_6$) [40], [189], [190], [192]. Although using physical discharge is relatively common, it risks thermal damage to the electrode material or battery casing when passivating LIBs [191]. These are the cornerstones of pre-treatment to eliminate reactive lithium and enable safe post-processing afterward [40], [190], [192]. To achieve and utilize the ohmic method for LIBs discharge, done by LIBs are connected to a resistor, which in turn extracts residual energy for reuse via electron flow, gradually depleting the electrolyte energy inside the cell, thus leading to passivation [94]. Although this method allows for simplicity, it has some drawbacks; it is labor-intensive due to the precise terminal contacts that must be achieved for the method to work, which is why the option of implementing robotics and smart systems has been in the process [188]. Overall, this method is impractical for larger-scale industries, which is why it is primarily used in research and laboratory-scale applications [94]. As the chemistry and pack design of those EV LIB batteries continue to differ, they become heavier and larger, led by the EV architecture [27], [189]. However, other methods, such as the use of aqueous salt-saturated solutions of halide salts, are viable [27], [189]. Salts that are most commonly employed in pre-treatment include Sodium Chloride (NaCl), Sodium Sulphate (Na_2SO_4), Magnesium Sulfate ($MgSO_4$), or Sodium Carbonate (Na_2CO_3) [27], [94], [191], [194]. These are all viable options and, to some extent, used industrially. What salts allow is to process larger batches of LIBs, as they minimize the short-circuiting in batteries and reduce the material deposition in anodes [94]. The main reasons for salt not being commercially adopted are due to the risk associated with it not being suitable for high-voltage components and that the process of submerging components into salts is time-consuming, hence reducing the efficiency of the process [190], [191]. Salts have also been seen to cause corrosion of electrodes and their materials due to their chemical reaction with the addition of sediments [27], [189], [194]. However, some studies have achieved none of

the before by utilizing NaCl, Na_2S, and $MgSO_4$ [194]. A more novel method of conductive powder has also been tested, but it has been found to be prone to thermal runaway reactions [189].

Disassembling one step before the separation is instrumental in the recovery rates of the LIB materials and making the process profitable, as the dismantling of the LIB makes residual components easy to access for other processes, and as the value of the components is high, as the CRMs market is in demand [98]. Disassembly can either be done manually or automatically, similarly to the separation step, but most typically, manual disassembly is adopted in laboratories, laboratory scale-ups, and pilots [27], [94]. Nevertheless, the pre-treatment of EV and NEV EoL batteries involves physical intervention in disassembly due to the lack of standardization in both recycling and manufacturing, as EV batteries and storage systems have a high voltage range and high energy density [98]. If disassembly is done manually, it typically involves the removal of the battery from the casing or the battery back so that the cell or core of it can be handled [94]. The importance of automation in future and current LIBs recycling pre-treatment is evident, as the masses and capacities of factories increase [189]. However, at the same time, technology seems to be immature and highly dependent on the LIBs design, which could be a key factor in scaling the circular economy [189]. Due to the immaturity of automation, human intervention is necessary to some extent, leading to risks associated with the LIBs, leading to precautions such as personal protective equipment (PPE) (e.g., masks, protective glasses, gloves, etc.) [27], [189]. The use of PPE is important when dismantling batteries, as PVDF risk and exposure increase, as residues of it may be found on cathodes, and these may go further in the process and hence the recycling process and contaminate the environment and waste material being separated [17]. Because of these, the importance of developing future automation would increase the efficiency and critical safety of the process [27], [189], [193]. Overall, manual disassembly yields high purity of the final separated product, but as stated in the long term, this is not an option/method as it is unsuited to large-scale industrial applications, as such fixing this would also enhance and benefit direct recycling [27], [189]. Automation can make battery pre-treatment more economical by enabling rapid disassembly into components, with UK researchers developing processes to safely recover materials while reducing worker risks [186], [193]. However, these are hindered by the current battery pack design, which is why more modular designs could improve repairability and disassembly, but as current battery

designs often use adhesives, complicating recycling by causing contamination and mixed phases, hence increasing operational costs [98], [142], [189], [193]. One way to improve this could be by implementing a shredding technique, which would allow for cleaner mechanical separation to produce material streams, thereby leading to more recovery of materials in a higher-value state by utilizing less of the post-treatments in the process [189]. To achieve these, several enterprises are working together to bring the necessary technology and technical information to enable the zeroth stage of recycling by automation as the onset of the Industry 4.0 [193].

Separation is the final step in the recycling process, and its importance determines the quality of the end results. Effective separation of battery components is critical prior to hydrometallurgical processing, as residuals of Al and Cu foils impair the leaching efficiency of the process [94]. After the spent batteries have been disassembled and their electrodes have been sorted out and forward stripped of their active materials, they undergo mechanical or chemical separation based on material properties like (density, magnetism, and solubility) to isolate active materials from current collectors and binders alike [190]. In addition to these two separation methods, other types can be added as sub-separation processes (thermal and mechano-chemical, etc.) [94]. As the impurity removal by these processes enables the subsequent recovery processes, they all subsequently stress the need for a commonly shared fundamental constraint: lithium recovery occurs terminally in the process chain, often resulting in significant losses and contaminated lithium carbonate [194]. By pre-separating the battery components from the waste streams, recycling provides more valuable and higher-purity renewable materials in addition to increasing recycling efficiency and lowering energy consumption across related later separation procedures [186], [194].

4.1.1.1. The Physical and Mechanical Separation

Many different separation methods are necessary, and each one differs from the others, as they are all designed to achieve one primary goal: separation. However, utilizing different properties of the material being separated (**Table 17**) reveals the separation methods employed in the pre-treatment of LIB recycling. Mechanical separation is a key automated pre-treatment step that maximises material integrity while prioritising safety and efficiency

[190]. Relying on physical properties (size, shape, and material type), post-dismantling, it separates components (plastics and non-ferrous metals) into distinct waste streams by particle size for optimal resource recovery [27], [94], [190]. While offering high-purity materials and scalability, challenges still remain, such as impurity introduction and incomplete separation due to component interpenetration, due to LIB's complex structures, subsequently rendering specific methods weak and insufficient to yield desirable results on complete separation [27], [186], [190]. Nonetheless, the physical/mechanical methods allow for downstream recycling by utilising the following:

- Isolating inorganic/organic components,
- sorting non-ferrous metals by particle size,
- and reserving material integrity [186], [190].

Table 17. Physical and Mechanical separation pre-treatment processes/methods in LIB Recycling. Table reproduced by Refs. [27], [94], [98], [186], [190], [192], [193].

Method	Advantages	Disadvantages
Mechanical Crushing	- Low cost and simple operation - High efficiency and strong processing capacity - Effectively releases valuable materials - Concentrates on useful components - Widely applicable in industry - Reduces the volume of spent LIBs	- Particle size distribution and release degree can affect subsequent recovery - Requires safety precautions (e.g., for toxicity, reactivity) - Significant gas emissions (e.g., CO_2, DMC, EMC) - High risk of short circuits and fire due to thermal reaction
Dry Crushing	- Enables selective crushing for better material separation - Avoids component loss (e.g., graphite) - Higher purity of active materials - Convenient for purification and regeneration - Safer when done in inert gas (avoids friction and impact hazards) - More practical - High processing efficiency - Prevents short-circuiting	- Potential emission of toxic substances if not done in an inert gas - Less effective at reducing toxic emissions - Safety risks from sparks and heat in a normal atmosphere - Particle size distribution may complicate downstream recovery - Cost because of inert gas
Wet Crushing	- Reduces and even prevents of toxic substance emissions (harmless treatment) - Reduced fire and explosion risk - Effective component release in salt solution	- Erosion from liquid turns materials into fine particles - Complex particle mixtures hinder separation - Loss of valuable materials like (e.g., Gr)

(*Continued on next page*)

Table 17. (*Continued*)

Method	Advantages	Disadvantages
Wet Crushing	- Reduces lithium reactivity - Uses salt solutions (e.g., NaCl, $MgSO_4$)	- Makes subsequent recovery more complex - May be less efficient for material recovery
Cryogenic Crushing	- Safe operation - Enhances subsequent processing Used in the Retriev process	High cooling costs (e.g., liquid nitrogen)
Mechanical Crushing	- Low cost and simple operation - High efficiency and strong processing capacity - Effectively releases valuable materials - Concentrates on useful components - Widely applicable in industry - Reduces the volume of spent LIBs	- Particle size distribution and release degree can affect subsequent recovery - Requires safety precautions (e.g., for toxicity, reactivity) - Significant gas emissions (e.g., CO_2, DMC, EMC) - High risk of short circuits and fire due to thermal reaction
Dry Crushing	- Enables selective crushing for better material separation - Avoids component loss (e.g., graphite) - Higher purity of active materials - Convenient for purification and regeneration - Safer when done in inert gas (avoids friction and impact hazards) - More practical - High processing efficiency - Prevents short-circuiting	- Potential emission of toxic substances if not done in an inert gas - Less effective at reducing toxic emissions - Safety risks from sparks and heat in a normal atmosphere - Particle size distribution may complicate downstream recovery - Cost because of inert gas
Wet Crushing	- Reduces and even prevents of toxic substance emissions (harmless treatment) - Reduced fire and explosion risk - Effective component release in salt solution - Reduces lithium reactivity - Uses salt solutions (e.g., NaCl, $MgSO_4$)	- Erosion from liquid turns materials into fine particles - Complex particle mixtures hinder separation - Loss of valuable materials like (e.g., Gr) - Makes subsequent recovery more complex - May be less efficient for material recovery
Cryogenic Crushing	- Safe operation - Enhances subsequent processing - Used in the Retriev process - Makes material brittle - Makes material electrochemically inactive	- High cooling costs (e.g., liquid nitrogen) - Complexity
Sieving	- Simple and effective preliminary separation based on particle size distribution - Separates fine (BM) from coarse components (e.g., Al-Cu foils) - Reduces downstream hydrometallurgical steps - Improves the separation efficiency of battery waste streams	- Components might not fully be separated if particle size differences are not distinct enough - Potential for material loss during separation - Efficiency depends on prior treatment/separation method (e.g., crushing)

(*Continued on next page*)

Table 17. (*Continued*)

Method	Advantages	Disadvantages
Sieving	- Can be automated with screening systems - Allows selective crushing performance of waste LIBs	- Cannot distinguish by material type
Selective Crushing & Sieving	- Enhances material purity for downstream recycling processes - High-purity fraction recovery (Al, Cu, Co/graphite) - Capitalises on LIBs' natural selective crushing behaviour, requiring minimal energy input - Utilises inherent material properties for efficient separation - Provides a simple, cost-effective mechanical solution compared to complex chemical methods - Low operational complexity and costs	- Density/chemistry-blind separation - Persistent material cross-contamination - Added processing costs (secondary purification required) - Material-agnostic (size-only approach) - Incomplete separation (residual mixed fractions)
Cathode Sorting with Sieving	- Reduces input material variability – Minimises uncertainty in feedstock composition - Enhances separation precision – Enables targeted recovery of specific materials (e.g., cathode components) by size fraction - Optimises downstream processing - Improves overall separation efficiency of waste streams - Enables battery-type specific sorting (particularly cathode materials) Stabilises input material characteristics for consistent processing - Maximises recovery efficiency through size-fraction-based separation	- Pre-Processing: Battery-type dependent (requires upfront classification) - System Complexity: Infrastructure-intensive (multiple sieving stages - Efficiency: Throughput-limited (batch processing constraints) - Separation: Universality gaps (fails for size-similar/size-insensitive components)
Eddy Current Separation	- Environmentally friendly - Effective for nonferrous metals (e.g., Al, Cu) separation - Works well for particle sizes (>1 mm) - Highly efficient for conductive materials - Recovery yield of 85%	- Limited to larger particle sizes (2–10 mm) - Not effective for fine particles - Requires optimised belt speed for different particle sizes
Pneumatic Separation	- Recovers metal foils from crushed products	- May be less selective - Efficiency depends on material flow properties
Electrostatic Separation	- Effective for collecting conductive materials and non-conductive dry particles - Works when particles are fully dried	- Requires completely dried particles - Less effective if moisture is present in the system

(*Continued on next page*)

Table 17. (*Continued*)

Method	Advantages	Disadvantages
Magnetic Separation	- Effective for separating Fe, Ni and Co cathode particles and Al-Cu electrodes from nonmagnetic materials (e.g., plastics) - Minimal cathode loss (1.7%) - Removes nonmagnetic materials (e.g., plastics) - Proven industrial applicability and commercialisation - Relatively low energy consumption	- Limited to materials with magnetic properties only - Lower recovery rates compared to fluid-magnetic methods
Wet Magnetic Separation	- Effective for processing mixed cathode materials - Enables purification of separated components - Recovery rate of >90% for component fractions	- Requires moisture or some sort of liquid medium handling and potential water treatment - May not be ideal for dry systems - Complex
Fluid-Magnetic Separation	- Environmentally friendly - High recovery rates (e.g., 98.26% overall, 99.21% for Co, 97.91% for Ni) - Excellent purity for target metals - Twice as efficient as standard magnetic separation	- Likely more complex and costly - Specific to vacuum reduction products - Requires specialised equipment
Gravity Separation	- Simple separation method - Separates materials based on density differences - Heavy metals from lighter plastics - Commonly used on an industrial scale	- Less effective when material density differences are small
Flotation	- Efficient for fine particles - Based on material differences in surface hydrophilicity (e.g., $LiCoO_2$ (hydrophilic) from graphite (hydrophobic))	- Organic coatings reduce selectivity - Requires surface modification for effectiveness - Organic material coating reduces effectiveness - PVDF binder masks wettability differences - PVDF binder can reduce selectivity - Solvent methods may introduce impurities
Surface Modification (pre-treatment for flotation)	- Improves flotation efficiency - Enhances wettability differences	- An additional processing step is required - This may increase the complexity and cost of the separation process
High Voltage Fragmentation (HVF)	- Effective for complex products - Target weak points at material boundaries - Selective disassembly - Uses shockwaves to break products via dielectric breakdown - No need for additional chemicals	- Expensive - Less cost-effective than conventional crushing - Limited to lab-scale - Electrolyte recovery remains uncertain

As one can see, there is a wide variety of different methods how physical and mechanical separation of pre-treat LIB waste, to achieve the end goal of high purity and effective recovery at the end of the processes, based on (**Table 17**) information listed.

4.1.1.2. The Chemical & Mechano-Chemical Separation

Chemical separation in LIB recycling refers to the process in which the selective extraction and purification of those metals (e.g., Li, Co, Ni, and Mn) and other components are retrieved at certain recovery rates using chemical methods. This step is crucial for recovering high-purity materials that can be reused in new batteries or other applications. As the batteries have binders in their structures, they are held by them in addition to SEI/CEI films, the use of alkaline solutions or organic solvents to liberate active materials from the current collectors, in comparison to those of physical and mechanical separation methods, that had problems or were not suitable for material recovery [190]. Mechano-chemical processes are processes that utilize both the chemical and mechanical properties of pre-treatment, such as integrating shredding and chelating agents (e.g., EDTA) to liberate active materials from LIB electrodes [94]. The method utilizes inducing structural modifications through mechanical forces (e.g., friction and collisions) to generate defects in recycled materials, allowing for phase transitions and reduced energy activation for the recovery of active materials and other elements from LIBs [190]. Hence, these methods have been implemented in the pre-treatment processes to improve leaching conditions; as such, different types of chemical and mechano-chemical pre-treatment methods are presented below (**Table 18**), along with their advantages and disadvantages in comparison to one another [27].

Table 18. Chemical and Mechano-chemical separations of the pre-treatment processes/methods in LIB recycling. Table reproduced by Refs. [27], [94], [190], [192].

Method	Advantages	Disadvantages
Chemical Separation	- Effective for separating electrode materials from Al foils - Works with various solvents (NMP, DMAC, DMSO, DMF, ionic liquids) - Alkaline solutions (NaOH) preserve cathodic oxides - High efficiency in extracting Al and other metals	- Solvents are expensive and toxic - Not suitable for large-scale processes - Binder-specific (no universal solvent) - NMP is ineffective for PTFE binders - Requires high temperatures (>90 °C) - Leaves impurities requiring calcination - Metal losses are unavoidable - Alkaline solutions introduce impurities
Mechano-Chemical Separation	- Combines the benefits of mechanical and chemical methods - Enhances particle surface area for better leaching - Enhances downstream acid leaching (e.g., efficiency) - Breaks bonds and increases surface area, hence reactivity - Uses eco-friendly chelates (e.g., EDTA or PVC)	- Long reaction time - Not practical for industrial scale
Chemical Separation (Organic Solvents)	- Effective at detaching active materials from Al foils and PVDF binders - Solvents like (NMP, DMAC, DMSO, DMF, and ionic liquids) can dissolve PVDF - DMF is more efficient, lower cost, and less toxic than NMP - Effective PVDF binder dissolution (200 g/kg at ~100°C) - Low energy consumption - Ultrasonic assistance improves efficiency - High separation efficiency - Al recovered in metallic form	- Solvent choice is binder-specific (e.g., chemistry) - Ineffective on PTFE binders - Toxic and expensive solvents - Not suitable for large-scale use - Residuals may require calcination - High solvent costs
Chemical Separation (Alkaline Solutions)	- Simple operation - Efficiently dissolves Al without reacting with cathodic oxides - Selective Al recovery via amphoteric properties - Preservation of other metals - High Al extraction efficiency (~97 wt.%) and high separation overall - Supports clean recovery of electrode active materials	- Material loss is unavoidable - Introduces impurities that hinder downstream recovery (e.g., alkaline wastewater) - Introduces hardly-leachable ions - High equipment cost for treating alkaline wastewater

(*Continued on next page*)

Table 18. (*Continued*)

Method	Advantages	Disadvantages
Green Solvents	- Environmentally friendly - Reduces toxicity and environmental impact - Can dissolve PVDF in (~20 min.) - Cheaper alternatives to synthetic solvents - Low impurity introduction - High separation efficiency	- Ineffective on PTFE - Requires high temperatures (>90 °C) - Lower efficiency compared to conventional solvents - High cost of green solvents - High energy consumption for electrochemistry
Mechanochemical Activation	- Improves metal extraction efficiency - Works under normal temperature/pressure - Environmentally friendly (no strong acids/reductants) - Shortens leaching reaction time - Enables selective extraction	- Requires specialized equipment - Limited industrial scalability due to process complexity
Ultrasonic-Assisted Leaching	- Higher leaching rates - Environmentally friendly - Increases solid-liquid contact area - Promotes binder degradation - Effective for both organic and inorganic acids - Efficient and targeted peeling	- Energy-intensive - Requires precise control of ultrasonic parameters - May involve chemical residues
Reduction Thermal Treatment	- Reduces the need for chemical reductants - Enhances subsequent acid leaching efficiency - High recycling yields for Co and Li	- High energy consumption (600°C) - Potential gas emissions from thermal decomposition

From (**Table 18**) can be seen that the methods have a more positive and advantageous impact in general than that of negative on the pre-treatment of the LIBs as it goes through them, yielding better results at the end. What also should be noted is that, as some may not be optimal for certain processes, the other/others are.

4.1.1.3. The Thermal Separation

As the demand for greener alternatives, such as EVs, NEVs, and energy storage systems, increases, so does the need for various pre-treatment techniques in the recycling of LIBs, including thermal processes. These pre-treatment processes play a pivotal role in conditioning the metallurgical recycling process, enabling the recovery of valuable materials from spent LIBs by removing hazardous elements. The most common thermal type of pre-treatment is pyrolysis, which reduces residual energy while eliminating organic components

and volatilizing halogenated compounds through exhaust gas streams, utilizing thermal principles [98]. Overall, the thermal pre-treatment may be that of pyrolysis may be that of pyrometallurgical processes, which, as has already been established, utilise high temperatures (e.g., smelting or incineration) to extract metals with different melting points from the spent LIBs and waste stream [142]. For a better understanding of different thermal pre-treatment separations, and to see what kinds of thermal separation processes are available, the following table (**Table 19**) provides an overview, including the advantages and disadvantages of each, regardless of whether they are industrial-scale or laboratory-scale methods.

Table 19. Thermal separations of the pre-treatment processes/methods in LIBs recycling with details of the methods, to advantages, and disadvantages. Table reproduced by Refs. [40], [94], [98], [192].

Method	Details	Advantages	Disadvantages
Thermal Pre-treatment	- Deactivate and stabilise LIBs before disassembly - Decomposes organic components and discharges residual energy - Removal of carbon (avoid Li absorption)	- Ensures safety by discharging and deactivating batteries - Removal of problematic organic materials before further processing - Improved leaching and solid-liquid separation efficiency - Widely applicable at the lab and industrial scale	- Some cathode powders may remain attached due to strong binder adhesion - Crushing and comminution may release toxic gases and cause loss of valuable powders - Improper binder removal affects froth flotation efficiency - Energy-intensive
Incineration Pre-treatment	- Burning of carbon and binder in air/oxygen at high temperatures - At 700°C for 60 min, enhances Li and Co recovery via carbon removal - The ANVIL method uses 500°C to neutralise adhesion and enables mechanical separation	- Improves recovery of Co and Li by complete removal of carbon - Can recover energy as steam - Metal encapsulation issues are minimised by using a moderate temperature	- High temperature (700°C) can cause Al foil melting, covering active material and reducing recovery - Risk of oxidation of metals - Cannot recover organics for reuse - Limited metal selectivity

(*Continued on next page*)

Table 19. (*Continued*)

Method	Details	Advantages	Disadvantages
High-Temperature Pyrolysis	- Decomposition of organic components (e.g., PVDF) at 500–600°C, allowing active material detachment from Al/Cu foils	- Enables easy separation of active material - Effective binder removal - Increases leaching efficiency due to phase transformation (e.g., $LiCoO_2 \rightarrow Co_3O_4$) - Li recovery (~90%) - Allows for (76–80 wt.%) solid residue for mechanical treatment - Prevents oxidation	- Above 600°C damages Al foil (melting/fragility) - Above 600°C causes aggregation, reducing the separation efficiency - Produces toxic gases (e.g., HF, dioxins, CO/CO_2) - Requires a gas filter or scrubber
Vacuum Pyrolysis	- Uses a vacuum chamber to prevent oxidation during high-temp treatment	- Protects metals from oxidation - Eliminates the need for continuous pressure monitoring	- Higher energy consumption - Requires vacuum systems and monitoring
Oxygen-Free Roasting	- Roasting in a nitrogen atmosphere	- Enhances magnetic separation efficiency - Co recovery (~75%) - Avoids oxidation - Enables Gr precipitation - Li_2CO_3 dissolves in water	- Involves high temperatures - Requires controlled inert gas setup - Requires additional separation steps
Cryogenic Treatment	- Uses very low temperature (to 200°C) to inactivate lithium, then combines it with wet grinding	- Safer handling of reactive lithium - Isolates cathodic material efficiently - Compatible with mechanical separation	- High energy consumption - Expensive and complex infrastructure required
Low-Temperature Treatment (100–150°C)	- 30-minute treatment	- Facilitates safer battery handling - Reduction in the risk of thermal runaway during crushing	- Incomplete binder removal

(*Continued on next page*)

Table 19. (*Continued*)

Method	Details	Advantages	Disadvantages
Intermediate-Temperature Treatment (300–500°C)	- 1-hour treatment post-crushing	- Separates $LiCoO_2$ from foils	- Energy-intensive - Partial organic removal only - Incomplete binder removal
Gas Treatment System	- Condensers and scrubbers capture pyrolytic gases - Separates organic constituents	- Recovers valuable organic compounds - Reduces environmental pollution	- High investing and operational costs - System complexity

Different thermal separations as per (**Table 19**) allow for effective and fast pre-treatment of the LIBs waste in a fast-growing industry, thus benefiting the recycling processes and allowing a high yield of return in them. Throughout industry life, each of the different methods has been tailored, used, and is still being used for that one goal, yielding high efficiency and purity in the end product in the process.

4.2. The Hydrometallurgical process of LIB recycling

Current industrial and commercial LIB recycling involves some form of metallurgical process, such as those employed in extraction metallurgy (pyrometallurgy and hydrometallurgy), out of which hydrometallurgy utilizes mechanical and thermal pre-treatment to facilitate the dissolution of LIB waste [195]. As shown before, the pre-treatments are the crucial part and needed for the spent LIBs, as the waste of active cathodic powder, cathodic black mass are to be separated and leached via different techniques for the separation and purification of the valuable metals from LIB, rich transition metals Co, Ni, and Li by hydrometallurgy [94], [97], [192]. Hydrometallurgy's working principle is highly dependent on the pre-treatment and how it is performed before the process, as it enhances the subsequent process or material recovery [94], [192]. Meaning stages involving (sorting, discharging, disassembly, and separation), (physical and mechanical separation), and (chemical and mechano-chemical separation) have occurred by involving some sort of methods as per (**Tables 17 – 19**) visible [195]. An important factor for hydrometallurgy is the pre-treatment increase in the surface area of the crushed BM, allowing for the process's effective recovery and exploitation of recovery methods [94]. However, these are not the

only reasons for utilizing pre-treatments before the recycling processes, as they enrich metals, minimize waste, boost recovery, and mitigate safety risks [195]. This is important as the process is already hindered by the presence of Al foils and organic binders (i.e., separating cathode materials and Al foil from binders (e.g. PVDF)) in the BM, which impede leaching efficiency and complicate subsequent leachate processing of resources, but this is not only in hydrometallurgy but also an issue in direct recycling process [94], [192], [194]. Extraction and recovery of BM resources are typically performed through three main steps: leaching, separation, and subsequent purification [40], [189], [191], [193], [195]. As such, the extraction is typically done commercially by a low-temperature (<200°C) solution-based process using water-immersion chemical methods, like those of leaching in acids (or alkalis), thus turning pre-treated battery material metal elements into ions, by strong chemical acid and reducing agents are allowed to attack the material due to increased surface area of the crushed BM [93], [94], [98], [186], [192], [193], [195]. Afterward, dissolved metal in the concentrated solution is subsequently separated using techniques such as selective chemical precipitation, crystallization, ion exchange, electrodeposition, and solvent extraction, after which the purification can be done using other methods for the subsequent refining and recovering metals as salts or as straight raw materials [40], [93], [98], [186], [189], [192], [195]. What makes this process itself lucrative and appealing to others in the market/industry around is the:

- Reduced energy, due to lower temperatures,
- Recovery of the Li in carbonate form,
- Leaching of metal to be reused in LIBs manufacturing,
- Good efficiency across all the different battery chemistries [192], [196].

What hydrometallurgy brings to the recycling is the offer of higher selectivity, enabling more direct and efficient recovery techniques for the optimized recovery, such as Li with recycling rates typically exceeding 90%, utilizing different arrays of steps, as shown above, to optimize efficiency by subsequently reducing and removal of impurities in process and recovered material alike, with the selective metal dissolution [98], [194]. While most methods of metallurgy are highly chemistry-oriented, some can process mixed Co-, Ni-, and Mn-based batteries [197]. However, few are compatible with all battery types, including phosphate-based systems [197].

For the past decade, hydrometallurgy processes have emerged as the dominant recycling approach, particularly in Asia, which is in clear correlation with that of (**Figure 15** (**b**)) data, which shows China's impact on patents and journals increases in that time frame [186], [191]. This is due to the process currently being the most widely adopted LIB recycling approach, with pyrometallurgy, which has also led to the combination of both techniques for the most optimal and efficient material recovery from secondary raw materials [93], [196]. Still, the major companies of China's GEM Co., Ltd, and Brunp use the hydrometallurgical processes in LIB recycling. Although the process may be widely adopted in China and South Korea, this is not the case for the US and Western countries, as the process is plagued by the high operational costs limit when looking at the prices of raw/transportation costs required for operation. [186] Commercial hydrometallurgical operations typically recover valuable compounds, including metal sulfates and lithium phosphate, from spent batteries and are the primary method for separating different valuable elements (i.e., Co, Ni, Mn, and Li) as single-element compounds [189], [197].

It has also been discussed that when BM is being processed, the re-synthesization of battery-grade materials happens in a sense, which can be viewed as a closed loop of recycling and leading to the principles of CE [99]. As the methodology involves the dissolution of the material via leaching, it requires considerable energy and water resources for the process to be continuous, leading to large consumption quantities of reactants, hence generating significant liquid waste streams [195]. This means that, while it may be viewed as a closed loop, it is far from the sustainable processes out there for LIB recycling [98], [195]. Additionally, recycling is overall only the third ladder on the Waste Hierarchy schematic, as per (**Figure 6**), being overtaken by prevention and preparing for re-use, which may and will lead to further changes and motivate changes in technology/recycling alike [195].

4.2.1. Leaching Processes with the Reducing Agents

Leaching is one of the most critical steps in hydrometallurgical processes for recovering valuable metals from spent LIB's BM mass that has all of the cathode material in it, which is dissolved into a concentrated solution for subsequent separation and purification at a later date [198]. Leaching as a process primarily employs inorganic acids (e.g., sulfuric (H_2SO_4),

hydrochloric (HCl), nitric acid (HNO_3), phosphoric acid (H_3PO_4)) because of their high leaching efficiency at low concentrations, enabling near-complete dissolution of metals from BM [27], [189]. There is also a wide use of the organic acids (e.g., citric ($C_6H_8O_7$), oxalic ($C_2H_2O_4$), tartaric ($C_4H_6O_6$)) that serve as more environmentally friendly alternatives, leveraging acidolysis and complexolysis mechanisms to dissolve metals while at the same time minimizing the secondary pollution, although they are and have that of weaker leaching capacity in them [196]. While alkaline and bioleaching methods are being explored, they remain less common compared to acid-based approaches for the moment being [190], [193]. Hydrometallurgical leaching has significant efficiency factors, as its efficiency process depends on key parameters such as the solid-to-liquid (S/L) ratio, temperature, leaching duration, and the use of reductants to enhance metal dissolution in the concentrated leaching solutions [192], [195]. Due to its effectiveness and adaptability, acid leaching stands as the predominant method in both research and industrial applications when it comes to LIB recycling [27].

4.2.1.1. The Organic Acid Leaching

Organic acids have gained increasing attention as sustainable alternatives for the inorganic acids in the LIB recycling, as their biodegradability and reduced environmental impacts are their biggest driving forces in the industry [27], [101]. Certain organic acids offer dual functionality, as they both act as leachers and chelating agents, facilitating direct metal recovery and simplifying subsequent processing steps directly from the concentrated solutions [27]. Thanks to studies and, more importantly, commonly used organic acids such as $C_6H_8O_7$, malic acid ($C_4H_6O_5$), aspartic acid ($C_4H_7NO_4$), oxalic ($C_2H_2O_4$), acetic acid (CH_3COOH), and ascorbic acid ($C_6H_8O_6$), organic acid leaching process as a whole has demonstrated effective leaching performance while minimizing toxic gas emissions (e.g., Cl_2, NO_x, SO_x), emissions are associated with inorganic acids [27], [98], [189], [196], [197]. While organic acid leaching may have advantages over inorganic acid, it also presents challenges in separating similar elements, such as Al, Cu, Ni, Mn, and Co, due to their similar properties [189]. Nevertheless, by using reducing agents, such as hydrogen peroxide (H_2O_2) or that of ($C_6H_8O_6$), the effectiveness of many organic acids can be further enhanced, which can convert insoluble Co^{3+} and Mn^{3+} compounds to more soluble Co^{2+} and Mn^{2+} forms, hence

improving leaching kinetics significantly [196]. Although these acids are more expensive than inorganic acids, their environmental advantages are significant [189], [190]. As the acids in the process generate no toxic gases and produce biodegradable waste liquids, and can be enhanced through pre-treatment methods like that of thermal treatment of LCO at 500°C [98], [190]. Thanks to the combination of adequate recovery efficiency and environmental benefits, organic acid leaching shows strong potential for sustainable battery recycling applications with practical recovery efficiency [27], [190], [191], [196].

The hydrogen ion (H^+) and its concentration in any sort of acid, but more importantly in organic, can affect the leaching speed of the leaching as in $C_6H_8O_7$, as it is decomposed in 3 different stages of ($pKa_1 = 3.28$, $pKa_2 = 4.71$ and $pKa_3 = 6.3$), where each mole of citric acid releases that 3 moles of H^+, enhancing metal dissolution, because of this the $C_6H_8O_7$ can easily produce metal complexes in acidic media, as it has properties of a strong chelating agent [196], [199]. When $C_6H_8O_7$ reacts with the BM, the reaction can be divided into three separate steps: 1. diffusion, where acid goes on the surface of the LCO, 2. Surface area, where acid forms Co citrate as it reacts with LCO, and 3. diffusion of the Co citrate from the solid-liquid interface into the bulk solution [196], [200]. In the case of using four different acids (Golmohammadzadeh et al. [199]), found that by dissolving Li and Co from the spent LIBs, the dissolution rates of the $C_6H8O_7 > C_4H_6O_5 > CH_3COOH > C_2H_2O_4$ was as follows, because of the 3 moles of H^+, and 2 moles of H^+ for the $C_6H_8O_7$ and $C_4H_6O_5$ respectively, which meant that the while Li leaching was due to H^+ concentration the Co was because of it also, but also because of the type of anion acid used [196]. Reaction of the Co and Li with the $C_4H_6O_6$ medium can be expressed as (Eqs. (**10.1**), (**10.2**) and (**10.3**)), where the dissolution of Li by (Eq. (**10.1**)) and precipitation of Co by (Eq. (**10.2**)), is possible by $C_4H_6O_6$ and further can lead to dissolution of Co as per (Eq. (**10.3**)), further selective separation and recovery of Co and Li as follow [190]:

$$LiCoO_2\ (s) + 2H^+\ (aq) + H_2H_2\ (l) \rightarrow Co^{2+}\ (aq) + Li^+\ (aq) + 2H_2O\ (l) + O_2(g) \quad (10.1)$$

$$Co^{2+}\ (aq) + 2Li^+\ (aq) + 2C_2H_4O_6^{2-}\ (aq) \rightarrow C_4H_4C_6Co\ (s) + C_4H_4O_6Li_2\ (aq) \quad (10.2)$$

$$C_4H_4C_6Co\ (s) + H^+\ (aq) + C_4H_5O_6^-\ (aq) \rightarrow (C_4H_5O_6)_2Co\ (aq) \quad (10.3)$$

(Gao et al. [201]), investigation and study found that by using mineral acids, metals can be dissolved at high efficiency, for the Al with 99 wt.%, while by organic acids, only 15 wt.%. This demonstrated that leaching was selective, as the Al's ions led to the complication of the purification and separation steps. [196] Three major factors affect the organic acids effectiveness, and what type of reducing agents are as such needed for their use:

1. Temperature
    - Higher temperatures enhance acid's dissociation, increasing H^+ availability and reaction kinetics.
    - Above 70°C, efficiency declines due to H_2O_2 decomposition.
2. Time
    - Longer contact times between solid and liquid phases improve dissolution rates and metal recovery.
3. Solid-to-liquid ratio
    - Optimising this balance is critical for maximising leaching yield. [196]

Based on the studies, $C_6H_8O_7$ is the most studied of all of the organic acids, and as such, it has been reported that $C_6H_8O_7$ solubilised efficiently, is 95% to 100% for all of the valuable metals from spent LIBs. Based on the studies and literature (**Table 20**), some of the organic acids with their recovery efficiencies of the spent LIBs of the valuable metals.

Table 20. Summary of some research results for the leaching of spent LIBs in inorganic acids based on the reference materials.

Organic Acid	Key Features & Performance	Optimal Conditions	Recovery Efficiency	Ref.
Citric Acid	- Most effective (citric > malic > acetic) - Eco-friendly, biodegradable - Works with H_2O_2 or waste tea leaves as reductant	Two-step dissolution at 90°C with H_2O_2	- >95% Li/Co/Ni/Mn - 99% Li, 93% Co, 91% Ni, 94% Mn ($LiNi_{1/3}Co_{1/3}Mn_{1/3}O_2$, 80°C, 2h)	[192], [202], [201], [203]
Oxalic Acid	- Selective leaching: Li soluble, transition metals precipitate - No additional reductant needed - Regenerates NCM cathodes (168 mAh/g)	0.1M, 80°C, 120 min, S/L = 50 g/L	- 98% Li/Co separation ($LiCoO_2$)	[27], [204], [205]
Formic Acid	- Emerging alternative - Near 100% efficiency for Li/Co	–	- ~100% Li/Co recovery	[193], [206]
Tartaric Acid	- Limited studies but promising - Forms Li-rich solution + precipitate	–	- 97% Li, 98% Co ($LiCoO_2$) - 99% Ni/Co/Li/Mn with H_2O_2	[94], [193]

While there is a wide variety of different acids that can be used as inorganic acids in hydrometallurgy, some are more commercially available than others and yield higher recovery rates than others, based on the (**Table 20**). It also must be noted that there are more studies and references to be found to citric acid than to those of formic or tartaric, leading to differences in research amount and problematic use.

4.2.1.2. The Inorganic Acid Leaching

Inorganic acid leaching is a widely used, if not the most widely used, method in hydrometallurgy due to its efficiency in extracting valuable metals from spent LIBs. This process typically utilizes a liquid solution containing strong mineral acids, with the addition of reducing agents as supplementary aids in the reaction. Important factors in the inorganic leaching kinetic mechanism are the heterogeneous phase transitions of the solid-liquid-gas

phase transitions, which can typically be and are industrially enhanced by the reducing agents (e.g., H_2O_2, $NaHSO_3$, glucose ($C_6H_{12}O_6$)). The use of reducing agents not only enhances but also accelerates the process, which is further enhanced by the temperature and concentration of the leaching solution and leachate, as the S/L ratio plays a crucial role. [98] The most common acids and most studied in this industry are those of (e.g., HCl, H_2SO_4, HNO_3, or H_3PO_4), which are strong acids and yield an efficiency of (>99% for Co/Li, >98% for Cu) from the spent LIB's BM [27], [93], [97], [188]. For instance, H_2SO_4 at 1M and 90°C can yield (>93% of Li, Ni, and Co) due to its strong acidity alone [94], [189]. This can then be further enhanced by reducing agents, as they can improve the low valence of the metal's solubility [94], [191]. When using strong acids, the risks also increase, and in the case of HCL, the generation of the Cl_2 toxic gas is a pressing issue, while others generate those of NO_x/SO_x emissions and acidic wastewater, leading to the need for specialized equipment in the process control emissions and thus ramping up operational costs on the current market [27], [189]. Due to various factors, as previously discussed in the context of organic acids, the study and development of new methods have led to alternative leaching methods that minimize risks and optimize processes alike, while inorganic acids may be effective and highly studied [189], [191], [198]. The principle of acid leaching can be shown by the HCl recycling of the BM from the LCO, known as the nitrate pathway, which would go as follows [94], [193], [196], [198]:

$$2LiCoO_2\ (s) + 8HCl\ (aq) \rightarrow 2CoCl_2(aq) + \ Cl_2(g) + 2LiCl\ (aq) + 4H_2O\ (aq) \qquad (11)$$

From the reaction of LCO with HCl, the Co is leached and reduced from Co^{3+} to Co^{2+}, as shown in (Eq. (**11**)). The Equation also highlights the emissions and risk associated with the production of Cl_2 gas, as it is toxic and corrosive, which can be neutralized by using the H_2SO_4 [94]. H_2SO_4 is one of the most analyzed acid paths, also known as the sulfate pathway or techniques in the literature, and would mean that the formed Co^{3+} is reduced to that of Co^{2+} by using a reducing agent of H_2O_2, leading to the following reaction (Eq. (**12**)) [94], [193]:

$$\begin{gathered} 2LiCoO_2\ (s) + 3H_2SO_4\ (aq) + \ H_2O_2\ (aq) \rightarrow \\ 2CoSO_4(aq) + \ O_2(g) + Li_2SO_4\ (aq) + 4H_2O\ (l) \end{gathered} \qquad (12)$$

Another well-studied acid, HNO_3, also enables highly efficient recovery of Li and Mn from battery materials without requiring reducing agents, however, it is less effective for LFP batteries [193]. Overall, the study of the inorganic acids is vast, and their used parameters differ from one another, as such some of them can be found in the (**Table 21**) below.

Table 21. Summary of some research results for the leaching of spent LIBs in inorganic acids based on the reference materials.

Leaching Reagent	Reducing Agent	Temp (°C)	Solid-to-liquid ratio (g/L)	Time	Recovery Efficiency (%)	Ref.
H_2SO_4	H_2O_2 Glucose, Sulfites	60–70	Varies (e.g., 3–8)	2 h	Up to 99 for Li, Co, Ni, Mn	[197], [207], [208]
HNO_3	H_2O_2 or Iron powder	–	~3 (low)	Slow kinetics	Enhanced Co/Ni leaching	[198], [209], [210], [211]
HCl (1 M)	H_2O_2 (1.7% v/v)	75	–	30 min	95 Li and Co	[94], [210]
H_2SO_4 (2 M)	H_2O_2 (5% v/v)	75	–	1 h	99.1 Li, 70 Co	[94], [202]
H_3PO_4 (0.7 M)	H_2O_2 (4% v/v)	40	–	1 h	>99 Li and Co	[94], [212]
H_3PO_4 (2% v/v)	H_2O_2 (2% v/v)	90	8	1 h	~99 Li and Co	[196], [212]
H_2SO_4 (4 M)	H_2O_2 (10% v/v)	85	100	2 h	Li:96, Co:95	[196], [213]
H_2SO_4 (2 M)	H_2O_2 (15% v/v)	75	50	10 min	Li:100, Co:100	[196], [214]
HCl (4 M)	–	90	50	18 h	Li:100, Co:100, Al:100	[196], [215]

Based on (**Table 21**), the importance of reducing agents can be seen, as all of the research and methods utilise them, to fasten and allow for reactions to happen in methods that have been studied. Based on the available data, it can be seen and stated that the leaching efficiency of the current methods presented is high, as all of them yield (>95%) for both Li and Co alike.

4.2.1.3. The Alkaline- and Ammonia-Based Leaching

BM by utilizing the kinetics of the alkaline environment [190]. Alkaline leaching is most commonly done by ammonia-based leaching, hence by ammonia (NH_3), ammonium sulfate

($(NH_4)_2SO_4$), ammonium sulfite ($(NH_4)_2SO_3$), ammonium carbonate ($(NH_4)_2CO_3$), ammonium hydroxide ($(NH_4)OH$), and ammonium oxalate ($(NH_4)_2C_2O_4$), is one way to leach valuable metal form the BM, by the ammonium ions (NH^{4+}) forming different stable complexes with specific metal, allowing for the metals to dissolve in the alkaline leachate [27]. Leaching of metals from the BM is achieved by selective leaching [27], [190], [198]. However, there are certain metals, those of the Mn and Al, for instance, that are difficult to leach due to their complexity being not readily available when leaching, meaning they stay in residue for the end, when the Ni, Co and Li for instance can be leached without issues, as their complexes in the concentrated alkaline solution are readily formed [27], [190], [198]. Hence, leaching is done with high efficiency [27], [190], [198]. Overall, alkaline leaching is one of the methods that has been studied. For the leaching of the Bm in hydrometallurgy, it is more commonly found in other steps of the hydrometallurgy, like the precipitation, when it comes to recycling. However, there have been some studies done on leaching alone, as shown in (**Table 22**).

Table 22. Summary of some research results for the Alkaline- and Ammonia-based leaching of spent LIBs in organic acids based on the reference materials.

Leaching System	Leaching Reagent(s)	Conditions / Notes	Recovery Efficiency	Ref.
Ammonia Leaching	$NH_3 \cdot H_2O$ + $(NH_4)_2SO_3$	Combined with thermal carbon reduction roasting, Mn remained as ammonium salts	Li: 82.2% (water leaching); Ni & Co: efficient separation	[27], [216]
Ammonia + Adsorption	NH_3-based leaching + Mn-type Li-ion sieve	Lithium separated via adsorption; recovered as Li_2CO_3, $NiSO_4$, $CoSO_4$; ammonia recyclable	Li: 76.19% Ni: 96.23% Co: 94.57%	[27], [217]
Ammoniacal System	NH_3, $(NH_4)_2CO_3$, $(NH_4)_2SO_3$	$(NH_4)_2SO_3$ as reductant; $(NH_4)_2CO_3$ as pH buffer; forms NH3-metal complexes	Co & Cu: fully Ni: moderate Mn & Al: remained	[190], [218]
NaOH	NaOH (15 wt.%)	5°C, 1 h, S/L = 0.1 g/mL; Co and most Li remained in the solid phase	58% Al	[198], [219]
NaOH	NaOH (5 wt.%)	Room temp, 4 h, S/L = 0.1 g/mL; Co and most Li remained in residue	99.9% Al	[198], [213]

From (**Table 22**) in comparison to other leaching processes, it is evident that the results based on the research are a bit lacking in recovery efficiency as in comparison to that of inorganic acids-based leaching that yielded of average of 95% or more, as to this alkaline- and ammonia-based leaching of. What can be seen as under of that 95%.

4.2.1.4. The Bio-metallurgy & Bioleaching

Bio metallurgy, or an environmentally friendly and emerging technology process, brings cost-effectiveness, a novel technology that utilizes the use of microorganisms, such as bacteria or fungi, to recover valuable metals from the spent LIBs, like the commonly used hydrometallurgy acids/leaching processes, but with a more sustainable option in mind [186], [190]. One of these methods under bio metallurgy is that of already being studied bio leaching, which for now is tested on a laboratory scale, but has been seen as a future for the hydrometallurgy and pyrometallurgy [27], [94], [190], [193], [198] Bio leaching unlike conventional methods, must be operated under specific ambient conditions, which in return reduce energy need, environmental emissions (e.g., greenhouse) and other discussed under inorganic and organic acid leaching, while also minimizing contamination risks associated with methods [189]. Unlike conventional and commercialised processes, this process utilizes microbial metabolites to generate acid for the leaching step, dissolving metals in LIB while at the same time making it cost-effective and an efficient alternative [27], [186], [189], [190], [198]. Although bio metallurgy may be well established in the mining industry for low-grade ores and e-waste recycling, its phase in LIB recycling is only at the start, as stated before, that of the R&D phase, with promising results on hand [193], [220].

One of the biggest issues and challenges with bioleaching is their slow kinetics due to long microbial cultivation time, which may be affected or even decimated by their sensitivity to toxicity, especially of metal ions, leading to issues with higher capacity/batch leaching, which can be related straight to industrial scalability issues [27], [189], [198]. For instance, a study has shown that when pulp density is increased from 2% to 4%, meaning that only of a 2% increase, the Co recovery efficiency drops drastically between these 2% from 89% to only 10%, and for the Li it is from 72% to 37% due to the inhibition of the microorganisms responsible for iron oxidation [198], [220]. Research has shown that fungi, as an alternative to bacteria, exhibit higher toxicity tolerance and a faster leaching rate, making them a promising candidate for future studies and techniques in hydrometallurgy, as more studies and optimization are being conducted [198]. Despite many of the shortcomings, the future of hydrometallurgy seems to be better and going more to a green solution direction, not only in for the LIB recycling but also in other industries that have similar waste and recovery needs but currently, the reality is that the large-scale implementation is not an

efficient and feasible option, leading to more research and study needed on the topic [193]. Currently, some of the research data and results can be seen in (**Table 23**).

Table 23. Summary of some research results for the Bio-Hydrometallurgy leaching of spent LIBs in organic acids based on the reference materials.

Method	Microorganisms / Agents	Leaching Mechanism / Metabolites	Key Parameters	Recovery Rates	Ref.
Fungal bioleaching	Aspergillus niger	Citric, malic, gluconic acids	pH = 5.44	Cu (100%), Li (100%), Mn (77%), Al (75%)	[27], [221]
Autotrophic bioleaching	Various autotrophic bacteria	In-situ generation of organic acids (cost-effective method)	lab-scale only	Effective but not industrialized due to slow kinetics and microorganism handling	[27], [222], [223]
Combined bioleaching + precipitation	Aspergillus niger + chemical method	Organic acids from fungi + precipitation reagents	–	CoS (100%), $Co(OH)_2$ (100%), CoC_2O_4 (88%), Li_2CO_3 (73.6%)	[27], [222]
Bacterial bioleaching	Alicyclobacillus sp.	–	Ore concentration: 1–4% (higher concentration inhibits microbes)	Li: ↓ from 52% to 10%, Co: ↓ from 80% to 37%	[71], [224]
Bioleaching (Spent Medium)	Aspergillus niger (unadapted)	Citric, malic, gluconic, oxalic acids (mainly citric acid)	16 days, spent medium, unadapted strain	Cu (100%), Li (95%), Mn (70%), Al (65%), Co (45%), Ni (38%)	[27], [224]
Fungal bioleaching	Aspergillus niger	Secretes citric, malic, gluconic, and oxalic acids	1% pulp density; 16-day bioleaching in spent medium	Cu (100%), Li (95%), Mn (70%), Al (65%), Co (45%), Ni (38%)	[198], [225]
Bacterial Bioleaching	Sulfur-oxidizing + Fe^{2+}-oxidizing bacteria	Biogenic H_2SO_4, Fe^{2+} oxidation + acid dissolution	1% pulp density, cathodes: LFP, LMO, NMC	Li, Co, Mn, Ni: all >95% after optimization	[190], [226]
Cu^{2+}-catalysed bacterial bioleaching	A. ferrooxidans + Cu^{2+}	Cu^{2+} catalyzes reduction of $Co^{3+} \rightarrow Co^{2+}$	(0.75 g/L Cu) in 6 days	Co: from 43.1% (no Cu) to 99.9%	[198], [227]

An innovative and somewhat trending leaching process (**Table 23**) yields high results and has been researched extensively based on the studies. The effectiveness of the methods can also be seen as the leaching efficiency of a wide range of different elements/metals can

be seen with high recovery rates, leading to a promising development and implementation on a larger scale when the process is refined to its final form.

4.2.2. Treatment and Purification of Valuable Metals from the Leaching Process

As the spent LIB has been pre-treated and leached by different acids, as done commercially, the separation of the valuable metals from the concentrated leachate, as they are in metallic ion form. For these reasons, methods like those mentioned at the start of hydrometallurgy are used for their separation: chemical precipitation, crystallization, ion exchange, electrodeposition, and solvent extraction are employed to extract and purify subsequent products for refining, as metal salts or as straight raw, pure metal compounds.

4.2.2.1. Chemical Precipitation

In lithium-ion battery recycling, once metals are solubilized by leaching, a separation step is required, such as chemical precipitation. Chemical precipitation is the most widely used method at an industrial scale for selective separation, which relies on alkaline neutralization to form insoluble compounds, as the process is heavily affected by key factors such as pH, temperature, and the choice of precipitant [195]. Key factors in precipitation are the understanding of thermodynamics and that of E-pH diagrams, as these indicate the stable regions of the compounds to be precipitated, helping the most commonly used, often carbonate ions (CO_3^{2-}) from Na_2CO_3 or $CaCO_3$, which effectively target a wide array of valuable metals [98], [195]. What makes the process appealing are its simplicity, low operational cost, quick processing time, and high metal-ion recovery efficiency; however, its flaws include the difficulties encountered during the separation and recycling of metals from complicated leached solutions [190], [193], [195]. When it comes to recycling of LIBs, researchers typically, when dealing with the first-generation $LiCoO_2$ cells, frequently yield Li_2CO_3 and Co_3O_4 [190]. However, the advent of more complex cathode chemistries like those of $LiFePO_4$ and $LiNi_xCo_yMn_zO_2$ batteries turns separation into challenge, as the chemically similar behavior of Ni, Co, and Mn, hinders purity of the recovery process, unless precipitation conditions are precisely controlled and tailored for the needs to yield high

purity of product [190]. For this reason, the precipitant selection becomes crucial, as the common agents included in the process are (sodium hydroxide (NaOH), Na_2CO_3, sodium phosphate (Na_3PO_4), oxalic acid ($H_2C_2O_4$), and $(NH_4)_2C_2O_4$), which are all selected for their individual ability to form insoluble metal hydroxides, carbonates, oxalates, or sulfides at specific pH points, allowing sequential removal strategies of Fe, Mg, Cu, Al, and hence further the transition metals, leading to that final lithium removal [27], [190], [195]. To maximize utility, the precipitation method not only isolates single metal ions but can also yield high-value precursors that can be regenerated for the new cathodes, which is one of the features driving research toward co-precipitation, where Ni, Co, and Mn are simultaneously recovered and recycled into battery material feedstocks, hence offering cost and complexity advantages over the other methods on the market and being utilized [27], [190]. As the R&D and more research is being done, innovative variations include using saturated Na_2CO_3 or bubbling CO_2 to the carbonate precipitate Li as carbonate with ~80% efficiency (Zhang et al. [228]), yet scaling these technologies commercially remains challenging due to the complexity of treating mixed leachates with overlapping ion stability ranges, which as a result may lead to that of to co-precipitation [98], [190], [193]. As such to enhance selectivity, thermodynamic insights and in particular, E–pH diagrams are used to reveal overlapping precipitation zones for Ni and Co to utilize selective oxidation strategies, such as converting Co^{2+} to Co^{3+} using NaClO, restricting the Co precipitation to narrower stability windows and avoid co-precipitation of that Ni^{2+}, while Mn can likewise be oxidized to Mn^{4+} with $KMnO_4$ to precipitate as MnO_2 at pH 2 level but at the same time the oxidation may lead to that of MnO_2 and Mn_2O_3 by Mn precipitation with same $KMnO_4$ [40], [98], [190]. Complementary separation techniques, such as electrochemical deposition and ion exchange, can further refine the outputs [189]. It is not uncommon for the research and specific processes in development to be that of complex recycling flowsheets and incorporating multiple separation stages, starting with the solvent extraction or oxidants, followed by sequential precipitation steps, which is to achieve high-purity metal recovery; for instance, one optimized route removed Fe^{3+} and Cu^{2+} via NaOH and an organic extractant, precipitated Mn via $KMnO_4$, separated Co with a novel extractant, and recovered $Ni(OH)_2$ and Li_3PO_4 through base additions, achieving 100% Cu, 99.2% Mn, 97.8% Co, 99.1% Ni, and 95.8% Li [98], [190].

Given precipitation's strengths and limitations, such as overlapping stability, co-precipitation, and extensive process requirements, the development of such hybrid routes by combining solvent extraction, oxidation, and staged precipitation are increasingly favored, because of this, these integrated systems can achieve near-complete recovery of battery metals while aligning with circular-economy goals and producing materials suitable for cathode refurbishment [27], [98], [101], [137], [195], [197]. For some context, the available literature includes results and a discussion on methods of precipitation (**Table 24**).

Table 24. Summary of some research results for the precipitation methods of spent LIBs in organic acids based on the reference materials.

Method	Reagents	Key Parameters	Recovery Efficiency	Ref.
Lithium carbonate precipitation from formic acid leachate	Na_2CO_3 (saturated)	After removing Ni, Co, Mn; saturated Na_2CO_3 addition	Li 98.22%	[190], [229]
Precipitation of Li from $LiNi_{0.5}Mn_{0.3}Co_{0.2}O_2$ using oxalic acid	Oxalic acid	Mn removal by KOH, then K_2CO_3 or Na_2CO_3 added	Li (6 mL 5 M K_2CO_3) 78.5%, Li (2 mL) 44.8%, Li (15 mL 3 M Na_2CO_3) 48.1%	[190], [230]
Selective oxidation precipitation of Co^{3+} as $Co_2O_3 \cdot 3H_2O$	NaClO	pH = 3; converts Co^{2+} to Co^{3+} for selective precipitation	Co 99.99%, Ni 100%	[190], [196], [215]
Leaching with citric acid, followed by precipitation using multiple agents	Citric acid (1.5 M), $KMnO_4$ (0.5 M), DMG, oxalic acid, H_3PO_4	Leaching: 80°C, 2 h; Precipitation: 20 min, 25°C, 300 rpm, 1 dosage	Ni: 98.5%, Co: 96.8%, Li: 92.7%	[196], [231]
Hybrid method for Fe, Mn, Li recovery	Leaching + flotation + precipitation	HCl leaching, flotation of Fe as $FeCl_3$, Mn as Mn oxides, Li as phosphate	$FeCl_3$: 97.91%, MnO_2/Mn_2O_3: 98.73%, Li_3PO_4: 99.32%	[196], [232]
Roasting mixed electrodes → Acid leaching → Solvent extraction and evaporation precipitation	Reduction roasting + H_2SO_4, evaporation/precipitation	Roasting: 600°C, 3 h; Leaching: 85°C, 1 h, L/S = 6 ml/g; 1.05x theoretical H_2SO_4	Mn: >97%, Ni, Co, Li: >99%	[196], [233]
Co-precipitation followed by sequential precipitation	Na_2CO_3	Co (II), Ni (II), Mn (II) co-precipitated; separation based on carbonate solubility	Regenerated NMC cathode up to 95% capacity	[197], [234], [235], [236], [237]

Chemical precipitation, one of the important aspects and steps of hydrometallurgy, with a wide variety of methods as seen by (**Table 24**), has been utilized on an industrial scale

and is being used around the globe. As one can see, the research and available data indicated those of high recovery efficiencies for different types of metals, with (>90%) rates by many studies, explaining the popularity of certain methods over others.

4.2.2.2. Solvent Extraction

Solvent extraction is one of the most widely applied techniques and has been shown to be an effective hydrometallurgy technique for separating and purifying different metal ions from the LIBs BM and other wastes alike at high selectivity by utilizing the immiscible aqueous and organic phases to do it from complex leach mixture solutions [93], [189]. Most commonly used extraction solvents or extractants in this case include di-(2-ethylhexyl) phosphoric acid (D2EHPA), 2-ethylhexyl phosphoric acid mono-2-ethylhexyl ester (PC-88A), and bis(2,4,4-trimethylpentyl) phosphinic acid (Cyanex 272), for Co and Cu with high selectivity [27], [40], [94], [198]. In particular, Cyanex 272 is favored for Co extraction, but it loses efficiency in the presence of Mn, necessitating the pre-removal of Mn, which can be achieved using another extractant (e.g., D2EHPA) to minimize Co losses from the solvent when dissolved [94]. Like any solvent/solution process, the extraction has factors that affect it; for this reason, the Synergistic extractant systems, such as Cyanex 272 mixed with PC-88A, are meant to enhance both extraction efficiency and metal selectivity, especially under optimized pH and organic-to-aqueous (O/A) ratios [27], [94]. For this reason, the usage of mixed systems to improve Mn, Co, and Cu recovery at high pH and low Na_2SO_4 concentrations demonstrates the potential for tailored multi-extractant approaches [27]. For instance, it has been studied and demonstrated that the recovery of Li from the pyrometallurgical processes could be made at an efficiency of (>90%) using β-diketone systems like benzoyl trifluoroacetone (HBTA) with trioctyl phosphine oxide (TOPO), offering energy-saving benefits due to low-temperature operation, as the Li recovery in the process has been far too long overlooked [27]. While solvent extraction may be common, it faces challenges, including the high costs of organic reagents and extractants, its complex multi-step processes leading to functional issues, and risks of secondary pollution from flammable solvents [27], [93]. Because of these, the comparison to ion exchange, which is simpler and more industrially scalable but requires careful resin regeneration, while the chemical precipitation, though cost-effective, struggles with co-precipitation of similar

metals like Ni, Co, and Mn, prompting innovations like oxidation-assisted selective precipitation (e.g., Co^{2+} to Co^{3+} conversion via NaClO) leading to more possibilities and technological processes for the LIBs recycling by solvent extraction [27], [40], [189]. While solvent extraction excels in purity and selectivity, its industrial adoption is hindered by economic and environmental trade-offs [27], [93]. As such, future directions include developing greener, recyclable extractants and hybrid systems that integrate solvent extraction with ion exchange or precipitation to balance efficiency, cost, and sustainability [27], [93].

4.2.2.3. Ion-Exchange and Ion-Exchange Resin

Ion-exchange is a process characterized by high selectivity, which utilizes resins to remove specific ions from a solution [195]. This is all due to the utilization of resins that contain chelating functional groups to form complexes with them in addition to utilizing chemical/physical properties based on differences in ionic size, charge, and concentration [189], [238]. In this method, the leachate is passed through specialized resins that exhibit high affinity for specific cations or anions, making it particularly effective for recovering trace metals from complex solutions by using their functional groups, selectivity ratio, cross-linking, porosity, and matrix geometry to achieve separation of the ions [40], [238]. Compared to chemical precipitation and solvent extraction, ion exchange has achieved superior selectivity compared to some other methods used in hydrometallurgy to some studies and developments [40]. The technique offers several advantages, including resin reusability and operational simplicity for large-scale applications [40], [195]. Additionally, the ease of operation, no reagent losses, no disengagement of phases, economic feasibility when using low concentrations of metal ions, and environmental safety can be considered as bonus advantages for an already relatively good process, as the disadvantages of high-quality resins being costly, operational oversight to maintain resin effectiveness and prevent either saturation (exhaustion) or premature ion leakage in the system, are relatively big issues of the current process [195], [238]. Additionally, resin regeneration requires chemical inputs, which leads to the creation of both economic and environmental concerns [195]. Nevertheless, the ion exchange at the current stage and what has been done/studied seems to be well-established for brine processing, but as technology matures, its application to LIB

leachates could increase as long as the economic constraints, process complexity, high chemical consumption, and waste generation can be removed or lowered drastically [196].

4.3. The Pyrometallurgical process of LIB recycling

The pyrometallurgical recycling process has emerged as one of the dominant methods for handling EoL in LIBs over the past decade, particularly due to its industrial maturity, simplicity, flexibility, rapidity, and ability to treat mixed or unsorted battery chemistries without extensive pre-treatment [40], [98], [190], [192]. The process itself is particularly suited for industrial-scale operations that have more than 1000 Mt/yr capacity, as it brings the rapid throughput and integration into existing metallurgical infrastructure as a key consideration factor, as the industry is evolving, and new sustainability targets and promises are being done across different actors [40], [94], [189,] [193], [239]. Pyrometallurgy technology utilizes high-temperature treatment methods, such as smelting, pyrolysis, incineration, roasting, and calcination, which convert battery waste into reusable metallic alloys, gases, and slag [95], [186], [189], [192], [193], [197], [240]. At its core, the process involves the reduction of metal oxides in spent batteries into alloys primarily composed of Co, Ni, Cu, and iron (Fe), while Li, Mn, and Al typically end up in the slag phase, posing recovery challenges [27], [98], [189], [192], [193], [195], [197].

The general starting point of the process recovery is that either batteries come as intact whole cells or modules, or as in BM form from pre-treatment [94], [191], [239], [241], [242]. Due to the maturity of the process, the need for the pre-treatment step is optional, as the battery mixtures can be burned all together in the shaft or electric arc furnace with the three commonly found zoned temperatures:

1. Preheating (<300°C) → remove electrolytes and avoid explosions [94], [193].

2. Pyrolysis (500–800°C) → Removes organic compounds such as plastics, binders, and separators through thermal degradation in an oxygen-free or inert atmosphere [40], [192], [242].

3. Smelting (>1000°C) → metal oxides are reduced to form alloys of Co, Ni, Cu, and Fe, while less reducible elements like Li and Al are oxidised and retained in the slag [40], [94], [189], [191], [192], [198], [242].

The exothermic combustion of organic electrolytes and graphite helps sustain the necessary thermal conditions, reducing external energy requirements [40], [93], [189], [239]. Nevertheless, energy demand remains high, and specialized off-gas systems are necessary to manage the release of hazardous substances, such as HF and dioxins, which occur significantly during smelting [186], [189], [193], [195]. Industrial scaling of pyrometallurgy is also in contrast, thanks to the unnecessary need for pre-treatment, sorting, or size reduction of batteries, which offers feedstock flexibility and simplifies logistics [195], [242]. However, this comes at the cost of selectivity, as the metallic products are recovered as mixed alloys, which necessitate even further hydrometallurgical refining or other processes/methods to achieve high-purity materials suitable for battery-grade reuse [40], [93], [98], [197]. Because of this, pyrometallurgy is heavily hybridized with hydrometallurgical steps downstream, particularly to reclaim Li from slag and separate Co and Ni from other metals [98], [189], [191], [195], [239], [242]. Nevertheless, the major drawback of conventional pyrometallurgical recycling is its inefficiency in recovering Li, as discussed earlier, due to its strong oxidizing behaviour at high temperatures, which causes it to integrate into the slag phase in an oxidized form. For this, the Li recovery is both technically and economically challenging unless additional processes like slag leaching or molten salt recovery are implemented [186], [189], [191], [194], [242].

From an economic and market value perspective, the process has traditionally hinged on the recovery of Co due to its high market value [94]. As battery chemistries evolve towards cobalt-free or low-cobalt cathodes (e.g., LFP, LMO, and NMC), the profitability and sustainability of pyrometallurgy have been questioned [94], [192], [195], [239]. To address this, innovations have been developed, including salt-assisted roasting, in-situ reduction pyrolysis, and molten salt-assisted recovery technologies, which are receiving more attention than before [27], [186], [242]. Salt-assisted roasting is a process that, for instance, can utilize compounds like ammonium sulfate ($(NH_4)_2SO_4$) or sublimed sulfur in controlled atmospheres to convert Li into soluble salts such as lithium sulfate (Li_2SO_4) while stabilizing other transition metal oxides for subsequent recovery [191], [242]. In light of these approaches, there are unified goals of lower energy demands, improved Li yield, and

support closed-loop recycling pathways for the LIBs recycling and pyrometallurgy as a process itself [98], [191].

Although the pyrolysis process is dominant industrially, it is highly capital-intensive, as the requirements and conditions of the process are, in some instances, extreme, which is further plagued by large labor and utility costs of energy [189]. But what really plagues current industrial processes, and in development or in literature research, are the environmental drawbacks, which include the generation of toxic gases, high CO_2 emissions, and slag waste, which itself may require additional processing or disposal strategies, as usually it is [93], [189], [197], [198]. Because of this, the metallic alloys recovered are, subsequently, not always straight suitable for direct reuse in batteries, that (open-loop recycling), leading them to re-enter the broader metallurgical market instead of returning to battery production (functional or closed-loop recycling) [93], [98], [193].

Thanks to these limitations and issues, the research into pyrometallurgy enables the development of new methods to enhance existing ones or integrate them. Alternative strategies, such as the carbothermal shock method synthesis, which reduces the ternary layered oxide cathodes, and microwave-assisted pyrolysis, which is being used as one of the pre-treatment methods, as well as molten salt pyrolysis, aim to improve process efficiency, recovery rates, and sustainability of current technologies [40], [189], [242]. Developments in industry not only reduce processing temperature but also mitigate metal losses and environmental impacts [40], [93], [189]. While interest in more sustainable and alternative options for pyrometallurgical recycling processes continues, the current issue with EoL LIBs and batteries alike is that their increased amount exceeds the current capacity for recycling. As such, the importance of adaptability and potential synergy with existing metallurgical infrastructures is needed [189]. Nonetheless, pyrometallurgy remains a useful process for processing battery chemistries with significant concentrations of Co and Ni content, as well as for large-scale applications where mechanical and thermal integration can offset some of the energy and cost disadvantages, while the market allows it. Nevertheless, the development and improvements in the current systems and alike the pyro-hybrid systems and greener roasting alternatives are the cornerstones of ensuring the long-term feasibility of this approach and battery recycling in a landscape increasingly dominated by low-cobalt or cobalt-free batteries as pyrometallurgical recycling industry is used mainly in the Western

countries, where the labor and prices of utility/energy are soaring up. [40], [98], [190], [191], [192], [193], [195], [197], [198], [242]

4.3.1. Extraction of the LIBs valuables by the Pyrometallurgy Process

The extraction from the LIBs, as per pyrometallurgy typically occurs in the industry at the process's third-zone temperatures, but with what method it is done depends, as it can be achieved via roasting/calcination or even smelting. Furthermore, these processes can be classified into the extraction mechanisms used and the atmosphere in which they are processed. In addition, processes can also be separated by their process chains, meaning that if they are direct or multi-step processes, the latter is what current development and research are aiming for. [27], [241] In this section, we will only look at the direct process. In addition, we will not delve too deeply into pyrometallurgy extraction methods but instead, examine what is used industrially and is currently being researched.

4.3.1.1. Roasting

Roasting is a pyrometallurgical process that involves a gas-solid reaction performed in an oxygen-rich atmosphere at elevated temperatures and has traditionally been used in the treatment of sulfide minerals [40], [93]. In contrast, calcination is conducted in inert or oxygen-limited conditions [40], [93]. As the pre-treated BM enters the process, it undergoes carbothermic reduction (CTR) roasting, by which the active material is processed [40]. Roasting as a process allows for material decomposition and oxidation of the compounds [93]. This is with regard to CTR, which makes it easier for Li and Co to escape and promote the reaction to progress further [40]. What roasting allows is the going from 1000°C to around 500°C, utilizing strategic additives such as reducing agents (e.g., carbon, charcoal, Al foil, Fe scrap) and salts to achieve metal leaching efficiencies of Li 81.8% → 94.3%, Ni 50.3% → 88.7%, and Co 43.2% → 96.3%, as the additives are to promote reduction metal ions in lithiated metal oxides [189]. The CTR methods use has been also further demonstrated by the (Reinhart et al. [241]) as the LCO mixed in Gr was roasted in an oxygen-free environment, further led by in-situ recovery of Co, Gr, and lithium carbonate (Li_2CO_3)

after the wet magnetic separation the recovery rates for the Li, Co, and Gr were of 98.93%, 95.72%, and 91.05% respectively, leading to show feasibility and process efficiency, that could be scaled [40], [190], [243]. Overall, roasting can be categorized into direct roasting and additive-assisted roasting, including sulfation, chlorination, and nitration roasting, but they also have different shortcomings, such as corrosive and toxic gases [242].

Salt-assisted roasting is a derivative of the pyrometallurgical process of roasting, which has gained significant attention over the past years due to its effective approach for recycling LIBs [191]. The goals and changes that the method brings are the utilization of chlorination, sulfation, and nitration as a roasting, aiming to enhance metal recovery efficiency while reducing acid consumption and minimizing toxic gas emissions [189], [191]. During this process, stoichiometric amounts of salts are added to the cathode material, which include NH_4Cl, $(NH_4)_2SO_4$, or H_2SO_4, forming metal salts and varying water-soluble salts that enhance the recovery of valuable metals from the LIBs [27], [189]. For instance, the use of sulfate roasting converts Li into Li_2SO_4, which is highly soluble in water is (13.3 g/L, 20°C) and can achieve a leaching efficiency of up to 99.3% [40], [189]. Using salt-assisted roasting on the NCM and the LFP, Li can be extracted by the following reaction using relatively low temperatures (Eq. (**13**)) [191].

$$4LiFePO_4\ (s) + O_2\ (g) + 2(NH_4)_2SO_4\ (s) \xrightarrow{300°C} 2Li_2SO_4(s) + 4NH_3\ (g)\ + 4FePO_4\ (s) + 2H_2O\ (g) \quad (13)$$

In this reaction, ammonium sulfate acts as a roasting assistant, allowing Li to form Li_2SO_4 as $(NH_4)_2SO_4$ decomposes under heat, releasing SO_4^{2-}, which then reacts with lithium to form Li_2SO_4, a water-soluble salt. This reaction and method allows for complete leaching but also complete sulfur recycling in the form of $SO_4^{2-}$to prevent SO_x emissions [27]. While additive-assisted roasting offers higher selectivity and faster reaction kinetics than direct roasting or hydrometallurgy, it also poses challenges, such as the generation of corrosive gases like Cl_2, NO_x, and SO_x, which require proper environmental controls in place [242]. Looking towards the future, it is also worth noting that the further optimization of process variables, such as temperature, pressure, atmosphere, and salt formulation, may enable even more sustainable and efficient closed-loop recycling of LIB materials if more study and research are put on the line [27].

LIB recovery via in-situ roasting technology involves the recovery of valuable metals from LIBs through the utilization of LIB waste itself, without the use of any reagents outside the process, embodying the concept of "waste + waste = valuable resources" [27]. This means that the process runs purely on the materials inside or those of LIB, reducing the need for reagents and lowering costs by drastically simplifying steps [27]. (Yan et al. [240]), For instance, did develop an in-situ thermite roasting method, which utilized the Al foil as a built-in reducing agent to recover Li and Co from the $LiCoO_2$, by a selective leaching and subsequent crystallization, of that 93.67% and 95.39%, respectively, demonstrating concepts work in metal recovery, that could be applied in LIBs recovery hence [185], [239]. The development does not end only on that, as (Li et al. [243]) further improved the process by combining in situ carbon reduction roasting, which is the same example mentioned in chapter (***4.3.1.1. Roasting***), showing the development and process feasibility [27].

4.3.1.2. Smelting

Smelting is one of the three core temperature zones of pyrometallurgy used in LIBs recycling and is an effective way of recovering high-value metals such as Co, Ni, Cu, and etc [40], [189], [195]. As stated in the pyrometallurgy, the recycling process can start with either untreated whole LIBs or black mass from pretreated batteries alike, which are then subsequently treated with those high temperatures exceeding 1000°C or more [40], [189], [195]. Before smelting, as shown, the battery materials are heated at a lower temperature to evaporate volatile components such as electrolytes and prevent explosive overpressure buildups [40]. By using high temperatures in the smelting reduction zone/phase, where the materials are melted to produce alloys such as Co, Ni, Cu, and Fe, for instance, and slag [40], [94], [193]. In the smelting process, all organic components, including binders and electrolyte solvents, are almost always oxidized or burned industrially during this phase to generate heat and energy that sustain the smelting reaction [27], [40]. Materials that stay in the slag and cannot be recovered as a separate material due to their properties, as in other steps of pyrometallurgy, as well as in hydrometallurgy, are those of Li, Al, Si, Ca, and Mn, are transferred a stay in the slag [40], [94], [190], [193], [195]. The choice between pre-treatment and no pre-treatment in the smelting is important, as when dealing with the BM, the addition of materials with contaminants into the process poses a risk to the efficiency

and purity of the resulting output [189]. As such, the use of the flux and its addition to the process allows for lowering the melting points and segregating impurities present in the battery waste into the forming formation of the consistent slag, while metals collect at the bottom of the furnace alloy in a pool [40]. For these metals, the next step is their purification, which is done as alloys are subsequently refined using hydrometallurgical methods to extract individual metals [40], [189], [190]. Nonetheless, the recovery of the Li at the current stage is unfeasible in most pyrometallurgical systems [40], [189]. In contrast, recovery via other means is an option, but with additional cost, leading to the same issues as discussed. But while smelting offers high productivity and broad compatibility with different battery chemistries, its energy-intensive aspect makes it more suitable for batteries with high Co and Ni content, as for the low-value chemistries like LFP or Mn-spinel oxides, its efficiency and profitability decline [40], [189]. As such, developments and advancements in the $CaO–SiO_2–Al_2O_3$ slag system with $MnO–SiO_2–Al_2O_3$, try to replace conventional methods, and hence aim to improve the Li recovery more effectively, while also reducing smelting temperatures to 500–600°C from those of current smelting 1000°C by utilizing Gr and plastics as internal fuels and reductants [189].

4.4. Direct Recycling of the LIBs

Direct recycling, one of the three most commonly used methods for recycling LIBs commercially, is an emerging and environmentally favorable method that aims to recover and regenerate active materials from spent LIBs without any type of disassembly or alteration to their chemical structures [142], [189], [195]. Unlike hydrometallurgical or pyrometallurgical processes, which are used to dissolve or reduce materials into their elemental forms, direct recycling preserves the crystal structure of cathode materials, thereby maintaining their embodied energy and economic value [142], [189]. This method and its approach are particularly beneficial for low-value cathodes such as LFP, as it avoids the need for energy-intensive resynthesis while at the same time enabling the reuse of regenerated materials in new batteries [94], [142], [195], [197].

The start of the process is typically achieved by disassembling LIBs, followed by the physical or thermal separation of components and the re-lithiation of degraded cathode

materials to restore their electrochemical performance [95], [189], [193], [195]. Re-lithiation methods used in the process steps include solid-state, hydrothermal, electrochemical, molten-salt, and ionothermal re-lithiation reaction techniques, each with specific advantages and implementation challenges in the current state of process development [189], [193]. One of the methods used in the process utilizes that of supercritical CO_2 (above 31°C and 74 bar) is often used to extract electrolytes safely and efficiently while preserving other cell components. In some studies, this method enabled up to 85–89% recovery of graphite anode materials [94], [193]. While the results were good, similar to those of the process, with slight modifications, the addition of CO_2 in liquid form enabled a better recovery efficiency of 85.07%, demonstrating progress in the field [193]. Similar to these methods, the thermal treatment at 650°C has been shown to revitalize degraded LFP cathodes and, subsequently, energy density and discharge capacity to levels comparable to fresh LIB materials [94], [193].

Over the course of research and development, experiments have demonstrated high material recovery rates using direct recycling. (Li et al. [244]) for instance, recovered high-quality $LiFePO_4$ through direct physical recovery and sintering, while (Zhang et al. [245]) reported that of 98.23% efficiency for cathode material liberation through pyrolysis and physical separation [94], [193]. What makes these processes and research fascinating is their typical avoidance of the use of harsh chemicals and reduced secondary pollution while demonstrating their effectiveness in recycling electrode scraps from battery manufacturers and single-chemistry battery waste [142], [195]. Despite process advantages, which include high recovery rates of 95% and more in some patented methods (e.g., Toyota's 2011), low energy consumption, and minimal environmental impacts of direct recycling faces notable limitations [94], [186], [193], [195]. These include the requirement for accurate sorting by cathode chemistry (e.g., distinguishing NMC333 from NMC811), the need to eliminate Al contamination from current collectors, and challenges in maintaining the purity and structural integrity of recycled materials to meet industrial standards, which leads to that processes can and are only tailored to processing of one cathode chemistry at the time, hence it is limited by its inflexibility [93], [142], [193]. Furthermore, the batteries of the different array in development and current use ranging from 10 to 20 years are so different that the struggle to recover mixed or outdated battery types and their cathode materials are generally only compatible with the same chemistry they were originally part of, as stated [142], [186], [197]. For these reasons, current research efforts focus on exploring techniques to convert

older cathode compositions into newer ones, such as upgrading NMC111 to NMC811, for instance [142], [197]. Nonetheless, most commercial applications are still limited to lab-scale demonstrations or restricted to homogeneous feedstocks such as electrode scrap [186], [197].

Ultimately, what is clear is that the scalability and industrial adoption of direct recycling will depend fully on overcoming its current limitations, such as incomplete anode recycling, chemistry-specific processing requirements, and a lack of standardization. Addressing these barriers while adapting to evolving battery chemistries is critical for unlocking the full potential of direct recycling as a sustainable and economically viable CE solution, as well as for developing other methods within the Waste Hierarchy, legislation, and protocols for the industry's LIBs recycling/ manufacturing industry as a whole. [93], [94], [142], [186], [193], [197]

4.5. Comparison of current Recycling Processes for the LIBs

As LIB demand soars and the growing demand for new energy storage increases, driven by the rapid expansion of EVs, NEVs, and stationary energy storage systems, the development and need for increasing EoL battery recycling process technologies have become increasingly critical. On the current market and up to date, three major recycling processes tackle these needs and bring solutions either already commercially available or in lab-scale under R&D. Pyrometallurgy, hydrometallurgy, and direct recycling all of these processes have their distinct advantages but also limitations in terms of metal recovery efficiency, energy and chemical consumption, environmental impact, and economic feasibility. Pyrometallurgy relies on high temperatures, allowing for large-scale processing, while hydrometallurgy employs chemicals in its methods but has a longer processing step compared to pyrometallurgy. Additionally, pyrometallurgy is used more in Western countries, while hydrometallurgy is used in Asian countries as a process method. Meanwhile, direct recycling aims to preserve the functional structure of battery materials and regenerate them with minimal processing, offering a promising route for circularity but being plagued by standardization and scalability issues. Because of these differences, this section will present differences of processes by (**Table 25**) showing the advantages and disadvantages

of the processes and (**Table 26**) showing the current processes implemented globally with their summary information. All of these are only for visual understanding of all three processes that have been discussed throughout this work to help understand where and how LIBs recycling is happening, and what is its maturity status.

Table 25. Summary on advantages and disadvantages of Hydrometallurgy, Pyrometallurgy and Direct Recycling processes, in different aspects, reproduced by Reference. [27], [40], [93], [94], [142], [188], [189], [190], [192], [193], [194], [195], [196], [197], [198], [239], [241], [242], [246].

Parameter	Hydrometallurgy	Pyrometallurgy	Direct Recycling
Process Description & Methology	- Wet chemical extraction / aqueous solutions; (leaching, precipitation, etc.)	- High-temperature reduction (typically >1000°C) to form alloys and slag	- Maintains and restores cathode structure and active materials (e.g., via re-lithiation)
Pre-treatment Needs	- Yes (discharging, shredding, separation)	- Not always (less selective, but riskier)	- High (precise sorting, careful handling)
Process Complexity	- Multi-step (leaching, purification, precipitation)	- Simple operation but complex emissions control	- Moderate to high (depends on restoration process)
Main Outputs	- Metal salts (Li, Co, Ni, Mn); high purity	- Metal alloys (Co, Ni, Cu), - Slag with Li, Mn, Al	- Regenerated cathode materials (e.g., NMC, LFP), graphite, electrolyte components
Temperature Range	- <200°C	- >1000°C	- 100–800°C, depending on method
Recovery Efficiency	- Co, Ni & Li (90–95% can be up to 99%)	- High for Co, Ni, Cu. - low for Li (lost to slag)	- high for LFP - moderate for NMC - Li & Co often >90%
Material Purity	- High	- Moderate to high (after refining)	- Requires careful control to match industrial standards
Energy Consumption	- Moderate	- Very high (due to smelting)	- Low to moderate
Chemical Consumption	- High (strong acids, alkalines)	- Low	- Low (mainly water, mild solutions)
Environmental Impact	- Potential wastewater and chemical disposal issues - Secondary pollution	- High CO_2 - toxic gas emissions (e.g., SO_x, NO_x)	- Lowest if closed-loop achieved; limited by material purity
Scalability	- High (commercially mature and widely used) - Widely used in Asia	- Highly scalable - established in large metal industries - Widely used in the West	- Early-stage or pilot scale; mostly lab-based

(*Continued on next page*)

Table 25. (*Continued*)

Parameter	Hydrometallurgy	Pyrometallurgy	Direct Recycling
Pre-treatment Requirement	- Requires precise sorting, discharging, and component separation	- Minimal (can handle mixed chemistries and formats)	- Requires clean, sorted, single-chemistry batteries
Flexibility to Chemistries	- Highly adaptable to various cathode materials	- Suitable mainly for high-value chemistries (NMC, NCA, LCO)	- Limited; optimal for specific chemistries (e.g., LFP, NMC111)
Circular Economy Potential	- Linear: breaks down materials to basic elements; recovered	- Linear: metals are downcycled; materials are lost	- High: regenerates usable materials; shorter loop
Challenges	- Secondary pollution, reagent cost, purification complexity	- High energy use, - Li recovery losses, - environmental emissions	- Sensitivity to feedstock composition, - material purity, - automation needs
Industrial Examples	- Umicore (Belgium), - GEM (China), - Li-Cycle (Canada/USA) - Recupyl (France)	- Glencore (Italy), - Umicore (Belgium), - Redux (France)	- OnTo, - ReCell, - Retriev, - Argonne Lab (pilot projects)

Table 26. Summary on current commercialised/industrial companies, with their locations, methods of processing and capacities, for the Hydrometallurgy, Pyrometallurgy and Direct Recycling processes, in different aspects, reproduced by Reference. [27], [40], [93], [94], [142], [188], [189], [190], [192], [193], [194], [195], [196], [197], [198], [239], [241], [242], [246].

Company	Country/Location	Capacity (if stated)	Recycling Type(s) Used
GEM Co., Ltd.	China	- >50,000 tons of Co & Ni cathodes	Hydrometallurgy
Brunp (subsidiary of CATL)	China	- ~5% global share (2030 projected.) (batteries + scrap)	Hydrometallurgy + Direct Recycling
Umicore	Belgium	- 7,000 tonnes/year	Pyrometallurgy + Hydrometallurgy
Revolt (Northvolt)	Sweden	- 2% of global recovery share (2030 projected.)	Hydrometallurgy Direct recycling (planned)
Ascend Elements	USA	- ~2–3% global share (2030 projected.)	Hydrometallurgy
Cirba Solutions	USA	- ~2–3% global share (2030 projected.)	Hydrometallurgy
Valdi Emerat	France	- 20,000 t/year	Pyrometallurgy
Sumitomo-Sony	Japan	- 150 t/year ($LiCoO_2$)	Pyrometallurgy + Hydrometallurgy

(*Continued on next page*)

Table 26. (*Continued*)

Company	Country/Location	Capacity (if stated)	Recycling Type(s) Used
LithoRec	Germany	- 100	Manual + Dry mech. + Hydro
Glencore/Xstrata	Canada, Norway	- 7,000	Pyrometallurgy + Hydrometallurgy
Batrec Industrie AG	Switzerland	- 200	Hydrometallurgy
Akkuser Ltd	Finland	- 4,000	Pre-treatment (sends to pyro)

Based on the information gathered in the tables, it can be seen that the current Wester. The approach, as stated, is that of pyrometallurgy, and Asia is of hydrometallurgy. What can also be seen from both tables (**Table 25**) is that Chinese companies have multiple times higher capacities than their counterparts across the globe, showing the current development and maturity of the recycling industry globally, which has already been mentioned many times throughout the paper, with insight to be of Asian and Chinese dominance. In addition, based on the (**Table 26**) information, hydrometallurgy on an industrial scale seems to have better recovery efficiency for the metals currently than the other two processes, with more optimized steps and flexibility in the current green energy trend, as new batteries are designed and discharged out of, allowing for faster adaptation of recycling flexibility.

4.6. The Electrochemistry

Electrochemistry is one of the branches of chemistry that explores the boundaries and interactions between electrical energy and chemical reactions, by encompassing phenomena such as (e.g., electrophoresis and corrosion), and the operation of devices like batteries, fuel cells, and electrochromic displays [247]. In addition to principles, the field also offers a wide variety of electroanalytical techniques, (e.g., coulometry, potentiometry, polarography and voltammetry) measuring current or potential in electrochemical cells, by which the analysis of substances with high precision, often across a broad concentration range (ppb to mg L^{-1}) can be done [247]. The development and research into electrochemistry equipment and methods have allowed for electrochemical analysis to become faster, and more affordable in instrumentation and rapid data acquisition, which in return has allowed for the fundamental understanding of complex reactions/phenomena at the electrodes [247], [248].

Beyond analytical applications, electrochemistry plays a crucial role in sustainable technology development, allowing and introducing the pathways to decarbonize industrial processes by integrating renewable electricity and thereby reducing reliance on high-carbon energy sources [248]. These are significant aspects, as in LIB recycling, as discussed and demonstrated, the industry is highly energy-intensive and utilizes a wide variety of different steps, methods, and utilities. As such, the progress in this area hinges on atomic-scale insights into electrode reactions, optimized reactor designs, and innovative electrocatalysts, that could help us unlock greener alternatives to conventional chemical manufacturing processes on an industrial scale [248].

While electrochemical methods help us optimize processes and understand chemistry on different levels, they also excel in material synthesis and modification, as exemplified by the production of graphene through electrochemical exfoliation of graphite [249]. This process is driven by the bias-induced OH^- generation in acidic electrolytes, which then allows the facilitate layer separation by the use of the gaseous expansion [249]. In addition to this, the electrochemical anodic oxidation and ion intercalation, also provide eco-friendly routes to synthesize metal oxides, hydroxides, and 2D materials, which is important as they offer advantages such as high yield, regulatable particle size, and minimal environmental impact compared to traditional wet-chemical methods, like found in hydrometallurgy [250]. For instance, the used and researched electrodeposition in hydrometallurgy selectively separates metals from the concentrated leachate solution, similar to those of ion exchange and precipitation methods, is one of the electrochemical processes, but we will not talk about them in this chapter, but about Electrochemical-Leaching (ECL) and Electrochemically-Assisted-Leaching (EAL) with addition to sub-categories of Direct Leaching and Indirect Leaching [195]. Nonetheless, what these different techniques underscore is electrochemistry's versatility, bridging fundamental research and industrial applications while aligning with global sustainability goals [248], [249], [250].

4.6.1. Electrochemical-Leaching

Electrochemical leaching is an emerging hydrometallurgical technique that employees and at the same time enhances the metal recovery from metal-rich waste like that of LIB, by

employing an external electric field/current to drive the dissolution of valuable metals from it by redox reactions and hence offering a sustainable alternative to conventional chemical leaching methods (chemical reductants as H_2O_2) [251], [252], [253]. Unlike the typical industrial wet leaching processes, the ECL utilises electrons and redox mediators (e.g., Fe^{2+}/Fe^{3+}) to reduce the use of metal oxides as high-valent (e.g., Co^{3+}, Ni^{3+}, Mn^{4+}) into soluble ions like the (Co^{2+}, Ni^{2+}, Mn^{2+}), thus improving leaching efficiency of the process while at the same time minimizing the need/use of the acids and generation of wastes (wastewater) [251], [252]. The theoretical basis of ECL involves both chemical-controlled reactions (surface dissolution) (Eq. (**14**)) and internal diffusion-controlled reactions (mass transport) mechanisms (Eq. (**15**)), that is modelled by the shrinking core leaching kinetics, which is the typical rate-controlled equations in the leaching as steps, involving reaction constants k_1 and k_2, and the leaching rate of a specific metal X dependent on the retention time t [254].

$$1 - (1 - X)^{1/3} = k_1 t \tag{14}$$

$$1 - 2/3X - (1 - X)^{2/3} = k_2 t \tag{15}$$

For instance, in processing LIBs, the increase of the current density accelerates cathodic and anodic reactions, which in return leads to enchanted leaching rates of (e.g., Li, Ni, Co, and Mn), but if the current is of excessive amount, then it causes premature metal deposition (e.g., Ni-Co co-deposition) hence to decrease of purity levels of metals [254].

Some of the challenges in the ECL also include those of slow kinetic reactions/processes (requiring ~7 hours for greater than 96% recovery) or competing side reactions occurring in chemistry (e.g., oxygen evolution) and limited mass transport due to heterogeneous reactions [253], [255]. Nevertheless, ECL's electric field can also directly pull Li^+ from solid phases, such as those of α-spodumene, which allows for lowering the electrochemical leaching but can lead to parasitic reactions, such as oxygen evolution, that reduce Faradaic efficiency and hence the process itself suffers [253]. The efficiency of the process and methodology can also be affected by the Gibbs free energy change (ΔG), which is associated with leaching reactions, as well as the influence of electrochemical potential (E_{rxn}), which also governs reaction spontaneity [253]. As such, the optimization of the current density is a critical aspect of the ECL, as it accelerates both anodic and cathodic reactions, thereby enhancing mass transfer [254]. Nonetheless, the over-excessive current

can also cause undesirable deposition of metals (e.g., Co and Ni), which would also lead to product purity reduction [254].

Current studies have been somewhat fruitful, as the ECL has been demonstrated by (Diaz et al. [6]) also to achieve metal recovery rates of (>96%), utilising a bipolar membrane electrolytic cell with soluble redox mediator Fe^{2+} as a reducing agent in a controlled acidic environment, with minimal waste [6], [251]. While there are challenges in every new and old process, the ECL future advancements in reactor designs and electron/mass transport optimization are critical, addressing today's challenges is important in developing sustainable and large-scale alternatives of ECL into traditional methods, particularly when powered by renewable energy sources [253], [255].

4.6.1.1. The Direct Leaching and Indirect Leaching

The difference between direct leaching and indirect leaching is quite simple, as the direct electrolysis method involves the execution of an oxidation reaction at the active site [256]. This means that the reaction is done on the electrode surface [256]. For instance, in acidic conditions, Li from the LFP cathode can be selectively recovered via electrochemical direct oxidation leaching, thereby allowing the separation of Li and Fe during the process and simplifying the recovery process [256]. This can be explained via (Eq. (**16.1**)),

$$2H_2O\,(l) - 4e^- \rightarrow 4H^-(aq) + O_2(g)\uparrow \quad (16.1)$$

$$LiFePO_4(s) + 4H^+(aq) + e^- \rightarrow Fe^{2+}(aq) + Li^+(aq) + H_3PO_4\,(aq) \quad (16.2)$$

Where the (Eq. (**16.1**)) is the anode oxidation, via water oxidation, which in return releases oxygen gas and protons H^+, leading to cathode reduction of (Eq. (**16.2**)) as the LFP is reduced, subsequently releasing Li^+ and Fe^{2+} into the solvent solution as phosphoric acid is being generated.

In indirect leaching, oxidation may occur not only on the anode but also on the cathode, as by homogeneous electron transfer, which enables indirect electrolysis at lower potentials than direct electrode transfer [256]. Thus, this reduces energy consumption and improves reaction efficiency, while lowering the electron transfer overpotential, and at the

same time, avoiding the direct electrolysis limitations [256]. As an example of LFP, through synergistic electrochemical and chemical leaching, the strong oxidants allow a selective metal separation from LFP leachates by creating high redox potentials [256], [257]. This allows Fe^{2+} to be separated from Li^{+} via cathodic precipitation, using the leaching solution as the initial catholyte [257]. As such, the reaction can be written as (Eq. (**17.1**)).

$$Fe^{2+}(aq) \rightarrow Fe^{3+}(aq) + e^{-} \quad (17.1)$$

$$LiFePO_4(s) + Fe^{3+}(aq) \rightarrow Li^{+}(aq) + Fe^{2+}(aq) + FePO_4(s) \downarrow \quad (17.2)$$

Where the (Eq. (**17.1**)) is oxidant regeneration on the anode, as the Fe^{3+} leaching agents are regenerated as the anodic oxidization occurs. In (Eq. (**17.2**)), the LFP is then leached by the Fe^{3+} as it oxidizes into Fe^{2+} in the LFP, hence releasing Li^{+} and forming the $FePO_4$ as the Li^{+} remains in the solution, and $FePO_4$ forms an insoluble precipitate and thus can be removed from the solution. As such (**Figure 19**) explains how the differences between direct and indirect electrochemical leaching.

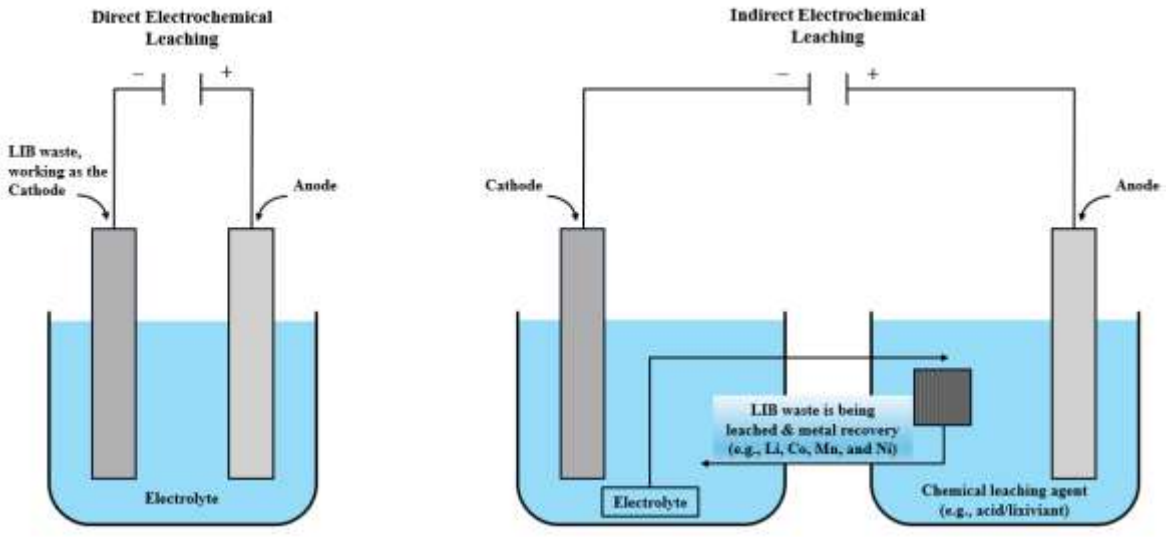

Figure 19. Difference between Direct and Indirect Electrochemical Leaching and their principles.

As one can see from the (**Figure 19**) the simple explanation is that in direct the LIBs waste works as a cathode, while in indirect the leaching happens by utilizing two separate

electrodes, out of which an anode and a cathode support leaching via a direct current (DC) power source, as the LIBs waste is being leached.

4.6.2. Electrochemically-Assisted Leaching

Electrochemically-assisted leaching for the past few years has gained a notable increase in attention as a sustainable, selective, and efficient technology for extracting critical and valuable metals from various primary and secondary resources, including low-grade ores, electronic waste, and spent batteries, those of LIBs of our interest [6], [258], [259], [260], [261]. The traditional hydrometallurgical leaching methods often rely on high temperatures, strong acids, and high concentrations of oxidising reagents, which contribute to significant environmental and energy burdens throughout the process's different steps [258], [259]. EAL's sustainable strategy in extractive hydrometallurgy is to utilise electrons ideally sourced from carbon-free energy, as well as clean redox agents, to drive metal dissolution reactions under milder conditions, which can be controlled and scaled to an industrial setting [259], [260]. In EAL systems, the direct anodic dissolution of aqueous and solid metal-bearing minerals and waste can be limited by passivation layers, especially in low-conductivity or uneven surfaces such as those found in BM or metallic alloys [258], [259]. Further, the EAL's ability to regenerate oxidising agents like Fe^{3+} or reactive oxygen species (ROS) (e.g., H_2O_2, OH, Cl_2) in situ environment by alkaline electrochemical advanced oxidation processes (EAOPs), allowing the dissolution discussed above [258]. For instance, the research done by (Xue et al. [262]) demonstrated that when ROS, are generated under alkaline conditions, it is possible to oxidatively dissolve metal ions (e.g., As, V, and Cr) even at room temperature, with potential implications of those efficient and selective recovery, with catalyst regeneration [258]. Because of these advantages and research, EAL can be fine-tuned through solution chemistry and applied potential, thereby overcoming and studying kinetic barriers to improve reaction efficiencies.

Recent studies have highlighted the highly efficient potential of EAL for LIB waste recycling, as high extraction efficiencies (e.g., 82% Li, 62% Co) have been achieved under mild conditions without pre-treatment [260]. Additionally, the development of deep eutectic solvents (DESs) and the use of hydroxylated electrolytes have been noted to further enhance

the selectivity and scalability of the EAL in battery recycling, both from a laboratory and theoretical standpoint [6], [250]. The development of reactors and other similar principles have also seen a positive development as integrated systems combining leaching and electrodeposition cell-like systems have gained systematic attention [261]. Various experimental setups including those of two-compartment electrochemical cells and three-electrode systems with titanium (Ti) mesh, glassy carbon, or stainless-steel electrodes, have demonstrated high metal recovery efficiencies (>96%) and the potential for selective metal separation by adjusting potential and electrolyte composition [6], [259], [260], [261]. (Hazotte et al. [261]) Ni-Cd-based battery recovery utilising cell-type technology has also proven effective for selectively recovering cadmium (Cd) over Ni and Co, by an energy-efficient separation method [261]. Despite their research having higher energy consumption than those (6–10 V cell voltage), the concept enhanced understanding of proton generation rates, migration barriers, and metal speciation, which are essential in optimising cell voltage [6], [261]. Hence, these methods demonstrate and align with decarbonization goals by utilizing renewable electricity, drastically minimizing chemical use, and employing cheaper and more environmentally friendly alternatives in the process [6], [261]. Overall, what EAL represents is a focus and promising technological advancements in the highly energy-intensive and concentrated chemical solution usage in hydrometallurgical LIBs recycling, by optimising kinetics and reducing costs for industrial adoption [6], [259], [260], [261], [263].

5. Methodology

This chapter is part of the experimental section, which outlines the systematic approach adopted to investigate the feasibility of electrochemical leaching for CRMs from the EoL spent-LIBs. The methodology encompasses the preparation of LIB materials, characterisation of black mass, design of the experimental reactor, literature-informed parameter selection based on the chemical and electrochemical leaching altogether, experimental testing protocols, data analysis, and comprehensive safety measures. Overall, the chapter consists of eight sections and further of eight sub-sections, which enable a clear review and understanding of the process experimentation and methodology in a detailed manner.

5.1. Research & Experimentation Purpose

This thesis and research aim to investigate whether electrochemical leaching, utilizing an experimental type of reactor modified from other research conducted and designed by Mohammad Reza Bilesan, in which gold extraction from motherboards was conducted, is feasible. Research is optimized to study the leaching efficiency (Eff.%) of CRMs and metals, such as those of Li, Co, Ni, and Mn, from spent/EoL LIBs under reasonable parameters, if possible. The research will also focus on studying the BM made of the LIBs in this thesis and determine its type, as well as what can be learned from it, using different analytical methods to yield explanatory results throughout the methodology section (***5. Methodology***). The use of kinetics and thermodynamics will be of utmost importance in explaining what happens and should happen on both theoretical and practical levels throughout the tests.

In this research, a flow-current-type reactor is utilized in a batch mode with a BM addition type in each experiment, subsequently with different types of reactor configurations and parameters, ranging from acid types and their concentrations to temperatures, flow rates, and current intensities.

The clarification must also be done, into the research and experimentation that the treatment being done is testing and determining the Eff.% for the stated metals beforehand,

and not through the additional extraction of them using further methods of ”recycling” or ”precipitation” of that matter. The Eff.% we are discussing in this thesis is how much of the concentrated metals in the BM is subsequently leached into the leaching solution from the BM’s initial metal concentration, which can then be extracted with various other methods, as stated in the hydrometallurgy segment.

Aspects that are taken into account when justifying the use/need for this type of reactor in comparison to other available methods:

1. What are the Eff.% rates of already available methods in the current type of reactor comparisons (literature review comparison)?
2. How do other compartment configurations compare to one another, not only in thesis, but also those in the literature and studies?
3. What type of changes and improvements are necessary for better results, based on available data, literature, as well as experimental results from the thesis and theoretical results in case of reactions taking place and could take place with changes?
4. Do our data collected in experiments resemble that of already conducted and reviewed data in any way, and if not, why, and what is different?

Experiments are designed to collect data on the leachate/lixiviate, which contains the mentioned metals of our interest and many more in the same samples and observe those samples after the changes have been implemented. The primary focus is put on the time the samples were taken from one another, what changes they have in comparison to one another, and whether these changes are desirable or not, and if so, why.

5.2. Preparation of Lithium-Ion Battery

This section goes over the preparation of the black mass from the EoL spent-LIBs, and then its preparation into as much as possible homogeneous mass, based on the particle size distribution. This was done by disassembly of the battery packs and then their internal parts separation and subsequent milling, to attain black mass. While taking all of the pre-cautions and safety regulations, which are part of the understanding process, into account and

following them. Black masses were then characterised and their morphology with elemental distribution were studied and confirmed by the SEM-EDS and ICP-MS as the main instrumental analytics throughout all of the experimental tests.

5.2.1. Spent-LIBs battery packs

The used spent-LIBs in this research are provided by LUT University and are of the type of laptop battery packs that have been decommissioned by LUT and made available for this research. This means that the batteries used were used and old type ones, which might have been at their end-of-life-cycle (EoLC), which were perfect for this type of research, as the goal is to recycle batteries and their content from the EoLC stream using a closed electrochemical flow reactor, which recovery efficiency was being tested.

It is also important to note that the battery packs provided were from multiple different manufacturers, hence their content may not have been similar to one another. What is also important to clarify is that EoLC LIBs contain different amounts of metals concentrated within them, with possibly even undefined elemental compounds. These are only one of many challenges in this type of research, as manufacturers are obligated only to present information regarding products, such as when they are being produced. What happens in the later stages of the LIB life cycle is shrouded in many factors, which are often UNK and cannot be traced. These factors all have a key influence on the state and, hence, the concentration of metals/elements in LIBs in EoLC in this instance.

Battery packs used in this research all come from laptops, and there were several different models used (**Figure 20**), manufactured for either Hewlett-Packard Company (HP), Dell Inc. (DELL), or ASUSTeK Computer Inc. (ASUS) laptops, as seen for some in (**Table 27**).

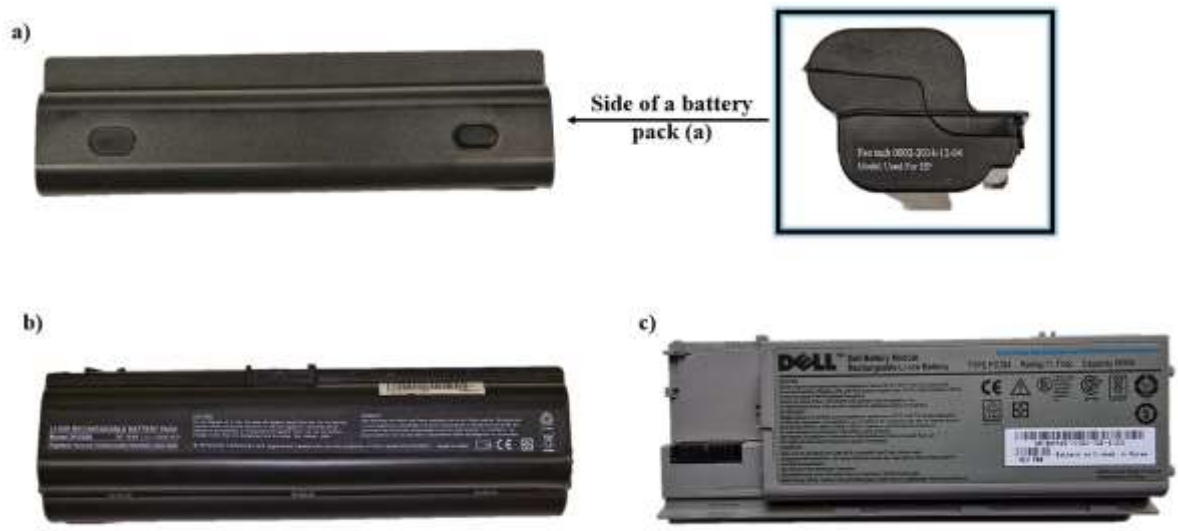

Figure 20. Some of the battery packs used in the research and disassembled in later stages.

Table 27. LIBs used in thesis with manufacturers and corresponding models, based on the (**Figure 20**) data for some of them.

Manufacturer	Model	Figure 20
HP	Series HSTINN-IB51	–
HP	DV2000	(b)
DELL	TYPE PC764	(c)
ASUS	A32-F3	–

Additionally, it is worth noting that these battery packs varied in shape and size, resulting in different weights. Furthermore, it is also notable that, although they were intended for DELL, HP, and ASUS laptops, their manufacturers were different subsidiary companies.

5.2.2. Disassembly of LIB battery packs

The first step of the dismantling procedure of the used LIBs in the research was the removal of the batteries from the (de-commissioned) laptops and then observing if any of them had any internal defects or any external abnormalities, which would have led to their removal from further research. After this, the batteries were pried open using a jigsaw on the groove of the LIBs casings, specifically at one of the corners between the top and bottom halves of the LIBs, to make a small cut. This then enables the opening of the batteries using more

conventional tools, like the linesman pliers or long nose pliers, which in turn opens up the internal structure of the LIBs as seen in (**Figure 20**), right side. The dismantling method of the battery packs was done as follows:

1. Small incision into the plastic casing of the battery pack by a prying tool and wire cutters.
2. After an incision and a small opening, long nose pliers were used to widen the opening.
3. Using an insulated screwdriver, pull along the edge of the opening, while at the same time prying/widening open with the long-nose pliers, to separate the two plastic faces from one another.

The use of an insulated screwdriver and other tools was important as the rupture of individual cells or the damage overall may have caused a short circuit if coming into contact with either the battery/cells end or the thermal reaction, as the Li is unstable and highly reactive when coming into contact with air. Additionally, the risk of puncturing battery cells inside meant risking the creation of toxic gases, such as HF, so the process was done under the fume hood. During the process, the following safety precautions were taken into account and used:

- Wear insulated gloves and safety goggles.
- Work in a well-ventilated, non-flammable area.
- Using as many insulated tools as possible.
- Avoid puncturing or crushing the battery cells.
- Make sure batteries were as much DISCHARGED or FULLY DISCHARGED.
- Having a Class D fire extinguisher nearby and a metal container with a lid for a case of thermal runaway.

After the separation between the top and lower covers was achieved, the battery pack was successfully opened, hence the 1st step was completed, leaving us with (**Figure 21 (b)**), battery cell assembly in (parallel connection) and connected to the circuit board, which is known as battery management system (BMS) or known as a safety protection circuit and has a key role in the stability of the battery throughout its usage life, by protecting it from different fault conditions from itself, which typically range from overvoltage/undervoltage and overcurrent [264].

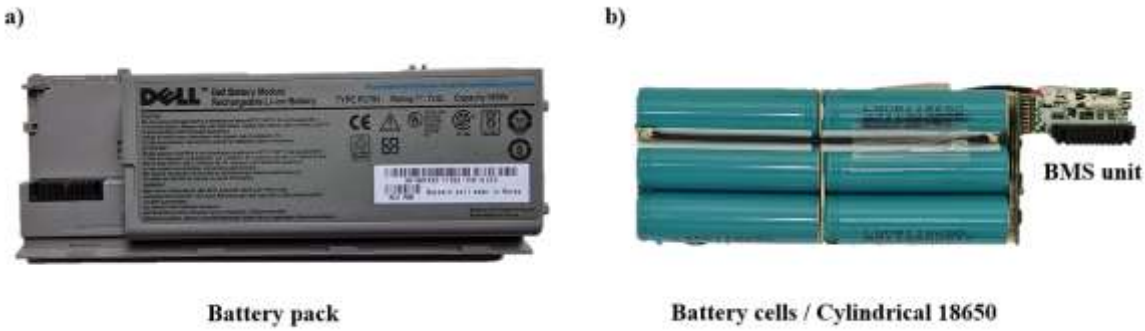

Figure 21. One of the tested LIBs and disassembled in the thesis, TYPE PC764 DELL battery pack on the right (a), and on the left, disassembled the same battery inside of battery cells 6x of LGDB118650 (cylindrical) and the BMS unit of the battery (b) that was tested subsequently**.**

Separation of the cells from the battery pack (parallelly connection) was done as follows:

1. Disconnect the battery pack cells from the BMS unit using wire cutters.
2. Cut the connection between the cell's spot-welded strips and avoid damaging the cells.

The same precautions, safety equipment, and environment as discussed above (**Figure 21**).

5.2.2.1. Discharge method of single Cell

After cells were separated into individual batteries, their dismantling must be done only after discharging them, to avoid residual electricity/charge in the battery. This is important as when the cell is opened, if there is a charge in the battery, the following risks and scenarios can occur:

- The anode and cathode touch each other due to a puncture/tool, leading to an internal short circuit, resulting in a rapid heating and thermal runaway (>500°C)
- Release of gases (e.g., HF and CO_2) and other vapours that may occur due to electrolytes (e.g., EC and PC), leading to acute poisoning and, in the worst case, lung damage.

- Li has high reactivity, with the moisture/air may lead to spontaneous thermal runaway and, in a worst-case scenario, explosion, risking yourself and the surrounding area.

Because of these reasons, the discharging of batteries is essential, as if the energy stored in the battery is still present, but the reaction inside the battery will not be as violent, and time for reaction and making current safety decisions will be sufficient. For instance, thermal runaway, the exothermal or simply put, overheating process, of a battery due to self-heating, because of the high-density energy stored in batteries, and by so creating one chemical reaction to cause a chain reaction of other processes/reactions [265], [266]. As this reaction starts increasing uncontrollably, it becomes self-sustaining, a phenomenon known in chemistry as the combustion of exothermic and redox reactions. The reaction continues, producing oxygen, which leads to SEI layer decomposition at 80°C and electrolyte breakdown at 100–120°C, resulting in the creation of vapours and toxic fumes [267].

Battery discharging as discussed in (***4.1.1. Sorting, discharging, disassembly and separation***) could be done via NaCl, Na_2CO_3, Na_2SO_4 and/or $MgSO_4$, but in this work, it was decided to be done simply and more easily, as the quantity of battery cells was not a ridiculous amount to demand for large-scale discharging as these salts are typically utilized in. Additionally, avoiding corrosion or any other reaction inside the LIBs was desired, so that the results of future experiments and characterization analysis would not be affected.

To understand and know if batteries were or had any sort of charge in them, they were first tested and connected to a Fluke 189 True RMS multimeter as shown (**Figure 22 (a)**), and then each cell that had charge was connected to the resistor by two wired alligator clips, one from each end of LIB polar ends. The other ends of the alligator-clipped wires were then connected to a 10-ohm (Ω) resistor and left connected for 18–24 hours to drain out energy capacity. LIB discharge efficiency could then be calculated by the following (Eq. (**18**)).

$$P = \frac{V^2}{R} \tag{18}$$

Where P is power (W), V is voltage (V), and R is resistance in ohms (Ω). By this (Eq. (**18**)), one could calculate discharge efficiency, which then could be used to calculate the time

needed for battery discharging. For this, one would need (Eq. (**19**)) to calculate capacity to energy, which then could be used to calculate (Eq. (**20**)) the time needed.

$$E = \frac{V \times \text{mAh}}{1000} \tag{19}$$

$$t = \frac{E}{P} \tag{20}$$

Where, in (Eq. (**19**)) E is capacity (Wh) and V is voltage (V), while in (Eq. (**20**)) t is time (hours), E is capacity (Wh), and P is power (W). Nonetheless, in this thesis, these were not done/calculated, or data was not collected as deemed unnecessary, but the discharging of the battery was done, and it can be seen as a schematic in (**Figure 22 (b)**).

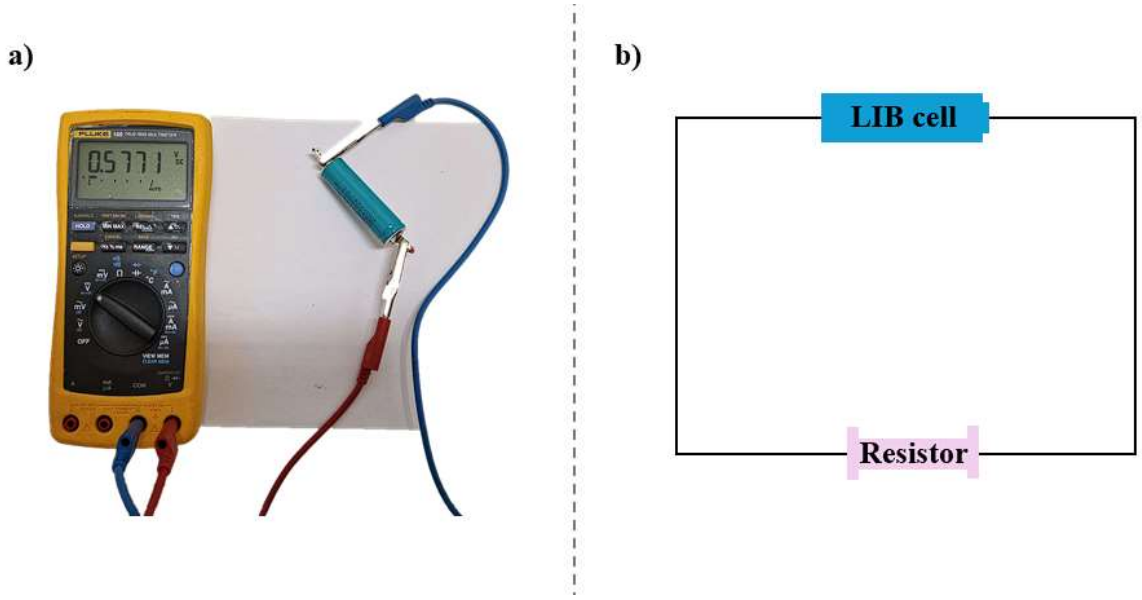

Figure 22. Use of the Fluke 189 True RMS multimeter to check the charge and capacity of energy inside the individual cells on the left (a), and schematic of the discharging method done for the individual LIB cells on the right (b).

5.2.2.2. Dismantling method of a single LIB cell

After battery cells had been discharged, their dismantling was performed for the collection of BM and to separate the Cu negative current collector (anode), Al positive current collector

(cathode), casing, separator, and plastic from one another. Battery disassembly was done as follows for each cell:

1. The plastic wrapper was removed from around the metal casing of the cell.
2. Cutter and wire cutter pliers were used to pry open one pole of the cell.
3. After one pole was open, the thin Fe rod was removed from the battery.
4. Cutters were then used to pry open the casing of the battery along the side to separate the casing from the rest of the battery cell.
5. The cells were then unrolled on the stainless-steel tray in a big plastic bag that could be zip-sealed for safe storage, and the cathode sheet/strip was left in it, while the other two more of similar trays and bags were nearby, where the separators and anode sheets/strips were then saved for later use.

Safety and other precautions that were taken into account were the same as in the (***5.2.2. Disassembly of LIB battery packs***), as the risks were the same throughout the whole battery dismantle to these steps.

5.2.3. Creation of the Black Mass

After the separation of battery materials into separate bags, the cathode and anode strips were mixed, and the ends of their strips were removed by cutting them just. The rest of the strips were then cut into approx. (5x5 mm) sizes (**Figure 23 (a)**) and put into a single bag, while the cut leftovers of the Cu and Al strips were put into separate bags, as they were not used to make the BM or the rest of the thesis. What also should be noted is the storing of the BM, which should have been preferably done in a desiccator, not to let moisture affect the BM, but this was not done, so the results of the further thesis may have been altered, to what extent UNK.

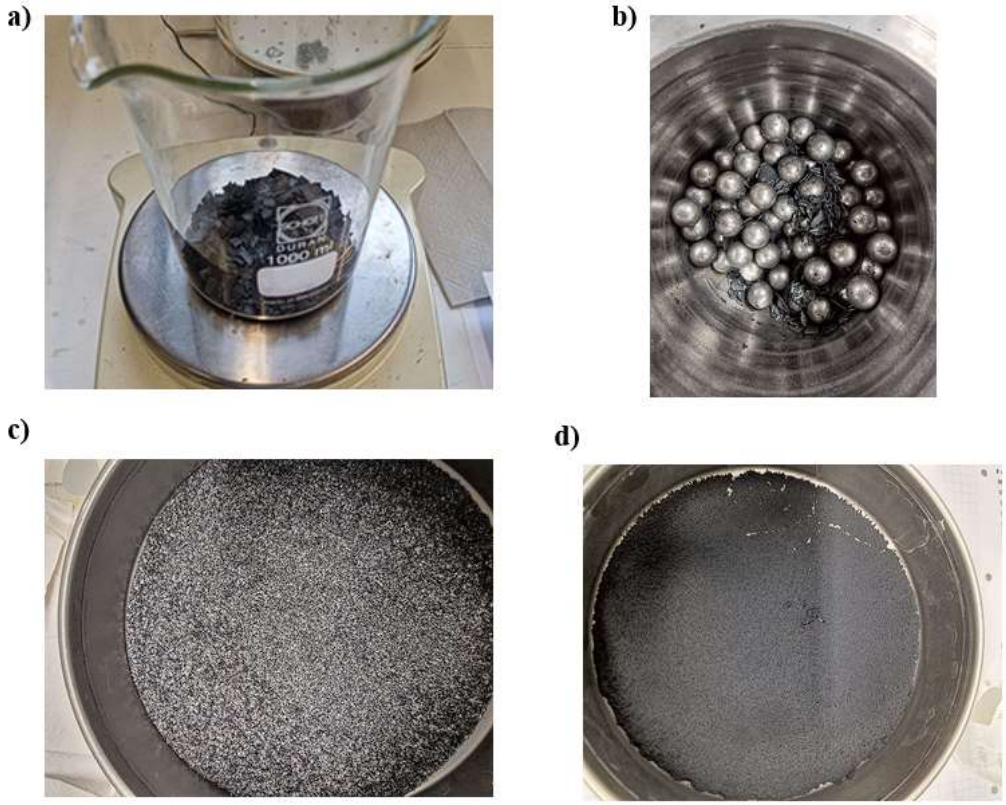

Figure 23. Image of the (5x5 mm) sized cathode/anode sheets in the upper left corner (a), 76x of (⌀ 1 cm) stainless-steel balls inside the planetary ball mill drum, with the cathode/anode sheets (partially shredded) in the upper right corner (b), biggest particles what is left of cathode/anode sheets BM material (particle size >250 μm) in the bottom left corner (c) and BM material of the finest size (<75 μm) in the bottom right corner (d).

The creation of the BM was done using a (Planetary Ball Mill PM 100) by RETSCH GmbH, Germany, and stainless-steel balls 76x size (⌀ 1 cm) in it, with several batches of approx. (100 grams) per batch as shown in (**Figure 23 (b)**) where the BM material was milled by the balls in the planetary ball mill.

The total time per batch was 95 minutes, which included milling with breaks in between. Breaks were important because the friction and heat generated by the balls were noted to be an issue, which was evident from the odour in the air. As such, the process of milling and breaking was as follows (**Table 28**).

Table 28. Process of milling BM into finer particles for the thesis.

	Time (min)
Milling (1)	5
Break (1)	5
Milling (2)	15
Break (2)	10
Milling (3)	15
Break (3)	10
Milling (4)	15
Break (4)	10
Milling (5)	10
Total	**95**
	Grams
Initial BM	360.11
Milled BM	357.09
Difference	**3.02**

After the milling, it was also noticed that the difference between the initial BM of (5x5 mm) particles was 360.11 grams, and afterwards, it was only 358.17, meaning that due to heat/friction (e.g., electrolyte or moisture removed by heat) and other things (e.g., material clinging to balls (electrostatic effects)) a 3.02 grams loss was recorded. After milling, the BM was filtered/sieved through different sieve grades, of (>250, 250–150, 125–90, 90–75, <75) μm (Analysensieb-Retsch-5657 HAAN W) by Germany and the recorded distribution of the BM was as in (**Table 29**).

Table 29. Distribution of 358.17 grams of BM material throughout different particle sizes.

	Particle size and distribution					**Unit**
Samples	**>250**	**250–150**	**125–90**	**90–75**	**<75**	μm
BM mass	78.72	50.1	108.08	71.24	48.95	Grams
Fraction/Percentage	22.04	14.03	30.27	19.95	13.71	%

In (**Figure 23 (c)** and **(b)**), one can also see the difference between large >250 μm large/coarse particles of Cu and Al foils and small particles of finely ground powder like BM (<75 μm) respectively.

5.2.4. Characterisation of the LIB cells and Black Mass

For characterising the batteries and BM, the most optimal approach is the use of various analytical instruments, such as SEM-EDS, ICP-MS, and CHNS analysis. However, a lot of information about LIBs and their cells can also be found by using the wraps' colour and codes that come with them on the side, as visible in (**Figure 21 (b)**). Companies and manufacturers typically only provide the following information when it comes to their batteries:

- Description and Model,
- Technical Information,
- Cell Dimensions,
- Appearances,
- Characteristics,
- Mechanical Characteristics,
- Environmental Test,
- Safety Test,
- Standard Test Conditions,
- Product Liability,
- And warranty [268], [269].

As was already discussed, cells contain different amounts of elements and are also manufactured either by the same manufacturer or by another. The identification of these is simple, as they have a different colour of the outer layer from one another, as seen in (**Figure 21 (b)**) and come with an identification code which consists of several segments, model & serial code, and date. Some of the cells tested in the thesis can be found in (**Table 30).**

Table 30. LIB cells tested in the thesis, with their information based on plastic wraps and using the tool (https://batterybro.com/pages/18650-date-code-lookup-tool) for deciphering Date codes [270].

Code	Manufacturer	Wrap Colour	Battery Chemistry	Model code	Date code	Date of manufacture
LGDB118650 Q3112608246 EKI72D7B1	LG Chem Ltd.	Teal	$LiCoO_2$ (LCO)	LGDB118650	Q311	Nov. 2017
ICR18650-26D SDI 972	Samsung SDI Co., Ltd.	Pink	$LiCoO_2$ (LCO)	ICR18650-26D	Code on casing	(UNK)
ICR18650-28A SDI 2A23	Samsung SDI Co., Ltd.	Purple (Light)	$LiCoO_2$ (LCO)	ICR18650-28A	SDI A23	Feb.03.2010
ASO GH40411EH 210557 SZN	(UNK)	Purple	(UNK)	ASO/SZN	(UNK)	(UNK)

As one can see, a lot can be found from only visual inspection of the battery cells, like the manufacturer and even the manufacturing date for some of the cells used in the thesis. (**Table 31**) shows the structure of the typical 18650 cell type in relation to all its components based on (Johnson et. al [271]).

Table 31. Typical measurements of the 18650 cell type battery components compared to one another, from minimal to maximal data for different manufacturers. (*Note! Data for Matsushita cells was taken separately due to too great of a difference from other manufacturers' cells*). Table reproduced from the Ref. [271].

Component	Measurement	Min & Max	Matsushita (cell)
	Total mass (g)	38.1–41.9	24. 1
	Mass of can (g)	6.6–9.1	4.5
Anode	Mass (g)	13.3–15.4	7.0
	Thickness (µm)	114–185	185
	Foil thickness µm)	25	25
	Length (cm)	49.2–78.1	35.0
	Width (cm)	5.3–5.5	3.7
	Active area (cm^2)	422–532	6.2
Cathode	Mass (g)	9.1–12.0	7.5
	Thickness (µm)	94–203	216
	Foil thickness µm)	18	18
	Length (cm)	51.9–76.8	42.2
	Width (cm)	5.5–5.7	3.9
	Active area (cm^2)	421–603	4.7
Separator	Mass (g)	1.3–2.2	1.6
	Thickness (µm)	25	25
	Length (cm)	109.6–173.4	101.6
	Width (cm)	5.3–5.9	4.4

Based on the information provided by (**Table 27**), it has been noted that the following laptop batteries and cells, in particular, provided for this research, were of origin from different manufacturers and of different ages when manufactured. Additionally, there is UNK information on how much each of the LIBs was used in comparison to one another. Hence, it can be said that batteries are at different stages of the EoLC relative to one another. Due to the factors mentioned above, it has been concluded that, in this research, all of the batteries will be treated the same and no differences/exceptions between one another will be conducted and taken into consideration at later stages of research/experiments.

- The decision is also being backed by the following factors:
- No available data for the (**Table 30**) battery cells regarding their elemental content before circulation and at the EoLC.
- Different manufacturers have different elemental compositions from one another (even when talking about LIBs).
- Research does not take into consideration differences between the manufacturers.
- BM is being simulated to what it could be in the real life of a recycling facility (different manufacturers, age of batteries, and consistency of elements/particles overall).

To solidify the meaning of this approach and the reasoning behind the choices regarding EoLC and not using new LIBs or ones that are suitable for a long time, the difference in elemental concentrations is crucial. However, it is challenging to prove the element concentration of spent LIB cells simultaneously in different single cells. In this research, to ensure that all single cells contain the same amount of every element, differentiation is performed based on the available data from the new LIBs and cells alike.

5.2.4.1. Characterisation of BM by ICP-MS analysis

Inductively coupled mass spectrometry (ICP-MS) analysis (model 7900 ICP-MC equipped with ASX-500 autosampler) manufactured by Agilent US, was used for identification and characterisation of this thesis throughout every experiment, and each single sampling was done/run as a triplicate, to avoid situations where one of the samples has a big

deviation/difference from the other samples. The use of ICP-MS is crucial throughout, as it enables the identification of the elemental composition of BM and its metal concentrations.

To prepare samples for the ICP-MS, which requires only dissolved or soluble samples, the BM samples need to be dissolved using the appropriate methods. For this reason, samples were dissolved using the microwave digestion system. Samples were also dissolved using the commonly applied AQUA regia, which was prepared by combining concentrated HCl and HNO_3 acids in a 3:1 ratio. This can then be put into (Eq. (**21**)), which shows the reaction of the HCl and NHO_3 further.

$$HNO_3\ (aq) + 3HCl\ (aq) \rightarrow NOCl\ (g) + Cl_2\ (g) + 2H_2O\ (l) \qquad (21)$$

Where the HNO_3 oxidizes chloride ions (Cl^-) from HCl to produce Cl gas with water and nitrosyl chloride (NOCl) as the primary reactive agent. When AQUA regia is created, it is a volatile and highly reactive species, which is seen as it decomposes relatively fast, which is seen in a yellow/orange vapour as a result when mixing acids (created under the hood and always fresh, not stored). This was observed as the bubbling started in the test tubes, and as such, reaction/decomposition can be written down as (Eqs. (**22.1**) and (**22.2**)).

$$2NOCl\ (g) \rightarrow 2NO\ (g) + Cl_2\ (g) \qquad (22.1)$$

$$2NO\ (g) + O_2\ (g) \rightarrow 2NO_2\ (g) \qquad (22.2)$$

As the AQUA regia is being formed the small number of different particle sizes of BM LCO, as in (**Table 29**), is added into a test tube 50 of around 0.1 grams with ± 0.0125 grams difference, due to the small amount needed and done as quadruplicate (four) as a majority of sampling for each particle size distribution meaning of three shadow samples. This addition of BM, composed of LCO, can then create the following reactions (Eqs. (**23.1**) – (**23.4**)).

$$LiCoO_2\ (s) + H^+\ (aq) \rightarrow H^+(aq) + CoO_2(s) + H_2O\ (l) \qquad (23.1)$$

$$Co^{3+}(aq) + Cl_2\ (g) \rightarrow Co^{2+}(aq) + 2Cl^-(aq) \qquad (23.2)$$

$$CoO_2(s) + 4H^+(aq) + Cl_2(g) \rightarrow Co^{2+}(aq) + 2H_2O\ (l) + 2Cl^-(aq) \qquad (23.3)$$

$$Co^{+2}\ (aq) + 4Cl^-(aq) \rightarrow [CoCl_4]^{2-}\ (aq) \qquad (23.4)$$

So, what happens is that in (Eq. (**23.1**)) Li is being released from LCO, and this leads to oxidation of Co^{3+} to Co^{2+} as seen in (Eq. (**23.2**)) and byproducts due to the reduction effect as a pathway one (1). Reaction (Eq. (**23.3**)) is also possible as a pathway two (2), in which the reduction happens in oxide form. As these have occurred, the complexation of dissolved Co can happen as per (Eq. (**23.4**)) via the Cl. Overall, the whole reaction between LCO and AQUA regia can be simplified as the (Eq. (**24**)).

$$\mathrm{LiCoO_2}\ (s) + 4\mathrm{HCl}\ (aq)\ + \mathrm{HNO_3}\ (aq) \rightarrow \mathrm{Li^+}(aq) + \ [\mathrm{CoCl_4}]^{2-}\ (aq) + \ \mathrm{Cl_2}(g) + \mathrm{NO}\ (g) + \ 2\mathrm{H_2O}\ (l) \tag{24}$$

After the mixing of the BM and AQUA regia had been done, the samples were put into a microwave digestion system for (1 hour) in two separate batches. The overall sampling/dissolving of the BM can be found below (**Table 32**). The sampling was done for fifteen (15) samples per batch, and both had blank samples in them. Also, the BM was dissolved primarily in quadruplicate sampling, but due to limited space and the need to fill empty racks, improvisation and what particle size to run more times was done.

Table 32. Sampling and dissolving of the BM via AQUA regia by microwave digestion system for the different particle size distribution of BM, as per (**Table 29**).

No.	Batch 1	Mass (grams)	Batch 2	Mass (grams)
1	>250	0.1043	90–75	0.1002
2	>250	0.0997	90–75	0.0997
3	>250	0.1056	90–75	0.1025
4	>250	0.096	90–75	0.1051
5	250–125	0.0991	<75	0.1058
6	250–125	0.1028	<75	0.101
7	250–125	0.0957	<75	0.1082
8	250–125	0.1014	<75	0.1045
9	125–90	0.1054	250–125	0.0993
10	125–90	0.1041	250–125	0.1019
11	125–90	0.1066	250–125	0.982
12	125–90	0.1072	Blank	0
13	Blank	0	Blank	0
14	Blank	0	Blank	0
15	Blank	0	Blank	0

After dissolving and digesting the samples, they were taken into the ICP-MS room, where they were prepared and diluted by a solution of a 2% NHO3 and 0.5% HCl solution

sample matrix mixture by 100x to analyse and find out BM's elemental composition weight percentage (Wt.%) to one another. In this thesis, the goal is to achieve and determine the recovery/leaching efficiency for the Li. In addition, also other elements like Co, Ni, Fe, Al, Cu, Mn, & Cr, for instance, if there are traces of them, but primarily Li, Ni, Co, & Mn. The samples were prepared into 50 mL plastic test tubes and diluted with the dilution solution by 100x after they were filtered through an RC-20 syringe micro filter, filtering (0.20) µm and larger particles, for precaution. A 0.5 mL sample was pipetted into a tube and then diluted with 49.5 mL of solution. Data that came out (**Table 32**) by ICP-MS for the samples can be found below (**Table 33**).

Table 33. Wt.% for the samples calculated from the ICP-MS concentration in parts per billion (ppb).

	BM Sample Size Range					
Element	**>250**	**250–125**	**125–90**	**90–75**	**<75**	**Unit**
7 Li	3.68	5.25	6.36	6.11	5.77	Wt.%
27 Al	30.55	14.08	1.19	0.66	0.56	Wt.%
55 Mn	4.39	6.15	6.60	6.45	4.94	Wt.%
59 Co	21.39	26.86	31.88	33.27	38.92	Wt.%
60 Ni	8.13	10.83	11.57	11.49	8.94	Wt.%
23 Na	-0.05	0.02	-0.09	0.13	0.11	Wt.%
39 K	-0.45	-0.42	-0.62	-0.09	-0.21	Wt.%
51 V	0	0	0	0	0	Wt.%
52 Cr	0.01	0.01	0.01	0.01	0.01	Wt.%
56 Fe	0.13	0.08	0.06	0.09	0.05	Wt.%
63 Cu	0.02	0.03	0.03	0.03	0.03	Wt.%

What is noticeable from the data is that the Co concentration is highest in particles of less than 75 µm in size, with a significant margin difference compared to other sizes. In contrast, the Li concentration is not particularly notable when compared to other sizes. What was also noticed was the precise distribution and concentration of Al in relation to larger particle size samples, as well as the precise distribution of Ni and Mn in relation to those particle sizes in the middle. Because of these reasons, it was decided to use throughout the thesis from this point on the smallest particle size of (<75) µm as BM material to leach elements out. The decision was also influenced by the reactor and electrodes in mind. Because of this, two months after the decision to use (<75) µm as the BM material for testing, a new analysis was conducted into Wt.% composition of elements was done, as it was discussed with (Analysis

Engineer) Liisa Puro, that a dilution of 1,000 or 15,000 would be better for the samples the thesis was dealing with.

Based on a preliminary analysis of the BM by ICP-MS (**Table 33**), it was determined that all of the following elements could be detected with 100% certainty: Li, Al, Mn, Co & Ni. Additionally, it was noted that theoretically the Na, & K also could also be detected with a certain level/percentage of certainty, as their CPS values are close to that of the minimum of the ICP-MS standard solution value given by it. On the other hand, based on the ICP result, the V, Cr, Fe, & Cu for 100% cannot be seen or detected by the ICP-MS, which means their results could not be used further in the thesis. The following statements can, as such, be represented in the table (**Table 34**) below.

Table 34. BM Elemental Detection & Reliability of the CPS-values/Concentrations of the Elements for the (<75 μm by AQUA regia).

Detected / Reliability	100%	50/50%	0%
	7 Li	23 Na	51 V
	27 Al	39 K	52 Cr
	55 Mn		56 Fe
	59 Co		63 Cu
	60 Ni		

The basis for choosing the best and most reliable concentrations from the 15,000 and 1,000 dilution samples was based on which one had the highest CPS value, as the CPS value corresponds to the reliability of the sample. This is done to all of the elements in (**Table 34**), presented regardless of whether they can be detected by the ICP-MS for later study. The CPS values that were chosen can be found below (**Table 35**). Based on the results between 1,000 and 15,000 dilutions, the CPS values of 15,000 were slightly better, which is why, afterwards, all of the thesis leaching and experimentation samples were diluted/treated into 15,000 dilutions when it came to ICP-MS analysis.

Table 35. Results of the CPS-value for samples and the minimal CPS-value of elemental detection by the ICP-MS for (<75 µm by AQUA regia) samples. (*Note! Elements in detection/reliability order, based on the* (**Table 34**) *100% → 50/50% → 0%*).

Elements	CPS-value of the Sample	CPS value of the ICP-MS standard minimum value
7 Li	594.46	80.00
27 Al	103.61	81.11
55 Mn	18450.48	1931.25
59 Co	637285.56	8841.63
60 Ni	45415.16	2616.93
23 Na	4452.56	4655.21
39 K	4918.27	5737.83
51 V	19.33	3551.11
52 Cr	624.47	5239.88
56 Fe	1743.66	4734.96
63 Cu	421.40	7708.78

Based on (**Table 35**) results, the Wt.% could be calculated by the concentration (ppb) value for the elementals and their calculation for the Wt.% and their corresponding Concentration values based on values. These are represented in (**Table 36**) below. Calculation of Wt.% from the ICP-MS data is relatively simple as it is done using the following equation (Eq. (**25**))

$$\text{Wt.\%} = \left(\frac{\text{ICP} - \text{MS Conc. (ppb)} \times \text{Dilution volume } (V)(\text{L}) \times \text{Dilution Factor } (DF)}{\text{Sample Weight } (W_s)(\text{g}) \times 10^6}\right) \times 100 \quad (25)$$

What happens in (Eq. (**25**)) is taking the raw ICP-MS concentration data in ppb and then multiplying it by the dilution volume of 50 mL. Multiplication by *DF* is not performed as the dilution after digestion was not done, since the sample dilution was already done at the digestion step. Hence, the whole upper side of (Eq. (**25**)) was divided by the *Ws* multiplied by 1,000,000, and the whole calculation was then multiplied by 100 to get a Wt.% as in (**Table 36**). Nonetheless, calculations done in this thesis were done a bit differently. Use of blank ppb's were used to calculate blank average values, which were then subtracted from the ICP-MS raw data, before (Eq. (**25**)) was used to calculate, as instructed. Additionally, the data were adjusted by removing values that were more or less 15% of the relative standard deviation (RSD) to make the data more cohesive.

Table 36. Results of the initial BM characterisation for the (<75 µm by AQUA regia), by the ICP-MS in the form of Wt.% & corresponding Concentration (ppb). (*Note! Elements in detection/reliability order, based on* (**Table 34**) *100% → 50/50% → 0%. Values for the C and Gr cannot be seen via ICP-MS, values for the Reference material can be*).

Elements	Wt.%	Concentration (ppb)	Literature avg. Wt.% Ref. [2], [6], [272], [273], [274]
7 Li	5.42	54,174.67	2.11
27 Al	0.64	6,385.49	2.02
55 Mn	4.69	46,906.46	8.68
59 Co	35.17	351,731.45	13.42
60 Ni	8.84	88,354.47	8.61
23 Na	0.05	458.68	–
39 K	-29.61	-29,6103.00	–
51 V	0.01	126.64	–
52 Cr	0.005	49.81	–
56 Fe	0.05	518.42	1.87
63 Cu	0.02	232.76	2.17
Gr or C	–	–	29.15

Based on (**Table 36**), we can see that BM consist primarily of the Co, which amounts to 35.17% of the total weight of the sample, meaning that BM is/should be that of $LiCo_{1/3}O_2$ basis and then the rest majority of the BM would be Ni 8.84 Wt.%, while Li 5.42 Wt.%, Mn 4.69 Wt.% and small traces of Al 0.64 Wt.% making the amount of 54.76 Wt.% of the BM of (<75 µm) particle size. From the results, it is evident that some of the values, such as those for potassium (K), are questionable, as their weight percentage Wt.% and concentration are negative. This can be explained by the (**Table 34**) observation of CPS-values and ICP-MS minimal detection not being met, meaning that we cannot be sure of the result being correct. However, if the result is correct, it would mean that, based on the ICP-MS, there is no K in the BM we were testing, which may indeed be the case. In addition to these results, the concentration of carbon (C) has been determined to be important, as BM gets its colouration, due to C or Gr, as BM is composed mainly of Gr and Li-metal complex oxides. The Gr/C in this situation is typically carbon black, and its many other variants are used. Due to this, we had to use the elemental analysis (CHNS) analysis method in C amount determination, which gave us the following (**Table 37**) results below, as the ICP-MS could not see C or Gr, as was discussed with Liisa Puro at the time. This analysis method could also see those of H, nitrogen (N), and sulfur (S).

Table 37. CHNS analysis results for the (<75 μm) particle size of BM.

Element	Carbon	Hydrogen	Nitrogen
Wt.%	3.351	0.484	-0.012

Based on (**Tables 36** and **37**), we can see that we have about a total of 58.11 Wt.% in 100% reliable known elements, in addition, know that it should have been around 1–8 Wt.% fluorine (F), also in the BM, totalling around in between 66.11 Wt.% known elements/compounds, meaning that the rest is of that most highly Gr primarily maybe even of 30% ± 2–3% and some other element, not detected [275]. What we can also see from the data (**Table 36**) is that our BM elemental Wt.% comparison to some of the reference materials' average BM's Wt.% tells us that, depending on how and what particle sizes are used in the research, will affect the end product of BM and its composition.

5.2.4.2. Characterisation of BM by SEM-EDS Analysis

Scanning Electron Microscopy with Energy Dispersive X-ray Spectroscopy (SEM-EDS) was used for the examination of the surface morphology and elemental composition of materials at a microscopic level. Use of SEM (The Hitachi SU3500) for imaging was performed, and EDS for chemical analysis. Samples tested in SEM-EDS were prepared as in (**Figure 24**) by adding a small two-sided carbon tape bond, which was used in SEM-EDS analysis, and then a small amount of BM of different particle size distribution, as in (**Table 32**), was added on top of it, coating the tape.

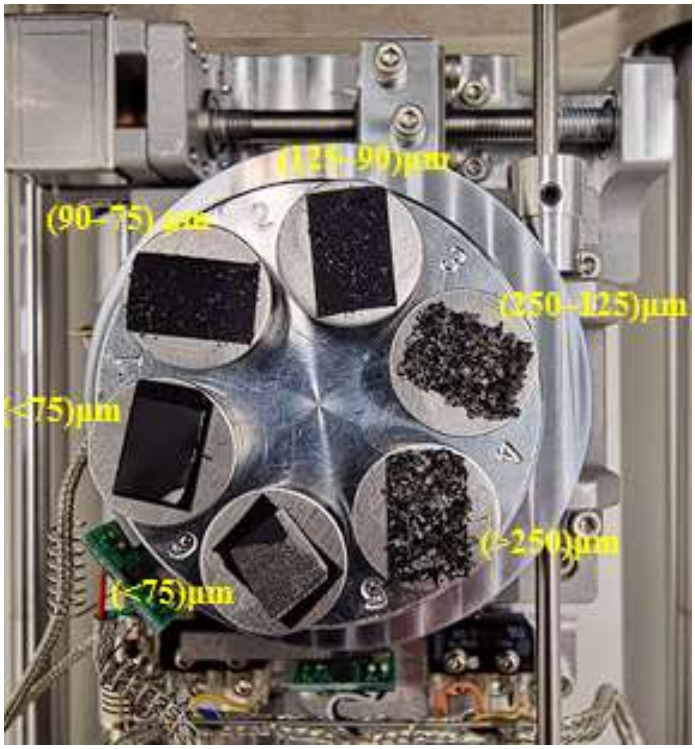

Figure 24. BM sample preparation for the SEM-EDS, with the six different samples, out of which No.5 and No.6 are the same samples of (<75 µm) particle size and the rest were sampled and used only once.

Studying SEM-EDS images revealed two distinguishable particles, one with darker colouration and the other with white colouration, which represent the Gr and metals, respectively, in BM [276]. As the analysis was done with the SEM, it was noticed that the results for Li and Gr could not be obtained reliably, while Gr could be visualised as it is the lightest element when comparing it with the metal elements present in the BM, the detection of Li was not visible even with EDS, which was also discussed and mentioned by the operator, when discussing SEM-EDS capabilities and its parameters present at LUT. The morphology as such of our BM in all five different particle size distributions was performed, as per (**Figure 25**), in which (**Figure 25 (a)**) is that of $LiCo_{1/3}O_2$ assumed. All images were captured using an accelerating voltage of 15.0 kV, a magnification of ×150, and secondary electron detection (SE).

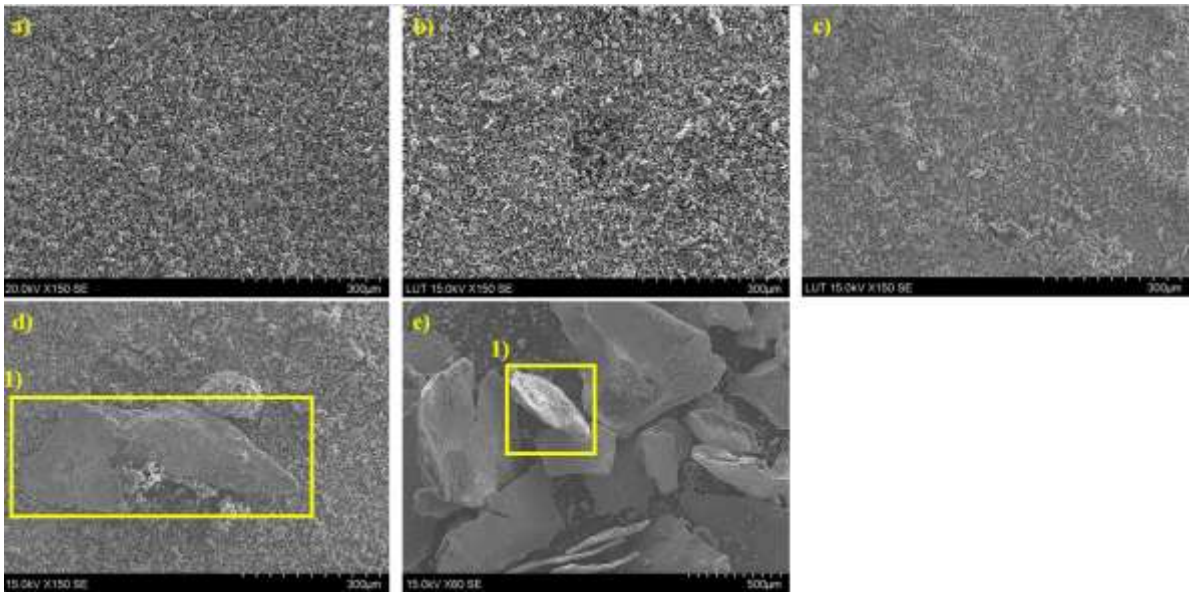

Figure 25. SEM images done at LUT, for the different CM particle size distributions, are as follows: (a) <75, (b) 90–75, (c) 125–90, (d) 250–125 and (e) >250.

What was observed in the SEM images was a clear, irregular shape with vague facets on the particle surface (**Figure 25 (d)** and **(e)**), which were further marked as (**d1** and **e1**). These are the particles of Al-foil shredded with high probability, as they can be seen in (**Figure 24**) of the (250–125) µm and (>250) µm, additionally, only these distributions had a high dosage of Al concentration on them, based on ICP-MS Wt.% analysis as per (**Table 33**), as the following shapes/particles were not observed in others. As one can see between particles, there are crevasses and cracks, which are really black/dark in comparison to other surrounding particles. These are due to carbon tape underneath the samples, and this is visible from (**Figure 25 (e)**), where the fine particle size in comparison to other samples was minimal, hence a lot of the sample was empty of particles on the carbon tape used. What was noted from (**Figure 25 (a)** and **(b)**) was a clear distribution of fine particles of that Gr, in comparison to other particle size samples. Based on (**Figure 25 (b)**), one could say it is the richest out of all five samples in Gr particles, as it is the most visible of them. However, as this thesis focused more on the (<75) µm, the other samples were only characterised partially.

As the data from the ICP-MS (**Table 36**) has shown, the Co 35.17 Wt.%, Ni 8.84 Wt.%, Li 5.42 Wt.% and Mn 4.69 Wt.% results are similar to those obtained by EDS (**Figure 28**), showing the results for Co, Ni, Mn and Al, in ((**a3**) 37.41, 13.31, 8.22 and 0.92 Wt.%), ((**b3**) 38.91, 14.65, 8.69 and 0.87 Wt.%), ((**c3**) 11.98, 11.2, 6.87 and 0.67 Wt.%) and ((**d3**)

14.85, 25.14, 15.35 and 0.47 Wt.%). What was noted, was that in the overall sampling of the (<75) μm BM, as per (**Figures 26** and **28)** (**a1**, **b1**, **a3** and **b3**) was that the Co and Ni were evenly spread around the BM as per (**Table 36**) data for the same elements with slight differentiation, in between of Co ± 3.74 Wt.% and Ni ± 5.81 Wt.%, depending which of the (**a3** and **b3**) were compared to that of ICP-MS data, showing the comparability in between SEM-EDS and ICP-MS analysis for BM, as many literature and research methods also utilise it for a reason. The only difference between (**a3** and **b3**) to that of ICP-MS is that of Mn, as the SEM-EDS gave almost two-fold results for it and for (**d3**) even that of more than three times, which is normal and is due to how the two analysis methods perform analysis and which method they utilise, as one is better for others like the SEM-EDS is perfect for the C analysis as seen from the (**Figures 27** and **28)**, EDS elemental mapping on the samples and the EDS spectrum and quantitative analysis results. Show a clear difference in ICP-MS capability to differentiate C and Gr from samples compared to that of SEM-EDS, which sees them, but which of them is in the sample is UNK, as Gr is an allotrope of C or one of the forms of its specific crystalline structure, for this a recommendation of using X-ray diffraction (XRD) would be made, which in this thesis was not done. (**Table 37**) data for C showed that BM had only 3.35 Wt.% of it, but based on the mapping and subsequent EDS analysis of (**a3**, **b3**, **c3** and **d3**), 14.75, 11.53, 33.75 and 13.92 Wt.% respectively were detected, coming back to that of the hypothesis in ICP-MS, that of around 30 Wt.% could be of C or Gr, out of which majority would be of that Gr, as it is used in anode, to allow for chemical reaction and allowing Li^- to move. Presence of the oxygen (O) was also noted, in large quantities, across the whole of the elemental mapping (**Figure 27**), showing that it is uniformly distributed across the samples of BM, with values based on (**Figure 28**) and (**a3**, **b3**, **c3** and **d3**) 24.96, 24.73, 26.16 and 26.44 Wt.% respectively for samples. This kind of distribution could mean that the transition metal ions have been mixed on an atomic level throughout the sample homogeneously; this is also true for the Co and Ni, as seen in (**Figure 27**).

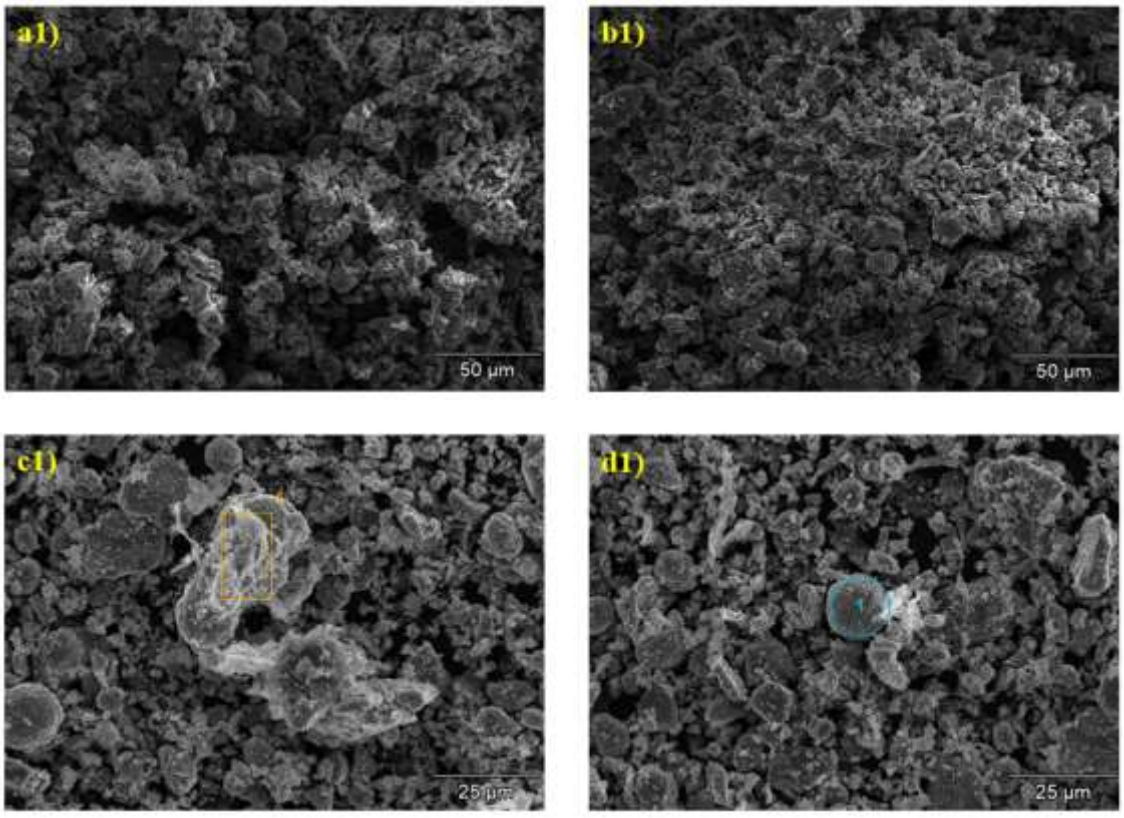

Figure 26. SEM images of (<75) µm particle size BM in (a1) and (b1), with two separate point analyses selected for the EDS (c1) and (d1) samples. (*Note! Samples (a1) and (c1) are that of No.5, and samples (b1) and (d1) are that of No.6 from* (**Figure 24**)).

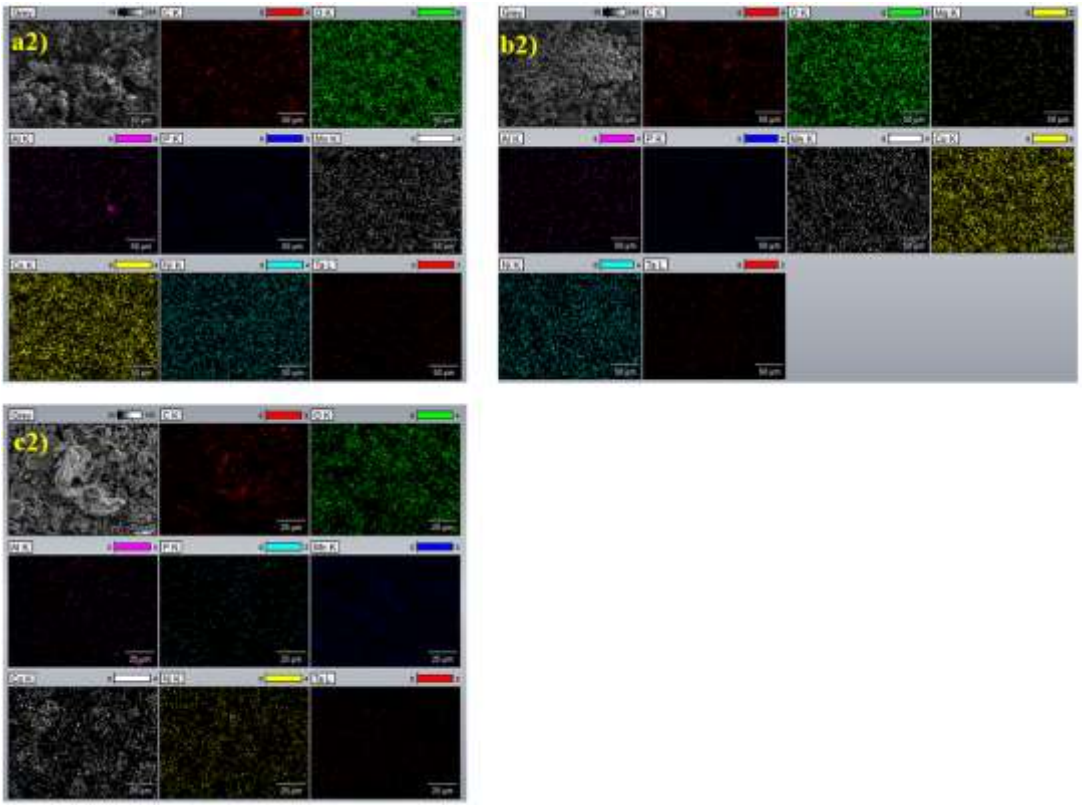

Figure 27. SEM image of the samples in (**Figure 25**) without the (d1) sample and their corresponding EDS elemental mapping on the (<75) µm particle size BM samples. (*Note! (d1) sampling was not done or lost in the data exchange*). Additionally, (*Note! Sample (a2) and (c2) are that of No.5, and sample (b2) is that of No.6 from* (**Figure 24**)).

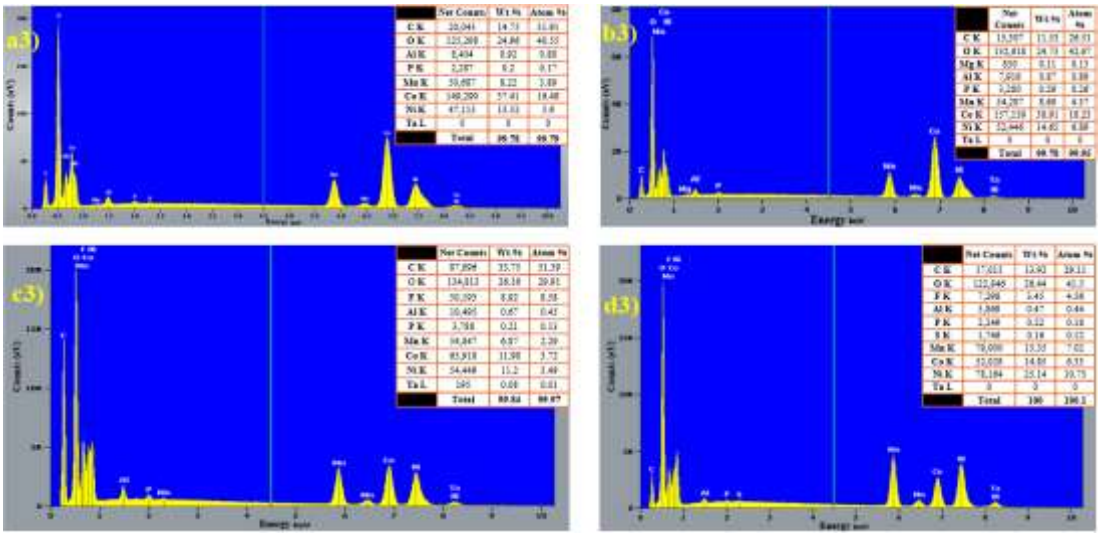

Figure 28. EDS spectrum and quantitative results for all the samples (**Figure 25**), all the samples with corresponding counts, atomic percentages and elemental Wt.% in the samples, as (a3) and (b3) for the whole sample, while (c3) and (d3) for the corresponding point analyses. (*Note! Samples (a3) and (c3) are that of No.5, and samples (b3) and (d3) are that of No.6 from* (**Figure 24**)).

Differences between the extensive sampling of (**a1/2/3** and **b1/2/3**) to that of (**c1/2/3** and **d1/3**), the point sampling can also be seen as the values as already pointed out for certain elements differ in between and a clear elemental concentration can be seen of greater in the point samples inside of the grids of (**Figure 26**) (**c1** and **d1**). This is especially true in the case of F, which was said to have that of in between 1 and 8 Wt.%, which was confirmed to be correct, as the (**c3** and **d3**), results were the only ones to point out F concentrations of 8.92 and 3.45 Wt.% respectively in samples, meaning that the F is highly dependent on to what element it is adhered to. SEM-EDS between ICP-MS is the only method to see it, as an element or a crystalline compound in the BM. Concentrations of F in the tested BM were not surprising, as it was known that when crushed/sieved, it would most likely have the highest chance to be in the smaller particle size distribution of that (<125) μm. Traces of F were due to the PVDF or PTFE binders, in addition to those of electrolyte $LiPF_6$, if it did not evaporate fully. Pre-treatment, if it may be called milling/grinding cathode/anode material into BM, as was stated, generated friction and as such thermal heat, which could and most likely did lead to loss of some F and in BM made, as decomposition was highly likely to some extend as in some form/species of a LiF most likely. The mentioned form is relatively stable thanks to its strong ionic bond and lattice energy being high unless it is subjected to strong acids like those of (HCl, H_2SO_4, and HNO_3), which are being used in the later experimentation and will be discussed in the corresponding section. As such, it is the most plausible explanation for the F traces due to binders, but it is even further ensured by the traces of phosphorus (P) as it was also present in (**c3** and **d3**), in 0.21 and 0.22 Wt.%, relatively small when compared to other elements, but never the less present throughout all of the (**a3**, **b3**, **c3** and **d3**) samples in relatively same amount. As such, it can be concluded that the traces of F and P are a clear testament to the PVDF and/or PTFE. Nonetheless, the high difference in F and P concentrations from one another clearly shows that F has formed mainly as LiF form.

The lithium amount in the SEM-EDS cannot possibly be verified by its methodology. However, as seen by ICP-MS (**Table 36**), it should have been that of 5.42 Wt.% for the BM of (<75) μm meaning that Li had formed some kind of stable form with some other elements present in the BM, out of which LiF had been one of the high likely forms. However, as data is sieved through, the pattern or spike in certain elements becomes apparent, particularly in point analysis and the overall characterization of sample differences. Looking between (**a3**

and **b3**) versus (**c3** and **d3**), there is a clear spike in Mn when it comes to (**d3**), as it goes from the same sample of (**b3**) 8.69 Wt.% to that of 15.35 Wt.%, because of the point analysis getting on the concentration Mn-rich spot, which also was seen as increase of Ni from the 14.65 Wt.% to 25.14 Wt.% was also observed, while the Co decreased from the initial 38.91 Wt.% to 14.85 Wt.%, changes in the between the (**a3** and **c3**) were also noted, but theirs were not as interesting, if not mention the decrease of Co from 37.41 Wt.% to 11.98 Wt.% due to spot analysis spot chosen. This means that the (**d1**) sphere shape type of spot is rich in metals and metal-oxides, in comparison to that of the (**c1**) polyhedron shape type of spot, which is not as rich in metals, but in C or Gr sure, as values are elevated in comparison to (**a3**) two times. Overall, across all the images (**a3**, **b3**, **c3**, and **d3**), a wide range of sizes and shapes, from a few μm to 40 μm, were observed. A clear difference between (**c3** and **d3**) is that the first is more balanced in Co, Ni, and Mn, almost as a 1:1 ratio, while the latter one is clearly Ni-based with a 2:1 ratio to those of Co and Mn, a 1:1 ratio. Hence, it can be said that some sort of clear metal-oxides can be seen/found in the (**c1** and **d1**). If we go based on the (**c1** and **c3**) data, the composition of metal oxide would be closer to that of $LiNi_xMn_yCo_zO_2$, where ($x + y + z = 1$), which would look like the $LiNi_{11.2}Mn_{6.87}Co_{11.98}O_2$, which then would be translated into $LiNi_{0.23}Mn_{0.4}Co_{0.37}O_2$, which would look very much similar to that commercially available and highly manufactured/used NMC 111 or $LiNi_{1/3}Mn_{1/3}Co_{1/3}O_2$. As for the (**d1** and **d3**), where Ni concentration is higher than that of the two others, Co and Mn, the data composition looks similar to that of NMC 532, as based on the data, NMC would look like the $LiNi_{0.45}Mn_{0.28}Co_{0.27}O_2$. In addition to these, the F could also have formed NiF_2, CoF_2, and MnF_2, for instance, which would also contribute to the results. What, in actuality, has happened to BM to make it look so close to those of NMC 111 and NMC 532 is not clear, as it should not be possible for the BM to change/metaphor from the LCO to NMC, as it should only be possible if systemization has been performed, which was not done at any point of samples and their storage. What the two-point analysis represents as compounds is a bit unclear, and more analysis would have been needed for morphology and clear characterisation, such as XRD, transmission electron microscopy (TEM), or laser-induced breakdown spectroscopy (LIBS) [276], [277], [278].

What was also done after experimentation and in between was the comparison of fresher BM, as in (**Figure 26**), to that of storage BM (**Figure 29**). Based on the available data from EDS, it can be seen that the Wt.% of all of the primary elements Co, Ni, and Mn

dropped between 1.22–8.62 Wt.%, depending on which one is studied. While this may have been for the metals, the C and O acted differently as their concentration increased, and in the case of C or Gr, it almost doubled. This is a clear result of the molecules in the air, in addition to moisture, such as (e.g., O_2, CO_2, H_2O), and degradation of organic components, such as PVDF and/or PTFE, and F forms/species formed, which were discussed. As such, a clear indication that BM should be stored correctly or BM created closer to experimentation, due to degradation and contamination risks.

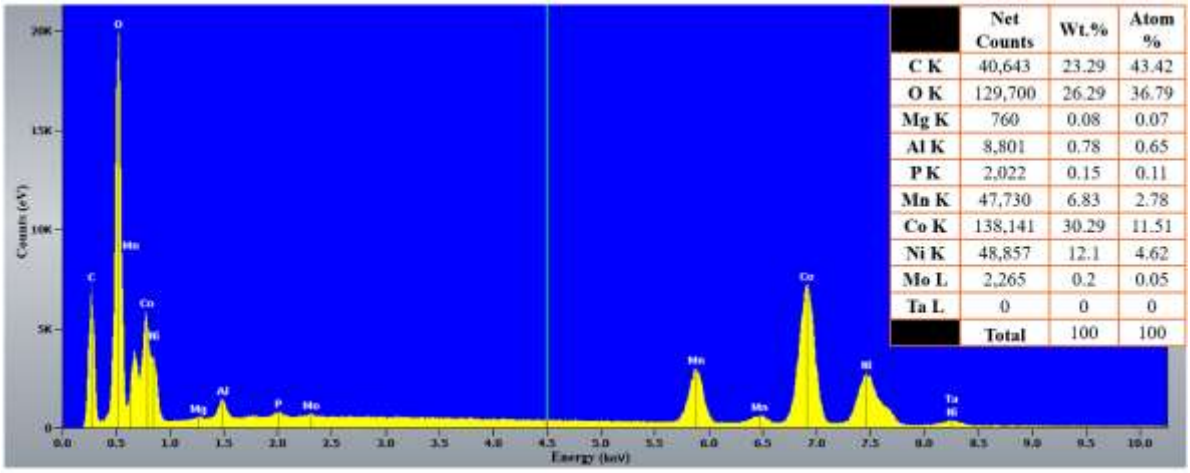

	Net Counts	Wt.%	Atom %
C K	40,643	23.29	43.42
O K	129,700	26.29	36.79
Mg K	760	0.08	0.07
Al K	8,801	0.78	0.65
P K	2,022	0.15	0.11
Mn K	47,730	6.83	2.78
Co K	138,141	30.29	11.51
Ni K	48,857	12.1	4.62
Mo L	2,265	0.2	0.05
Ta L	0	0	0
	Total	100	100

Figure 29. EDS spectrum and quantitative results for the separate sample of (<75) µm particle size BM, after it was stored to see the effect of moisture/air and other factors that can affect the sample morphology, as it is waiting to be tested.

5.3. Experimental Reactor and Other Equipment for it

The experimental reactor was designed and constructed by Mohammad Reza Bilesan out of polypropylene. The reactor went through the thesis a few iterations/modular changes, as to the number of compartments used in the reactor as cells, where the reactions occurred. Modularity and changes to the reactor were possible because it was 3D printed from polypropylene (PP), as seen in (**Figure 30**). Which was treated in the heated water over the course of several hours, to remove plastic residue from the 3D printed reactor (**Figure 30** (**a**)) and solidify/increase its durability, to make it into its final form as in (**Figure 30** (**b**)). What should be noted are the channels in (**Figure 30** (**a**)), which theoretically should have allowed for the better material flow of BM in and out and made the flow of BM to those of

electrodes more balanced on the surface and in between rods in electrodes. To allow current throughout the reactor system, a slight protrusion of the electrode surface can be seen in (**Figure 30** (**c**)) for alligator-clip wires to be connected to the DC. From (**b**), (**c**) and (**d**), a clear channel/lower level could be seen, which was for placing the electrode securely in the reactor, which protruded by a few millimetres and was topped with a fluoroelastomer (FKM) solid 2 mm thick gasket and solid 3D printed plate, from both sides of the reactor and then subsequently clamped by clamps and secured from all four sides by screws. From the images, it is also possible to see inlet and outlet tube protrusions, which were used to connect the tubes used in the experimentations to transfer acids and material inside the reactor and out into beakers used as storage tanks.

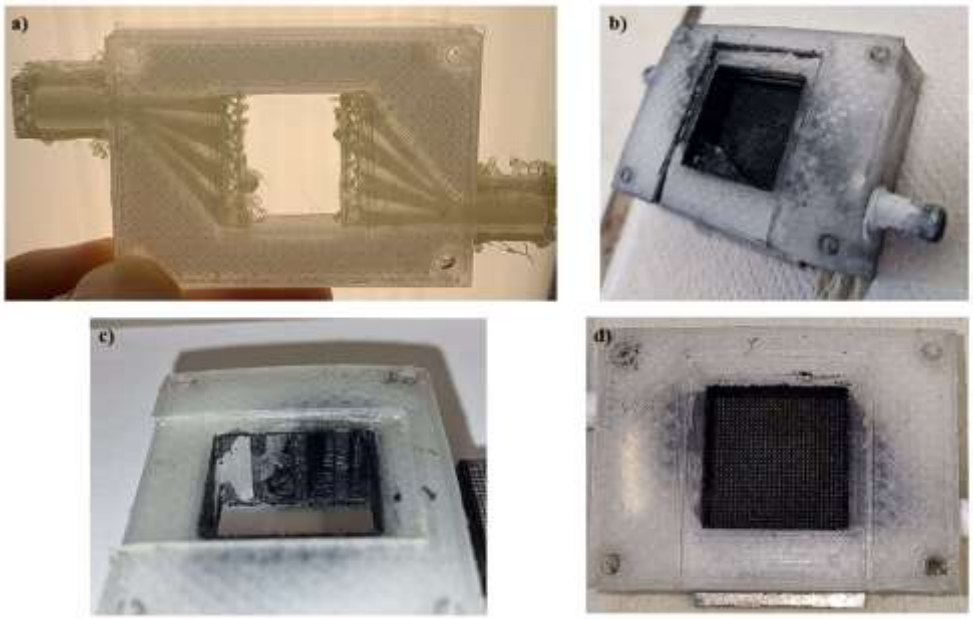

Figure 30. 3D printed and used in the thesis, reactor taken from the 3D printer in its raw form with filaments/residue plastics (a), reactor just used in experimentation from an angled view with electrode still in it (b), reactor from an angled view where the channels inside of the reactor can be seen (c) and view of reactor from the top with electrode inside after experimentation (d).

The reactor utilized two electrodes, one from each side, facing one another in one compartment/cell without anything in between them, as was the intention. The electrodes used were custom-made and 3D printed from Ti and stainless steel (SS) metals. In (**Figure 31**), electrode visual and technical parameters for measurements can be seen. As an anode,

Ti was used, and as a cathode, SS was used, both of these had some of the same projected surface area (*PA*) of 2*2 cm or 4 cm^2 as seen in (**Figure 31** (**a**) and (**b**)). The fundamental basis of using Ti as an anode and SS as a cathode stems from Ti's ability to resist corrosion as it forms a stable passivation/protective oxide layer between Ti and O, namely TiO_2. Additionally, the printing technique or the structure of electrodes played a role, as one is of 4 rods and the second of 8 rods seen in (**Figure 32**), as the cathode of 4 rods has less surface area in comparison to that of the 8 rods, in addition to having higher current density per rod, as the 8 rods have higher capacity/rate capability, translating to that of greater ion and electron transportation capacity/capability.

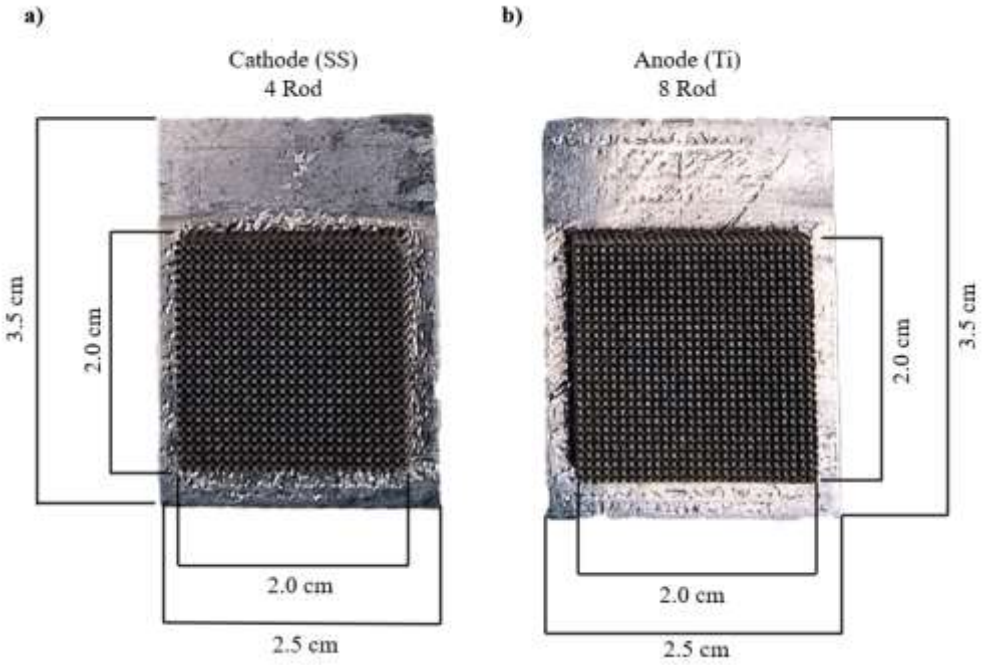

Figure 31. Two electrodes used in the reactor with their parameters: a cathode made of SS in a 4-rod mesh style per rod on the left (a) and an anode made of Ti in an 8-rod mesh style per rod on the right (b).

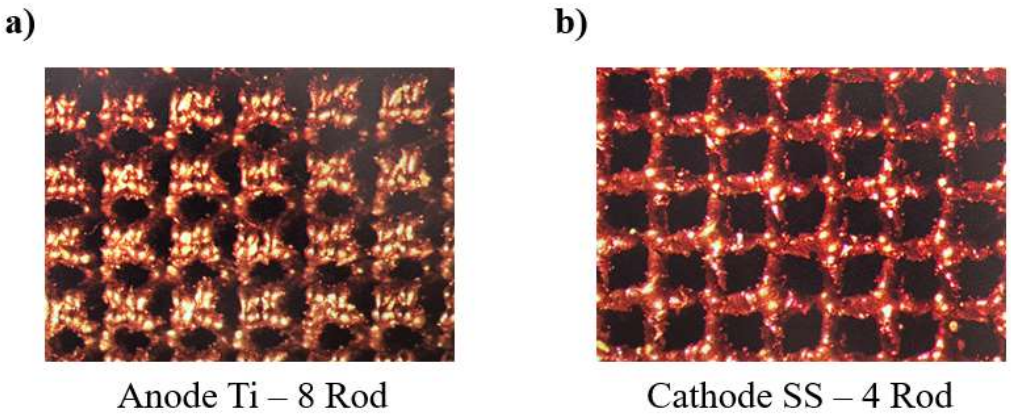

Figure 32. Visual images of the anode's Ti 8 rod surface structure on the left (a) and the cathode's SS 4 rod surface structure on the right (b). Images/photos were captured by the Olympus DF PL 2x Stereo Microscope Objective and captured by the Leica Microsystems.

Other important utilities used in the experimentation were the tubes, as they as the transportation of acids and BM contained in them with other liquids, such as alkaline, in the later tested experimentations, were done by the Masterflex® L/S® Precision Pump Tubing, Platinum-Cured Silicone, L/S 16 tubes, connected to the reactor and then to those of storage tanks containing liquids and BM mass in certain S/L ration.

5.4. Literature review & Selection of aspects

For understanding the recycling and recovery efficiency of valuable minerals and metals from LIBs, the importance of seeking and finding already conducted experiments and literature reviews on scientific methods is crucial. However, to understand and have some sort of reference data for the tested BM and to be able to validate the results from the experiments, a more studied approach, involving only chemical leaching, needed to be performed on the BM. As such, the literature review has been divided into two separate sections: chemical leaching and electrochemical leaching. In the latter, it will also be taken into account that the material and review should primarily focus on the indirect leaching mechanism, as the reactor utilizes two electrodes for BM leaching, and the material is suspended in a liquid leachate.

5.4.1. Chemical Leaching of BM Literature

Most commonly found chemical leaching reagents and acids used in the literature with sufficient results have been found to be those of H_2SO_4 and HCL primarily, as seen in (***4.2.1. Leaching Processes with the Reducing Agents***) when the chemical leaching tests were conducted. Not that these were the only acids used, as the other acids were also tested, like those of an organic type of $C_6H_8O_7$, $C_6H_{12}O_7$, and $C_2H_2O_4$. What was also duly noted was that the use of H_2O_2 as a reducing agent was fairly common in many of the scientific papers and research reviewed throughout thesis for chemical leaching. A collection of reviewed results/parameters found for some sort of BM can be found below (**Tables 38 – 42**).

Table 38. Chemical leaching of BM method/settings/parameters/leaching Efficiency.% from the Ref. [273]. (*Note! Table of 1/5 set of chemical leaching collection*).

ACID	Reducing agent	Settings	S/L	Leaching Efficiency.%	BM (⌀)
H_2SO_4 2 M	(NONE)	T = 40 & 60°C P = (UNK) t = 180 min stir = 300 rpm (magnetic)	S/L 1:50 (g/mL)	- Li – 71–84 at 40°C (Untreated) - Li – 97 at 60°C (Untreated) - Mn – 76 at 60°C (Untreated) - Ni – 85 at 60°C (Untreated) - Co – 88 at 60°C (Untreated) - Cu – 10 at 60°C (Untreated) - Al – 40 at 60°C (Untreated)	under 75 µm
H_2SO_4 2 M	(NONE)	T = 25°C P = (UNK) t = 180 min stir = 300 (magnetic)	S/L 1:50 (g/mL)	- Li – 84 at 25°C (Incinerated at 600°C) - Li – 83 at 25°C (Incinerated at 500°C) - Cu – 60 at 25°C (Incinerated at 500°C) - Al – 70 at 25°C (Incinerated at 400°C)	under 75 µm
H_2SO_4 2 M	(NONE)	T = 25°C P = (UNK) t = 180 min stir = 300 rpm (magnetic)	S/L 1:50 (g/mL)	For all 80 – 99 at 25°C (Pyrolyzed at 600°C) PYROLYSIS BETTER OPTION IN THIS STUDY	under 75 µm

Table 39. Chemical leaching of BM method/settings/parameters/leaching Efficiency.% from the Ref. [2], [3], [4], [230]. (*Note! Table of 2/5 set of chemical leaching collection*).

ACID	Reducing agent	Settings	S/L	Leaching Efficiency.%	BM (⌀)
HCl 2 M	(NONE)	T = 60–80°C P = (UNK) t = 90 min stir = (UNK)	S/L 50	- Li – 94.5 ± 0.33 + Co (mobilization) - Li – extraction 88 (in 20 min at 60/80°C) - Co – Co-extraction 55 (in 20 min at 60/80°C)	(UNK)
H_2SO_4 1.5 M	H_2O_2 30 vol.%	T = 90°C P = (UNK) t = 120 min stir = (UNK)	S/L 10	- Li – 99.91 - Co – 87.85 (co-extracted) - Ni – 91.46 (co-extracted)	(UNK)
Oxalic acid 1 M	(NONE)	T = 95°C P = (UNK) t = 12 h stir = 500	S/L 10	- Li – <90 - Mn – <90	(UNK)

Table 40. Chemical leaching of BM method/settings/parameters/leaching Efficiency.% from the Ref. [279]. (*Note! Table of 3/5 set of chemical leaching collection*).

ACID	Reducing agent	Settings	S/L	Leaching Efficiency.%	BM (⌀)
H_2SO_4 0.5 M	(NONE)	T = 20, 40, 60 & 80°C P = (UNK) t = 30 min stir = 400 rpm (constant) V = 800mL glass reactor (thermostatically controlled water bath)	S/L 50	- Li – 90 (20°C) – in 30 min - Li – 90 (40°C) – in 15 min - Li – 97 (60°C) – in 10 min - Li – 99 (80°C) – in 10 min, & then degreased afterwards - Al – 88 (20°C) – in 30 min - Al – 90 (40°C) – in 20 min - Al – 98 (60°C) – in 8 min - Al – 99 (80°C) – in 8 min - Si – 40 (20°C) – in 30 min - Si – 47 (40°C) – in 30 min - Si – 50 (60°C) – 12 min - Si – 45 (80°C) – in 5 min	(UNK)

(*Continued on next page*)

Table 40. (*Continued*)

ACID	Reducing agent	Settings	S/L	Leaching Efficiency.%	BM (⌀)
H_2SO_4 1 M	(NONE)	T = 20, 40, 60 & 80°C P = (UNK) t = 30 min stir = 400 rpm (constant)	S/L 50	- Li – 93 (20°C) – in 25 min - Li – 97 (40°C) – in 7 min - Li – 98 (60°C) – in 5 min - Li – 99 (80°C) – in 5 min - Al – 90 (20°C) – in 30 min - Al – 90 (40°C) – in 15 min - Al – 97 (60°C) – in 10 min - Al – 99 (80°C) – in 10 min - Si – 85 (20°C) – in 30 min - Si – 90 (40°C) – in 15 min - Si – 90 (60°C) – in 15 min - Si – 99 (80°C) – in 7 min	(UNK)

Table 41. Chemical leaching of BM method/settings/parameters/leaching Efficiency.% from the Ref. [272]. (*Note! Table of 4/5 set of chemical leaching collection*).

ACID	Reducing agent	Settings	S/L	Leaching Efficiency.%	BM (⌀)
H_2SO_4 4 N 95 vol.%	(NONE)	T = 50°C P = (UNK) t = 2 h stir = 100 rpm	10 Wt.% of solid residue	- Al – 47 - Co – 44 - Cu – 50 - Fe – 32 - Mn – 38 - Ni – 40	(UNK)
HCl 4 N 37 vol.%	(NONE)	T = 50°C P = (UNK) t = 2 h stir = 100 rpm	10 Wt.% of solid residue	- Al – 68 - Co – 75 - Cu – 67 - Fe – 40 - Mn – 80 - Ni – 64	(UNK)
Citric acid 4 N 99 vol.%	(NONE)	T = 50°C P = (UNK) t = 2 h stir = 100 rpm	10 Wt.% of solid residue	- Al – 25 - Co – 38 - Cu – 60 - Fe – 19 - Mn – 70 - Ni – 10	(UNK)

(*Continued on next page*)

Table 41. (*Continued*)

ACID	Reducing agent	Settings	S/L	Leaching Efficiency.%	BM (⌀)
Gluconic acid 4 N 50 vol.%	(NONE)	T = 50°C P = (UNK) t = 2 h stir = 100 rpm	10 Wt.% of solid residue	- Al – 16 - Co – 28 - Cu – 50 - Fe – 10 - Mn – 55 - Ni – 5	(UNK)
H_2SO_4 4 N 95 vol.%	H_2O_2 2 vol.% TEST 0–6 Highest at 2, after 2–6 degreased Eff.%	T = 230°C P = (UNK) t = 2 h stir = 100 rpm	10 Wt.% of solid residue	- Al – 65 (2 vol.% H_2O_2) - Co – 57.5 (2 vol.% H_2O_2) - Cu – 70 (2 vol.% H_2O_2) - Fe – 35 (2 vol.% H_2O_2) - Mn – 82.5 (2 vol.% H_2O_2) - Ni – 45 (2 vol.% H_2O_2)	(UNK)
HCl 4 N 37 vol.%	H_2O_2 4 vol.% TEST 0–6 Highest at 4, after 4–6 degreased Eff.%	T = 50°C P = (UNK) t = 2 h stir = 100 rpm	10 Wt.% of solid residue	- Al – 75 (4 vol.% H_2O_2) - Co – 82.5 (4 vol.% H_2O_2) - Cu – 70 (4 vol.% H_2O_2) - Fe – 40 (4 vol.% H_2O_2) - Mn – 87.5 (4 vol.% H_2O_2) - Ni – 75 (4 vol.% H_2O_2)	(UNK)
Citric acid 4 N 99 vol.%	H_2O_2 0 vol.% TEST 0–6 Highest at 0, after 0–6 degreased eff.%	T = 50°C P = (UNK) t = 2 h stir = 100 rpm	10 Wt.% of solid residue	- Al – 25 (0 vol.% H_2O_2) - Co – 39 (0 vol.% H_2O_2) - Cu – 60 (0 vol.% H_2O_2) - Fe – 19 (0 vol.% H_2O_2) - Mn – 72 (0 vol.% H_2O_2) - Ni – 10 (0 vol.% H_2O_2)	(UNK)
Gluconic acid 4 N 50 vol.%	H_2O_2 6 vol.% H_2O_2 0 vol.% TEST 0–6 Highest at 6 Eff.%	T = 50°C P = (UNK) t = 2 h stir = 100 rpm	10 Wt.% of solid residue	- Al – 21 (6 vol.% H_2O_2) - Co – 32 (6 vol.% H_2O_2) - Cu – 60 (6 vol.% H_2O_2) - Fe – 12 (6 vol.% H_2O_2) - Mn – 62 (6 vol.% H_2O_2) - Ni – 5 (6 vol.% H_2O_2)	(UNK)

Table 42. Chemical leaching of BM method/settings/parameters/leaching Efficiency.% from the Ref. [280]. (*Note! Table of 5/5 set pf chemical leaching collection*).

ACID	Reducing agent	Settings	S/L	Leaching Efficiency.%	BM (⌀)
Citric acid 2 M	(NONE)	T = 25°C P = (UNK) t = 24 h stir = (UNK)	slurry density = 5% (w/v)	- Li – yield 63 - Co – yield 42 - Ni – yield 35	(UNK)
Oxalic acid 1 M	(NONE)	T = 25°C P = (UNK) t = 24 h stir = (UNK)	slurry density = 5% (w/v)	- Li – yield 75 - Co – yield 2 - Ni – yield 2	(UNK)
H_2SO_4 2 M	(NONE)	T = 25°C P = (UNK) t = 24 h stir = (UNK)	slurry density = 5% (w/v)	- Li – yield 100+ - Co – yield 80 - Ni – yield 75	(UNK)
HCl 4 M	(NONE)	T = 25°C P = (UNK) t = 24 h stir = (UNK)	slurry density = 5% (w/v)	- Li – yield 100+ - Co – yield 90 - Ni – yield 85	(UNK)
HNO_3 1 M	(NONE)	T = 25°C P = (UNK) t = 24 h stir = (UNK)	slurry density = 5% (w/v)	- Li – yield 92 - Co – yield 70 - Ni – yield 62	(UNK)
Citric C6 acid 2 M	H_2O_2 1% (v/v)	T = 25°C P = (UNK) t = 24 h stir = (UNK)	slurry density = 5% (w/v)	- Li – yield 72 - Co – yield 54 - Ni – yield 39	(UNK)
Oxalic acid 1 M	H_2O_2 1% (v/v)	T = 25°C P = (UNK) t = 24 h stir = (UNK)	slurry density = 5% (w/v)	- Li – yield 80 - Co – yield 2 - Ni – yield 0	(UNK)
H_2SO_4 2 M	H_2O_2 1% (v/v)	T = 25°C P = (UNK) t = 24 h stir = (UNK)	slurry density = 5% (w/v)	- Li – yield 100+ - Co – yield 87 - Ni – yield 78	(UNK)
HCl 4 M	H_2O_2 30 vol.%	T = 25°C P = (UNK) t = 24 h stir = (UNK)	slurry density = 5% (w/v)	- Li – yield 100+ - Co – yield 98 - Ni – yield 80	(UNK)
HNO_3 1 M	H_2O_2 1% (v/v)	T = 25°C P = (UNK) t = 24 h stir = (UNK)	slurry density = 5% (w/v)	- Li – yield 96 - Co – yield 83 - Ni – yield 78	(UNK)

Based on the (**Tables 38 – 42**), one could conclude that the leaching with H_2SO_4 yields the best results for the Li, Ni, Co, and Mn metal recovery efficiency when it comes to chemical leaching purely, as the majority of the studies/research material use it as a leaching agent. This is not surprising, as the hydrometallurgical recycling of LIBs and the recovery of metals from them are the most common industrial methods applied. This can be further

shown by (Diaz et al. [6]), where they and colleagues showed the most common S/L and pulp densities used in hydrometallurgy recovery, in comparison to that of ECL and its advantages (**Figure 33**) [6]. What they found is that the majority of the H_2SO_4 and HCL leaching industrially happens in between 2 to 4 mol/L and 3 to 4 mol/L operating ranges, respectively, and pulp densities reported and found were those of around 20/50/100/200 and 50/100 S/L ratios, respectively [6].

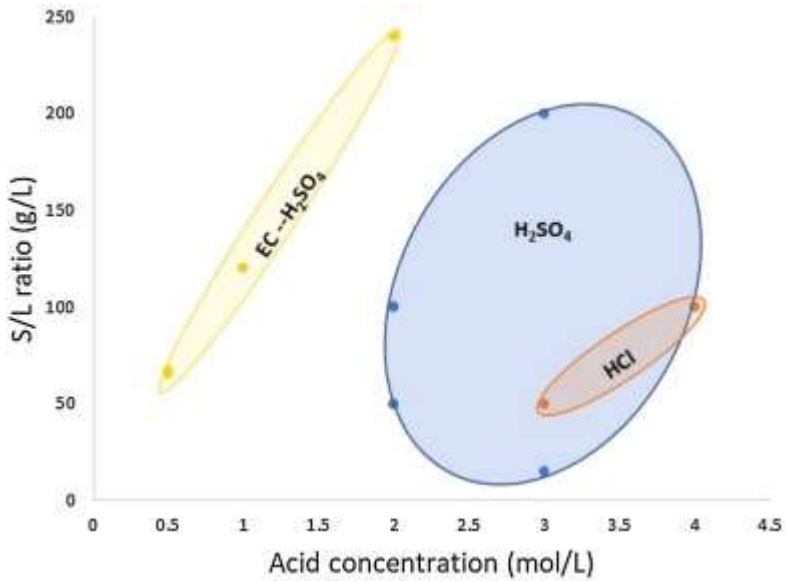

Figure 33. Operation parameters, pulp density vs. acid concentration from the LIBs by (Diaz et al. [6]). (*Note! Solid points represent reported pulp densities at the corresponding acid concentration, and regional colours are operational ranges (yellow is of electrochemical leaching, while blue/red are of chemical leaching)*) [6].

Hence, it was decided to conduct chemical leaching for the BM, characterised on the basis that H_2SO_4 is the most studied and has the best leaching efficiency and recovery rate among all the acids examined. What should be noted is that BM used in thesis has not been pre-treated in any way, as the grinding/milling of it was done as much as possible in a controlled manner so that the thermal aspects of kinetics would not have affected BM. The experimental condition and setup are visible in the (***5.5.1. Chemical Leaching***) segment.

5.4.2. Electrochemical Leaching of BM Literature

Based on the fact that the method used in this thesis is ECL. There is a need to find similar recovery methods, based on their literature study/research and kinetics, if possible, and those that have tested ELC in some sort of reactor-type concept. For this reason, we have collected similar kinds of research and their settings with different necessary parameter values, which may be useful in determining the course of thesis's ECL parameters. As it has been discussed with hydrometallurgy, the ECL's use commercially and on an industrial scale as of now is not of the highest level, while the theoretical and laboratory scale research has seen sufficient progress in recovery rates and technological state, when it comes to perfection and finding substitutes for current hydrometallurgical technologies/methods. In (**Tables 43 – 46**) below can be found a collection of different research in literature for the ECL, that utilised some sort of reactor in LIB's or BM's metal recovery at the time this thesis experimental section and testing were conducted.

Table 43. Electrochemical Leaching data/parameters based on the literature/research review references, for the LIB and/or BM. (Geometric area (GA) and immersed surface area (IA)). (*Note! Table of a 1/4 set of electrochemical leaching collection*).

Parameter	**[6]**	**[8]**
Black Mass – BM	LIB's metal oxide filter cake (MOFC)	$LiCoO_2$ – (BL-5CA, Nokia)
Pre-Treatment of BM	NOT DONE	Calcined, (650°C – 3 h)
Mass (g) TESTed	–	0.1
BM addition Compartment	Cathode side	Anodic/Cathodic side
Solid-to-liquid ratio (S/L), (g/L)	65/120/240 (given)	0.67 (calculated)
Anode (Pos.Ele)	Nickel foam – GA = 36 cm^2	Platinum (Pt) plate
Cathode (Neg.Ele)	Stainless-steel (SS) – IA = 36 cm^2	$LiCoO_2$ ((⌀) = 1.5 cm in circular mould)
Reference Electrode	BASi RE-5B Ag/AgCl	–
Membrane	Bipolar membrane (BPM) – (Fumasep FBM-PK)	N/A
Potentiostat	1x – Biologic SP-300	N/A
Leaching Solution Acid – LSA	H_2SO_4 & 10mM $FeSO_4$	Malic Acid ($C_4H_6O_5$)
LSA Concentration, (M)	0.5/1.0/2.0 & 10 (mM)	0.5–1.5 → 1.25 experimented
LSA Volume, (mL)	200	150

(*Continued on next page*)

Table 43. (*Continued*)

Parameter	**[6]**	**[8]**
Anolyte – An	KOH	Malic Acid ($C_4H_6O_5$)
An Concentration, (M)	1	0.5–1.5 → 1.25 experimented
An Volume, (ml)	200	150
Catholyte – Ca	30% molar H_2SO_4 + $FeSO_4$	Malic Acid ($C_4H_6O_5$)
Ca Concentration, (M)	0.5/1.0/2.0 + 10 (mM)	0.5–1.5 → 1.25 experimented
Ca Volume, (ml)	200	150
Reducing Agent – RA	Fe^{2+}	N/A
Ra amount, (–)	1 g/L per Ca	N/A
Final pH of TESTs	1–3	–
Temperature (°C)	20–23	20–80
Flow Rate (L/min)	–	N/A
Stirring speed (rpm)	–	50
Time (min)	1 800 → achieved at 480	180
Current Density, ($A \cdot m^{-2}$)	–	–
Working Voltage (V)	1.5–2.25 for (65 g/L)	2–10 → 8 experimented
Electric Current (A)	–	–
Cells/Compartments in the reactor	TWO	ONE
Reactor (Open or Closed) air	OPEN	CLOSED
Operation Mode	BATCH	BATCH
Direct or Indirect Leaching	INDIRECT	DIRECT
Direct or Assisted Leaching	ASSISTED	ASSISTED
Additional Information	Three (3) electrode system	–

Table 44. Electrochemical Leaching data/parameters based on the literature/research review references, for the LIB and/or BM. (*Note! Table of a 2/4 set of electrochemical leaching collection*).

Parameter	**[7]**	**[11]**
Black Mass – BM	Spent LIBs ($LiNi_{1/3}Co_{1/3}Mn_{1/3}O_2$) – (6.01% Li, 19.87% Co, 19.65% N & 17.95% Mn)	Spent LIBs of positive electrodes
Pre-Treatment of BM	Binder dissolution by (N-methyl pyrrolidone (NMP)) & Thermal Treatment (650°C – 2 h)	Washing in Distilled Water (40°C – 24 h)
Mass (g) TESTed	–	9.17
BM addition Compartment	Cathodic side (in polypropylene bag)	Anodic/Cathodic side
Solid-to-liquid ratio (S/L), (g/L)	0.02 (given)	18.34 (calculated)
Anode (Pos.Ele)	Titanium (Ti)	Platinum (Pt) Auxiliary electrode – GA = 3.75 cm^2
Cathode (Neg.Ele)	Graphite (G)	Aluminium (Al) foil 99% – GA = 0.40 cm^2
Reference Electrode	–	Ag/AgCl/NaCl (saturated)
Membrane	Anion Exchange Membrane (G1204)	N/A
Potentiostat	–	–

(*Continued on next page*)

Table 44. (*Continued*)

Parameter	[7]	[11]
Leaching Solution Acid – LSA	Sulfuric Acid (H_2SO_4)	HCl & H_2O_2
LSA Concentration, (M)	0.5/1.0/1.5/2.0 → 1.5 optimal	3.0 & 30% (v/v)
LSA Volume, (mL)	–	470 & 30
Anolyte – An	–	HCl & H_2O_2
An Concentration, (M)	–	3.0 & 30% (v/v)
An Volume, (ml)	–	470 & 30
Catholyte – Ca	Sulfuric Acid (H_2SO_4)	HCl & H_2O_2
Ca Concentration, (M)	0.5/1.0/1.5/2.0 → 1.5 optimal	3.0 & 30% (v/v)
Ca Volume, (ml)	–	470 & 30
Reducing Agent – RA	N/A	N/A
Ra amount, (–)	N/A	N/A
Final pH of TESTs	–	1.5/2.0/2.7/4.0/5.40 (adjusted)
Temperature (°C)	–	80
Flow Rate (L/min)	N/A	N/A
Stirring speed (rpm)	N/A	–
Time (min)	30/60/120/150/180 → 150 optimal	120
Current Density, ($A \cdot m^{-2}$)	–	-0.185–0.00
Working Voltage (V)	N/A	incl.
Electric Current (A)	0.2/0.4/0.6/0.8/1.0 → 0.4 optimal	–
Cells/Compartments in the reactor	TWO	ONE (assumption)
Reactor (Open or Closed) air	OPEN	OPEN (assumption)
Operation Mode	BATCH	BATCH (assumption)
Direct or Indirect Leaching	INDIRECT	INDIRECT
Direct or Assisted Leaching	ASSISTED	ASSISTED
Additional Information	–	–

Table 45. Electrochemical Leaching data/parameters based on the literature/research review references, for the LIB and/or BM. (*Note! Table of a 3/4 set of electrochemical leaching collection*).

Parameter	[12]	[9]
Black Mass – BM	Spent LIBs – (6.87 Wt.% Li, 58.79 Wt.% Co, 0.06 Wt.% Ni, 0.03 Wt.% Mn & 0.08 Wt.% Al) → ($LiCoO_2$, experimented)	Spent LIBs ($LiNi_{1/3}Co_{1/3}Mn_{1/3}O_2$) – (19.87% Ni, 19.56% Co, 19.14% Mn & 6.93% Li) – (0.15 mm)
Pre-Treatment of BM	Calcination & grounding	Calcined (650°C – 4 h)
Mass (g) TESTed	1.5/1.875/2.25 (calculated)	0.1
BM addition Compartment	Anodic/Cathodic side	N/A

(*Continued on next page*)

Table 45. (*Continued*)

Parameter	[12]	[9]
Solid-to-liquid ratio (S/L), (g/L)	6.0/7.5/9.0	0.667 (calculated)
Anode (Pos.Ele)	Corrosion-resistant DSA electrode	Platinum (Pt) plate
Cathode (Neg.Ele)	Copper (Cu) foil (from spent LIBs)	$LiNi_{1/3}Co_{1/3}Mn_{1/3}O_2$
Reference Electrode	N/A	N/A
Membrane	N/A	N/A
Potentiostat	N/A	N/A
Leaching Solution Acid – LSA	$CuSO_4$	Malic Acid ($C_4H_6O_5$)
LSA Concentration, (M)	0.1–0.2	0.5–2.5 →1.5 experimented
LSA Volume, (mL)	250	150
Anolyte – An	–	–
An Concentration (M)	–	–
An Volume (ml)	–	–
Catholyte – Ca	$CuSO_4$	Malic Acid ($C_4H_6O_5$)
Ca Concentration, (M)	0.1–0.2	0.5–2.5 →1.5 experimented
Ca Volume, (ml)	250	150
Reducing Agent – RA	N/A	N/A
Ra amount, (–)	N/A	N/A
Final pH of TESTs	1.0–2.0 / 2.0–2.5 / 2.5–3.0 / 3.5–4.0 / 4.0–4.5	–
Temperature (°C)	30–80	25–90 → 60 experimented
Flow Rate (L/min)	N/A	N/A
Stirring speed (rpm)	–	100–500 → 300 experimented
Time (min)	0–70	10–60 → 60 experimented
Current Density, ($A \cdot m^{-2}$)	200–700 (300/500/700)	–
Working Voltage (V)	–	2–10 → 8 experimented
Electric Current (A)	–	–
Cells/Compartments in the reactor	ONE (assumption)	ONE
Reactor (Open or Closed) air	OPEN (assumption)	CLOSED
Operation Mode	BATCH (assumption)	BATCH
Direct or Indirect Leaching	INDIRECT	DIRECT
Direct or Assisted Leaching	ASSISTED	ASSISTED
Additional Information	–	–

Table 46. Electrochemical Leaching data/parameters based on the literature/research review references, for the LIB and/or BM. (*Note! Table of a 4/4 set of electrochemical leaching collection*).

Parameter	[10] (discontinuous process)		[10] (reconstructed BM)	
	Ni/Cd batteries	Zn/MnO_2 batteries	Ni/Cd batteries	Zn/MnO_2 batteries
Black Mass – BM	Industrial BM by (Eurodieuze Industrie)	Industrial BM by (Eurodieuze Industrie)	Reconstructed BM from Spent (SANYO-end-of-life)	Industrial BM by (Eurodieuze Industrie)
Pre-Treatment of BM	–		–	
Mass (g) TESTed	30 (5 g initially + 5 g/h)	3.25	20	–
BM addition Compartment	Cathode side	Central chamber	Cathode side	Central chamber
Solid-to-liquid ratio (S/L), (g/L)	136.36/(30 g) or 22.73/(5 g) (Calculated)	–	117.65 (Calculated)	–
Anode (Pos.Ele)	Platinized Tinamium (Pt-Ti)	Lead (Pb) plate	Platinized Tinamium (Pt-Ti)	Lead (Pb) plate
Cathode (Neg.Ele)	Aluminium (Al) plate – SA = $53cm^2$	Aluminium (Al) plate – SA = $53cm^2$	Aluminium (Al) plate – SA = $53cm^2$	Stainless Steel (SS) or Aluminium (Al) plate – SA = $53cm^2$
Reference Electrode	–		–	
Membrane	Polypropylene (PP) cloth		Polypropylene (PP) cloth	
Potentiostat	–		–	
Leaching Solution Acid – LSA	H_2SO_4 & $CdSO_4$	–	H_2SO_4	H_2SO_4 & $ZnSO_4$
LSA Concentration, (M)	0.5 & 0.49	–	0.05	0.01 & 0.5
LSA Volume, (mL)	220	–	170	100
Anolyte – An	H_2SO_4 & $CdSO_4$	H_2SO_4 & $ZnSO_4$	H_2SO_4 & $CdSO_4$	–
An Concentration, (M)	0.1 & (2.0 – addition of 3 mL per h)	0.1 & 0.2	0.05 & 0.6	–
An Volume, (ml)	170	150	156	–
Catholyte – Ca	H_2SO_4 & $CdSO_4$	H_2SO_4 & $ZnSO_4$	H_2SO_4	H_2SO_4 or H_2SO_4 & $ZnSO_4$
Ca Concentration, (M)	0.5 & 0.49	0.25 & 0.5	0.05	. 0.01 or 0.5 & 0.5
Ca Volume, (ml)	220	150	170	125 or 125
Reducing Agent – RA	–		–	
Ra amount, (–)	–		–	

(*Continued on next page*)

Table 46. (*Continued*)

Parameter	[10] (discontinuous process)		[10] (reconstructed BM)	
	Ni/Cd batteries	Zn/MnO_2 batteries	Ni/Cd batteries	Zn/MnO_2 batteries
Final pH of TESTs	–		–	
Temperature (°C)	–		–	
Flow Rate (L/min)	–		–	
Stirring speed (rpm)	–		–	
Time (min)	360	480	300	360
Current Density, ($A \cdot m^{-2}$)	350	450	350	450
Working Voltage (V)	–		–	
Electric Current (A)	–		–	
Cells/Compartments in the reactor	TWO	THREE	TWO	THREE
Reactor (Open or Closed) air	OPEN		OPEN	
Operation Mode	BATCH		BATCH	
Direct or Indirect Leaching	INDIRECT		INDIRECT	
Direct or Assisted Leaching	ASSISTED		ASSISTED	
Operation Mode	–	BM waste was added to the central compartment.	–	BM waste was added to the central compartment.

Based on (**Tables 43 – 46**), there has been extensive research and methodology to develop and test different types of ECLs. What can be seen from all of them is that the majority of them are indirect EACLs, and all of them are of batch type. Understanding is also between direct and indirect, and/or even assisted, is important, as the direct has been discussed; it is that of compounds that react at the electrodes or in the indirect, where the chemical reagents and reducing agents are used to generate the electrodes to perform leaching, which is also the same principle for the assisted term [10]. It is also visible that the spread of ECLs in one or two-compartment cell reactors, with a few more, which have been utilising a membrane cloth to separate cells. Using membranes is a viable option, as cation exchange membranes (CEMs) and anion exchange membranes (AEMs) are two types of ion-exchange membranes (IEMs) that have been used in hydrometallurgy on a laboratory scale to separate Li from LIB waste [281]. For Li separation from the suspension, it is done using CEM. However, (Diaz et al. [6]) used bipolar membrane (BPM), which uses CEM's and AEM's properties, as they needed to control the electrolyte's pH, and prevent electrolyte

crossover [6]. But as shown by (Lei et al. [7]), the use of only one membrane, such as AEM (G1204), is also an option, but as shown by (Hazotte et al. [261]) and her team, when using the AEM Eurodia membrane, the problem of sampling and damaging the membrane needs to be taken into account.

While investigating and reading those (**Tables 43 – 46**) references and what was done in those studies, it was noted that, when some may have really delved into detail/explanations of what happened and what they were investigating, some of them lacked a lot of experimental information. This may have made some of the reading and understanding of what has been done a bit harder for the reader, as in some cases, certain information mentioned is conflicting with one another. Because of these reasons, the line between what research is best suited or more important than the other one has no clear line, as they all bring some good and insightful information in search of valid material needed to understand reactions and what is important for our experimentation, and we can additionally expect from them.

As such, a wide variety of different choices were made. For the experimental section, it was decided to go with a three-compartment/cell reactor configuration, with the addition of BM and anolyte of H_2SO_4 0.5 M into the anodic compartment of the Ti electrode (anode). In comparison, the KOH 1 M would have been used as catholyte, while the NaCl 2 M would have been used in the middle compartment separated by AEM and CEM, while also having circulation/flow in it, based on the (**Tables 43 – 46**) results and what kind of setups were observed. Based on the review of ECL, tests should yield, in comparison to chemical leaching, better results in lower concentration, while boasting a similar S/L ratio capability as per (**Figure 45**), when comparing H_2SO_4 between two different hydrometallurgy methods.

5.5. Experiment & Test methods

This section is divided into two main sections: (***5.5.1. Chemical Leaching***) and (***5.5.2. Electrochemical Leaching***). In both of these sections, all of the necessary parameters and conditions for and how the experiments of both types with the selected BM had been conducted can be found. With the calculations and reagent preparations, mainly of the

lixiviant of sulfuric acid. All of the setups for the experiments and sampling can also be found under the following sections, to keep coherence and systematicity of the thesis.

5.5.1. Chemical Leaching

The following section goes over the CL in four subsections, which walk through the CL from the experimental conditions, reagent preparations, testing setup used, and sampling with the parameter collection throughout the whole testing phase, done for the CL concept, using the particle size of BM smaller than 75 μm.

5.5.1.1. Experimental conditions

As discussed in the (***5.4.1. Chemical Leaching of BM Literature***) and taking into account the (**Table 38**) research/studies and results based on the BM from LIB, in addition to particle size smaller than 75 μm, which is the BM used in thesis. Using primarily (Petranikova et al. [1]), (Vieceli et al. [5]), and (Klimko et al. [279]), the following three chemical leaching tests (CL-T-1–3) and their experimental parameters under the (**Table 47**) were created and tested subsequently in the laboratory. What was also important to some extent was, if possible, to have data purely based on the acids, without any reducing agents, to also then later support BM's theoretical kinetics and their explanation.

Table 47. Experimental tests of theoretical and actual conditions based on the literature reviews, mainly influenced by (Petranikova et al. [1]), (Vieceli et al. [5]) and (Klimko et al. [279]).

	Experiments		
Parameter	**CL-T-1**	**CL-T-2**	**CL-T-3**
Acid	H_2SO_4	H_2SO_4	H_2SO_4
Concentration (M)	0.5	0.5	2
Temperature (°C)	25	50	50
Acid Volume (mL)	200	200	200
BM mass theoretical (grams)	5	5	5
BM mass used (grams)	5.2601	5.1377	5.1154
S/L theoretical (g/mL)	1/40	1/40	1/40
S/L used (g/mL)	38.0221	38.928	39.098
Stirring (rpm)	300	300	300
Time (min)	180	180	180

5.5.1.2. H_2SO_4 lixiviant preparation

For all three experiments, the same particle size of 75 µm BM was used, and the same H_2SO_4 95% (liquid form) by Sigma-Aldrich, which was then prepared into 0.5 and 2 M concentrations, via the normal dilution formula of (Eq. (**26**)).

$$C_1 \times V_1 = C_2 \times V_2 \tag{26}$$

Where C_1 is the concentration (M) of stock acid, which consists of (Eq. (**27.1**)), while C_2 is the desired concentration of 0.5 or 2 M acid wanted, and V_2 is the desired final volume of 200 mL for all 1/2/3 Tests.

$$C_1 = \frac{Precentage \times \rho \times 10}{M_{mass}} \tag{27.1}$$

Where C_1 is the concentration (mol/L or M) of stock acid, percentage is the percentage/purity of the S_2HO_4 on the package of the S_2HO_4 Sigma-Aldrich of 95%, ρ is the density (g/mL) of the H_2SO_4 of 1.84 g/mL and M_{mass} is the molar mass (g/mol) of S_2HO_4, which is 98.08 g/mol, meaning the calculation goes as (Eq. (**27.2**)).

$$C_1 = \frac{95 \times 1.84\ \text{g/mL} \times 10}{98.08\ \text{g/mol}} \approx 17.82\ \text{M} \tag{27.2}$$

Based on the C_1, calculation of the V_1 can be done based on the (Eq. (**26**)), when it is changed into (Eq. (**28.1**)) as follows,

$$V_1 = \frac{C_2 \times V_2}{C_1} \tag{28.1}$$

Calculated using parameters for the C_2 is 0.5 M, V_2 is 200 mL and C_1 is 17.82 M, resulting in the following result of (Eq. (**28.2**)).

$$V_1 = \frac{0.5\ \text{M} \times 200\ \text{mL}}{17.82\ \text{M}} \approx 5.61\ \text{mL} \tag{28.2}$$

Meaning that to create that 200 mL of 0.5 M H_2SO_4 one needs to take a beaker large enough and fill it to the 200 mL mark or that of 194.39 mL water or preferably deionised water (DI), or if creating that of 2 M H_2SO_4, then via same equations just changing in (Eq. (**28.2**)) 0.5 to 2 M and resulting in 22.45 mL of H_2SO_4 needed for the 200 mL of solution.

5.5.1.3. Testing setup

The experimental setup can be seen in (**Figure 34**) for all three Tests, which consisted of a heater, a magnetic stirrer, two bench clamps, a support stand, a thermometer, parafilm, a magnetic stir bar, a 250 mL Erlenmeyer flask and a well-ventilated environment (fume hood).

Figure 34. Experimental setup for the chemical leaching Tests 1/2/3 for the BM.

The addition of the BM was done after the temperature of the desired test, as per (**Table 48**) was achieved. The measured BM was of those 5 grams per 200 mL S_2HO_4, to achieve a 40 S/L ratio, and the magnetic stir was set up for 300 rpm. All three of the tests were run for 180 minutes or three hours.

5.5.1.4. Sampling & Parameter collection CL

Sampling was done through the top of the parafilm through a small hole as seen in (**Figure 34**), using the 5 mL single-use pipette tip. Sampling was also performed using a triplicate system, out of which two were essentially shadow samples of the other, to eliminate the possibility of contamination or other factors affecting the sample if something seemed off in the analysis stage. The amount of sample taken each time was 1.5 mL or 4.5 mL per triplicate, totalling 64 mL from the 200 mL reactor/batch volume, which was used for the samples and subsequently transferred to the ICP-MS room for analysis. When taking a sample from the flask/decanter beaker, the pipette tip was submerged around 1–2 cm under the surface of the lixiviate/BM solution, and between the centre of the glassware and its wall.

Sampling started from the point just before BM was added and was then taken at intervals, as seen in (**Table 48**).

Table 48. Addition of BM material at 0 minutes, but the sample was taken before the addition of BM, a total of 14 samplings of three per No. A total of 42 samples were taken in 180 minutes, BM added at * mark.

	No BM	**BM in lixiviant**												
Sampling No.	1	2*	3	4	5	6	7	8	9	10	11	12	13	14
Time (min)	0	5	15	30	45	60	75	90	105	120	135	150	165	180

In addition to sampling temperature and pH values, chemical leaching content was also collected; however, its results and content were deemed unnecessary to analyze, as no values could be salvaged from them. The results for the elemental detection and reliability for all three chemical leaching tests can be found in (**Table 49**), which is based on the CPS values by ICP-MS, for the samples collected in (**Table 48**).

Table 49. Elemental Detection & Reliability by the ICP-MS from the samples for the CL-Ts 1–3.

Detected / Reliability	**CL-T-1**	**CL-T-2**	**CL-T-3**
100%	7 Li / 55 Mn / 59 Co / 60 Ni	7 Li / 55 Mn / 59 Co / 60 Ni	7 Li / 55 Mn / 59 Co / 60 Ni
50/50%	23 Na / 27 Al / 39 K	23 Na / 39 K	23 Na / 39 K
0%	51 V /52 Cr / 56 Fe / 63 Cu	27 Al / 51 V /52 Cr / 56 Fe / 63 Cu	27 Al / 51 V /52 Cr / 56 Fe / 63 Cu

The same reliability and detections for the elements as in (**Table 34**), except for 27 Al, where the reliability/detection dropped, as the leaching was performed in the case of CL-T-1, and they became fully undetectable in CT-L-2 and CT-L-3.

5.5.2. Electrochemical Leaching

The following section goes over the ECL in four subsections, which walk through the ECL from the experimental conditions, reagent preparations, testing setup used, and sampling with the parameter collection throughout the whole testing phase, done for the ECL concept, using the particle size of BM smaller than 75 μm.

5.5.2.1. Experimental conditions

In the thesis, three different configurations of ECL were tested with the experimental reactors using one / two / three compartment reactor configurations. Out of these, one and three were successful to some extent, while two-compartment configuration datasets had to be scrapped due to faulty methodology. For some reference and comparison between chemical leaching, the decision was made to conduct tests in all three cases for a duration of 180 minutes, using H_2SO_4 as the lixiviant, based on the (***5.4.2. Electrochemical Leaching of BM Literature***), this led to following ECL test parameters for Test-1/2/3 as seen per (**Table 50**). When it came to the ECL-T-2 and ECL-T-3, it was discussed to keep the KOH concentration at a higher level than the H_2SO_4, for higher conductivity in the cell/reactor.

Table 50. Experimental tests of theoretical and actual conditions based on the literature reviews and compromises between their parameters.

	Experiments			
Parameter	**ECL-T-1**	**ECL-T-2**	**ECL-T-3**	**Unit.**
Cell compartments	1	2	3	–
Anode	Ti	Ti	Ti	–
Cathode	SS	SS	SS	–
Lixiviant	H_2SO_4 – (0.5)	–	–	M
Anolyte (M)	–	H_2SO_4 – (2.0)	H_2SO_4 – (0.5)	M
Catholyte (M)	–	KOH – (2.0)	KOH – (1.0)	M
Middle compartment	–	–	NaCl – (2.0)	–
Membranes used	–	CEM	CEM & AEM	–
BM added a compartment	Anode	Anode	Anode	–
BM mass theoretical	5	5	5	g
BM mass	5.0039	5.0143	5.2600	g

(*Continued on next page*)

Table 50. (*Continued*)

Parameter	Experiments			Unit.
	ECL-T-1	**ECL-T-2**	**ECL-T-3**	
S/L theoretical	40	40	40	g/mL
S/L used	39.969	39.886	38.023	g/mL
Flow Rate	40	40	40	mL/min
Volume	200	200	200	mL
Current	140	160	160	mA
Temperature	24	25	23–27	°C
Stirring	300	300	300	rpm
Time	180	180	180	min
Data availability	**YES**	**NO**	**YES**	–

The (**Table 50**) in addition to test parameters referred to and based on the literature review ECL studies, does have in it also includes the actual ECL Test-1/2/3 values of certain parameters (e.g., S/L used, BM mass and Temperature) written down when they were conducted, with the addition to data availability for tests in thesis itself.

5.5.2.2. Reagent preparation

For all experiments, the particle size of 75 μm BM was used, and chemicals were from Sigma-Aldrich. Their initial information can be found in (**Table 51**) with their information and in what form they were, as H_2SO_4 was in liquid form. However, NaCl and KOH were in powder and pellet forms, respectively, so different calculations were required for their preparations.

Table 51. Solution preparation for the initial and desired parameters for the ECL-T-1/2/3, with all the needed information for the calculations to be done using the correct Equations. To create 200 mL volume of solutions for tests.

Parameter	Solutions		
	H_2SO_4	**KOH**	**NaCl**
Initial purity %	95	–	–
Form	liquid	pellet	powder
Volume (mL) needed, V	200	200	200
Density, ρ	1840	–	–
Concentration (M) needed, C	0.5 & 2.0	1.0 & 2.0	2.0
Molar mass (g/mol), M_{mass}	98.1	56.11	58.44
Eq. needed to calculate	**26 / 28.1**	**29.1**	**29.1**
Measured volume or weight needed	5.61 & 22.45 (mL)	11.22 & 22.44 (grams)	23.38 (grams)

Calculations and preparations for the different concentrations of the H_2SO_4 can be found in the (***5.5.1.2. H_2SO_4 lixiviant preparation***) section, while for the KOH and NaCl, as they are in solid forms, a different type of calculation is needed, as per (Eq. (**29.1**)).

$$m = M \times V \times M_{mass} \tag{29.1}$$

Where m is mass/weight needed (grams), M is the molarity of the desired solution (mol/L), V total volume of solution needed/wanted to make (L), and M_{mass} is the molar mass of the solute, in this case, of KOH and NaCl. Calculations for the KOH 1 M, as such, can be done as follows (Eq. (**29.2**)),

$$m = 1.0\ \text{M} \times 0.2\ \text{L} \times 58.44 \frac{\text{g}}{\text{mol}} = 23.38\ \text{g} \tag{29.2}$$

Meaning that the needed mass for the preparation of the KOH 1 M was 11.22 grams, for the 2 M was 22.44 grams, and for the NaCl of 2 M is 23.38 grams. Preparations of all of the solutions was done by filling a beaker with 150 mL of DI, and stirred with magnetic stirrer to dissolve solid particles, after wards the beakers were filled till the 200 mL mark, hence creating the 1/2 M KOH and 2 M NaCl solution of 200 mL volume for all of the ECL tests.

5.5.2.3. Testing setup

All three ECLs were conducted in a well-ventilated (fume hood) as per (**Figure 35**). From (**a**) to (**c**), different reactor configurations can be observed, ranging from one compartment to two and, lastly to that of three, which can be seen via Erlenmeyer and decanter glassware amount in separate photos. In (**Figure 35**) are also shown steps or more precisely adjustments and modifications done throughout the experimentations. In (**d**), we can see the addition of the FKM gasket and a special slot for it in the two-compartment and three-compartment reactors, which was designed for the sealant between compartments and the membranes used in the testing. In (**e**), a silicone-based sealant paste by (Würth Oy), which was applied on all of the crevices/joints in between different components, from where solutions and BM could seep through, as this was a constant issue. The application was completed one (1) hour before the tests were conducted, as the paste needed six (6) hours to harden and procure, meaning it would be difficult to remove after three (3) hours of testing,

as it would have formed a bond with the reactor. In (**d**), a photo shows precisely how the voltage was applied via DC to the electrodes in the reactor, along with their connections.

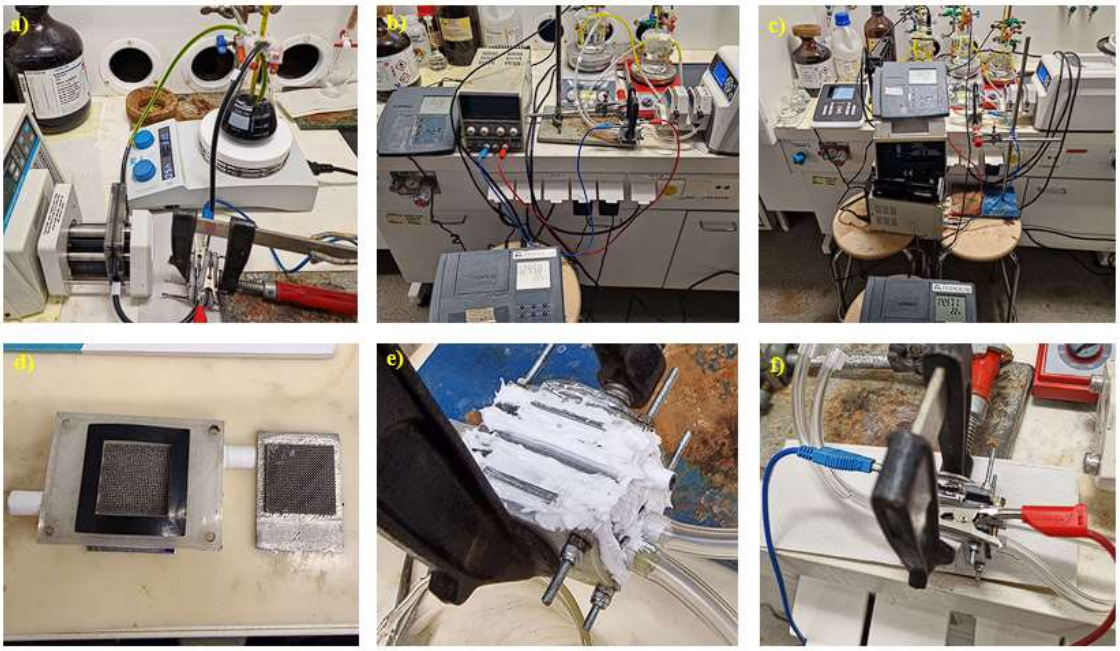

Figure 35. Electrochemical leaching TESTs 1–3, with their setup photos, and additional modifications for the reactor. ELC-T-1 testing setup in the photo of (a), ELC-T-2 testing setup in the photo of (b), ELC-T-3 testing setup in the photo of (c), an addition of the gasket between the two parts that hold electrodes so that the membrane has a tight sealing in the reactor separating electrode compartments (d), use of silicone based sealant base to minimise leakage from the reactor when testing (e), and connection of electrode to that of DC, via alligator clips (f).

Equipment and all of the other necessary hardware needed for different tests can be seen (**Table 52)**, not taking into consideration the solutions and other small necessities if needed.

Table 52. The necessary equipment amounts in different ELC tests performed in addition to the reactor.

	Tests		
Equipment	**ELC-T-1**	**ELC-T-2**	**ELC-T-3**
pH meter	1	2	3
Pump	1	2	3
Erlenmeyer/Decanter	1	2	3
DC-power supply	1	1	1
Pump	1	1/2	2/3
Heater	1	2	3
Magnetic stirrer/stick	1	2	3
Bench clamp	3	5	7
Support stand	2	3	4
Wires + alligator clip	2	2	2
Tubes	2	4	6
Membrane	0	1	2
Gasket	3	5	8

5.5.2.4. Sampling & Parameter collection ECL

Sampling, as in the chemical leaching processes, was performed using a triplicate sampling methodology. This involved pipetting 1.5 mL from each solution three times, resulting in a total sample volume of 4.5 mL, as the sampling was conducted each time. The procedure was performed for all reagents in the ECLs to verify the elemental composition of the solutions throughout the tests and to determine if metal/elemental concentration spikes were visible in those of NaCl and KOH alike. A total of 64 mL of various samples from solutions were prepared, depending on the tests. Sampling was performed through the parafilm's self-made hole on top of each solution container as the top cover and taken in between the centre and wall of the container, of about 1–2 cm under the surface of the solution, to avoid particles of BM and to prevent touching the stirring bar at the bottom. Different parameters and information regarding the proceedings in ECL-T-1 and ECL-T-3 can be seen in (**Appendix 1**). Sampling was conducted at all stages, times, and when a parameter was added or applied, as in the case of the BM and Voltage, for instance, as observed by time and sampling. ECL-T-2 was removed at this point, as its data/values, as stated, were faulty. Data for the ECL-T-1 pH values are also not available, as they were not taken, and a re-test was not deemed necessary. For achieving the initial voltage in ECL-T-1 and ECL-T-2, the use of the current (A) was applied to DC. This then gave the voltage as seen in (**Appendix 1**). The current was constant and kept at a constant level, while the voltage fluctuated due to electrodes and solvents reacting in the reactor. This was achieved by utilising PA and current density (j) to

produce the desired current (I) in DC, which was then translated into a voltage, as follows (Eq. (**30.1**)).

$$I = j \times PA \tag{30.1}$$

Where, I is the current (A), j is the current density (A/m^2 or A/cm^2), and PA is projected surface area (m^2 or cm^2), which if inputting parameters in the test and literature review of for instance that of 400 A/cm^2 based on the studies of (Meng et al. [9]), (Leclerc et al. [10]), and (Li et al. [12]), the needed current applied to that of DC, can be calculated as follow using (Eq. (**30.1**)) as (Eq. (**30.2**)) for the ELC-T-3.

$$I = 400 \frac{\text{A}}{\text{cm}^2} \times 0.4 \text{ cm}^2 = 160 \text{ A or } 0.16 \text{ mA} \tag{30.2}$$

This would and was the simplest way of doing the voltage by DC, without taking into account resistance and other factors that come in electrochemical systems, as DC just gives it. For instance, if everything is taken into account, it could be broken down into five steps. 1. Determination of the current density (j) as (Eq. (**31.1**)), 2. Calculation of the overpotential (η) as (Eq. (**31.2**)), 3. Equilibrium potential (E_{eq}) addition into equation as per (Eq. (**31.2**)), after the using the Tafel equation and calculation of overpotential (η), per (Eq. (**31.2**)), 4. Inclusion of the ohmic losses (IR_{drop}) as (Eq. (**31.3**)) and 5. Calculation and sum of all the steps 1-4 into the last step of the voltage as (Eq. (**31.4**)). Hence, this can be put as follows,

$$j = \frac{I}{PA} \tag{31.1}$$

Where j is current density (A/m^2 or A/cm^2), I is current (A), and PA is the projected surface area of the electrode (m^2 or cm^2).

$$\eta = a + b \log(j) \tag{31.2}$$

Where η is overpotential (V), a and b are the Tafel equation constants or parameters, and j is current density (A/m^2 or A/cm^2) in a log. Overpotential depends on reaction kinetics.

$$IR_{drop} = I \times R_{cell} \tag{31.3}$$

Where IR_{drop} is the ohmic loss or the resistive (V), I is current (A), and R_{cell} is the cell resistance (Ω)

$$V = E_{eq} + \eta + IR_{drop} \quad (31.4)$$

Where V is the voltage (V), E_{eq} is the equilibrium potential (V), η is the overpotential (V), and IR_{drop} is the ohmic losses (V). This would give the total voltage as was observed in the DC power supply, as the current was set up into it. As such it could be possible to calculate others factors from the Eq (**31.1**) till the (**31.4**) if one wanted, but this is just for theoretical explanation of how and what affect electrochemistry of electrodes and electrolytes alike, as the resistance and other factors/parameters do also affect the results what are achieved.

To verify and validate data correctness, the ICP-MS analysis was done, as for all of the samples, out of which the CPS values were studied, to determinate, which element could be seen and which not based on the 100%, 50% and 0% reliability, as shown in (**Table 53**) below.

Table 53. Elemental Detection & Reliability by the ICP-MS from the samples for the ECL-T-1 and ECL-T-3.

Detected / Reliability	ECL-T-1	ECL-T-3
100%	7 Li / 55 Mn / 59 Co / 60 Ni	7 Li / 55 Mn / 59 Co / 60 Ni
50/50%	23 Na / 39 K	23 Na / 39 K
0%	27 Al / 51 V /52 Cr / 56 Fe / 63 Cu	27 Al / 51 V /52 Cr / 56 Fe / 63 Cu

Based on the ICP-MS CPS values and by using (**Table 35**) in addition, the following decibel values for elements were observed, which are similar to those of CL-Ts results (**Table 49**).

5.6. Filtering and BM collection

After each individual experimentation, from chemical to electrochemical leaching, the BM's concentration in the lixiviant and suspension was left. To not waste, and also because the collection of this waste and hazardous material was deemed necessary, as the concentration of different metals, especially those of F. For this reason, the filtering of the BM was conducted after each test for the solution with BM, using Whatman 50 filter paper, which

can filter particles up to 2.7 µm in size using the Büchner vacuum system [282]. This method of filtering has also been used by (Porvali et al. [283]) to collect leach residues of the BM used in their work by the team, showing promising results and effectiveness, which is why it has also been chosen for the current BM filtration, from the lixiviant residue. The system used for the filtering of the BM can be seen below (**Figure 36**), which consists of a Büchner funnel, a Büchner flask, and a rubber bung between them. The entire system is then connected to a vacuum inlet, creating suction that filters liquid, lixiviant, and moisture through the filter paper, leaving the BM on top of the filter paper.

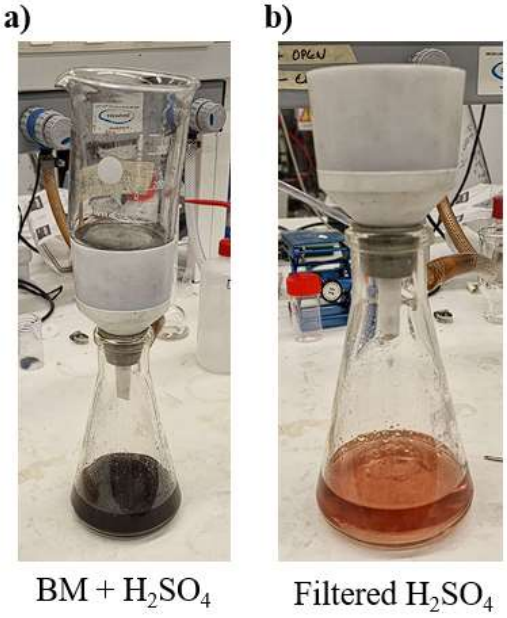

Figure 36. The filtration system of BM from the lixiviate (in the picture of 2 M H_2SO_4) using Whatman 50 grade filter paper, BM in lixiviate from the testing after cooling black colour in H_2SO_4 on the left (a) and filtered H_2SO_4 with some residue from the BM, which colours its colour into pinkish on the right (b).

After filtration, the filter paper with the BM residues was left to harden for approximately 20 to 30 minutes, so that it would be easier to take out from the funnel. For any data and measurements to be valuable or available at all for further studies and calculations of how much BM or metals have leached out of it, using the initial mass of the BM in tests as per (**Table 47**), for example, BM mass used (grams), the filter paper had to

be weight at the start of the filtering, to know later after it has been left to dry in an oven overnight. Only after that could the amount of the undissolved and not leached metals be calculated from the filter paper, as some particles were so small but not less than 2.7 μm got in between filter papers pores, and as such should also be taken into consideration with the free bigger particles that form a new undissolved BM, based on what one could calculate the difference before and after tests. These BMs could also be used for other types of analysis, such as familiar SEM-EDS to see the lixiviants' effect on the BM, for instance, or that of ECL, or by XRD analysis, or by ICP-MS after microwave digestion system and AQUA regia. Nonetheless, data for some of the data/values can be found under (**Table 54**).

Table 54. Collected values of the Whatman grade 50 filter paper and BM before the chemical leaching (CL) tests 1 & 2, and after the tests, to calculate/get undissolved BM and leached BM total mass/weight in grams.

	Experiments		
Parameter	**TEST-CL-2**	**TEST-CL-3**	**Unit**
Filter paper (initial)	0.364	0.377	grams
BM mass (initial)	5.138	5.115	grams
Filter paper (after)	0.417	0.390	grams
Undissolved BM	2.637	2.379	grams
Left on the Filter paper	0.053	0.013	grams
Undissolved BM in TOTAL	**2.690**	**2.392**	grams
Leached BM in TOTAL	**2.448**	**2.723**	grams

As such, the process of filtering and collecting mass/weight data from the BM can be put into the following steps:

1. Take Whatman 50-grade filter paper.
2. Weight mass of the filter paper.
3. Assembly of the filter system Büchner flask → a rubber bung → a Büchner funnel → a connecting vacuum inlet tube to the Büchner flask adapter → putting Whatman filter paper on top of a Büchner funnel → moistening filter paper a tiny bit with DI.
4. Let lixiviate with BM cool off.
5. Pour carefully on top of the moisture filter paper in small portions
6. Filter until clear, as in (**Figure 36 (b)**), done 2–4 times in thesis.
7. After filtering/closing the vacuum pump, let it sit for 20–30 minutes.

8. Take the filter paper out and put it on a Petri dish, and put it into the oven overnight.
9. Weigh the mass of the filter paper with the BM → weigh BM separately → weigh filter paper separately → (**Table 54**) result done.

Lixiviate and other reagents, after use and sampling, if done, were disposed of in separate liquid containers. The pipette tips and single-use plastic testing tubes were then disposed of in separate plastic bags and placed in boxes for hazardous waste collection, following LUT guidelines.

5.7. Data Calculation and Leaching Efficiency

The purpose of these experiments and tests is to calculate and determine the leaching recovery efficiency rates for the CRMs, such as Li, Co, Ni, and Mn, that can be found in LIBs and their BM during the recycling process. To achieve results from the lixiviate and solution, the best method is ICP-MS. Samples from the sections (***5.5.1.4. Sampling & Parameter collection CL*** and ***5.5.2.4. Sampling & Parameter collection ECL***), as discussed with the ICP-MS analysis method, were diluted 15,000 times for further analysis and before any ICP-MS dilutions were done, were filtered through an RC-20 syringe micro filter, filtering (0.20) μm and larger particles, for precaution and ICP-MS analysis/machine safety. To calculate leaching efficiency or the Eff.%, one needs to do the following steps:

1. Have the elemental concentrations in the original BM as per (**Table 33**).
2. Measure and get data for the element under investigation (concentrations).
3. Calculate the mass or Wt.% of elements in leachate/lixiviant.
4. Calculate the Eff.% by dividing step (3) by (**Table 33)'s** Wt.% and multiplying by 100.

To put this into and mathematical equation, it can be represented as (Eq. (**32.1**)).

$$\text{Eff.}\,\% = \left(\frac{C_{LIX} \times V_{LIX}}{m_s \times C_s}\right) \times 100 \qquad (32.1)$$

Where C_{LIX} is the metal ion concentration in lixiviant (mg/L), V_{LIX} is the recovered volume (L) of the lixiviant used for the leaching or in this case the reactor volume, m_s is the mass of the solid material used for the leaching (kg), and the C_s is the concentration of the metal used in the material before the leaching ($mg \cdot kg^{-1}$). As an example, let's take the ICP-MS data value for the (7 Li) of the CL-T-1 at 90 minutes, and as we have the sampling done in triplicate, these values can be found in (**Table 55**) below. The calculation itself is based on (Eq. (**29.1**)), which can be shown/written as an example (Eq. (**32.2**)) for the first data of the ICP-MS concentration at 90 minutes as follows using (**Table 55**).

$$\text{Eff.}\,\% = \left(\frac{545 \frac{\text{mg}}{\text{L}} \times 0.2\ \text{L}}{5260.1\ \text{mg} \times 0.0542} \right) \times 100 = 38.25 \ldots \% \qquad (32.2)$$

The value for the leaching efficiency is 38.25%, as determined for Li at 90 minutes for the first sample out of three, after subtracting all units from each other to obtain a percentage. According to this equation, a leaching Eff.% can be calculated for all of the experiments/tests if using data available from (**Table 33**) for the initial BM Wt.% for elements and parameters used in the experiments/tests.

Table 55. This resulted in values for the 90 minutes of the CL-T-1, out of which the average value was taken for later use. Steps for the (Eq. (**32.1**)) with the conversion of the units for the calculations as shown in (Eq. (**32.2**)).

Parameter	ppb by ICP-MS	Divided by 1,000	Initial BM	Divided by 1000	Volume of Reactor	Divided by 1000	(Table 36) Wt.% for (7 Li)	Divided by 100	Result
Data value 1	545,002.7385	545.0027385	5.2601	5,260.1	200	0.2	5.42	0.0542	38.25134275
Data value 2	501,852.3608	501.8523608	5.2601	5,260.1	200	0.2	5.42	0.0542	35.22280771
Data value 3	560,415.5689	560.4155689	5.2601	5,260.1	200	0.2	5.42	0.0542	39.33310146
Units	ppb = µg/L	mg/L	grams	mg	mL	L	Wt.%	–	%
(Eq. (32.2))		C_{LIX}		m_s		V_{LIX}		C_s	Eff.%

5.8. Safety Operations in Thesis

There are many different things done in the thesis, and some of the substances are corrosive, acidic, toxic particles when breathed in fire hazards, or explosion risks. These should be noted and taken into account throughout the thesis and overall, when working in the laboratory and making sure that others around are safe, as laboratories were open, but restricted to personnel with credentials. Such understanding of risk throughout the whole thesis involves different steps, where risk for ourselves and our surroundings must be broken down.

The importance of safety during the creation of BM from the battery packs is the most crucial part of the whole safety in thesis, as there are multiple steps and risks are never-ending, as new ones come from the processing material into the next form/step, as such safety operations for these steps can be seen in (**Table 56**) below.

Table 56. Safety procedures and mitigations during Battery packs → BM creation.

Order	Stage	Operational Steps	Safety Precautions	Potential Accidents & Mitigations
1.	Disassembly of Laptop Battery Packs	- Pry open the outer casing using insulated tools throughout a small incision between the top/bottom covers - Identify and disconnect battery modules/cells - Separate cells from the BMS unit	- Wear cut-resistant gloves, safety goggles, and a flame-resistant lab coat - Use as many insulated tools as possible - Avoid puncturing or crushing the battery cells - Work in a well-ventilated, non-flammable area - Class D extinguisher is at least nearby (Currently no class in Finland)	- Thermal runaway: Cells may ignite if punctured → keep cells cool / avoid metal tools near terminals/poles - Short-circuit: Avoid metal contact between terminals → thermal runaway / keep Class D fire extinguisher and/or sand nearby - Toxic Gas leakage (HF): Well-ventilated area and a fume hood - Disconnect cells safely → insulated tools - Sharp edges → gloves working under & nitrile on top

(*Continued on next page*)

Table 56. (*Continued*)

Order	Stage	Operational Steps	Safety Precautions	Potential Accidents & Mitigations
1.	Disassembly of Laptop Battery Packs	- Separate cells from the BMS unit	- Class D extinguisher is at least nearby (Currently no class in Finland)	- Sharp edges → gloves working under & nitrile on top
2.	Discharging Battery Cells	- Confirm voltage <0.5 V before for safe handling - Discharge batteries, via a closed circuit, using a resistor (**Figure 22 (b)**) - Verify full discharge with a multimeter - Ensure full discharge	- Monitor voltage continuously - Use a multimeter - Make sure batteries were as much DISCHARGED or FULLY DISCHARGED - Perform in a fume hood or a ventilated area - Class D extinguisher is at least nearby	- Electrical shock/Short-circuit**:** Discharge in a plastic container; avoid water contact with exposed terminals - Chlorine gas**:** Perform in a well-ventilated area or under a fume hood - Gas evolution (H_2): Ventilated environment - Toxic Gas leakage (HF): Well-ventilated area and a fume hood - Residual charge: Confirm the cells are discharged → use insulated tools
3.	Dismantling LIB Cells	- Remove the plastic wrapper from around the metal casing of the cell (Collect) - Use insulated cutters and pliers to pry open one pole of the cell - Remove the thin Fe rod from the battery Separate the anode/cathode foils and separator manually - Use separate bags/containers for all parts	- Wear an N95 mask, face shield, and/or protective glasses with closed sides to avoid metal particles/dust shrapnel/inhalation - Work in a well-ventilated, non-flammable area - Work under a fume hood → electrolyte vapours - Ground equipment to prevent static sparks - Use as many insulated tools as possible Use a respirator when dry handling - A Class D extinguisher is at least nearby	- Toxic electrolyte leakage ($LiPF_6$) & (toxic/flammable): Neutralise spills with sodium bicarbonate ($NaHCO_3$) → store waste in sealed containers - Dust inhalation: Ventilated environment and/or under a fume hood - Thermal runaway: keep a Class D fire extinguisher and/or sand nearby
4.	Black Mass (BM) Creation	- Dry anode/cathode under inert air or vacuum, to remove moisture and other fumes released	- Use an explosion-proof mill - Use ground equipment to prevent static sparks - Wear anti-static clothing	- Dust explosion/Fire: Stay in well well-ventilated area & keep an eye out for thermal/kinetic hazards, stay in a humid environment

(*Continued on next page*)

Table 56. (*Continued*)

Order	Stage	Operational Steps	Safety Precautions	Potential Accidents & Mitigations
4.	Black Mass (BM) Creation	- Grind and mill electrodes and their materials Sieve through different meshes to have a consistent, homogeneous particle size distribution	- Minimum requirement: N95 mask, in the best scenario, if particles are highly aerosolised, a respirator - Eye protection is better if goggles with closed sides and a tight seal to the skin - Glove protection - Class D extinguisher is at least nearby	- Fire risk: Store BM in sealed, grounded containers - Inhalation of fine metal/graphite dust: Use PPE → N95 mask or respirator - Static ignition: Ground equipment, avoid plastic tools

Working with the chemical and other equipment when doing laboratory work in the experimental part, mainly under the fume hood, with strong acids. This means risks and safety precautions that need to be taken into account. (**Table 57**) has the basic and important minimal safety precautions to work in a laboratory with acids and BM.

Table 57. Safety precautions and operational steps in the experimental part of the laboratory, when dealing with chemical substances (e.g., acids and BM).

Order	Stage	Safety Precautions	Operation Steps	Potential Accidents & Mitigation
1.	Personal Protective Equipment (PPE)	- Chemical-resistant gloves (nitrile) - Lab coat (acid-resistant) - Lab coat with closed sleeves - Eye protection - N95 mask if needed	- Cover the skin surface that is under the fume hood	- Chemical burns → Immediately rinse with water - Inhalation & fumes → Leave the room & close the fume hood sash - Changing gloves when contaminated
2.	Experimental Setup	- Work in a fume hood - Use acid-resistant containers (glassware) - Label all containers clearly	- Prepare an acid solution in a beaker under a fume hood - Bm addition slowly	- Acid splashes → Neutralise spills with $NaHCO_3$ or spill kits

(*Continued on next page*)

Table 57. (*Continued*)

Order	Stage	Operational Steps	Safety Precautions	Potential Accidents & Mitigations
3.	Experimental Process	- Temperature monitoring - Use of a magnetic stirrer - Add BM to acid slowly & in small portions	- Heat reagents & lixiviants slowly to temperatures - Use magnetic stirrers, and keep rpm optimal	- Violent reactions → Add reagents slowly (foaming → stop heating) - Perform in the ventilated fume hood - Monitor pH - Keep neutralizing agents ($NaHCO_3$ & NaOH) on hand
4.	Filtration & Waste Handling	- Use a Büchner funnel when vacuuming (no pressure build-up) - Throw acids in contact with the BM into a separate container (market) - Labelling waste properly	- Filter leachate to separate solids - Rinse residues with DI	- Toxic filtrate → dispose of as hazardous waste (big container in laboratory separately)
5.	Post- and cleanup	- Decontaminate tools with DI - Allow residues to cool before handling	- Wash glassware with a dilute base of NaOH 1M and DI. - Label waste correctly if needed	- Residual acid → Test the pH of waste & dilute if needed - Cross-contamination → clean workstation, with towel/wipes

5.9. Theoretical Reactions

Four metals can be detected reliably by the ICP-MS, based on (**Tables 33**, **47,** and **50**), Li, Mn, Co, and Ni. Reactions that can and could occur in chemical leaching can be divided into Li, Mn, Co, and Ni reactions between $LiCoO_2$ or LCO and H_2SO_4, primarily, as it is used in both CL and ECL in the same compartment with the BM.

Reactions and reaction mechanisms that can occur in chemical leaching for the Li, Mn, Co and Ni can occur as follows: For Li, there could be more reactions, but we will look at two more important (Eq. (**33.1**) and (**33.2**)).

$$Li_2O\ (s) + H_2SO_4\ (aq) \rightarrow Li_2SO_4(aq) + H_2O\ (l) \quad (33.1)$$

$$2LiF\ (s) + H_2SO_4(aq) \rightarrow Li_2SO_4(aq) + 2HF\ (g) \uparrow \quad (33.2)$$

In (Eq. (**33.1**)), what happens is that the chemical bonds between Li^+ and O^{2-} break, due to H_2SO_4, leading to the formation of H^+ and SO_4^{2-}. These then lead to the formation of Li_2SO_4 salt and H_2O. Like in the previous equation, a similar mechanism happens in the (Eq. (**33.2**)), as chemical bonds between Li^+ and F^- break, because of acid. This process leads to the reaction between F^- and H^+ ions, resulting in the formation of hydrogen fluoride gas and subsequently to the formation of a salt.

For the Mn reaction between Mn in LCO the H_2SO_4, the reaction mechanism could be that of (Eq. (**34**)).

$$4LiMnO_2\ (s) + 6H_2SO_4(aq) \rightarrow 2Li_2SO_4(aq) + 4MnSO_4(aq) + 6H_2O\ (l) + O_2(g) \uparrow \quad (34)$$

In (Eq. (**34**)), H_2SO_4 attacks the Li metal oxide Mn by making it release Li^+ and Mn^{3+}, leading to the reduction of Mn^{3+} into Mn^{2+} as it happens in $MnSO_4$, leading to oxygen being released as the oxidation happens, as metal oxides are being oxidised.

Reactions and mechanisms that can occur in chemical leaching with Co can go as follows:

$$4LiCoO_2(s) + 6H_2SO_2(aq) \rightarrow 4CoSO_2(aq) + 2Li_2(SO_4)_3(aq) + 6H_2O\ (l) + O_2(g)\ \uparrow \quad (35.1)$$

$$2Co_3O_4(s) + 6H_2SO_4(aq) \rightarrow 6CoSO_4(aq) + 6H_2O\ (l) + O_2(g)\ \uparrow \quad (35.2)$$

$$Co\ (s) + H_2SO_4(aq) \rightarrow CoSO_4(aq) + H_2\ (g) \uparrow \quad (35.3)$$

In (Eq. (**35.1**)), a displacement by the H^+ of Li^+ happens, then in return leads to the reduction of Co^{3+} to Co^{2+}, leading to the oxygen evolution, which also leads to that of Li^+ being bound to SO_4^{2-} and the creation of stable salts Li_2SO_4 and $CoSO_4$. In (Eq. (**35.2**)), a formation of oxygen evolution occurs, as the H_2SO_4 does a proton donation, which leads to the formation of oxygen and Co bond break as the reduction of Co^{3+} to Co^{2+} occurs and the formation of salt $CoSO_4$. In (Eq. (**35.3**)), that is possible that hydrogen gas evolution occurs, as the Co is being oxidised to Co^{2+}, which should lead to energy release and corrosion.

Ni with the Li in H_2SO_4 reaction could react of (Eq. (**36.1**)) in a leaching reaction of LCO.

$$4LiNiO_2(s) + 6H_2SO_4\ (aq) \rightarrow 2Li_2SO_4\ (aq) + 4NiSO_4(aq) + 6H_2O\ (l) + O_2(g) \uparrow \quad (36.1)$$

In (Eq. (**36.1**)), a release of those Li^+ and Ni^{3+} occurs as the H_2SO_4 attacks the structural crystal structure inside of that $LiNiO_2$, which hence leads to the of reduction of Ni^{3+} to Ni^{2+} and oxygen evolution due to Ni^{2+} reduction reaction, leading to that of SO_4^{2-} combining with the Li^+ and Ni^{2+}. A different type of mechanism between Li and Co is possible, that of protonation of carbonate, where CO_3^{2-} will act as a base in accepting H^+ from that of an acid in reaction in (Eq. (**36.2**)).

$$Li_2CO_3\ (s) + H_2SO_4\ (aq) = Li_2SO_4\ (aq) + H_2O\ (l) + CO_2(g) \uparrow \quad (36.2)$$

Like in those of (Eq. (**33.1**) and (**33.2**)) the dissociation occurs due to H_2SO_4, which allows for the (Eq. (**36.3**)) protonation of carbonate by.

$$HCO_3^-\ (aq) + H^+(aq) \rightarrow H_2CO_3\ (aq) \quad (36.3)$$

And further to that of H_2CO_3 decomposition as per (Eq. (**36.4**)) and formation of the salt per (Eq. (**36.5**)).

$$H_2CO_3\ (aq) \rightarrow H_2O\ (l) + CO_2(g) \uparrow \quad (36.4)$$

$$2Li^+(aq) + SO_4^{2-}(aq) \rightarrow Li_2SO_4\ (s) \quad (36.5)$$

As it was mentioned in the SEM-EDS result (***5.2.4.2. Characterisation of BM by SEM-EDS Analysis***), the BM seemed to have those spots with the NMC 532, so when we look at it, a reaction of it in H_2SO_4 could go as (Eq. (**37.1**)).

$$2LiNiMnCoO_2(s) + 6H_2SO_4\ (aq) \rightarrow Li_2SO_4(aq) + 2NiSO_4(aq) + 2MnSO_4(aq) + 2CoSO_4(aq) + 6H_2O\ (l) + O_2(g) \uparrow \quad (37.1)$$

Where H_2SO_4 acts as a strong acid, it would attack the metal oxide, releasing Li^+ subsequently, which in turn would allow the reduction of Mn from the Mn^{4+} to a much lower Mn^{2+} valence, and in the case of Co^{3+} to normal Co^{2+}. These would then allow for the $Ni^{2+,}$ which is is/has been stable enough to allow all four metals to combine with that of SO_4^{2-}, to bond and form that of sulfates as seen in (Eq. (**37.1**)) via the (Eq. (**37.2**)) mechanism route as shown.

$$2Li^+(aq) + 2Ni^{2+}(aq) + 2Co^{2+}(aq) + 2Mn^{2+}(aq) + 6SO_4^{2-}(aq) \rightarrow Li_2SO_4(aq) + 2NiSO_4(aq) + 2MnSO_4(aq) + 2CoSO_4(aq) \quad (37.2)$$

In electrochemical leaching of T-3 or ECL-T-3, the use of three different solutions of H_2SO_4 in the anode compartment, which had BM, NaCl in the middle compartment, and KOH in the cathode compartment. All three work as electrolytes, as it is in their nature to dissociate into ions in aqueous solutions. As such, hydrogen evolution occurs in H_2SO_4, allowing metal oxides to oxidize at the anode compartment. As KOH is in the cathode, its role in OH^- providing to that of ECL is important, thus allowing for the cell's principle to work. Importance of NaCl in the middle compartment divided by AEM and CEM does not allow for KOH and H_2SO_4 to mix, but also acts as a salt bridge, leading to migration of (Na^+ to the cathode and Cl^+ to the anode) for a balanced charge, to close the circuit of ECL**.**

One of the risks in ECL, when using Ti as an electrode, is the F corrosion, which may occur as the BM does have residues of F and P in it; hence, (Eq. (**38**)), it could be possible under correct conditions, like those of pH value.

$$Ti_2O_3\ (s) + 6HF\ (aq) \rightarrow 2TiF_3(aq) + 3H_2O\ (l) \quad (38)$$

For this reason, the use of H_2SO_4 could be important as the TiO_2 layer via anodic oxidation could be possible to created, a layer that would/protect the Ti from corrosion in ECL.

6. Results

The following chapter presents the experimental results obtained from the CL and ECL tests conducted on BM. The chapter is divided into two main sections: ***(6.1. Chemical Leaching Results***) and (***6.2. Electrochemical Leaching Results***), detailing the extraction efficiencies of Li, Mn, Co and Ni. In CL, the outcomes, including the effects of varying parameters such as acid concentration, temperature, and leaching time, are investigated based on the gathered results for the four metals and further then the results are compared with a reference study to contextualise the findings. While in the ECL, leaching results are compared between two reactor configurations and their performance in metal recovery, alongside the comparison with literature studies. Lastly, the section (***6.3. Comparison of CL and ECL results***), a comparative analysis of the CL and ECL methods, evaluates their respective efficiencies for each metal and discusses the implications of the observed differences.

6.1. Chemical Leaching Results

The importance of these three tests can be explained by the fact that what is wanted is to see how BM in v behaves when it is subjected to a basic chemical leaching test. For these reasons, as previously mentioned, the reference material or the values for similar, if not the same, conditions/experimental environment were examined. For this reason, it was decided to use (Vieceli et al. [5]) data/values for the H_2SO_4 and their results as a reference to those in this thesis BM. For this reason, a reconstructed and made (**Figure 37**) was made for the visual representation of this thesis values comparison of Eff.% for BM, in both cases. At this point, it should be noted that only elements based on the detection and reliability of that 100% based on (**Table 49**) are going to be included in the results of chemical leaching, meaning Li, Mn, Co, and Ni only.

To understand the results of our three experiments, TEST 1–3, we should compare them to the reference article, which we enclosed in the previous chapter. What we can see from their results is that overall, the leaching Eff.% of the elements like the Li, Mn, Co, & Ni increased over time and by the increase of the concentration of the H_2SO_4, when they did

the experiments for the 60 minutes at 50 Celsius and between the 0.5–2.5 M concentration. From their results, we can see that for Li, at 2.5 M, they got over 100% Eff.%, with other concentrations being between 80 and 100% of the range also. For the other elements, we can see Eff.% ranging from 10% to 100%, depending on the element and the concentration applied by the H_2SO_4. What we can see from the Eff.% is that as the concentration increases, the Eff.% also increases, in a nearly linear correlation with time. Of course, there are some exceptions, as in the case of (**Figure 37** (**a**)) Li, where a clear stabilisation/slowdown of Eff.% is observed at 1/2.5 M and even an apparent decrease in 0.5 M, and also a slight decrease in 2.5 M at their end parts. It is also noted that the Li Eff.% of 0.5 M decreases at 30 minutes, and the Eff.% increases at 1.5 M at the same time. Also, what can be seen in (**Figure 37** (**d**)) of Ni, where at 0.5 M, the slow/stabilisation of Eff.% can be observed. These are the cases where they are clearly seen. However, when looking at the (**Figure 37**) results, a clear pattern at 0.5 M is observable in comparison to other concentrations, as Eff.% results stabilise.

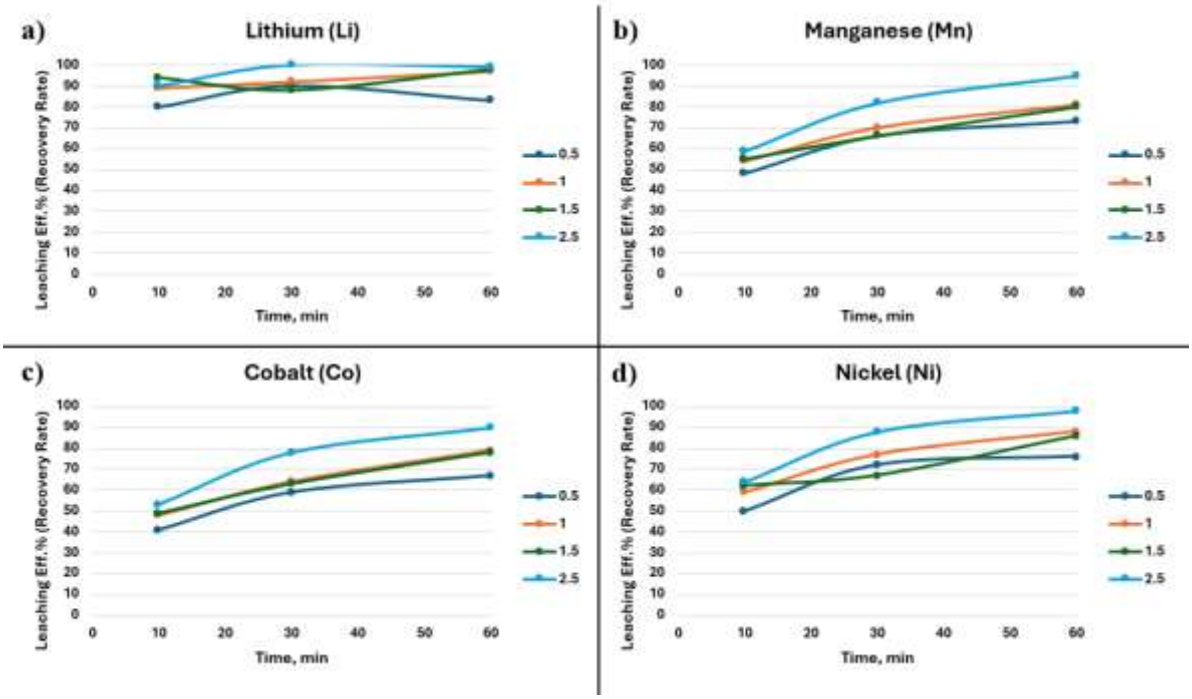

Figure 37. Results of the (Vieceli et al. [5]) reconstructed, for elements with their respective Leaching Eff.% from the BM in correlation to time (min) for the 0.5/1.0/1.5/2.5 M concentration of H_2SO_4 at a temperature of 50°C, Lithium (Li) Eff.% in (a), Manganese (Mn) Eff.% in (b), Cobalt (Co) Eff.% in (c), and Nickel (Ni) Eff.% in (d).

Compared to the results of the reference material (**Figure 37**), the tests CL-T-1/2/3 (**Figure 38**) show similarities that can be seen. Like the increase of Eff.%, over time, but clearly the leaching of (**Figure 38**) yielded worse results than that of (Vieceli et al. [5]). Hence the needs to be taken into account in the (**Figure 38)** are the parameters of the CL-T-1/2/3, as the CL-T-1 and CL-T-2 were done using lixiviate concentration of 0.5 M but, the first one being done at 25°C and the latter at 50°C, while the CL-T-3 done with 2.5 M and 50°C, as per (**Table 47**) information. An observation of those CL-T-2 and CL-T-3 shows a clear Eff.% surge of increase in comparison to that of CL-T-1 in all of the metals (**Figure 38**). This increase in tests indicates that the CL-T-3 achieves a greater Eff.% than the CL-T-2, with a difference of around 30 minutes or more. This can be seen as when CL-T-3 archives that of 77.48 Eff.%, 39.68 Eff.%, 33.20 Eff.%, and 39.08 Eff.% in 5 minutes, as per (**Figure 38** (**a**), (**b**), (**c**), and (**d**)), respectively. The CL-T-2 achieves similar or close to results 77.14 Eff.%, 38.72 Eff.%, 31.86 Eff.%, and 38.53 Eff.% at 30 minutes based on the (**Figure 38** (**a**), (**b**), (**c**), and (**d**)), respectively.

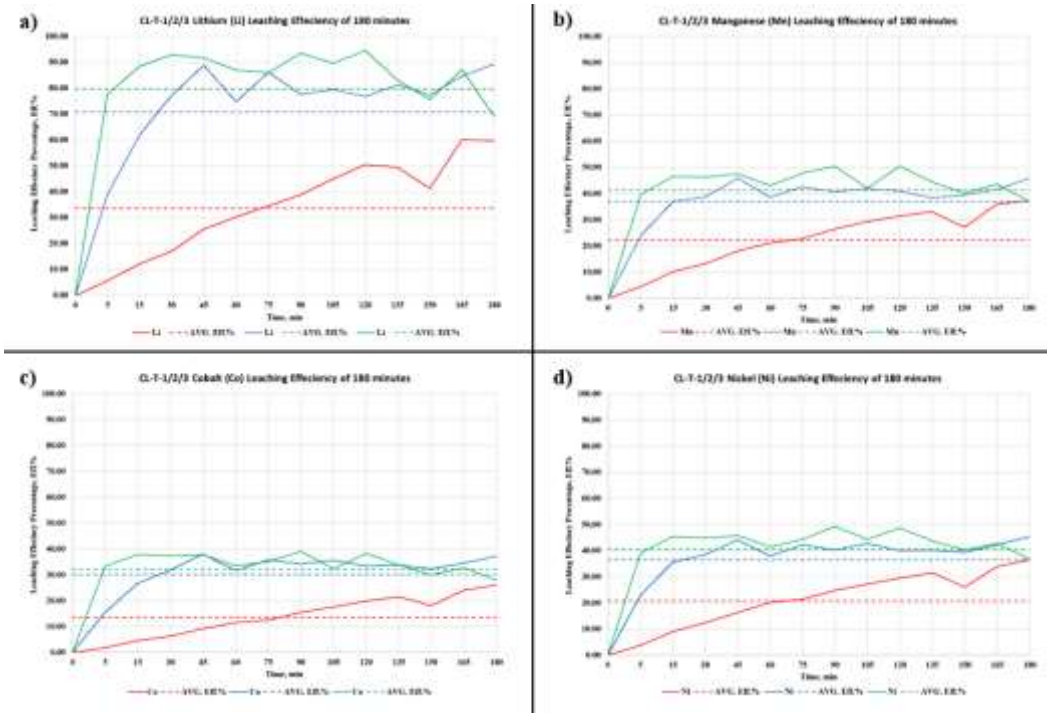

Figure 38. Results of Chemical Leaching (CL) for the TEST's 1–3, where the x-axis is time (min) and the y-axis of Leaching Eff.%. Results for CL-T-1 are in red, CL-T-2 in blue, and CL-T-3 in green. Additionally, results for the corresponding times per TEST are in solid line that of in Eff.% per sampling, while the dotted line is the result for the whole TEST's average value of the Eff.%. Results for the Lithium (Li) are in (a), Manganese (Mn) are in (b), Cobalt (Co) are in (c), and Nickel (Ni) are in (d), respectively.

Comparing the results of CL-T-1 to those of two other tests, a clear pattern of stability and fluctuation can be observed in all three tests. While the CL-T-1 Eff.% rises steadily and is that of constant, the same cannot be said for CL-T-2 and CL-T-3. A clear pattern of ups and downs is observed in all (**Figure 38** (**a**), (**b**), (**c**), and (**d**)) in Eff.%. These constant fluctuations eventually lead to an increase in the Eff.% in CL-T-2, while a drastic decrease in the Eff.% of CL-T-3 occurs. CL-T-2 ending Eff.% are at 180 minutes 89.32, 45.72, 37.25, and 45.37 in (**Figure 38** (**a**), (**b**), (**c**), and (**d**)) respectively, while those of CL-T-3 at 180 minutes Eff.% were 68.99, 37.13, 27.84, and 36.83 in (**Figure 38** (**a**), (**b**), (**c**), and (**d**)) respectively. Showing an apparent decrease, which, when looking at the graphs of a CL-T-2 and a CL-T-3, goes mainly as follows: when CL-T-2 reaches the same or close to the level of the Eff.% value of CL-T-2, the CL-T-3 starts or has already been decreasing for 15 minutes, but then at around 75 minute mark they both start increasing, only exception is in that of (**Figure 38** (**a**)) graphs, as shown in between 60 and 75 minutes. Nonetheless, afterwards, there is a clear pattern of when CL-T-3 is at peak, the CL-T-2 is at bottom, and vice versa till the 150 minutes mark, where they are almost of equal Eff.%, until at 165 minutes the sharp decrease of Eff.% in CL-T-3 takes place and increase in CL-T-2 respectively as mentioned previously. While those behave as they do, CL-T-1 steadily climbs till the 135-minute mark and sharply drops in all of the metals till 150 minutes, and afterwards it increases back sharply. These spikes can be seen as decreases of 8.11, 6.00, 3.47, and 5.51 Eff.% and increases afterwards of 18.71, 8.91, 5.98, and 7.87 Eff.% values for the Li, Mn, Co, and Ni, respectively, at the 135- and 150-minute marks. Overall, at the 180-minute mark, CL-T-1 reaches the same Eff.% or close to that of CL-T-3, which decreases to levels of 68.99, 37.13, 27.84, and 36.83 Eff.%, while the CL-T-1 increases to those of 59.77, 37.19, 26.20, and 36.47 Eff.%, meaning of only 9.22, -0.06, 1.64, 0.36 Eff.% difference in between them for the Li, Mn, Co and Ni respectively. From the results, it can also be noted that the end value of the CL-T-1 for the Mn is higher by 0.06 Eff.% in comparison to that of the CL-T-3 value. By these results, it is clear that the results of CL-T-1 are getting closer at the 180-minute mark, while those of CL-T-3 are decreasing, as the result of Eff.% for the Mn, Co, and Ni are so close to one another as observed by the (**Figure 38** (**b**), (**c**), and (**d**)), while those result of Li (**Figure 38** (**a**)) are of higher in CL-T-3. Nonetheless, when comparing the results of CL-T-1/2/3 tests, a clear conflict with the results of the reference (**Figure 37**) can be seen and stated, as the test results are relatively low in comparison.

To simplify the findings, let's look at the results from the value perspective, with (**Figure 39**). In (**Figure 39** (**a**)), the results of the (Vieceli et al. [5]) for the 30-minute and 60-minute can be seen with comparison to those of the tests in thesis, both for the H_2SO_4 of 0.5 M concentration. The key difference is that the reference material was thermally pre-treated and leached at 50°C, compared to 25°C. Clear differences in Eff.% can be observed for all of the metals when comparing them to one another; hence, it can be said that the leaching done in the laboratory did not achieve the literature values with drastic differences, primarily due to the temperature difference, but also because of the pre-treatment of the BM. This can be proven with comparison to the results of the leaching of the BM with the H_2SO_4 2.5 M as seen in (**Figure 39**), from both (**a**) and (**b**) was done by H_2SO_4 0.5 M, but at the same having that of 50°C, hence comparison in between both (**a**) and (**b**) can be done. Based on the (**Figure 39** (**a**)), although pre-treatment was performed in the reference material, its effect on the CL-T-2 results is that of only 12.86 Eff.% higher for the Li, while in case of the Mn, Co and Ni, the pre-treatment affection on the Eff.% can be seen at levels of 27.28, 27.14, and 33.47 Eff.% respectively. Results of (**Figure 39** (**a**)) indicate that at 30 minutes leaching, the temperature plays a 77% role in the Li recovery/Eff.% and leads to a value of 12.86% as disclosed previously. Meaning that, pre-treatments affect when comparing CL-T-1/2/3 BM to that of reference materials in the case of Li. In the cases of Mn, Co, and Ni, temperature plays a role of only 27.28%, 27.14%, and 33.47% in leaching, respectively, which we showcased earlier. In comparison to that of CL-T-2 and the reference material alike. This can then further be seen as the CL-T-1 values for the 30 minutes are miserably low in comparison to those of CL-T-2, to be precise, CL-T-2 results are of higher 78.03, 65.97, 80.45, and 68.00 in percentage (%) than those of CL-T-1 Li, Mn, Co, and Ni, respectively. Further indicating the temperature factor in the BM leaching, when it comes to 30 minutes.

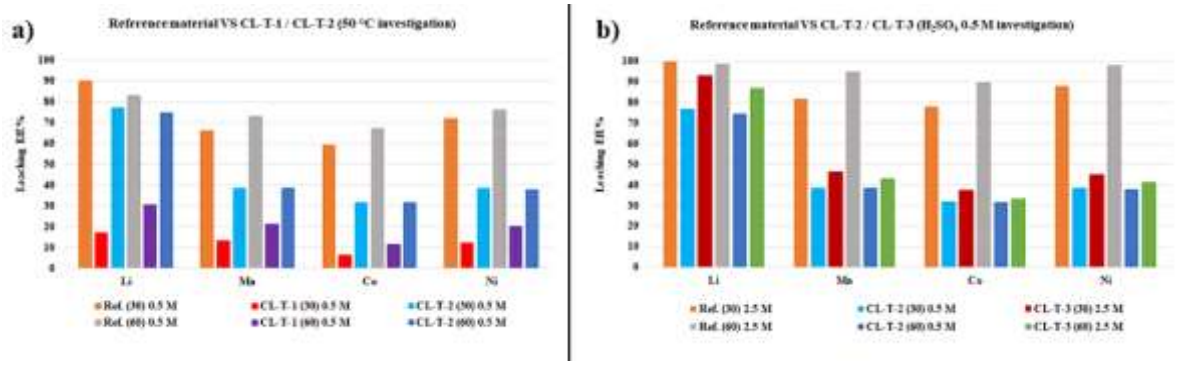

Figure 39. Investigation of the temperature and concentration on the leaching, when comparing 30- and 60-minute leaching results of the reference material to those of the CL-T-1 and CL-T-2. Temperature investigation using 50°C temperature on 0.5 M concentration results at 25°C temperatures on the left (a), and concentration investigation using 0.5 M concentration in 2.5 M concentration result at 50°C temperatures on the right (b). (*Note! Reference BM has been thermally pre-treated, so the investigation of 50°C and 0.5 M is optimal*).

When it comes to the 60-minute leaching results, similarities continue, but a clear difference can be seen in those results in the 30-minute leaching, as the CL-T-1 Eff.% increases over time. The difference between the results of CL-T-1 and CL-T-2 is only that of 59.40, 45.26, 63.59, and 46.82% for Li, Mn, Co, and Ni, respectively, when compared to those of the 30-minute result of 78.03, 65.97, 80.45, and 68.00%. Meaning that over time, the leaching at lower concentrations yields similar results as at higher temperatures, which also correlates with the (**Figure 38**) results. Result of Eff.% increases and percentage increases in comparison to CL-T-1 and CL-T-2 can be found in (**Table 58**) below. What can also be observed is that at 60-minute leaching, the factor effect of the pre-treated BM is greater, as it increases from the 30-minute leaching values of 27.28, 27.14, and 33.47% to 34.44%, 35.28%, and 38.06% for 60-minute leaching, respectively, for Mn, Co, and Ni. A noticeable difference when it comes to increased percentages.

Table 58. Difference between the reference values/data, and comparison with the values for the CL-T-1 and CL-T-2.

	Metal element				
Parameter	**Li**	**Mn**	**Co**	**Ni**	**Unit**
Ref. (30) 0.5 M	90.00	66.00	59.00	72.00	Eff.%
CL-T-1 (30) 0.5 M	16.94	13.17	6.23	12.33	Eff.%
CL-T-2 (30) 0.5 M	77.14	38.72	31.86	38.53	Eff.%
Pre-treatment effect on BM	12.86	27.28	27.14	33.47	%
Difference in Eff.% T-1 vs T-2	78.03	65.97	80.45	68.00	%
Ref. (60) 0.5 M	83.00	73.00	67.00	76.00	Eff.%
CL-T-1 (60) 0.5 M	30.36	21.11	11.55	20.18	Eff.%
CL-T-2 (60) 0.5 M	74.76	38.56	31.72	37.94	Eff.%
Pre-treatment effect on BM	8.24	34.44	35.28	38.06	%
Difference in Eff.% T-1 vs T-2	59.40	45.26	63.59	46.82	%
Decrease between 30 & 60 of Eff.%	23.88	31.40	20.95	31.15	%

In (**Figure 39** (**b**)), every test and result in it are done at 50°C, but CL-T-2 is done using 0.5 M concentrated H_2SO_4, lixiviate, hence the BM's behaviour can be seen to some extent, when it is pre-treated thermally in reference material + that how the concentration affects leaching when it is done at same temperatures. Based on the initial results of Li, all six results are decreasing at different rates. When it comes to CL-T-2, the decrease is minimal, at 0.16 Eff.%, and for the reference material, that is 1.0 Eff.%. CL-T-3, on the other hand, decreases from 92.99 Eff.% at 30-minute leaching to 87.10 Eff.%, a decrease of 5.89 Eff.% or 6.33% respectively. While the reference materials Eff.% keeps increasing for all of the rest metals, Mn, Co and Ni, a clear trend of vice versa behaviour is seen in the CL-T-2 and CL-T-3, that greater in the latter, which was seen and noted in the (**Figure 38**) discussion about CL-T-3 graph overall and its trend in comparison to others. Overall, a pre-treatment is affected primarily based on the result by temperature, and less so by concentration, as seen in the comparison between (**Figure 39** (**a**) and (**b**)). A pre-treatment effect at the 30-minute mark is that of 7.01, 35.70, 40.53, and 43.11% for Li, Mn, Co, and Ni, respectively, while at 60 minutes, 11.90, 52.01, 56.52, and 56.47%. From the results as in (**Figure 39** (**a**)), pre-treatment has a greater effect on the latter three metals than on Li. Based on the (**Table 59**) values, a difference of the Eff.% for metals in between CL-T-2 and CL-T-3 is that of 17.05, 16.38, 14.99 and 14.18% difference to that of Eff.% reported in 30 minutes of leaching in 60 minutes mark, these numbers decrease to having differences of 14.16, 10.32, 5.23 and 8.64% meaning that the difference in between 30 and 60 minutes Eff.% difference in % decreased by 16.95, 37.00, 65.11 and 39.07% in comparison. Meaning that the slowing down

of Eff.% from 30 to 60 minutes is 16.95, 37.00, 65.11, and 39.07% respectively for Li, Mn, Co, and Ni.

Table 59. Difference between the reference values/data, and comparison with the values for the CL-T-2 and CL-T-3.

	Metals				
Parameter	**Li**	**Mn**	**Co**	**Ni**	**Unit**
Ref. (30) 2.5 M	100.00	82.00	78.00	88.00	Eff.%
CL-T-2 (30) 0.5 M	77.14	38.72	31.86	38.53	Eff.%
CL-T-3 (30) 2.5 M	92.99	46.30	37.47	44.89	Eff.%
Pre-treatment effect on BM	7.01	35.70	40.53	43.11	%
Difference in Eff.% T-2 vs T-3	17.05	16.38	14.99	14.18	%
Ref. (60) 2.5 M	99.00	95.00	90.00	98.00	Eff.%
CL-T-2 (60) 0.5 M	74.76	38.56	31.72	37.94	Eff.%
CL-T-3 (60) 2.5 M	87.10	42.99	33.48	41.53	Eff.%
Pre-treatment effect on BM	11.90	52.01	56.52	56.47	%
Difference in Eff.% T-2 vs T-3	14.16	10.32	5.23	8.64	%
Decrease between 30 & 60 of Eff.%	16.95	37.00	65.11	39.07	%

A decrease has also been noted in the (**Table 58**), but it is greater in (**Table 59**) when it comes to Mn, Co, and Ni, while Li is greater in (**Table 58**) by 6.93% units. For comparison of the leaching efficiencies for the CL-T-1/2/3 and those of the average and maximum Eff.% (**Table 60**), a clear difference is observed between the reference and tested samples, as only CL-T-3 came close to the reference values, peaking at 92.99 Eff.% at 30 minutes in a 2.5 M H_2SO_4 lixiviate. Overall, the CL-T-3 had the best Eff.% values out of all tested, which was expected, but at different times compared to others, which are visible, meaning that at different concentrations and temperatures, the different Eff.% values are possible.

Table 60. Values of the Eff.% in cases of different experimentations and their comparisons with one another. (*Note! Values with the * maximum values of the Eff.% for the metals and consist of the maximum value X Eff.% and time mark Y minutes data in → X/Y*).

Experiments	**Li**	**Mn**	**Co**	**Ni**	**Unit**
Ref. (0.5 M)	84.33	62.33	55.67	66	Average
Ref. (2.5 M)	96.33	78.67	73.67	83.33	Average
CL-T-1	33.87	22.26	13.47	20.98	Average
CL-T-2	32.56	16.91	13.72	16.95	Average
CL-T-3	81.18	42.63	32.77	41.66	Average
Ref. (0.5 M) *	90 / 30	73 / 60	67 / 60	76 / 60	Max/Time
Ref. (2.5 M) *	100 / 30	95 / 60	90 / 60	98 / 60	Max/Time
CL-T-1 *	59.99 / 165	37.19 / 180	26.20 / 180	36.47 / 180	Max/Time
CL-T-2 *	40.59 / 180	20.86 / 45	17.27 / 45	20.85 / 180	Max/Time
CL-T-3 *	93.60 / 90	50.45 / 120	39.03 / 90	49.28 / 90	Max/Time

6.2. Electrochemical Leaching Results

There were done two of different ECL tests were done with reactor prototype configurations, which have results as seen in (**Figure 40**). In (**Figure 40** (**a**)), the results of Li, Mn, Co, and Ni can be found with their respective average values over the course of the 180-minute testing run, for the Eff.% for the four metals discussed. In (**Figure 40** (**b**)), the result of the same metals but in a three-cell compartment configuration can be found with the same definitions as in (**Figure 40** (**a**)). Overall, all of the data from the (**Figure 40**) can be represented as a (**Table 61**), in which all of the Eff.% in correlation to times and metals from both of the tests can be seen as shown below.

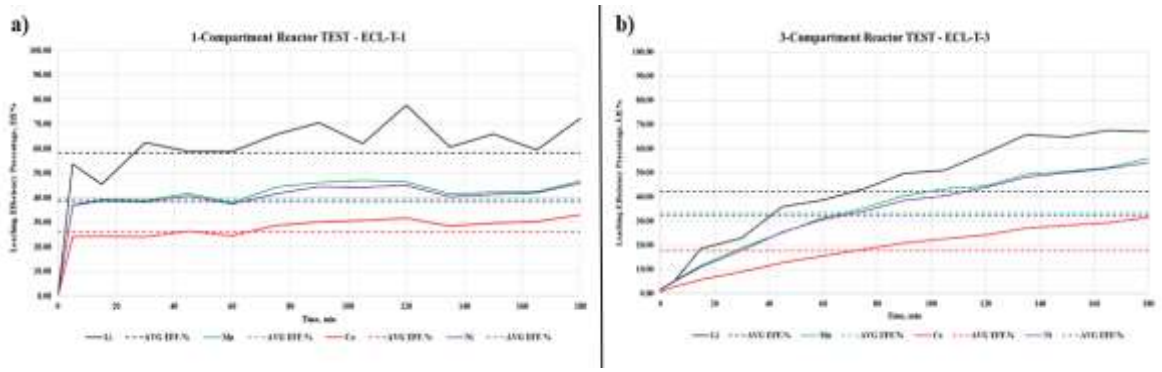

Figure 40. Result of the ECL-T-1 and ECL-T-3 for the Eff.% values of the Li, Mn, Co and Ni in straight graph line and their averages respectively in the same colour as dotted graph lines, in a time frame of 0 to 180 minutes. Test 1 or ECL-T-1 for the one-compartment cell type of reactor results on the left (a) and Test 3 or ECL-T-3 for the three-compartment cell type of reactor results on the right (a).

Table 61. Result for the ECL-T-1 and ECL-T-3 in comparison to one another's metals at their corresponding times, in addition to their average values, all of the results are in Eff.%.

Time, min	ECL-T-1 Li	ECL-T-3 Li	ECL-T-1 Mn	ECL-T-3 Mn	ECL-T-1 Co	ECL-T-3 Co	ECL-T-1 Ni	ECL-T-3 Ni	Unit.
0	0.00	1.52	0.00	1.65	0.00	0.00	0.00	1.28	Eff.%
5	53.80	4.98	37.05	5.26	24.17	36.74	36.74	4.89	Eff.%
15	45.57	18.55	39.35	11.67	24.31	38.84	38.84	11.08	Eff.%
30	62.39	22.98	38.81	18.87	24.07	38.31	38.31	17.86	Eff.%
45	58.81	35.91	41.74	25.21	26.45	40.75	40.75	25.43	Eff.%

(*Continued on next page*)

Table 61. (*Continued*)

Time, min	ECL-T-1 Li	ECL-T-3 Li	ECL-T-1 Mn	ECL-T-3 Mn	ECL-T-1 Co	ECL-T-3 Co	ECL-T-1 Ni	ECL-T-3 Ni	Unit.
60	58.76	38.70	37.97	31.20	24.62	37.48	37.48	30.61	Eff.%
75	65.61	43.39	44.23	35.31	28.75	41.59	41.59	34.03	Eff.%
90	70.61	49.68	46.13	40.42	30.04	44.58	44.58	38.56	Eff.%
105	62.03	50.99	47.05	43.36	30.72	44.33	44.33	40.49	Eff.%
120	77.77	58.22	46.43	44.51	31.67	45.08	45.08	43.86	Eff.%
135	60.72	65.69	41.65	49.29	28.46	40.39	40.39	48.14	Eff.%
150	66.01	64.81	42.28	50.55	29.58	41.29	41.29	50.02	Eff.%
165	59.58	67.47	42.54	52.11	30.27	42.09	42.09	51.82	Eff.%
180	72.31	67.09	46.79	55.80	32.97	45.99	45.99	54.09	Eff.%
AVG.	**58.14**	**42.14**	**39.43**	**33.23**	**26.15**	**17.74**	**38.39**	**32.30**	Eff.%

Analysing result of those in (**Figure 40** (**a**)), shows a clear difference of what metals leaching efficiency of higher than others, as it can be seen Li, has the hight through out the whole 180 minutes of testing, while Mn and Ni have similar and go in similar graph to one another, over the course of time. At the same time, the results of the Mn are slightly higher than those of the Ni throughout the 180 minutes. Similar graphs to those of Mn and Ni can also be seen in Co, but its values are the lowest of the four groups. All of the four metals Eff.% start similarly with a sharp climb at the start of those 5 minutes, which then over time stabilizes into a steady slow Eff.% increase from those of 5-minute values of 37.05, 24.17 and 36.74 Eff.% for the Mn, Co and Ni respectively and end at 180 minutes at levels of 46.79, 32.97 and 45.99 Eff.%, meaning of change in between 175 minutes of 9.74, 8.80, 9.25 Eff.% in the increase direction. What is also noted is the exact constant change occurring simultaneously in all three metals. These are clear changes of increases or when they start at 30/60/75/90/135/140/165-minute marks of tests, although it must be noted that already at 90 minutes, the value of Eff.% did decrease in the case of the Ni, in comparison to the two other metals. Decreases for the three metals, on the other hand, are or start at the 15/45/105/120 marks, which can all be seen from (**Figure 40** (**a**)) and (**Table 61**). On the other hand, when looking at the Li, the whole graph is full of ups and downs and does not have a correlation or pattern with those of the three other metals tested. What can be said of Li is that its Eff.% values react in a much sharper and more aggressive manner compared to the other three. Overall, the Eff.% of all Li, Mn, Co, and Ni metals increases over time. With an increase of yield or Eff.% increase in percentage-wise of those in the span of 5 to 180 minutes by 34.42,

26.30, 36.40, and 25.17% respectively, which results can also be found in (**Table 62**), where also for the ECL-T-3 later can be found. What strikes the most is that of ECL-T-1 result of the data set at the 120-minute mark, which of 77.77 Eff.%, which, when compared to other metals in the same tests, behave too much more differently in comparison, while other metals also do decrease quite sharply between 120 and 135 minutes, but the increase afterwards is then much higher in comparison to other metals afterward in between 135 and 150 minutes. Overall, the Li behaves in these time frames by decreasing by 17.05 Eff.% and then increasing rapidly by 5.29 Eff.% while other metals decrease by only 4.78, 3.21, and 4.69 Eff.% and increase afterwards by 0.64, 1.12, and 0.90 Eff.% in ECL-T-1 for the Mn, Co, and Ni, respectively.

Table 62. Difference of Eff.% between 5 and 180 minutes in a percentage-wise wise for the ECL-T-1 and ECL-T-3 results.

	ECL-T-1	**ECL-T-1**	**ECL-T-1**	**ECL-T-1**	**ECL-T-3**	**ECL-T-3**	**ECL-T-3**	**ECL-T-3**	
Time, min	**Li**	**Mn**	**Co**	**Ni**	**Li**	**Mn**	**Co**	**Ni**	**Unit.**
5	53.80	37.05	24.17	36.74	4.98	5.26	2.67	4.89	Eff.%
180	72.31	46.79	32.97	45.99	67.09	55.80	31.48	54.09	Eff.%
Difference	**+34.42**	**+26.30**	**+36.40**	**+25.17**	**+1,245.81**	**+960.47**	**+1,078.48**	**+1,007.27**	**%**

Results found in (**Figure 40** (**b**)) show a clear divide between the four metals into three groups. What can be seen is that Li has the highest Li Eff.% of all of the metals, which is followed by Mn and Ni Eff.% coming close to one another, latter having less than in comparison to first one by a bit, and lastly the Co, that has the lowest Eff.% out of all the four metals. All four of the metals have a relatively stable and constant increase in the Eff.% when compared to one another in the three-compartment reactor setting. Based on the (**Figure 40** (**b**)) and (**Table 61**), the Li Eff.% trend is that of increasing one, but at the end of the 150- and 180-minute marks, a decrease can be seen of 0.89 and 0.38 Eff.% or of 1.34 and 0.56% respectively. Decreases in Eff.% can also be seen in the Co case, where they occurred at 30/60/90/105/135-minute marks. What is also noticeable from these is that there was an initial increase, followed by a decrease at the subsequent sampling. The only difference occurs at the 90- and 105-minute marks, where a decrease occurred twice in a row. Compared to others, it increased only once after its initial increase. Results for those of Mn and Ni, on the other hand, show a decline in Eff.% at any given time frame, as the

increase was steady and stabilised in addition. Overall, the result of the show those of 67.09, 55.80, 31.48 and 54.09 Eff.% results for the Li, Mn, Co and Ni respectively, and if we look a the time frame of in between 5 minutes and 180 minutes Eff.% rates, they have increased in between time fame by 1,245.81, 960.47, 1,078.48 and 1,007.27% or simply put they are 10-times of greater at 180 minutes, than they were at 5 minutes as seen in (**Table 62**).

A comparison between the ECL-T-1 and ELC-T-2 highlights the apparent differences in how fast and what type of leaching procedure occurs in both methodologies utilising electrochemical-assisted leaching. ECL-T-1 achieves a high Eff.% from the start, or more precisely, at the 5-minute mark of testing, when BM has been in the reactor for 5 minutes. It has increased from 0 Eff.% to 53.80, 37.05, 24.17, and 36.74 Eff.% for the Li, Mn, Co, and Ni, respectively. Then it increases at a low pace, which can be seen from the (**Table 62**), as the increase for metals is that of 18.51, 9.74, 8.8, and 9.25 Eff.% or 34.42, 26.30, 36.40, and 25.17% for the Li, Mn, Co, and Ni, respectively. In contrast, the increase in metal Eff.% in the ECL-T-3 is that of a gradual and steady stabilized increase from 0 to 180 minutes. As we noted, there is a difference in results at the 5- and 180-minute marks, with a 1,245.81%, 960.47%, 1,078.48%, and 1,007.27% leaching increase. Result as such show that ELC-T-1 with one compartment leaches metals faster from the BM or more precisely in 5 minutes, and the rest 175 minutes is extra Eff.% of leaching metals from BM, while the ECL-T-3 does it gradually at a slower pace, but steadily, which also can be seen in it stability, based on (**Table 61**)'s ECL-T-1 result fluctuating across in between those 180 minutes more than in that of ECL-T-2. Average values of those metals in ECL-T-1 also show those of 16.00, 6.20, 8.41 and 6.09 Eff.% higher values, or to put in percentage of 27.52, 15.72, 32.16 and 15.86% higher Eff.% values in comparison to the more complicated three-compartment reactor result, for the Li, Mn, Co and Ni, respectively.

Based on the different methodologies and aspects that were tested and used in the different literature review studies and research, based on (**Tables 43 – 46**), three of the articles and their results were taken, based on how close and if their results could be compared to thesis, based on their chemicals, voltages, cell compartment numbers and BM consistency for instance. Based on these results the studies by (Lei et al. [7]), (Meng et al. [8]) and (Li et al. [12]) were chosen and based on those the (**Table 63**) was formatted, where the leaching efficiencies and their parameters how they were achieved can be found for the ECL-T-1 and ECL-T-2 comparison.

Table 63. Data for the leaching efficiencies Eff.% and other parameters used to achieve them based on the literature review studies by (Lei et al. [7]), (Meng et al. [8]) and (Li et al. [12]).

Parameter	Reference material/study			Unit.
	[7]	[8]	[12]	
Cell compartments	TWO	ONE	ONE	–
BM used	NCM 111	LCO	$LiCoO_2$	–
Acid used	H_2SO_4	$C_4H_6O_5$	$CuSO_4$	–
Concentration	1.5	1.25	0.15	M
Current density	–	–	500	A/m^2
Voltage	–	8	–	V
Electric current	0.8	–	–	A
Temperature	Room Temp.	70	60	°C
Time	150	180	60	min
Li	100	94.17	97	Eff.%
Mn	66.40	–	–	Eff.%
Co	90.53	90.45	92	Eff.%
Ni	90.59	–	–	Eff.%
	Avg. Li	97.06	Eff.%	
	Avg. Mn	66.40	Eff.%	
	Avg. Co	90.99	Eff.%	
	Avg. Ni	90.59	Eff.%	

The most notable differences between reference materials or studies are the very high leaching efficiencies for the four metals of Li, Mn, Co, and Ni throughout different time periods, ranging from 60 to 180 minutes, as used in ECL-T-1 and ECL-T-3. It is also notable that different leaching agents were used, as only (Lei et al. [7]) used the H_2SO_4, while others used different chemicals. Differences in times and concentrations are interesting and notable, as the (Li et al. [12]) used only $CuSO_4$ of 0.15 M for 97 and 92 Eff.% for the Li and Co, respectively. Based only on the average result of the metals' Eff.% of reference materials/studies in comparison to those of highest Eff/% values in the ECL-T-1 and ECL-T-3 have -24.74, -19.61, -58.02 and -44.60 Eff.% result and of -29.97, -10.60, -59.51 and -36.50 Eff.% respectively per test for the Li, Mn, Co and Ni respectively. Meaning that the Eff.% results in a percentage of 25.49, 29.53, 63.77, and 49.23% are worse/less in ECL-T-1 and ECL-T-3 of 30.88, 15.96, 65.40, and 40.29% are worse/less in comparison to those of the reference material/studies results as per (**Table 64**) underneath.

Table 64. Investigation of the reference materials from (**Table 63**) in comparison to ECL-T-1 and ECL-T-3, Eff.% and percentage differences of their values.

Parameter	Metal				Information	Unit.
	Li	Mn	Co	Ni		
Ref. material	97.06	66.40	90.99	90.59	Avg. [Ref]	Eff.%
ECL-T-1	72.31	46.79	32.97	45.99	High. Eff.%	Eff.%
ECL-T-3	67.09	55.80	31.48	54.09	High. Eff.%	Eff.%
ECL-T-1	-25.49	-29.53	-63.77	-49.23	Avg. [Ref] VS High. Eff.%	%
ECL-T-3	-30.88	-15.96	-65.40	-40.29	Avg. [Ref] VS High. Eff.%	%
ECL-T-1	42.14	33.23	17.74	32.30	Avg.T-1	Eff.%
ECL-T-3	58.14	39.43	26.15	38.39	Avg.T-3	Eff.%
ECL-T-1	-40.10	-40.62	-71.26	-57.62	Avg. [Ref] VS Avg.T-1	%
ECL-T-3	-56.58	-49.95	-80.50	-64.35	Avg. [Ref] VS Avg.T-3	%

Not to mention the differences of ECL-T-1 and ECL-T-3 average values of Eff.% for the Li, Mn, Co and Ni in comparison to those of reference materials/studies average results, which are 38.92, 26.97, 64.84, and 52.20 Eff.% higher and 54.92, 33.17, 73.25, and 58.29 Eff.% in comparison to those of ECL-T-1 and ECL-T-3 result of (Li, Mn, Co, and Ni) respectively. Which translates, as seen above, to those of 40.10, 40.62, 71.26, and 57.62% result in (**Table 63**) being better and in the case of ECL-T-3 by 56.58, 49.95, 80.50, and 64.34% higher.

6.3. Comparison of CL and ECL results

A small look into reference materials and their results in CL and ECL shows that the results based on (**Figure 37**) and those of (**Table 63**) look similar to one another in leaching efficiencies of Eff.%. Minor differences in their end values can be observed as in (**Table 65**), where the results of reference materials regarding the metals Li, Mn, Co, and Ni can be found. Looking at the result, it can be seen that ECL can achieve the same if not even better, result in Eff.% for the metals of particular interest, in the case of Co, for instance, having of 2.00 Eff.% better value than that of the CL method and in the Li case achieving that of 100 Eff.% as in CL alike parring on par. But nonetheless, results show CL's advantage in Mn of 28.6 Eff.% difference and in the case of Ni that of a 7.41 Eff.% difference compared to the ECL results of 95 and 98 Eff.% for metals, respectively.

Table 65. Comparison of the highest values based on the reference materials for the metals Li, Mn, Co, and Ni, in Eff.% value, with the addition of the average value (Avg.) for three ECL methodology references.

Method	Reference material	Metal				Unit.
		Li	Mn	Co	Ni	
CL	[5]	100	95	90	98	Eff.%
ECL	[7]	100	66.4	90.53	90.59	Eff.%
ECL	[8]	94.17	–	90.45	–	Eff.%
ECL	[12]	97	–	92	–	Eff.%
ECL	Avg. ([7], [8], [12])	97.06	66.4	90.99	90.59	Eff.%

Differences in CL and ECL result in thesis, via (**Figure 38**) and (**Figure 40**), showcase that the CL Eff.% is higher when comparing the results of metals, which can be found under (**Table 66**) for all of the CL-T-1/2/3 and ECL-T-1/3 for the 5/90/180 minutes periods. Out of all the conducted tests, CL-T-3 has the highest values for all the metals, at 77.48, 39.68, 33.20, and 39.08 Eff.% at the 5-minute mark. Eff.% per test went from the highest to smaller as follows: CL-T-3 → ECL-T-1 → CL-T-2 for all of the metals present. In the case of ECL-T-3 and CL-T-1, the results differed, as Li Eff.% was higher in CL-T-1 by 0.72 Eff.%, whereas the rest of the metals, Mn, Co, and Ni, were lower at values of 0.84, 0.94, and 1.09 Eff.%, respectively. At 90 minutes, CL-T-3 has the highest Eff.% for all of the metals, while other tests have mixed Eff.% for metals. Overall, CL-T-1 at this point has the lowest Eff.% of the four remaining tests. While CL-T-2 had the best result for the Li and Co out of the three remaining tests at 77.59 and 34.12 Eff.% respectively, its Mn and Ni were lacking compared to the results of ECL-T-1 at 46.13 and 44.58 Eff.% respectively, while the ECL-T-3 has second lowest result out of all five test for all of metals Eff.% tested. At the end of the tests, CL-T-1, on the other hand, had the highest Li and Co Eff.% at 89.32 and 37.25, while the ECL-T-3 had those of 55.80 and 54.09 Eff.% for the Mn and Ni. The overall best result and balanced Eff.% were achieved by the ECL-T-1 test, which had 72.31, 46.79, 32.97, and 45.99 Eff.% for Li, Mn, Co, and Ni, respectively, when compared to other tests. Differences between CL-T-2 and CL-T-3 were then minor in Mn and Co, as CL-T-3 had higher Mn by 0.06 Eff.% when CL-T-2 had higher Co by 1.64 Eff.%. While the differences in Li and Ni were of 9.22 and 10.27 Eff.%, similar to those in Mn and Co.

Table 66. Comparison between CL and ECL tests at times of 5/90/180 minutes to one another in Eff.% and in average (Avg.) Eff.%.

		Test					
Time	**Metal**	**CL-T-1**	**CL-T-2**	**CL-T-3**	**ECL-T-1**	**ECL-T-3**	**Unit.**
5 min	Li	5.70	38.72	77.48	53.80	4.98	Eff.%
	Mn	4.43	24.00	39.68	37.05	5.26	Eff.%
	Co	1.73	15.48	33.20	24.17	2.67	Eff.%
	Ni	3.80	23.01	39.08	36.74	4.89	Eff.%
90 min	Li	38.79	77.59	93.60	70.61	49.68	Eff.%
	Mn	26.47	40.59	50.39	46.13	40.42	Eff.%
	Co	15.43	34.12	39.03	30.04	20.92	Eff.%
	Ni	24.81	40.30	49.28	44.58	38.56	Eff.%
180 min	Li	89.32	68.99	59.77	72.31	67.09	Eff.%
	Mn	45.72	37.13	37.19	46.79	55.80	Eff.%
	Co	37.25	27.84	26.20	32.97	31.48	Eff.%
	Ni	45.37	26.20	36.47	45.99	54.09	Eff.%
Avg.	Li	33.57	71.00	79.72	58.14	42.14	Eff.%
	Mn	22.14	36.81	41.35	39.43	33.23	Eff.%
	Co	13.45	30.03	32.05	26.15	17.74	Eff.%
	Ni	20.89	36.55	40.48	38.39	32.30	Eff.%

Overall, the Eff.% of tests performed in the thesis went from the highest to the lowest as follows: CL-T-3 → CL-T-2 → ECL-T-1 → ECL-T-3 → CL-T-1, starting at 79.72, 41.35, 32.05, and 40.48 Eff.% and ending to that of 33.57, 22.14, 13.45, and 20.89 Eff.% for the Li, Mn, Co, and Ni respectively.

If we look at the highest and lowest Eff.% results from (**Figure 38**) and (**Figure 40**), they would be for (Li / 120 min / 94.49 Eff.% / CL-T-3), (Mn / 180 min / 55.80 Eff.% / ECL-T-3), (Co / 90 min / 39.03 Eff.% / CL-T-3), and (Ni / 180 min / 54.09 Eff.% / ECL-T-3). Meaning that for the Mn and Ni, better results were achieved via ECL methods or ECL-T-3 setup, while for the Li and Co, better results were achieved by CL methods, with CL-T-3 parameters for the leaching. As such, when doing a comparison to those of the highest result of CL and ECL alike, in percentage terms, CL-T-3 yields Li and Co, 94.49 and 39.03 Eff.% respectively, to those of ECL-T-1 highest values of 77.77 and 32.97 Eff.% for Li and Mn, meaning that CL yields for Li and Co 17.70 and 34.65% higher than ECL-T-1 or ECL tests/methods overall. On the other hand, ECLs or ECL-T-3 have the highest Eff.% for the Mn and Ni, as 55.80 and 54.09 Eff.%, while the similar criteria can only be met by the CL-T-3's Mn and Ni at 50.45 and 49.28 Eff.%, meaning that the ECLs have a higher yield in percentage to those of CLs methods by 9.59 and 8.89%.

As such, from the results of CLs and ECLs, a clear difference in the yield of Li and Co can be observed, with the CLs yielding, percentagewise, much higher Eff.% rates, by 17.70 and 34.65% higher, while the ECLs yield for Mn and Ni by only 9.59 and 8.89% higher, respectively. The result markup between Li and Co, compared to those of Mn and Ni, is twice as high in percentage. However, a clear distribution and dispersion in the percentages of Li and Co can be observed, as the former is approximately twice as large as the latter, while Mn and Ni are relatively close to one another. Meaning that the CL and ECL methods have similar kinetics and aspects when it comes to recovering Mn and Ni from the BM using different methodologies, but a clear difference in mechanisms when it comes to Li and Co, as the differences are greater, as seen by the results and comparison.

7. Discussion

The CL experiments demonstrated that higher acid concentrations (2.5 M H_2SO_4) and elevated temperature 50°C significantly improved the leaching efficiency Eff.% for the Li, Mn, Co, and Ni CRM results. Li, for instance, yields 93.60% efficiency in CL-T-3 at 90 minutes, and that of 77.48 Eff.% at 5 minutes, or that of Mn 50.45 Eff.% at 120 minutes. These result, based on a study by (Vieceli et al. [5]), aligns with the theory and kinetics of Li, as acid concentration and temperature allow for much greater and enhanced dissolution as proton diffusion ramps up. The kinetics and thermodynamics as studied in (Meng et al. [8]) of the chemical-reaction model (Eq. (**14**)) and the diffusion control model (Eq. (**15**)), could be used for the explanation/study of the reaction and mechanisms for leaching. Hence, aligning with the Arrhenius principle, where temperature has a straight factor correlation to that of reaction kinetics via temperature, as the proton diffusion and ion in the medium increase in speed, leading to more frequent bombardment of each other. Based on the Li result at 120 minutes in CL-T-3 of 94.49 Eff.%, it strongly suggests that H_2SO_4, by (Eqs. (**33.1**) and (**33.2**)), breaks down Li forms in BM, such as Li_2O and LiF, to form salt Li_2SO_4.

However, on the other hand, concentration, in fluctuations of Eff.% over time in CL-T-2 and CL-T-3 may also suggest a vice versa reaction/kinetics, which is seen in a sharp decline of Eff.% at 165 minutes as the leaching equilibrium has been achieved close to those of 45 and 30 minutes respectively, as the competing reactions or passivation effects may have occurred. Such as layer formation on particle surfaces, leading to the formation of Li_2O and LiF, hence lower recovery rates (**Figure 38** (**a**)). A presence of other residual metals and elements, such as Al and F from the (e.g., PVDF/PTFE binders) could also hinder leaching by forming stable compounds like LiF discussed, but also those of $Al_2(SO_4)_3$, meaning a re-adsorption of the metals in BM. Because these sub-species (e.g., O_x and/or SO_4^{2-}). For this reason, a typical reducing agent such as H_2O_2 is commonly used industrially for improved recovery rates and problem resolution. Another reason could also be related to sampling, as 3.5 mL was taken on average every 15 minutes from the volume of the beaker, thereby reducing the availability of acid for sustained kinetic/reaction. Hence, concentration increase led to initially rapid dissolution, but afterwards to the aforementioned mechanisms. Because

of these, there should/be and exist optimal leaching/retention times outside of the parameters shown.

The importance of pre-treatment in CL, like that of pyrolysis in literature (Vieceli et al. [5]), enhances the result of recovery values for Mn, Co and Ni by up to 40 Eff.%, as the (PVDF/PTFE)'s are decomposed, and allowing for the metal phases oxidation, hence leading to H_2SO_4 or any acids penetration into metal bondages in-between structures liberating metals from complex matrices. CL-T-1 and CL-T-2 both highlight this as their temperatures differ while concentrations are the same, to of the results by (Vieceli et al. [5]), of the critical role of both pre-treatment and higher temperatures in accelerating reaction kinetics. Pre-treatments are important not only for treating binders, but also because Gr and C lead to better results, as discussed in the pyro- and hydrometallurgy sections.

The one-compartment reactor ECL-T-1 achieved a rapid initial Li leaching of 53.80 Eff.% in 5 minutes but stabilized over time at only 72.31 Eff.% after 180 minutes, meaning that in 5 minutes it had reached its leaching equilibrium, which is likely due to electrode passivation, electrode saturation, or mass transfer limitations inside the system. This could also be due to uncontrolled side reactions, such as hydrogen evolution in the cathode compartment, which competes with the metal reduction kinetics.

In contrast, the result of the three-compartment reactor ECL-T-3 exhibited slower but more stable leaching as per (**Figure 40**), reaching in the end of 67.09 Eff.% for the Li. This can be attributed to the improved ion selectivity and separation achieved by using AEM and CEM membranes, which reduce side reactions within the ECL system. But as leaching efficiencies were slower, this can be explained by the membrane resistance in leaching kinetics. NaCl could also be a culprit in membrane permeability, but at the same time, it could, from a theoretical standpoint, enhance ion migration between compartments and electrolytes. ECL-T-3 results in those of ECL-T-1 lagging initially, may also be due to the concentration difference (lower), but as it has been shown by (**Figure 33**) and (Diaz et al. [6]) literature, it should not have such a significant effect. The use of membranes in separating anolytes and catholytes also leads to minimized hydrogen evolution, resulting in a more stable ECL overall.

Clear outperformance of ECL-T-3 in comparison to those of CL-T-1/2/3 leaching result for the Mn 55.80 Eff.% and Ni 54.09 Eff.% are most highly and likely due to those of

electrochemical reduction at the cathode as per (Eqs. (**34**) and (**36.1**)), as Ni^{3+} is being reduced to Ni^{2+}. Nonetheless, results in relation to those of (Lei et al. [7]), the literature results were 40.10, 40.62, 71.26, and 57.62% worse and 56.58, 49.95, 80.50, and 64.35 percentagewise in ECL-T-1 and ECL-T-3 for the Li, Mn, Co, and Ni, respectively. These are either due to the BM composition differences or to the three-compartment reactor settings (e.g., current density), of which solution/electrolyte goes and where the BM goes, into which compartment or due to Ti and Pt anode differences, with relation to reducing agents (e.g., Fe^{2+}) and pre-treated BM. Apparent differences in graphs of ECL can be observed, leading to the belief of highlighting the trade-off between leaching speed and efficiency in reactor design and overall parameters in both of them and the reference material.

While CL achieves high results peaking at 94.49 and 39.03 Eff.% in Li and Co, respectively, due to aggressive acid conditions, such as H_2SO_4, making it simpler and more scalable for industrial use. This is because it is widely used in hydrometallurgy to recover CRMs and other metals. On the other hand, this is accompanied by declining efficiency over time, likely due to acid depletion or saturation, as previously disclosed. In contrast to this, ECL results in comparison to those of CL, for Mn and Ni of 55.80 and 54.09 Eff.% respectively, highlight the difference and metal recovery per methodology, reaction mechanisms, kinetics, and thermodynamics. Highlighting the ECLs benefitting from redox-assisted dissolution at the electrodes, leading to those of lower acid consumption and reduced waste generation [7], [12]. While ECL offers better control and selectivity, its complex setup (membranes and compartmentalisation), as tested in thesis, with the slower kinetics, resulted in lower overall efficiency compared to those in CL Eff.% values for Li and Co, especially. Overall, both methods, when tested with untreated BM, showed worse results than those reported in the literature, as residual binders and graphite hinder leaching. Although pre-treatment could enhance the recovery rates of metals in both methodologies, it is up to what metals are wanted to be recovered, which leads to which method should be implemented and how exactly.

Results by CL-T-3 at 50°C proved most effective for Li recovery, up to 94.49 Eff.%, while the ECL-T-3 showed superior selectivity for Mn 55.80 Eff.% and Ni 54.09 Eff.% by utilizing a membrane and three-compartment cells for leaching. Results from all the tests conducted in this thesis are lower when compared to those in the literature. Both in the thesis and literature, the ECL has proven to be relatively selective and has shown good results in

Mn recovery, highlighting the selective reduction of Mn^{3+} into Mn^{2+}. Different ECL methods, as presented in (**Tables 43 – 46**), show the use of different acids and also those of electrolytes, hence, with different electrode materials and differences in the used BM morphologies. Overall, the results of the tests are similar in ECL, as the Eff.% in both tests increases; however, it is much lower than the literature values for all four metals investigated. The efficiency gaps versus literature values (Vieceli et al. [5]) primarily stem from:

- The absence of pre-treatment to remove organic binders and convert metal phases.
- Suboptimal reactor configurations, like those of membrane resistance.
- BM heterogeneity of LCO, as the aspects of NCM were found by SEM-EDS.

Industrially CL currently has a leading and dominant position in LIBs recovery/recycling, in hydrometallurgy, which is highlighted by many studies alike, due to simplicity and throughput, despite generating acidic waste, which current ECL studies are trying to mitigate by improving result of other more friendly organic acids, with combining them with ECL and lower concentrations, by different use reducing agents if used. As such, ECL offers greener potential through reduced acid consumption, but requires optimization of current density, as suggested by 500 A/m^2, as well as electrode materials and membrane selection to address energy costs. All these aspects and parts of the ECL lead to impediments in scalability, at current levels, as research and literature experiments have been conducted in experimental reactors. Critical environmental concerns include F and P have also been an aspect of leaching from PVDF, as the risk of HF and $LiPF_6$, and even electrode corrosion due to F presence in BM, if not pre-treated, and transition metal re-precipitation, necessitating secondary treatments are necessity in all of the ECL reviews, as the recovery of metals by assisted or deposition to electrodes, must be carried by others methods, which would also be true in thesis reactors case, for metal recovery from medias.

The absence of kinetic and thermodynamic models in the thesis plays a significant role, as they enable a more in-depth understanding of energies and the direction of reactions, whether they are spontaneous or not. These would allow for more in-depth simulation and understanding of what happens at what given time in a cell, especially. Certain reactions are not even possible at certain stages of leaching due to kinetic limitations and what occurs in reactions themselves. Using these, optimization and further research could be possible with

a more accurate and in-depth understanding. The simulation and prediction of the BM used could also be done with higher/more certain insight and what is/should be expected of it. Although there were lots of parameters that could have been studied, only a small part of them, if at all, were taken into consideration. Hence, the result does not reveal much about what happens and why, to be precise, or why/how/what effect is more pronounced in the reactor in particular. In CL, the use of literature reviews was sufficient to some extent, but in ECL, the need for many more tests and different parameter comparisons should have been conducted, with certain parameters left unchanged. For instance, increasing the S/L ratio and keeping other parameters constant, or changing the current density or flow rate of the electrolytes, would have provided a comparison between different aspects/parameters in the cell. Using these, a different array of electrolytes/chemicals/acids could have been tested to see optimizations or how they compared to others. The use of a different array of analytic methods in the study of BM and solvent residues could have also increased the data/results in the thesis, and helped to show the reader and experiment maker, how and what actually happened and why, if so.

Research on the current cell and BM tested should be divided into two separate topics, but with more in-depth and detailed analysis. The understanding of BM morphology, what affects it, and whether our methods of making it had an impact, is limited. This is because the consequences of this could not be observed due to the lack of an analysis before and after its creation. A clear study into kinetics and thermodynamics is needed for the current reactor, and it should be done in three different segments:

- Test either one or two, or three-compartment cells, but not all at the same time.
- Compare BM morphology before and after the cell use, by ICP-MS/SEM-EDS/XRD.
- Test the left residue and see what it has.
- With multiple compartments, research and analyse all of the residues and take samples from all of the compartments.
- Increase the volume of the solutions used, so that solution defects in tests would be minimised.
- Compartment configuration studies and all of the under it should be done as three different topics and not in one research or study, as there would be

too much data to analyse, hence, a more comprehensive kinetics and thermodynamics could be achieved.

- After all of these three have been done separately, a more comprehensive study as a fourth could be done in comparing each of the ECLs to one another could be achieved.

These results and findings could then lead to the optimization of even some type of hybrid development between CL and ECL, in addition to that of pre-treatment integration to balance the efficiency yield of LIBs recycling and the recovery of CRMs and other elements. Developing a more sustainable and economical commercial method for ECL, which is currently limited to small-scale reactors/cells, is far from achieving a scalable commercial/industrial methodology. One of the key changes in the current reactor that was tested would be the use of a different polymer that is 3D printed, as well as the addition of a larger space for electrode and wire connections. Additionally, the electrodes, instead of mesh, should be of some other geometry for easier cleaning and maintenance overall.

8. Conclusion

What this research has successfully been able to demonstrate is the recovery of CRM's metals from the EoL LIB of those laptops, with the primary study focusing on the EOL and validation of BM via CL. The characterisation of BM derived from spent LIBs involves comparing the performance of CL and ECL under laboratory conditions, and assessing the feasibility of electrochemical recovery in a prototype flow reactor system, which are part of the thesis's objectives.

Under the optimised condition of utilising the lixiviant of the H_2SO_4 as a leaching chemical to leach Li and Co at 89.32% and 37.25% at leaching efficiency respectively, (with analogous high recovery of manganese and relatively low nickel dissolution), when it came to CL. The achieved results for the ECL tests were about leaching Li and Co at 72.31% and 32.97% at leaching efficiency, respectively, (with correspondingly high Mn recovery and moderate Ni), hence showing the particular effectiveness in enhancing the selective recovery of theirs. This selectivity highlights ECL's potential for process tailoring and metal-specific recovery in future recycling flows. The highest Co content of 38.92 wt.% and significant Li presence of 5.77 wt.% in the <75 μm BM fraction emphasise the importance of fine particle size separation in optimising CRM recovery. As such, the results indicate that the thesis's objectives of recovering CRM, primarily those of Li, Co, Ni, and Mn, were largely met, as substantial fractions of each metal were dissolved into solution by both methods, with ECL showing promising results. The results of both CL and ECL concepts of BM leaching also showed a clear trend in metal recoverability, with Mn and Li leaching most readily, followed by moderate leaching of Co, and the least leaching of Ni. These are attributed to the varied chemistry and physical form of the source material of BM and the metals, their leachability with H_2SO_4 as lixiviant, and other factors. Overall, based on the results and outcomes, one can derive from these that the primary goals were achieved in a proof-of-concept sense. While at the same time highlighting that further optimization is much needed to approach complete extraction of all target elements at a sustainable and efficient rate.

The leaching efficiencies observed in the thesis were broadly consistent with known trends and research studies in the literature, but somewhat lower than those obtained under

idealised laboratory conditions. For instance, studies using concentrated acids industrially or those of the inorganic acids (e.g., H_2SO_4) with the assistance of the most commonly used reducing agent (e.g., H_2O_2), have achieved those of ≥98–100% extraction of Li, Co, Ni and Mn in CL and hydrometallurgical recycling processes from the E-waste and with the more laboratory scale and more immature ECL of ≥66.40–100% extraction of Li, Co, Ni and Mn as per (**Table 63**) [284]. In contrast, this thesis with both CL and ECL yielded (89% Li, ~33–37% Co), reflecting the non-utilization of the pre-treatment and that of any reducing agent. Leading to the limited dissolution of higher-valent transition metals, and metals subsequently leaching partially as of Co and Ni alike, while that of Mn mostly [284]. On the other hand, the results of the thesis confirm and align with those of the literature on the dependency of leaching efficiency on temperature, acid concentration, and S/L ratios. In summary, the findings of the thesis confirm general patterns of/from the literature (Li > Mn > Co > Ni leachability) and underscore how the leached mass composition and reagent chemistry drive the absolute recoveries of the elements, such as CRMs and metals alike [5], [5], [8], [12], [284]. However, this thesis expands the understanding of EAL by introducing and incorporating a novel, small-scale flow-reactor setup. While there are studies on ECL, they are primarily focused on batch-type setups. The flow reactor approach, for these reasons, allows for continuous processing and potential modular scalability, with the features not often addressed in batch-based ECL studies. Hence, the thesis provides both practical insights and technical validation to the emerging body of knowledge on flow-assisted electrochemical recovery systems in hydrometallurgy and their batch-dominant recycling processes.

On a theoretical basis, the following thesis contributes to the growing interdisciplinary discourse on combining electrochemical engineering with hydrometallurgy for sustainable material recovery, with sustainability as a secondary goal. Tested reactors' advantages on a laboratory scale, in the direction of those of industrial applicability, have demonstrated that ECL can serve as a complementary or alternative method to conventional CL or be implemented as a hybrid system between conventional hydrometallurgy CL and its relatively new, emerging ECL recycling processes. In complementing, driving, and, importantly, enhancing the more selective recovery or greener processing routes for future generations of hydrometallurgy engineering processes.

From a broader societal perspective, the research in this thesis aligns with the EU's CE and its critical material supply chains, as well as the relevant initiatives. In addition to its imposed and revised CRM Act of 2024 strategy goals. By these measures, the EU is reinforcing the importance of secondary raw material sources for ensuring supply security, mitigating environmental degradation, and reducing reliance on geopolitically sensitive mining regions, such as the DRC, as well as the reliance on the supply/demand of LIB components dominantly (e.g., cathodes and anodes) by China. The EU's Batteries Regulation is one of the many steps that envision to minimise the risk associated with the critical-material supply chains, as by classifying batteries BM as a recoverable material or raw material, rather than an exportable waste, hence boosting battery recycling and CE, with its value chains, while providing that of security supply for raw materials and enhancing strategic autonomy of EU a whole. As such, these subsequently enhance the recyclability of LIBs through efficient material recovery methods, supporting both energy transition and digitalization initiatives, which are important for the current and future development of the battery industry. This thesis contributes to a vision that helps establish a more localized recycling infrastructure, reducing risks that are emerging in association with CRMs and current battery recycling capacities globally, including their distribution. This could undoubtedly impact future battery development while enabling and fostering sustainable battery manufacturing in a circular manner. Recycling, as a whole, "*is not just about waste — it is about access and accessibility*" to those critical materials needed for domestic energy industries, by ensuring supply chains can withstand geopolitical shocks, which is achieved through recycling.

Nonetheless, the following thesis and its study have several limitations. As the laboratory tests were conducted under controlled, small/bench-scale conditions (e.g., limited feedstock volumes and without complexities of industrial processing), this may not directly translate to industrial scalability. With the relatively narrow range of parameters (e.g., acid concentration, temperature, current density, and S/L ratio) explored, it is possible that the optimal conditions may lie outside the tested space. The variability in BM composition, as it was primarily sourced from the EoL spent LIBs of laptops, as such, utilising the one feedstock (e.g., LCO battery material), does not accurately represent the diversity of LIB chemistries and different cathode/anode blends industrially. The lack of comprehensive life cycle analysis and techno-economic analysis, combined with the absence of downstream

purification and its metal refining stages, constrains a complete assessment of process sustainability and economic viability. Hence, the environmental impacts, energy use, and economic viability of the processes remain to be assessed. Furthermore, the prototype reactor design requires further optimization (e.g., electrode geometry/membrane integration), flow distribution, membrane integrity, and long-term operational stability.

Future research as a whole should focus primarily on the four cornerstones, based on the thesis and its findings and limitations, in that direction of those:

- Scale-up and pilot testing → ECL process using modular reactor designs.
- Reactor and process optimization → Refinements to the ECL reactor (e.g., configuration and flow patterns).
- Exploration of eco-friendly, greener and biodegradable leaching agents and electrolyte systems.
- Comprehensive sustainability assessment → Life-cycle, techno-economic and environmental impact assessments of the proposed recovery routes, with comparison of CL vs. ECL routes, enabling the evaluation of the real-world feasibility and environmental benefits of the proposed methods.

By addressing these future tasks could help with the translation of the present findings into robust, large-scale recycling technologies.

In conclusion, the current thesis demonstrates the technical viability and strategic relevance of CE-based-aligned leaching of CRM battery metals and their subsequent recovery/reclamation from EoL LIBs using both CL and ECL methods. At the same time, providing and identifying clear paths for a foundation of future research into more sustainable and selective battery recycling technologies, while offering valuable insights for the development of next-generation circular material systems, which consist of even more effective and sustainable technologies, if the current 5% of the LIBs recycling degree dilemma should and/or shall be broken.

References

[1] M. Petranikova, Pol Llorach Naharro, N. Vieceli, G. Lombardo, and Burçak Ebin, "Recovery of critical metals from EV batteries via thermal treatment and leaching with sulphuric acid at ambient temperature," *Waste management*, vol. 140, pp. 164–172, Mar. 01, 2022, doi: https://doi.org/10.1016/j.wasman.2021.11.030.

[2] S. Pavón, D. Kaiser, R. Mende, and M. Bertau, "The COOL-Process—A Selective Approach for Recycling Lithium Batteries," *Metals*, vol. 11, no. 2, p. 259, Feb. 03, 2021, doi: https://doi.org/10.3390/met11020259.

[3] W. Urbańska, "Recovery of Co, Li, and Ni from Spent Li-Ion Batteries by the Inorganic and/or Organic Reducer Assisted Leaching Method," *Minerals*, vol. 10, no. 6, p. 555, Jun. 20, 2020, doi: https://doi.org/10.3390/min10060555.

[4] Z. Takacova, T. Havlik, F. Kukurugya, and D. Orac, "Cobalt and lithium recovery from active mass of spent Li-ion batteries: Theoretical and experimental approach," *Hydrometallurgy*, vol. 163, pp. 9–17, Aug. 2016, doi: https://doi.org/10.1016/j.hydromet.2016.03.007.

[5] N. Vieceli, R. Casasola, G. Lombardo, B. Ebin, and M. Petranikova, "Hydrometallurgical recycling of EV lithium-ion batteries: Effects of incineration on the leaching efficiency of metals using sulfuric acid," *Waste Management*, vol. 125, pp. 192–203, Apr. 15, 2021, doi: https://doi.org/10.1016/j.wasman.2021.02.039.

[6] L. A. Diaz, M. L. Strauss, B. Adhikari, J. R. Klaehn, J. S. McNally, and T. E. Lister, "Electrochemical-assisted leaching of active materials from lithium ion batteries," *Resources, Conservation and Recycling*, vol. 161, p. 104900, Oct. 2020, doi: https://doi.org/10.1016/j.resconrec.2020.104900.

[7] S. Lei *et al.*, "Strengthening Valuable Metal Recovery from Spent Lithium-Ion Batteries by Environmentally Friendly Reductive Thermal Treatment and Electrochemical Leaching," *ACS Sustainable Chemistry & Engineering*, vol. 9, no. 20, pp. 7053–7062, Apr. 21, 2021, doi: https://doi.org/10.1021/acssuschemeng.1c00937.

[8] Q. Meng, Y. Zhang, and P. Dong, "Use of electrochemical cathode-reduction method for leaching of cobalt from spent lithium-ion batteries," *Journal of Cleaner Production*, vol. 180, pp. 64–70, Apr. 10, 2018, doi: https://doi.org/10.1016/j.jclepro.2018.01.101.

[9] Q. Meng, Y. Zhang, P. Dong, and F. Liang, "A novel process for leaching of metals from $LiNi_{1/3}Co_{1/3}Mn_{1/3}O_2$ material of spent lithium ion batteries: Process optimization and kinetics aspects," *Journal of Industrial and Engineering Chemistry*, vol. 61, pp. 133–141, May. 25, 2018, doi: https://doi.org/10.1016/j.jiec.2017.12.010.

[10] N. Leclerc *et al.*, "Recovery of Metals from Secondary Raw Materials by Coupled Electroleaching and Electrodeposition in Aqueous or Ionic Liquid Media," *Metals*, vol. 8, no. 7, p. 556, Jul. 2018, doi: https://doi.org/10.3390/met8070556.

[11] M. B. J. G. Freitas and E. M. Garcia, "Electrochemical recycling of cobalt from cathodes of spent lithium-ion batteries," *Journal of Power Sources*, vol. 171, no. 2, pp. 953–959, Sep. 2007, doi: https://doi.org/10.1016/j.jpowsour.2007.07.002.

[12] S. Li, X. Wu, Y. Jiang, T. Zhou, Y. Zhao, and X. Chen, "Novel electrochemically driven and internal circulation process for valuable metals recycling from spent lithium-ion batteries," *Waste Management*, vol. 136, pp. 18–27, Dec. 2021, doi: https://doi.org/10.1016/j.wasman.2021.09.023.

[13] S. Leuthner, "Lithium-ion battery overview," *Lithium-Ion Batteries: Basics and Applications*, pp. 13–19, May. 03, 2018, doi: https://doi.org/10.1007/978-3-662-53071-9_2.

[14] Y. Nishi, "The development of lithium ion secondary batteries," *The Chemical Record*, vol. 1, no. 5, pp. 406–413, Sep. 13, 2001, doi: https://doi.org/10.1002/tcr.1024.

[15] M. V. Reddy, A. Mauger, C. M. Julien, A. Paolella, and K. Zaghib, "Brief History of Early Lithium-Battery Development," *Materials*, vol. 13, no. 8, p. 1884, Apr. 17, 2020, doi: https://doi.org/10.3390/ma13081884.

[16] N. T. M. Balakrishnan *et al.*, "The Great History of Lithium-Ion Batteries and an Overview on Energy Storage Devices," *Electrospinning for Advanced Energy Storage Applications*, pp. 1–21, Feb. 16, 2021, doi: https://doi.org/10.1007/978-981-15-8844-0_1.

[17] M. Wang *et al.*, "Challenges in Recycling Spent Lithium-Ion Batteries: Spotlight on Polyvinylidene Fluoride Removal," *Global Challenges*, vol. 7, no. 3, p. 2200237, Feb. 05, 2023, doi: https://doi.org/10.1002/gch2.202200237.

[18] R. Schröder, M. Aydemir, and G. Seliger, "Comparatively Assessing different Shapes of Lithium-ion Battery Cells," *Procedia Manufacturing*, vol. 8, pp. 104–111, 2017, doi: https://doi.org/10.1016/j.promfg.2017.02.013.

[19] A. Dixit, "Cathode Materials for Lithium Ion Batteries (LIBs): A Review on Materials related aspects towards High Energy Density LIBs," *Academia.edu*, vol. 10, no. 3, Dec. 2019. https://www.academia.edu/71289393/Cathode_Materials_for_Lithium_Ion_Batteries_LIBs_A_Review_on_Materials_related_aspects_towards_High_Energy_Density_LIBs?auto=download. [Accessed: Oct. 12, 2024].

[20] D. Kushnir, "Lithium Ion Battery Recycling Technology 2015 Current State and Future Prospects," *Environmental Systems Analysis. Chalmers University,* Göteborg, Sweden. ESA, REPORT, Dec. 2015. [Online]. Available: https://pdfs.semanticscholar.org/71a7/07e359d962a9ea49d57312924cd52b34750c.pdf. [Accessed: Oct. 07, 2024].

[21] I. Nagai, Y. Shimaura, T. Shibata, and Y. Moritomo, "Performance of tertiary battery made of Prussian blue analogues," *Applied Physics Express*, vol. 14, no. 9, p. 094004, Aug. 19, 2021, doi: https://doi.org/10.35848/1882-0786/ac1b0f.

[22] B. E. Murdock, K. E. Toghill, and N. Tapia-Ruiz, "A Perspective on the Sustainability of Cathode Materials used in Lithium-Ion Batteries," *Advanced Energy Materials*, vol. 11, no. 39, p. 2102028, Sep. 19, 2021, doi: https://doi.org/10.1002/aenm.202102028.

[23] L. Yun *et al.*, "Metallurgical and mechanical methods for recycling of lithium-ion battery pack for electric vehicles," *Resources, Conservation and Recycling*, vol. 136, pp. 198–208, Sep. 2018, doi: https://doi.org/10.1016/j.resconrec.2018.04.025.

[24] K. M. Winslow, S. J. Laux, and T. G. Townsend, "A review on the growing concern and potential management strategies of waste lithium-ion batteries," *Resources, Conservation and Recycling*, vol. 129, no. 0921-3449, pp. 263–277, Feb. 2018, doi: https://doi.org/10.1016/j.resconrec.2017.11.001.

[25] T. P. M, C. Dyer, and V. Subramanian, "Lithium-ion battery recycling—a review of the material supply and policy infrastructure," *NPG Asia Materials*, vol. 16, no. 1, pp. 1–20, Aug. 30, 2024, doi: https://doi.org/10.1038/s41427-024-00562-8.

[26] R. Sommerville, P. Zhu, M. A. Rajaeifar, O. Heidrich, V. Goodship, and E. Kendrick, "A qualitative assessment of lithium ion battery recycling processes," *Resources, Conservation and Recycling*, vol. 165, p. 105219, Feb. 2021, doi: https://doi.org/10.1016/j.resconrec.2020.105219.

[27] K. Du, E. H. Ang, X. Wu, and Y. Liu, "Progresses in Sustainable Recycling Technology of Spent Lithium-Ion Batteries," *ENERGY & ENVIRONMENTAL MATERIALS*, vol. 5, no. 4, Sep. 12, 2021, doi: https://doi.org/10.1002/eem2.12271.

[28] L. Zhou *et al.*, "Recent Developments on and Prospects for Electrode Materials with Hierarchical Structures for Lithium-Ion Batteries," *Advanced Energy Materials*, vol. 8, no. 6, p. 1701415, Nov. 16, 2017, doi: https://doi.org/10.1002/aenm.201701415.

[29] E. S. Pampal, E. Stojanovska, B. Simon, and A. Kilic, "A review of nanofibrous structures in lithium ion batteries," *Journal of Power Sources*, vol. 300, pp. 199–215, Dec. 30, 2015, doi: https://doi.org/10.1016/j.jpowsour.2015.09.059.

[30] J. B. Goodenough, "Battery Components, Active Materials for," *Springer eBooks*, pp. 51–92, Nov. 28, 2012, doi: https://doi.org/10.1007/978-1-4614-5791-6_3.

[31] Tuyet Nhung Pham *et al.*, "Combination-based nanomaterial designs in single and double dimensions for improved electrodes in lithium ion-batteries and faradaic supercapacitors," *Journal of Energy Chemistry*, vol. 38, pp. 119–146, Nov. 2019, doi: https://doi.org/10.1016/j.jechem.2018.12.014.

[32] W. Qi, J. G. Shapter, Q. Wu, T. Yin, G. Gao, and D. Cui, "Nanostructured anode materials for lithium-ion batteries: principle, recent progress and future perspectives," *Journal of Materials Chemistry A*, vol. 5, no. 37, pp. 19521–19540, 2017, doi: https://doi.org/10.1039/c7ta05283a.

[33] X. Lin, M. Salari, L. M. R. Arava, P. M. Ajayan, and M. W. Grinstaff, "High temperature electrical energy storage: advances, challenges, and frontiers," *Chemical Society Reviews*, vol. 45, no. 21, pp. 5848–5887, Aug. 26, 2016, doi: https://doi.org/10.1039/C6CS00012F.

[34] H. Cheng, J. G. Shapter, Y. Li, and G. Gao, "Recent progress of advanced anode materials of lithium-ion batteries," *Journal of Energy Chemistry*, vol. 57, pp. 451–468, Jun. 2021, doi: https://doi.org/10.1016/j.jechem.2020.08.056.

[35] W. Zhang, C. Xu, W. He, G. Li, and J. Huang, "A review on management of spent lithium ion batteries and strategy for resource recycling of all components from them," *Waste Management & Research*, vol. 36, no. 2, pp. 99–112, Dec. 14, 2017, doi: https://doi.org/10.1177/0734242x17744655.

[36] P. U. Nzereogu, A. D. Omah, F. I. Ezema, E. I. Iwuoha, and A. C. Nwanya, "Anode materials for lithium-ion batteries: A review," *Applied Surface Science Advances*, vol. 9, p. 100233, Jun. 2022, doi: https://doi.org/10.1016/j.apsadv.2022.100233.

[37] X. Huang, "Separator technologies for lithium-ion batteries," *Journal of Solid State Electrochemistry*, vol. 15, no. 4, pp. 649–662, Dec. 30, 2010, doi: https://doi.org/10.1007/s10008-010-1264-9.

[38] M. F. Lagadec, R. Zahn, and V. Wood, "Characterization and performance evaluation of lithium-ion battery separators," *Nature Energy*, vol. 4, no. 1, pp. 16–25, Dec. 31, 2018, doi: https://doi.org/10.1038/s41560-018-0295-9.

[39] C. Hartnig and M. Schmidt, "Electrolytes and conducting salts," *Lithium-Ion Batteries: Basics and Applications*, pp. 59–74, May. 03, 2018, doi: https://doi.org/10.1007/978-3-662-53071-9_6.

[40] B. Makuza, Q. Tian, X. Guo, K. Chattopadhyay, and D. Yu, "Pyrometallurgical options for recycling spent lithium-ion batteries: A comprehensive review," *Journal of Power Sources*, vol. 491, no. 229622, p. 229622, Apr. 15, 2021, doi: https://doi.org/10.1016/j.jpowsour.2021.229622.

[41] S. Kainat, J. Anwer, A. Hamid, N. Gull, and S. M. Khan, "Electrolytes in Lithium-Ion Batteries: Advancements in the Era of Twenties (2020's)," *Materials Chemistry and Physics*, vol. 313, p. 128796, Feb. 01, 2024, doi: https://doi.org/10.1016/j.matchemphys.2023.128796.

[42] Y. Wang, S. Song, C. Xu, N. Hu, J. Molenda, and L. Lu, "Development of solid-state electrolytes for sodium-ion battery–A short review," *Nano Materials Science*, vol. 1, no. 2, pp. 91–100, Jun. 2019, doi: https://doi.org/10.1016/j.nanoms.2019.02.007.

[43] V. Aravindan, J. Gnanaraj, S. Madhavi, and H.-K. Liu, "Lithium-Ion Conducting Electrolyte Salts for Lithium Batteries," *Chemistry - A European Journal*, vol. 17, no. 51, pp. 14326–14346, Nov. 24, 2011, doi: https://doi.org/10.1002/chem.201101486.

[44] S. Luiso and P. Fedkiw, "Lithium-ion battery separators: Recent developments and state of art," *Current Opinion in Electrochemistry*, vol. 20, pp. 99–107, Apr. 2020, doi: https://doi.org/10.1016/j.coelec.2020.05.011.

[45] C. M. Costa, Y.-H. Lee, J.-H. Kim, S.-Y. Lee, and S. Lanceros-Méndez, "Recent advances on separator membranes for lithium-ion battery applications: From porous membranes to solid electrolytes," *Energy Storage Materials*, vol. 22, pp. 346–375, Nov. 2019, doi: https://doi.org/10.1016/j.ensm.2019.07.024.

[46] C. F. J. Francis, I. L. Kyratzis, and A. S. Best, "Lithium-Ion Battery Separators for Ionic-Liquid Electrolytes: A Review," *Advanced Materials*, vol. 32, no. 18, p. 1904205, Jan. 20, 2020, doi: https://doi.org/10.1002/adma.201904205.

[47] K. Vuorilehto, "Materials and function," *Lithium-Ion Batteries: Basics and Applications*, pp. 21–28, 2018, doi: https://doi.org/10.1007/978-3-662-53071-9_3.

[48] V. A. Agubra and J. W. Fergus, "The formation and stability of the solid electrolyte interface on the graphite anode," *Journal of Power Sources*, vol. 268, pp. 153–162, Dec. 05, 2014, doi: https://doi.org/10.1016/j.jpowsour.2014.06.024.

[49] B. Chen *et al.*, "Polymeric Binders Used in Lithium Ion Batteries: Actualities, Strategies and Trends," *ChemElectroChem*, vol. 11, no. 14, Apr. 23, 2024, doi: https://doi.org/10.1002/celc.202300651.

[50] M. Srivastava, A. K. M. R., and K. Zaghib, "Binders for Li-Ion Battery Technologies and Beyond: A Comprehensive Review," *Batteries*, vol. 10, no. 8, p. 268, Jul. 26, 2024, doi: https://doi.org/10.3390/batteries10080268.

[51] C. M. Costa, E. Lizundia, and S. Lanceros-Méndez, "Polymers for advanced lithium-ion batteries: State of the art and future needs on polymers for the different battery components," *Progress in Energy and Combustion Science*, vol. 79, p. 100846, Jul. 2020, doi: https://doi.org/10.1016/j.pecs.2020.100846.

[52] H. Adenusi, G. A. Chass, S. Passerini, K. V. Tian, and G. Chen, "Lithium Batteries and the Solid Electrolyte Interphase (SEI)—Progress and Outlook," *Advanced Energy Materials*, vol. 13, no. 10, p. 2203307, Jan. 18, 2023, doi: https://doi.org/10.1002/aenm.202203307.

[53] M. M. Doeff, "Battery Cathodes," *Batteries for Sustainability*, pp. 5–49, Nov. 2012, doi: https://doi.org/10.1007/978-1-4614-5791-6_2.

[54] B. Li *et al.*, "A Review of Solid Electrolyte Interphase (SEI) and Dendrite Formation in Lithium Batteries," *Electrochemical Energy Reviews*, vol. 6, no. 1, Mar. 03, 2023, doi: https://doi.org/10.1007/s41918-022-00147-5.

[55] U. S. Meda, L. Lal, S. M, and P. Garg, "Solid Electrolyte Interphase (SEI), a boon or a bane for lithium batteries: A review on the recent advances," *Journal of Energy Storage*, vol. 47, p. 103564, Mar. 2022, doi: https://doi.org/10.1016/j.est.2021.103564.

[56] A. M. Colclasure, K. A. Smith, and R. J. Kee, "Modeling detailed chemistry and transport for solid-electrolyte-interface (SEI) films in Li–ion batteries," *Electrochimica Acta*, vol. 58, pp. 33–43, Dec. 30, 2011, doi: https://doi.org/10.1016/j.electacta.2011.08.067.

[57] B. Writer, "Anode Materials, SEI, Carbon, Graphite, Conductivity, Graphene, Reversible, Formation," *Lithium-Ion Batteries*, pp. 1–71, Apr. 02, 2019, doi: https://doi.org/10.1007/978-3-030-16800-1_1.

[58] G. D. Smith and O. Borodin, "Lithium Battery Electrolyte Stability and Performance from Molecular Modeling and Simulations," *Batteries for Sustainability*, pp. 195–237, Nov. 28, 2012, doi: https://doi.org/10.1007/978-1-4614-5791-6_7.

[59] Z. Wang, R. Deng, Y. Wang, and F. Pan, "Comparison of Construction Strategies of Solid Electrolyte Interface (SEI) in Li Battery and Mg Battery—A Review," *Molecules*, vol. 29, no. 19, pp. 4761–4761, Oct. 08, 2024, doi: https://doi.org/10.3390/molecules29194761.

[60] X. Wang, X. Li, H. Fan, and L. Ma, "Solid Electrolyte Interface in Zn-Based Battery Systems," *Nano-Micro Letters*, vol. 14, no. 1, Oct. 19, 2022, doi: https://doi.org/10.1007/s40820-022-00939-w.

[61] J. Seok *et al.*, "Aging Mechanisms of Lithium-ion Batteries," *Journal of Electrochemical Science and Technology*, vol. 15, no. 1, pp. 51–66, Jan. 29, 2024, doi: https://doi.org/10.33961/jecst.2023.00724.

[62] P. Peljo and H. H. Girault, "Electrochemical potential window of battery electrolytes: the HOMO–LUMO misconception," *Energy & Environmental Science*, vol. 11, no. 9, pp. 2306–2309, Jul. 28, 2018, doi: https://doi.org/10.1039/c8ee01286e.

[63] O. Baum, "A Quiet Revolution in Energy Storage aided by Raman Spectroscopy," *Advancing Materials*, Feb. 05, 2019. https://www.thermofisher.com/blog/materials/a-quiet-revolution-in-energy-storage-aided-by-raman-spectroscopy/. [Accessed: Apr. 16, 2025].

[64] P. J. Sideris and S. G. Greenbaum, "Lithium Ion Batteries, Electrochemical Reactions in," *Batteries for Sustainability*, pp. 239–283, Nov. 28, 2012, doi: https://doi.org/10.1007/978-1-4614-5791-6_8.

[65] M. Root, "Medical Device Batteries," *Batteries for Sustainability* , pp. 359–392, Nov. 28, 2012, doi: https://doi.org/10.1007/978-1-4614-5791-6_11.

[66] European Parliament and Council of the European Union, "DIRECTIVE 2006/66/EC OF THE EUROPEAN PARLIAMENT AND OF THE COUNCIL of 6 September 2006 on batteries and accumulators and waste batteries and accumulators and repealing Directive 91/157/EEC," *eur-lex.europa.eu*, Brussel, Belgium, Jul. 04. 2018. [Online]. Available: https://eur-lex.europa.eu/eli/dir/2006/66/2018-07-04. [Accessed: Dec 23, 2024].

[67] European Commission, "Study on the calculation of recycling efficiencies and implementation of export article (Art. 15) of the Batteries Directive 2006/66/EC," *circabc.europa.eu*, Brussel, Belgium, May. 28, 2009. [Online]. Available: https://circabc.europa.eu/ui/group/636f928d-2669-41d3-83db-093e90ca93a2/library/18b1d111-de37-43c9-943d-665298870003/details?download=true.

[68] European Parliament and Council of the European Union, "REGULATION (EU) 2023/1542 OF THE EUROPEAN PARLIAMENT AND OF THE COUNCIL of 12 July 2023 concerning batteries and waste batteries, amending Directive 2008/98/EC and Regulation (EU) 2019/1020 and repealing Directive 2006/66/EC," *eur-lex.europa.eu*, Brussel, Belgium, Jul. 28, 2023. [Online]. Available: https://eur-lex.europa.eu/eli/reg/2023/1542/oj. [Accessed: Dec 23, 2024].

[69] European Parliament and Council of the European Union, "Directive 2008/98/EC of the European Parliament and of the Council of 19 November 2008 on waste and repealing certain Directives," *eur-lex.europa.eu*, Brussel, Belgium, Feb. 18, 2024. [Online]. Available: http://data.europa.eu/eli/dir/2008/98/2024-02-18. [Accessed: Dec 23, 2024].

[70] C. Rasmussen *et al*., "Rethinking the Waste Hierarchy," *ETDEWEB*, Institut for Miljøvurdering / Environmental Assessment Institute, Copenhagen (Denmark), Mar. 01, 2005. [Online]. Available: https://www.osti.gov/etdeweb/biblio/20623175. [Accessed: Dec 26, 2024].

[71] J. L. Price and J. B. Joseph, "Demand management - a basis for waste policy: a critical review of the applicability of the waste hierarchy in terms of achieving sustainable waste management," *Sustainable Development*, vol. 8, no. 2, pp. 96–105, Apr. 28, 2000, doi: https://doi.org/10.1002/(sici)1099-1719(200005)8:2%3C96::aid-sd133%3E3.0.co;2-j.

[72] S. Van Ewijk and J. A. Stegemann, "Limitations of the Waste Hierarchy for Achieving Absolute Reductions in Material Throughput," *Journal of Cleaner Production*, vol. 132, pp. 122–128, Sep. 20, 2016, doi: https://doi.org/10.1016/j.jclepro.2014.11.051.

[73] G. D'Inverno, L. Carosi, and G. Romano, "Meeting the challenges of the waste hierarchy: A performance evaluation of EU countries," *Ecological Indicators*, vol. 160, p. 111641, Mar. 2024, doi: https://doi.org/10.1016/j.ecolind.2024.111641.

[74] A. Pires and G. Martinho, "Waste hierarchy index for circular economy in waste management," *Waste Management*, vol. 95, pp. 298–305, Jul. 15, 2019, doi: https://doi.org/10.1016/j.wasman.2019.06.014.

[75] C. Zhang, M. Hu, F. Di Maio, B. Sprecher, X. Yang, and A. Tukker, "An overview of the waste hierarchy framework for analyzing the circularity in construction and demolition waste management in Europe," *Science of The Total Environment*, vol. 803, p. 149892, Jan. 10, 2022, doi: https://doi.org/10.1016/j.scitotenv.2021.149892.

[76] J. M. Allwood, "Squaring the Circular Economy," *Handbook of Recycling*, pp. 445–477, 2014, doi: https://doi.org/10.1016/b978-0-12-396459-5.00030-1.

[77] European Commission, "Waste Framework Directive," *European Commission*, 2023. [Online]. Available: https://environment.ec.europa.eu/topics/waste-and-recycling/waste-framework-directive_en. [Accessed: Dec 12, 2024].

[78] J. Niskanen, J. Anshelm, and D. McLaren, "Local conflicts and national consensus: The strange case of circular economy in Sweden," *Journal of Cleaner Production*, vol. 261, p. 121117, Jul. 10, 2020, doi: https://doi.org/10.1016/j.jclepro.2020.121117.

[79] J. Korhonen, A. Honkasalo, and J. Seppälä, "Circular Economy: the Concept and Its Limitations," *Ecological Economics*, vol. 143, pp. 37–46, Jan. 2018, Available: https://www.sciencedirect.com/science/article/pii/S0921800916300325.

[80] J. Kirchherr *et al.*, "Barriers to the Circular Economy: Evidence From the European Union (EU)," *Ecological Economics*, vol. 150, pp. 264–272, Aug. 2018, doi: https://doi.org/10.1016/j.ecolecon.2018.04.028.

[81] E. Chioatto and P. Sospiro, "Transition from waste management to circular economy: the European Union roadmap," *Environment, Development and Sustainability*, vol. 25, Jan. 21, 2022, doi: https://doi.org/10.1007/s10668-021-02050-3.

[82] Ellen MacArthur Foundation, "The EU's Circular Economy Action Plan," *ellenmacarthurfoundation.org*, Jan. 12, 2022. [Online]. Available: https://www.ellenmacarthurfoundation.org/circular-examples/the-eus-circular-economy-action-plan. [Accessed: Jan. 15, 2025].

[83] H. Jintao, "Circular Economy Promotion Law," *www.greenpolicyplatform.org*, Aug. 29, 2008. [Online]. Available: https://www.greenpolicyplatform.org/sites/default/files/downloads/policy-database/CHINA)%20Circular%20Economy%20Promotion%20Law%20(2008).pdf. [Accessed: Jan. 15, 2025].

[84] R. Stewart and M. Niero, "Circular economy in corporate sustainability strategies: A review of corporate sustainability reports in the fast-moving consumer goods sector," *Business Strategy and the Environment*, vol. 27, no. 7, pp. 1005–1022, Mar. 01, 2018, doi: https://doi.org/10.1002/bse.2048.

[85] S. Leipold *et al.*, "Lessons, narratives, and research directions for a sustainable circular economy," *Journal of Industrial Ecology*, vol. 27, no. 1, pp. 6–18, Dec. 27, 2022, doi: https://doi.org/10.1111/jiec.13346.

[86] N. Millar, E. McLaughlin, and T. Börger, "The Circular Economy: Swings and Roundabouts?," *Ecological Economics*, vol. 158, pp. 11–19, Apr. 2019, doi: https://doi.org/10.1016/j.ecolecon.2018.12.012.

[87] Amundi Asset Management, "ESG Thema #4–Investing in the Circular Economy: Closing the Loop," Paris, France, Oct. 2021. [Online]. Available: https://research-center.amundi.com/files/nuxeo/dl/03587038-62a5-4c7a-a255-92a9792ef1f7?inline=. [Accessed: Jan. 15, 2025].

[88] M. Geissdoerfer, P. Savaget, N. M. P. Bocken, and E. J. Hultink, "The Circular Economy - a New Sustainability paradigm?," *Journal of Cleaner Production*, vol. 143, no. 1, pp. 757–768, Feb. 01, 2017, doi: https://doi.org/10.1016/j.jclepro.2016.12.048.

[89] T. Dzhengiz, E. M. Miller, J. Ovaska, and S. Patala, "Unpacking the circular economy: A problematizing review," *International Journal of Management Reviews*, vol. 25, no. 2, pp. 270–296, Feb. 02, 2023, doi: https://doi.org/10.1111/ijmr.12329.

[90] "Circular Economy," *Australia's linear 'take-make-dispose' economy is unsustainable,* 2022. [Online]. Available: https://research.csiro.au/circulareconomy/about/ [Accessed: Feb. 15, 2025].

[91] S. Vanhamaki *et al.*, "Bio-based circular economy in European national and regional strategies," *International Journal of Sustainable Development and Planning*, vol. 14, no. 01, pp. 31–43, Mar. 2019, doi: https://doi.org/10.2495/sdp-v14-n1-31-43.

[92] J. Korhonen, C. Nuur, A. Feldmann, and S. E. Birkie, "Circular economy as an essentially contested concept," *Journal of Cleaner Production*, vol. 175, no. 175, pp. 544–552, Feb. 20, 2018, doi: https://doi.org/10.1016/j.jclepro.2017.12.111

[93] A. Mariele Domingues and R. Gabbay, "Review of life cycle assessment on lithium-ion batteries (LIBs) recycling," *Next Sustainability*, vol. 3, p. 100032, Jan. 2024, doi: https://doi.org/10.1016/j.nxsust.2024.100032.

[94] M. C. Etude *et al.*, "Recycling lithium-ion batteries: A review of current status and future directions," *Sustainable Chemistry One World*, vol. 4, p. 100027, Oct. 2024, doi: https://doi.org/10.1016/j.scowo.2024.100027.

[95] J. Heelan *et al.*, "Current and Prospective Li-Ion Battery Recycling and Recovery Processes," *JOM*, vol. 68, no. 10, pp. 2632–2638, Jun. 20, 2016, doi: https://doi.org/10.1007/s11837-016-1994-y.

[96] V. Halleux, "BRIEFING EU Legislation in Progress–New EU regulatory framework for batteries - Setting sustainability requirements," *EPRS | European Parliamentary Research Service*, Sep. 2024. [Online]. Available: https://www.europarl.europa.eu/thinktank/en/document/EPRS_BRI(2021)689337. [Accessed: Feb. 15, 2025].

[97] European Commission, "Waste statistics - recycling of batteries and accumulators," *Eurostat Statistics Explained*, Nov. 2023. [Online]. Available: https://ec.europa.eu/eurostat/statistics-explained/index.php?title=Waste_statistics_-_recycling_of_batteries_and_accumulators. [Accessed: Feb. 15, 2025].

[98] S. Windisch-Kern *et al.*, "Recycling chains for lithium-ion batteries: A critical examination of current challenges, opportunities and process dependencies," *Waste Management*, vol. 138, pp. 125–139, Feb. 01, 2022, doi: https://doi.org/10.1016/j.wasman.2021.11.038.

[99] NAATBatt International, "Laws, Regulations and Best Practices for Lithium Battery Packaging, Transport and Recycling in the United States and Canada," naatbatt.org. [Online]. Available: https://naatbatt.org/lithium-recycling-laws/. [Accessed: Jan. 26, 2025].

[100] Call2Recycle, “Recycling Laws By State | Call2Recycle | United States.” [Online]. Available: https://www.call2recycle.org/recycling-laws-by-state/. [Accessed: Feb. 7, 2025].

[101] M. J. Willey, Q. Huang, W. Martin, and J. Lochala, “North American Lithium Battery Materials Industry Report Version 1.2,” Pacific Northwest National Laboratory, Richland, Washington 99354, Feb. 2025. [Online]. Available: https://www.pnnl.gov/projects/north-american-lithium-battery-materials-industry-report. [Accessed: Feb. 7, 2025].

[102] Battery Council International and EBP US, “United States Lead Battery Industry Segment Economic Contribution in 2023 - Published 2025,” *Battery Council International*, Boston, MA, USA: EBP US, Mar. 17, 2025. [Online]. Available: https://batterycouncil.org/resource/new-study-shows-economic-impact-of-the-u-s-lead-battery-industry/. [Accessed: Feb. 8, 2025].

[103] L. Azhari, S. Bong, X. Ma, and Y. Wang, “Recycling for All Solid-State Lithium-Ion Batteries,” *Matter*, vol. 3, no. 6, pp. 1845–1861, Dec. 02, 2020, doi: https://doi.org/10.1016/j.matt.2020.10.027.

[104] Mordor Intelligence, “Lithium-ion Battery Market Size & Share Analysis - Growth Trends & Forecasts (2025 - 2030),” *www.mordorintelligence.com*. updated Jul. 04, 2025. [Online]. Available: https://www.mordorintelligence.com/industry-reports/lithium-ion-battery-market. [Accessed: Feb. 10, 2025].

[105] K. A. Gerardino, “LITHIUM-ION BATTERY RECYCLING: PROCESSES, LATEST TRENDS, & CHALLENGES,” *Industry EMEA*, Oct. 25, 2023. [Online]. Available: https://www.industryemea.com/market-overview/73428-lithium-ion-battery-recycling-processes. [Accessed: Feb. 10, 2025].

[106] S. Sasaki, “Toward the Creation of the Asian xEV Battery Recycling Zone,” *Research & Development in Material Science*, vol. 16, no. 5, Mar. 08, 2022, doi: https://doi.org/10.31031/rdms.2022.16.000896.

[107] Y. Chen, X. Dai, P. Fu, G. Luo, and P. Shi, “A review of China’s automotive industry policy: Recent developments and future trends,” *Journal of Traffic and Transportation Engineering (English Edition)*, vol. 11, no. 5, Oct. 2024, doi: https://doi.org/10.1016/j.jtte.2024.09.001.

[108] S. Wang and J. Yu, “Evaluating the electric vehicle popularization trend in China after 2020 and its challenges in the recycling industry,” *Waste Management & Research: The Journal for a Sustainable Circular Economy*, vol. 39, no. 6, p. 0734242X2095349, Sep. 03, 2020, doi: https://doi.org/10.1177/0734242x20953495.

[109] A. Tripathy, A. Bhuyan, R. K. Padhy, S. Kumar Mangla, and R. Roopak, “Drivers of lithium-ion batteries recycling industry toward circular economy in industry 4.0,” *Computers & Industrial Engineering*, vol. 179, p. 109157, May 2023, doi: https://doi.org/10.1016/j.cie.2023.109157.

[110] Natural Resources Canada, "Lithium facts - Natural Resources Canada," *Canada.ca*, updated Mar. 12, 2025. [Online]. Available: https://natural-resources.canada.ca/minerals-mining/mining-data-statistics-analysis/minerals-metals-facts/lithium-facts. [Accessed: Feb. 16, 2025].

[111] European Commission, "Communication COM(2020) 474 final — Critical Raw Materials Resilience: Charting a Path towards greater Security and Sustainability," *eur-lex.europa.eu*, Brussel, Belgium, Sep. 03, 2020. https://eur-lex.europa.eu/legal-content/EN/TXT/?uri=CELEX:52020DC0474. [Accessed: Feb. 02, 2025].

[112] D. Müller, D. I. Groves, M. Santosh, and C.-X. Yang, "Critical metals: Their applications with emphasis on the clean energy transition," *Geosystems and Geoenvironment*, vol. 4, no. 1, p. 100310, Feb. 2024, doi: https://doi.org/10.1016/j.geogeo.2024.100310.

[113] T. Vranken, "Critical raw materials in Li-ion batteries," Researcher - Inorganic and Physical Chemistry, University of Hasselt/EnergyVille, Jan. 2023. [Online]. Available: https://innoenergy.com/uploads/2023/01/critical-raw-materials-in-li-ion-batteries.pdf. [Accessed: Feb. 02, 2025].

[114] European Parliament & Council, "Regulation (EU) 2024/1252 of 11 April 2024 establishing a framework for ensuring a secure and sustainable supply of critical raw materials and amending Regulations (EU) No 168/2013, 2018/858, 2018/1724 and 2019/1020," *Official Journal of the European Union*, May. 03, 2024. [Online]. Available: https://eur-lex.europa.eu/eli/reg/2024/1252/oj/eng. [Accessed: Feb. 02, 2025].

[115] U.S. Geological Survey, "Mineral Commodity Summaries 2025," *U.S. Geological Survey, Reston, VA*, ver. 1.2, p. 212, Mar. 03, 2025, doi: https://doi.org/10.3133/mcs2025.

[116] F. Calvão, C. E. A. Mcdonald, and M. Bolay, "Cobalt mining and the corporate outsourcing of responsibility in the Democratic Republic of Congo," *The Extractive Industries and Society*, vol. 8, no. 4, Feb. 2021, doi: https://doi.org/10.1016/j.exis.2021.02.004.

[117] J. Alajoki, A. Karppinen, T. Rinne, R. Serna-Guerrero, and M. Lundström, "Leaching strategies for the recovery of Co, Ni, Cu and Zn from historical tailings," *Minerals Engineering*, vol. 217, pp. 108967, Sep. 2024, doi: https://doi.org/10.1016/j.mineng.2024.108967.

[118] Q. Dehaine, L. T. Tijsseling, H. J. Glass, T. Törmänen, and A. R. Butcher, "Geometallurgy of cobalt ores: A review," *Minerals Engineering*, vol. 160, no. 160, p. 106656, Jan. 01, 2021, doi: https://doi.org/10.1016/j.mineng.2020.106656.

[119] P. Anderson, "Cobalt and Corruption: The Influence of Multinational Firms and Foreign States on the Democratic Republic of the Congo," *Journal for Global Business and Community*, vol. 14, no. 1, Mar. 01, 2023, doi: https://doi.org/10.56020/001c.72664.

[120] M. Bell "The Cobalt Mines of the Democratic Republic of Congo" in *Global Encounters: New Visions*, vol. IV, Dept. of Geography and Planning, Queen's Univ., Kingston, ON, Canada, pp. 24–29, Apr. 2024. [Online]. Available: https://www.queensu.ca/geographyandplanning/genv-volume-4-now-available. [Accessed: Mar. 10, 2025].

[121] L. Thome, K. Walsh, J. Zimmerman, and B. Escobar, "Chasing copper and cobalt: China's mining operations in Peru and the DRC," *Aiddata.org*, Feb. 27, 2025. [Online]. Available: https://www.aiddata.org/blog/chasing-copper-and-cobalt-chinas-mining-operations-in-peru-and-the-drc. [Accessed: Mar. 10, 2025].

[122] A. K. Koech, Gershom Mwandila, F. Mulolani, and Phenny Mwaanga, "Lithium-ion Battery Fundamentals and Exploration of Cathode Materials: A Review," *South African Journal of Chemical Engineering*, vol. 50, pp. 321–339, Oct. 2024, doi: https://doi.org/10.1016/j.sajce.2024.09.008.

[123] R. T. Nguyen, R. G. Eggert, M. H. Severson, and C. G. Anderson, "Global Electrification of Vehicles and Intertwined Material Supply Chains of Cobalt, Copper and Nickel," *Resources, Conservation and Recycling*, vol. 167, p. 105198, Apr. 2021, doi: https://doi.org/10.1016/j.resconrec.2020.105198.

[124] Cobalt Institute, "Cobalt Market Report 2024," *www.cobaltinstitute.org & Benchmark Mineral Intelligence*, May. 14, 2025. [Online]. Available: https://www.cobaltinstitute.org/resource/cobalt-market-report-2024/. [Accessed: Feb. 16, 2025].

[125] K. van Wieringen, "Will the EU help build a cobalt refinery in the Democratic Republic of the Congo?," *European Parliamentary Research Service, Policy Foresight Unit*, Jun. 03, 2024. [Online]. Available: https://www.europarl.europa.eu/thinktank/en/document/EPRS_ATA(2024)757828. [Accessed: Feb. 15, 2025].

[126] Energy Capital & Power, "Chinese Investments Driving Economic Development in RoC," *Energy Capital & Power*, Sep. 26, 2024. [Online]. Available: https://energycapitalpower.com/chinese-investments-driving-economic-development-in-roc/. [Accessed: Feb. 15, 2025].

[127] F. Gregory and P. Milas, "China in the Democratic Republic of the Congo: A New Dynamic in Critical Mineral Procureme," *US Army War College - Strategic Studies Institute*, Oct. 17, 2024. [Online]. Available: https://ssi.armywarcollege.edu/SSI-Media/Recent-Publications/Article/3938204/china-in-the-democratic-republic-of-the-congo-a-new-dynamic-in-critical-mineral/. [Accessed: Feb. 16, 2025].

[128] U.S. Geological Survey, "Mineral Commodity Summaries 2024," *U.S. Geological Survey, Reston, VA*, p. 212, Jan. 31, 2024, doi: https://doi.org/10.3133/mcs2024.

[129] E. Alonso *et al.*, "World Minerals Outlook—Cobalt, Gallium, Helium, Lithium, Magnesium, Palladium, Platinum, and Titanium Through 2029," *U.S. Geological Survey*, ver. 1.1, p. 19, Mar. 11, 2025, doi: https://doi.org/10.3133/sir20255021.

[130] A. Cremona, "COBALT PERSPECTIVES," *CHIMICA & MATERIALI*, vol. 8, no. 4, 2024, doi: https://doi.org/10.17374/CI.2024.106.4.44.

[131] Cobalt Institute, "Cobalt Market Report 2023," *www.cobaltinstitute.org & Benchmark Mineral Intelligence*, May. 13, 2024. [Online]. Available: https://www.cobaltinstitute.org/resource/cobalt-market-report-2023/. [Accessed: Feb. 16, 2025].

[132] L. Chen *et al.*, "Impact of cobalt recycling on China's electrification process: Assessing the potential reduction in cobalt demand from battery recycling," *Journal of Cleaner Production*, vol. 434, p. 139917, Jan. 01, 2024, doi: https://doi.org/10.1016/j.jclepro.2023.139917.

[133] M. Rezaei *et al.*, "A review of lithium-ion battery recycling for enabling a circular economy," *Journal of Power Sources*, vol. 630, p. 236157, Feb. 28, 2025, doi: https://doi.org/10.1016/j.jpowsour.2024.236157.

[134] A. Cook and S. Shaw, "DRC imposes export suspension on cobalt," *Fastmarkets*, Feb. 24, 2025. https://www.fastmarkets.com/insights/drc-imposes-export-suspension-on-cobalt. [Accessed: Feb. 16, 2025].

[135] Daily Metal Prices, "Metal Spot Price Charts–Cobalt Price Chart (USD / Metric Ton) for the Last Available years," Daily Metal Prices. [Online]. Available:https://www.dailymetalprice.com/metalpricecharts.php?c=co&u=mt&d=0. [Accessed: Jul. 02, 2025].

[136] Cobalt Institute, "Cobalt Market Report 2022," *www.cobaltinstitute.org & Benchmark Mineral Intelligence*, May. 10, 2023. [Online]. Available: https://www.cobaltinstitute.org/resource/cobalt-market-report-2022/. [Accessed: Feb. 16, 2025].

[137] Natural Resources Canada, "Cobalt facts - Natural Resources Canada," *Canada.ca*, updated Mar. 13, 2025. [Online]. Available: https://natural-resources.canada.ca/minerals-mining/mining-data-statistics-analysis/minerals-metals-facts/cobalt-fact. [Accessed: Feb. 16, 2025].

[138] Cobalt Institute, "Cobalt Market Report 2020–'State of the Cobalt market' report," *www.cobaltinstitute.org & Roskill Consulting Group*, May. 17, 2021. [Online]. Available: https://www.cobaltinstitute.org/resource/state-of-the-cobalt-market-report-2020/. [Accessed: Feb. 16, 2025].

[139] V. Balaram, M. Santosh, M. Satyanarayanan, N. Srinivas, and H. Gupta, "Lithium: A review of applications, occurrence, exploration, extraction, rercycling, analysis, and environmental impact," *Geoscience Frontiers*, vol. 15, no. 5, p. 101868, Sep. 2024, doi: https://doi.org/10.1016/j.gsf.2024.101868.

[140] C. Ruas, "Bolivian communities push back against foreign-backed lithium projects," *Mongabay Environmental News*, Apr. 17, 2025. [Online]. Available: https://news.mongabay.com/2025/04/bolivian-communities-push-back-against-foreign-backed-lithium-projects/. [Accessed: Feb. 18, 2025].

[141] L. Paz, "Lithium-rich Bolivia lags behind in race to mine key metal," *France 24*, Dec. 12, 2024. https://www.france24.com/en/live-news/20241212-lithium-rich-bolivia-lags-behind-in-race-to-mine-key-metal. [Accessed: Feb. 18, 2025].

[142] International Energy Agency, "Recycling of Critical Minerals Strategies to Scale Up Recycling and Urban Mining - World Energy Outlook Special Report," *www.iea.org*, Nov. 18, 2024. [Online]. Available: https://www.iea.org/reports/recycling-of-critical-minerals. [Accessed: Feb. 18, 2025].

[143] M. Gutsch and J. Leker, "Costs, carbon footprint, and environmental impacts of lithium-ion batteries–From cathode active material synthesis to cell manufacturing and recycling," *Applied Energy*, vol. 353, part B, p. 122132, Jan. 01, 2024, doi: https://doi.org/10.1016/j.apenergy.2023.122132.

[144] V. Srivastava *et al.*, "A comprehensive review of the reclamation of resources from spent lithium-ion batteries," *Chemical Engineering Journal*, vol. 474, p. 145822, Oct. 15, 2023, doi: https://doi.org/10.1016/j.cej.2023.145822.

[145] Reuters Staff, E. Scheyder, L. Jackson, M. Burton, and A. Lv, "Chinese lithium company halts tech exports as trade tensions build," *Mining.com & Reuters*, Feb. 18, 2025. [Online]. Available: https://www.mining.com/web/chinese-lithium-company-halts-tech-exports-as-trade-tensions-build/. [Accessed: Feb. 18, 2025].

[146] Daily Metal Prices, "Metal Spot Price Charts–Lithium Price Chart (USD / Kilogram) for the Last Available years," *DailyMetalPrice.com*. [Online]. Available: https://www.dailymetalprice.com/metalpricecharts.php?c=li&u=kg&d=240. [Accessed: Jul. 02, 2025].

[147] International Energy Agency, "Global Critical Minerals Outlook 2025," *www.iea.org*, May 2025. [Online]. Available: https://www.iea.org/reports/global-critical-minerals-outlook-2025. [Accessed: Feb. 18, 2025].

[148] X. Sun, H. Hao, P. Hartmann, Z. Liu, and F. Zhao, "Supply risks of lithium-ion battery materials: An entire supply chain estimation," *Materials Today Energy*, vol. 14, p. 100347, Dec. 2019, doi: https://doi.org/10.1016/j.mtener.2019.100347.

[149] X. Guo, Y. Lu, Q. Zhang, J. Ren, and W. Cai, "The Geological Characteristics, Resource Potential, and Development Status of Manganese Deposits in Africa," *Minerals*, vol. 14, no. 11, p. 1088, Oct. 28, 2024, doi: https://doi.org/10.3390/min14111088.

[150] European Commission, "RMIS - Raw materials' profiles - Nickel," *Joint Research Centre*, 2025. [Online]. Available: https://rmis.jrc.ec.europa.eu/rmp/Nickel. [Accessed: Feb. 19, 2025].

[151] Natural Resources Canada, "Nickel facts - Natural Resources Canada," *Canada.ca*, updated Jan. 31, 2025. [Online]. Available: https://natural-resources.canada.ca/minerals-mining/mining-data-statistics-analysis/minerals-metals-facts/nickel-facts. [Accessed: Feb. 19, 2025].

[152] U.S. Geological Survey, "Manganese Statistics and Information," *National Minerals Information Center*, 2025. [Online]. Available: https://www.usgs.gov/centers/national-minerals-information-center/manganese-statistics-and-information. [Accessed: Feb. 19, 2025].

[153] European Commission, "RMIS - Raw materials' profiles - Manganese," *Joint Research Centre*, 2025. [Online]. Available: https://rmis.jrc.ec.europa.eu/rmp/Manganese. [Accessed: Feb. 19, 2025].

[154] Trading Economics, "Nickel | Price & Historical Chart," *TradingEconomics.com*. [Online]. Available: https://tradingeconomics.com/commodity/nickel. [Accessed: Jul. 02, 2025].

[155] Trading Economics, "Manganese | Price & Historical Chart," *TradingEconomics.com*. [Online]. https://tradingeconomics.com/commodity/nickel. [Accessed: Jul. 02, 2025].

[156] Reuters Staff, G. De Clercq, G. Trompiz, M. Akalaare Adombila, and A. Kacher , "Eramet's shares slide as Gabon plans manganese ore export ban," *Reuters*, Jun. 02, 2025. [Online]. Available: https://www.reuters.com/world/africa/frances-eramet-says-it-will-work-with-gabon-despite-manganese-export-ban-2025-06-02/. [Accessed: Jun. 04, 2025].

[157] Natural Resources Canada, "Graphite facts - Natural Resources Canada," *Canada.ca*, updated Mar. 01, 2024. [Online]. Available: https://natural-resources.canada.ca/minerals-mining/mining-data-statistics-analysis/minerals-metals-facts/graphite-facts. [Accessed: Feb. 19, 2025].

[158] H. Tian, M. Graczyk-Zajac, A. Kessler, Anke Weidenkaff, and R. Riedel, "Recycling and Reusing of Graphite from Retired Lithium-ion Batteries: A Review," *Advanced Materials*, vol. 36, no. 13, p. 2308494, Dec. 16, 2023, doi: https://doi.org/10.1002/adma.202308494.

[159] H. Zhang, Y. Yang, D. Ren, L. Wang, and X. He, "Graphite as anode materials: Fundamental mechanism, recent progress and advances," *Energy Storage Materials*, vol. 36, pp. 147–170, Apr. 2021, doi: https://doi.org/10.1016/j.ensm.2020.12.027.

[160] IMARC Group, "Graphite Prices, Trend, Chart, Demand, Market Analysis, News, Historical and Forecast Data Report 2025 Edition," *www.imarcgroup.com*, 2025. [Online]. Available: https://www.imarcgroup.com/graphite-pricing-report. [Accessed: Feb. 19, 2025].

[161] Fortune Business Insights, "Graphite Market Size, Share & Industry Analysis, By Product (Synthetic and Natural), By Application (Refractories, Foundries, Batteries, Friction Products, Lubricants, Recarburizing, and Others), and Regional Forecast, 2025-2032," *www.fortunebusinessinsights.com*, 2024. [Online]. Available: https://www.fortunebusinessinsights.com/graphite-market-105322. [Accessed: Feb. 19, 2025].

[162] Future Markets, Inc., "The Global Graphite Market 2024-2035 - Research and Markets," *Researchandmarkets.com*, 2024. [Online]. Available: https://www.researchandmarkets.com/reports/5663766/the-global-graphite-market-2024-2035. [Accessed: Feb. 19, 2025].

[163] ChemAnalyst, "Graphite Prices, News, Monitor, Market Analysis & Demand," *Chemanalyst.com*, 2025. [Online]. Available: https://www.chemanalyst.com/Pricing-data/graphite-1433. [Accessed: Feb. 19, 2025].

[164] International Energy Agency, "Global EV Outlook 2025 Expanding sales in diverse markets," *www.iea.org,* May. 2025. [Online]. Available: https://www.iea.org/reports/global-ev-outlook-2025#overview. [Accessed: Feb. 25, 2025].

[165] International Energy Agency, "Global EV Outlook 2024: Moving Towards Increased Affordability," *www.iea.org,* Apr. 2024. [Online]. Available: https://www.iea.org/reports/global-ev-outlook-2024. [Accessed: Feb. 25, 2025].

[166] Cobalt Institute, "SMM Global Cobalt Industry Chain Report 2018-2025," *www.cobaltinstitute.org*, May. 19, 2025. [Online]. Available: https://www.cobaltinstitute.org/resource/focus-on-chinas-cobalt-market/. [Accessed: Feb. 25, 2025].

[167] P. María, "The price of electricity, the silent tariff that weighs down Europe in the trade war: 'We pay four times more in Basque factories than in Texas,'" *El Mundo América*, Apr. 14, 2025. [Online]. Available: https://www.mundoamerica.com/news/2025/04/14/67fce2ecfc6c834a358b457a.html. [Accessed: Jul. 11, 2025].

[168] F. Meng and Y. Zhao, "How does digital economy affect green total factor productivity at the industry level in China: from a perspective of global value chain," *Environmental Science and Pollution Research*, vol. 29, pp. 1–19, Jun. 2022, doi: https://doi.org/10.1007/s11356-022-21434-0.

[169] U.S. Department of Energy, "Critical Materials Assessment," *U.S. Department of Energy Critical Materials Assessment*, 2023. [Online]. Available: https://www.energy.gov/sites/default/files/2023-05/2023-critical-materials-assessment.pdf. [Accessed: Apr. 20, 2025].

[170] N. T. Nassar and S. M. Fortier, "Methodology and technical input for the 2021 Review and Revision of the U.S. Critical Minerals List,"*Open-File Report, U.S. Geological Survey*, pp. 1–31, May. 07, 2021, doi: https://doi.org/10.3133/ofr20211045. [Accessed: Apr. 21, 2025].

[171] IRENA, "BATTERIES FOR ELECTRIC VEHICLES," *International Renewable Energy Agency (IRENA),* Abu Dhabi, 2024. [Online]. Available: https://www.irena.org/-/media/Files/IRENA/Agency/Publication/2024/Sep/IRENA_Critical_materials_Batteries_for_EVs_2024.pdf. [Accessed: Apr. 21, 2025].

[172] A. Miatto, B. K. Reck, J. West, and T. E. Graedel, "The rise and fall of American lithium," *Resources, Conservation and Recycling*, vol. 162, p. 105034, Nov. 2020, doi: https://doi.org/10.1016/j.resconrec.2020.105034.

[173] C. Reichl and M. Schatz, "World Mining Data 2025," *Federal Ministry Republic of Austria Finance*, vol. 40, pp. 3–264, Apr. 10, 2025. [Online]. Available: https://www.bmf.gv.at/en/topics/mining/mineral-resources-policy/wmd.html. [Accessed: Apr. 21, 2025].

[174] A. Khurshid, Y. Chen, A. Rauf, and K. Khan, "Critical metals in uncertainty: How Russia-Ukraine conflict drives their prices?," *Resources Policy*, vol. 85, part B, p. 104000, Aug. 2023, doi: https://doi.org/10.1016/j.resourpol.2023.104000.

[175] N. Hensel, "The Russia-Ukraine Crisis: How Regional Conflicts Impact the Global Economy How Regional Conflicts Impact the Global Economy," *PRISM*, vol. 4, no. 4, pp. 102–122, 2024. [Online]. Available: https://www.jstor.org/stable/48785858. [Accessed: Jul. 11, 2025].

[176] Małgorzata Jakimów, Vsevolod Samokhalov, and B. Baldassarre, "Achieving European Union strategic autonomy: circularity in critical raw materials value chains," *International affairs*, vol. 100, no. 4, pp. 1735–1748, Jun. 10, 2024, doi: https://doi.org/10.1093/ia/iiae127.

[177] T. Zadorozhnyy and L. Bivings, "Ukraine, US sign additional agreements for minerals deal, Economy Ministry says," *The Kyiv Independent*, May. 13, 2025. [Online]. Available: https://kyivindependent.com/ukraine-signs-additional-agreements-for-minerals-deal-economy-ministry-says/. [Accessed: Jul. 11, 2025].

[178] M. Baranowski, P. Jabkowski, and D. M. Kammen, "From the Russian invasion of Ukraine to the battlefield of the future: The geopolitical fight for Ukraine's mineral wealth," *Energy Research & Social Science*, vol. 123, p. 104043, May. 2025, doi: https://doi.org/10.1016/j.erss.2025.104043.

[179] D. Kumar, K. Amudha, K. Gopakumar, and G.A. Ramadass, "Air-lift pump systems for vertical solid particle transport: A comprehensive review and deep sea mining potential," *Ocean engineering*, vol. 297, p. 116928, Apr. 01, 2024, doi: https://doi.org/10.1016/j.oceaneng.2024.116928.

[180] D. J. Amon *et al.*, "Assessment of scientific gaps related to the effective environmental management of deep-seabed mining," *Marine Policy*, vol. 138, p. 105006, Apr. 2022, doi: https://doi.org/10.1016/j.marpol.2022.105006.

[181] K. Du, W. Xi, S. Huang, and J. Zhou, "Deep-sea Mineral Resource Mining: A Historical Review, Developmental Progress, and Insights," *Mining, Metallurgy & Exploration*, vol. 41, pp. 173–192, Jan. 05, 2024, doi: https://doi.org/10.1007/s42461-023-00909-9.

[182] A. Hallgren and A. Hansson, "Conflicting Narratives of Deep Sea Mining," *Sustainability*, vol. 13, no. 9, p. 5261, May. 08, 2021, doi: https://doi.org/10.3390/su13095261.

[183] D. Qian, C. Yan, L. Xiu, and K. Feng, "The impact of mining changes on surrounding lands and ecosystem service value in the Southern Slope of Qilian Mountains," *Ecological Complexity*, vol. 36, pp. 138–148, Dec. 2018, doi: https://doi.org/10.1016/j.ecocom.2018.08.002.

[184] N. R. Haddaway *et al.*, "Evidence of the impacts of metal mining and the effectiveness of mining mitigation measures on social–ecological systems in Arctic and boreal regions: a systematic map protocol," *Environmental Evidence*, vol. 8, no. 1, Feb. 21, 2019, doi: https://doi.org/10.1186/s13750-019-0152-8.

[185] H. Goyal, "Innovations in lithium-ion battery recycling," *Cas.org*, Mar. 07, 2025. [Online]. Available: https://www.cas.org/resources/cas-insights/innovations-in-lithium-ion-battery-recycling. [Accessed: Apr. 16, 2025].

[186] Y. Miao, L. Liu, Y. Zhang, Q. Tan, and J. Li, "An overview of global power lithium-ion batteries and associated critical metal recycling," *Journal of Hazardous Materials*, vol. 425, p. 127900, Mar. 05, 2022, doi: https://doi.org/10.1016/j.jhazmat.2021.127900.

[187] CAS (American Chemical Society) & Deloitte, "Lithium-ion Battery Recycling Market and Innovation Trends for A Green Future," Feb. 18, 2025. [Online]. Available: https://web.cas.org/marketing/pdf/INSGENENGBRO102412-CAS-Insights-Lithium-Ion-Full-Report-Digital.pdf. [Accessed: Apr. 16, 2025].

[188] Z. J. Baum, R. E. Bird, X. Yu, and J. Ma, "Lithium-Ion Battery Recycling─Overview of Techniques and Trends," *ACS Energy Letters*, vol. 7, no. 2, pp. 712–719, Jan. 19, 2022, doi: https://doi.org/10.1021/acsenergylett.1c02602.

[189] X. Ma *et al.*, "The evolution of lithium-ion battery recycling," *Nature Reviews Clean Technology*, vol. 1, no. 1, pp. 75–94, Jan. 15, 2025, doi: https://doi.org/10.1038/s44359-024-00010-4.

[190] S. Jin *et al.*, "A comprehensive review on the recycling of spent lithium-ion batteries: Urgent status and technology advances," *Journal of Cleaner Production*, vol. 340, p. 130535, Mar. 15, 2022, doi: https://doi.org/10.1016/j.jclepro.2022.130535.

[191] Y. Lan *et al.*, "Current status and outlook of recycling spent lithium-ion batteries," *Journal of Energy Storage*, vol. 110, p. 115374, Feb. 28, 2025, doi: https://doi.org/10.1016/j.est.2025.115374.

[192] E. Mossali, N. Picone, L. Gentilini, O. Rodrìguez, J. M. Pérez, and M. Colledani, "Lithium-ion batteries towards circular economy: A literature review of opportunities and issues of recycling treatments," *Journal of Environmental Management*, vol. 264, p. 110500, Jun. 15, 2020, doi: https://doi.org/10.1016/j.jenvman.2020.110500.

[193] A. R. Shekhar, M. H. Parekh, and V. G. Pol, "Worldwide ubiquitous utilization of lithium-ion batteries: What we have done, are doing, and could do safely once they are dead?," *Journal of Power Sources*, vol. 523, p. 231015, Mar. 01, 2022, doi: https://doi.org/10.1016/j.jpowsour.2022.231015.

[194] M. T. Islam and U. Iyer-Raniga, "Lithium-Ion Battery Recycling in the Circular Economy: A Review," *Recycling*, vol. 7, no. 3, p. 33, May 28, 2022, doi: https://doi.org/10.3390/recycling7030033.

[195] Maria, M. Villen-Guzman, C. Vereda-Alonso, Jose Miguel Rodriguez-Maroto, and Juan Manuel Paz-Garcia, "Towards Sustainable Lithium-Ion Battery Recycling: Advancements in Circular Hydrometallurgy," *Processes*, vol. 12, no. 7, pp. 1485–1485, Jul. 15, 2024, doi: https://doi.org/10.3390/pr12071485.

[196] E. Asadi Dalini, Gh. Karimi, S. Zandevakili, and M. Goodarzi, "A Review on Environmental, Economic and Hydrometallurgical Processes of Recycling Spent Lithium-ion Batteries," *Mineral Processing and Extractive Metallurgy Review*, vol. 42, no. 7, pp. 1–22, Jul. 13, 2020, doi: https://doi.org/10.1080/08827508.2020.1781628.

[197] F. Larouche *et al.*, "Progress and Status of Hydrometallurgical and Direct Recycling of Li-Ion Batteries and Beyond," *Materials*, vol. 13, no. 3, p. 801, Feb. 10, 2020, doi: https://doi.org/10.3390/ma13030801.

[198] Y. Yao, M. Zhu, Z. Zhao, B. Tong, Y. Fan, and Z. Hua, "Hydrometallurgical Processes for Recycling Spent Lithium-Ion Batteries: A Critical Review," *ACS Sustainable Chemistry & Engineering*, vol. 6, no. 11, pp. 13611–13627, Sep. 05, 2018, doi: https://doi.org/10.1021/acssuschemeng.8b03545.

[199] R. Golmohammadzadeh, F. Faraji, and F. Rashchi, "Recovery of lithium and cobalt from spent lithium ion batteries (LIBs) using organic acids as leaching reagents: A review," *Resources, Conservation and Recycling*, vol. 136, pp. 418–435, Sep. 2018, doi: https://doi.org/10.1016/j.resconrec.2018.04.024.

[200] Y. Zheng *et al.*, "Leaching Procedure and Kinetic Studies of Cobalt in Cathode Materials from Spent Lithium Ion Batteries using Organic Citric acid as Leachant," *International Journal of Environmental Research*, vol. 10, no. 1, pp. 159–168, Feb. 2016, doi: https://doi.org/10.22059/ijer.2016.56898.

[201] W. Gao *et al.*, "Selective recovery of valuable metals from spent lithium-ion batteries–Process development and kinetics evaluation," *Journal of Cleaner Production*, vol. 178, pp. 833–845, Mar. 20, 2018, doi: https://doi.org/10.1016/j.jclepro.2018.01.040.

[202] M. K. Jha, A. Kumari, A. K. Jha, V. Kumar, J. Hait, and B. D. Pandey, "Recovery of lithium and cobalt from waste lithium ion batteries of mobile phone," *Waste Management*, vol. 33, no. 9, pp. 1890–1897, Sep. 2013, doi: https://doi.org/10.1016/j.wasman.2013.05.008.

[203] Z. Zheng *et al.*, "High Performance Cathode Recovery from Different Electric Vehicle Recycling Streams," *ACS Sustainable Chemistry & Engineering*, vol. 6, no. 11, pp. 13977–13982, Sep. 20, 2018, doi: https://doi.org/10.1021/acssuschemeng.8b02405.

[204] R. Golmohammadzadeh, F. Rashchi, and E. Vahidi, "Recovery of lithium and cobalt from spent lithium-ion batteries using organic acids: Process optimization and kinetic aspects," *Waste Management*, vol. 64, pp. 244–254, Jun. 2017, doi: https://doi.org/10.1016/j.wasman.2017.03.037.

[205] X. Chen, C. Luo, J. Zhang, J. Kong, and T. Zhou, "Sustainable Recovery of Metals from Spent Lithium-Ion Batteries: A Green Process," *ACS Sustainable Chemistry & Engineering*, vol. 3, no. 12, pp. 3104–3113, Nov. 13, 2015, doi: https://doi.org/10.1021/acssuschemeng.5b01000.

[206] X. Zeng, J. Li, and B. Shen, "Novel approach to recover cobalt and lithium from spent lithium-ion battery using oxalic acid," *Journal of Hazardous Materials*, vol. 295, pp. 112–118, Sep. 15, 2015, doi: https://doi.org/10.1016/j.jhazmat.2015.02.064.

[207] P. Meshram, B. D. Pandey, and T. R. Mankhand, "Extraction of lithium from primary and secondary sources by pre-treatment, leaching and separation: A comprehensive review," *Hydrometallurgy*, vol. 150, pp. 192–208, Dec. 2014, doi: https://doi.org/10.1016/j.hydromet.2014.10.012.

[208] H. Li, S. Xing, Y. Liu, F. Li, H. Guo, and G. Kuang, "Recovery of Lithium, Iron, and Phosphorus from Spent $LiFePO_4$ Batteries Using Stoichiometric Sulfuric Acid Leaching System," *ACS Sustainable Chemistry & Engineering*, vol. 5, no. 9, pp. 8017–8024, Aug. 10, 2017, doi: https://doi.org/10.1021/acssuschemeng.7b01594.

[209] J. Guan *et al.*, "Mechanochemical Process Enhanced Cobalt and Lithium Recycling from Wasted Lithium-Ion Batteries," *ACS Sustainable Chemistry & Engineering*, vol. 5, no. 1, pp. 1026–1032, Nov. 08, 2016, doi: https://doi.org/10.1021/acssuschemeng.6b02337.

[210] C. K. Lee and K.-I. Rhee, "Reductive leaching of cathodic active materials from lithium ion battery wastes," *Hydrometallurgy*, vol. 68, no. 1–3, pp. 5–10, Feb. 2003, doi: https://doi.org/10.1016/s0304-386x(02)00167-6.

[211] Y. Yang *et al.*, "Selective recovery of lithium from spent lithium iron phosphate batteries: a sustainable process," *Green Chemistry*, vol. 20, no. 13, pp. 3121–3133, 2018, doi: https://doi.org/10.1039/c7gc03376a.

[212] E. G. Pinna, M. C. Ruiz, M. W. Ojeda, and M. H. Rodriguez, "Cathodes of spent Li-ion batteries: Dissolution with phosphoric acid and recovery of lithium and cobalt from leach liquors," *Hydrometallurgy*, vol. 167, pp. 66–71, Jan. 2017, doi: https://doi.org/10.1016/j.hydromet.2016.10.024.

[213] L. Chen, X. Tang, Y. Zhang, L. Li, Z. Zeng, and Y. Zhang, "Process for the recovery of cobalt oxalate from spent lithium-ion batteries," *Hydrometallurgy*, vol. 108, no. 1–2, pp. 80–86, Jun. 2011, doi: https://doi.org/10.1016/j.hydromet.2011.02.010.

[214] S. M. Shin, N. H. Kim, J. S. Sohn, D. H. Yang, and Y. H. Kim, "Development of a metal recovery process from Li-ion battery wastes," *Hydrometallurgy*, vol. 79, no. 3–4, pp. 172–181, Oct. 2005, doi: https://doi.org/10.1016/j.hydromet.2005.06.004.

[215] M. Joulié, R. Laucournet, and E. Billy, "Hydrometallurgical process for the recovery of high value metals from spent lithium nickel cobalt aluminum oxide based lithium-ion batteries," *Journal of Power Sources*, vol. 247, pp. 551–555, Feb. 01, 2014, doi: https://doi.org/10.1016/j.jpowsour.2013.08.128.

[216] Y. Ma *et al.*, "A promising selective recovery process of valuable metals from spent lithium ion batteries via reduction roasting and ammonia leaching," *Journal of Hazardous Materials*, vol. 402, p. 123491, Jan. 15, 2021, doi: https://doi.org/10.1016/j.jhazmat.2020.123491.

[217] H. Wang *et al.*, "Recovery of Lithium, Nickel, and Cobalt from Spent Lithium-Ion Battery Powders by Selective Ammonia Leaching and an Adsorption Separation System," *ACS Sustainable Chemistry & Engineering*, vol. 5, no. 12, pp. 11489–11495, Oct. 31, 2017, doi: https://doi.org/10.1021/acssuschemeng.7b02700.

[218] H. Ku *et al.*, "Recycling of spent lithium-ion battery cathode materials by ammoniacal leaching," *Journal of Hazardous Materials*, vol. 313, pp. 138–146, Aug. 05, 2016, doi: https://doi.org/10.1016/j.jhazmat.2016.03.062.

[219] D. A. Ferreira, L. M. Z. Prados, D. Majuste, and M. B. Mansur, "Hydrometallurgical separation of aluminium, cobalt, copper and lithium from spent Li-ion batteries," *Journal of Power Sources*, vol. 187, no. 1, pp. 238–246, Feb. 01, 2009, doi: https://doi.org/10.1016/j.jpowsour.2008.10.077.

[220] N. J. Boxall, K. Y. Cheng, W. Bruckard, and A. H. Kaksonen, "Application of indirect non-contact bioleaching for extracting metals from waste lithium-ion batteries," *Journal of Hazardous Materials*, vol. 360, pp. 504–511, Oct. 15, 2018, doi: https://doi.org/10.1016/j.jhazmat.2018.08.024.

[221] N. Bahaloo-Horeh and S. M. Mousavi, "Enhanced recovery of valuable metals from spent lithium-ion batteries through optimization of organic acids produced by Aspergillus niger," *Waste Management*, vol. 60, pp. 666–679, Feb. 2017, doi: https://doi.org/10.1016/j.wasman.2016.10.034.

[222] B. K. Biswal, U. U. Jadhav, M. Madhaiyan, L. Ji, E.-H. Yang, and B. Cao, "Biological Leaching and Chemical Precipitation Methods for Recovery of Co and Li from Spent Lithium-Ion Batteries," *ACS Sustainable Chemistry & Engineering*, vol. 6, no. 9, pp. 12343–12352, Jul. 17, 2018, doi: https://doi.org/10.1021/acssuschemeng.8b02810.

[223] J. Wang *et al.*, "Functional exploration of extracellular polymeric substances (EPS) in the bioleaching of obsolete electric vehicle LiNixCoyMn1-x-yO2 Li-ion batteries," *Journal of Hazardous Materials*, vol. 354, pp. 250–257, Jul. 15, 2018, doi: https://doi.org/10.1016/j.jhazmat.2018.05.009.

[224] Z. Niu, Y. Zou, B. Xin, S. Chen, C. Liu, and Y. Li, "Process controls for improving bioleaching performance of both Li and Co from spent lithium ion batteries at high pulp density and its thermodynamics and kinetics exploration," *Chemosphere*, vol. 109, pp. 92–98, Aug. 2014, doi: https://doi.org/10.1016/j.chemosphere.2014.02.059.

[225] N. B. Horeh, S. M. Mousavi, and S. A. Shojaosadati, "Bioleaching of valuable metals from spent lithium-ion mobile phone batteries using Aspergillus niger," *Journal of Power Sources*, vol. 320, pp. 257–266, Jul. 15, 2016, doi: https://doi.org/10.1016/j.jpowsour.2016.04.104.

[226] Y. Xin, X. Guo, S. Chen, J. Wang, F. Wu, and B. Xin, "Bioleaching of valuable metals Li, Co, Ni and Mn from spent electric vehicle Li-ion batteries for the purpose of recovery," *Journal of Cleaner Production*, vol. 116, pp. 249–258, Mar. 10, 2016, doi: https://doi.org/10.1016/j.jclepro.2016.01.001.

[227] G. Zeng, X. Deng, S. Luo, X. Luo, and J. Zou, "A copper-catalyzed bioleaching process for enhancement of cobalt dissolution from spent lithium-ion batteries," *Journal of Hazardous Materials*, vol. 199–200, pp. 164–169, Jan. 15, 2012, doi: https://doi.org/10.1016/j.jhazmat.2011.10.063.

[228] P. Zhang, T. Yokoyama, O. Itabashi, T. M. Suzuki, and K. Inoue, "Hydrometallurgical process for recovery of metal values from spent lithium-ion secondary batteries," *Hydrometallurgy*, vol. 47, no. 2–3, pp. 259–271, Jan. 1998, doi: https://doi.org/10.1016/s0304-386x(97)00050-9.

[229] W. Gao *et al.*, "Lithium Carbonate Recovery from Cathode Scrap of Spent Lithium-Ion Battery: A Closed-Loop Process," *Environmental Science & Technology*, vol. 51, no. 3, pp. 1662–1669, Jan. 12, 2017, doi: https://doi.org/10.1021/acs.est.6b03320.

[230] Q. Li, K. Y. Fung, L. Xu, C. Wibowo, and K. M. Ng, "Process Synthesis: Selective Recovery of Lithium from Lithium-Ion Battery Cathode Materials," *Industrial & Engineering Chemistry Research*, vol. 58, no. 8, pp. 3118–3130, Jan. 25, 2019, doi: https://doi.org/10.1021/acs.iecr.8b04899.

[231] X. Chen, B. Fan, L. Xu, T. Zhou, and J. Kong, "An atom-economic process for the recovery of high value-added metals from spent lithium-ion batteries," *Journal of Cleaner Production*, vol. 112, part 4, pp. 3562–3570, Jan. 20, 2016, doi: https://doi.org/10.1016/j.jclepro.2015.10.132.

[232] Y. Huang *et al.*, "A stepwise recovery of metals from hybrid cathodes of spent Li-ion batteries with leaching-flotation-precipitation process," *Journal of Power Sources*, vol. 325, pp. 555–564, Sep. 01, 2016, doi: https://doi.org/10.1016/j.jpowsour.2016.06.072.

[233] Y. Zhang, W. Wang, Q. Fang, and S. Xu, "Improved recovery of valuable metals from spent lithium-ion batteries by efficient reduction roasting and facile acid leaching," *Waste Management*, vol. 102, pp. 847–855, Feb. 01, 2020, doi: https://doi.org/10.1016/j.wasman.2019.11.045.

[234] Y. Weng, S. Xu, G. Huang, and C. Jiang, "Synthesis and performance of $Li[(Ni_{1/3}Co_{1/3}Mn_{1/3})_{1-x}Mg_x]O_2$ prepared from spent lithium ion batteries," *Journal of Hazardous Materials*, vol. 246–247, pp. 163–172, Feb. 15, 2013, doi: https://doi.org/10.1016/j.jhazmat.2012.12.028.

[235] Y. Yang, S. Xu, and Y. He, "Lithium recycling and cathode material regeneration from acid leach liquor of spent lithium-ion battery via facile co-extraction and co-precipitation processes," *Waste Management*, vol. 64, pp. 219–227, Jun. 2017, doi: https://doi.org/10.1016/j.wasman.2017.03.018.

[236] Chung, K. Y., Lee, H. Y., & Cho, B.-W. "*Recovery and Synthesis Method for Metaloxidic Cathodic Active Material for Lithium ion Secondary Battery,*" U.S. Patent 8835026 B2, Sep. 16, 2014.

[237] L.-P. He, S.-Y. Sun, and J.-G. Yu, "Performance of $LiNi_{1/3}Co_{1/3}Mn_{1/3}O_2$ prepared from spent lithium-ion batteries by a carbonate co-precipitation method," *Ceramics International*, vol. 44, no. 1, pp. 351–357, Jan. 2018, doi: https://doi.org/10.1016/j.ceramint.2017.09.180.

[238] V. Gunarathne *et al.*, "Hydrometallurgical processes for heavy metals recovery from industrial sludges," *Critical Reviews in Environmental Science and Technology*, vol. 52, no. 6, pp. 1022–1062, Dec. 2020, doi: https://doi.org/10.1080/10643389.2020.1847949.

[239] A. Holzer, S. Windisch-Kern, C. Ponak, and H. Raupenstrauch, "A Novel Pyrometallurgical Recycling Process for Lithium-Ion Batteries and Its Application to the Recycling of LCO and LFP," *Metals*, vol. 11, no. 1, p. 149, Jan. 14, 2021, doi: https://doi.org/10.3390/met11010149.

[240] Y. Yan *et al.*, "Plasma Hydrogenated TiO_2/Nickel Foam as an Efficient Bifunctional Electrocatalyst for Overall Water Splitting," *ACS Sustainable Chemistry & Engineering*, vol. 7, no. 1, pp. 885–894, Nov. 22, 2018, doi: https://doi.org/10.1021/acssuschemeng.8b04496.

[241] L. Reinhart *et al.*, "Pyrometallurgical recycling of different lithium-ion battery cell systems: Economic and technical analysis," *Journal of Cleaner Production*, vol. 416, p. 137834, Sep. 01, 2023, doi: https://doi.org/10.1016/j.jclepro.2023.137834.

[242] C. Pan and Y. Shen, "Pyrometallurgical recycling of spent lithium-ion batteries from conventional roasting to synergistic pyrolysis with organic wastes," *Journal of Energy Chemistry*, vol. 85, pp. 547–561, Oct. 2023, doi: https://doi.org/10.1016/j.jechem.2023.06.040.

[243] J. Li, G. Wang, and Z. Xu, "Environmentally-friendly oxygen-free roasting/wet magnetic separation technology for in situ recycling cobalt, lithium carbonate and graphite from spent $LiCoO_2$/graphite lithium batteries," *Journal of Hazardous Materials*, vol. 302, pp. 97–104, Jan. 25, 2016, doi: https://doi.org/10.1016/j.jhazmat.2015.09.050.

[244] X. Li, J. Zhang, D. Song, J. Song, and L. Zhang, "Direct regeneration of recycled cathode material mixture from scrapped $LiFePO_4$ batteries," *Journal of Power Sources*, vol. 345, pp. 78–84, Mar. 31, 2017, doi: https://doi.org/10.1016/j.jpowsour.2017.01.118.

[245] G. Zhang, Z. Du, Y. He, H. Wang, W. Xie, and T. Zhang, "A Sustainable Process for the Recovery of Anode and Cathode Materials Derived from Spent Lithium-Ion Batteries," *Sustainability*, vol. 11, no. 8, p. 2363, Apr. 20, 2019, doi: https://doi.org/10.3390/su11082363.

[246] S. Windisch-Kern, A. Holzer, C. Ponak, and H. Raupenstrauch, "Pyrometallurgical Lithium-Ion-Battery Recycling: Approach to Limiting Lithium Slagging with the InduRed Reactor Concept," *Processes*, vol. 9, no. 1, p. 84, Jan. 02, 2021, doi: https://doi.org/10.3390/pr9010084.

[247] A. R. Jalalvand, M. Roushani, H. C. Goicoechea, D. N. Rutledge, and H.-W. Gu, "MATLAB in electrochemistry: A review," *Talanta*, vol. 194, pp. 205–225, Mar. 01, 2019, doi: https://doi.org/10.1016/j.talanta.2018.10.041.

[248] S. Luo, K. Elouarzaki, and Z. J. Xu, “Electrochemistry in Magnetic Fields,” *Angewandte Chemie International Edition*, vol. 61, no. 27, p. e202203564, Apr. 24, 2022, doi: https://doi.org/10.1002/anie.202203564.

[249] K. Liu *et al.*, “Innovative Electrochemical Strategy to Recovery of Cathode and Efficient Lithium Leaching from Spent Lithium-Ion Batteries,” *ACS applied energy materials*, vol. 3, no. 5, pp. 4767–4776, Apr. 28, 2020, doi: https://doi.org/10.1021/acsaem.0c00395.

[250] H. Shuai *et al.*, “Electrochemically Modulated $LiNi_{1/3}Mn_{1/3}Co_{1/3}O_2$ Cathodes for Lithium-Ion Batteries,” *Small Methods*, vol. 3, no. 5, Mar. 20, 2019, doi: https://doi.org/10.1002/smtd.201900065.

[251] M. Li, R. Mo, A. Ding, K. Zhang, F. Guo, and C. Xiao, “Electrochemical technology to drive spent lithium-ion batteries (LIBs) recycling: recent progress, and prospects,” *Energy Materials*, vol. 4, no. 6, Jul. 22, 2024, doi: https://doi.org/10.20517/energymater.2024.29.

[252] Birendra Babu Adhikari *et al.*, “Electrochemical leaching of critical materials from lithium-ion batteries: A comparative life cycle assessment,” *Resources Conservation and Recycling*, vol. 193, p. 106973, Jun. 2023, doi: https://doi.org/10.1016/j.resconrec.2023.106973.

[253] H. Zhang *et al.*, “Direct extraction of lithium from ores by electrochemical leaching,” *Nature Communications*, vol. 15, no. 1, p. 5066, Jun. 13, 2024, doi: https://doi.org/10.1038/s41467-024-48867-0.

[254] S. Pei, S. Yan, X. Chen, J. Li, and J. Xu, “Novel electrochemical process for recycling of valuable metals from spent lithium-ion batteries,” *Waste Management*, vol. 188, pp. 1–10, Nov. 15, 2024, doi: https://doi.org/10.1016/j.wasman.2024.07.018.

[255] D. M. M. de Oca, M. Shi, L. A. Diaz, and T. E. Lister, “Electrochemical leaching of spent LIBs: Kinetics, novel reactor, and modeling,” *Sustainable Materials and Technologies*, vol. 40, p. e00898, Jul. 2024, doi: https://doi.org/10.1016/j.susmat.2024.e00898.

[256] S. Tian *et al.*, “Selective recovery of lithium from spent $LiFePO_4$ powders with electrochemical method,” *Journal of Environmental Chemical Engineering*, vol. 12, no. 3, p. 112871, Jun. 2024, doi: https://doi.org/10.1016/j.jece.2024.112871.

[257] J. Sun, Z. Wang, and Z. He, “Indirect electrochemical leaching and separation of cobalt and lithium from spent $LiCoO_2$ through recovery and reuse of sulfuric acid,” *Separation and Purification Technology*, vol. 364, part 3, p. 132587, Aug. 30, 2025, doi: https://doi.org/10.1016/j.seppur.2025.132587.

[258] W. Jin, “Towards source reduction and green sustainability of metal-bearing waste streams: The electrochemical processes,” *Electrochimica Acta*, vol. 374, p. 137937, Apr. 01, 2021, doi: https://doi.org/10.1016/j.electacta.2021.137937.

[259] Reyixiati Repukaiti *et al.*, "Electrochemical Leaching of Cobalt from Cobaltite: Box-Behnken Design and Optimization with Response Surface Methodology," *ACS Omega*, vol. 10, no. 1, pp. 655–664, Dec. 23, 2024, doi: https://doi.org/10.1021/acsomega.4c07361.

[260] H. Bastos, N. Schaeffer, J. M. Pringle, M. Eftekharnia, J. A. P. Coutinho, and C. Pozo-Gonzalo, "Electrochemically-assisted leaching of active cathode materials from spent batteries with minimal pre-treatment using hydroxylated solvents," *Separation and Purification Technology*, vol. 364, part 1, p. 132354, Aug 30. 2025, doi: https://doi.org/10.1016/j.seppur.2025.132354.

[261] C. Hazotte, E. Meux, N. Leclerc, and F. Lapicque, "Electroassisted leaching of black mass solids from Ni–Cd batteries for metal recovery: Investigation of transport and transfer phenomena coupled to reactions," *Chemical Engineering and Processing: Process Intensification*, vol. 96, pp. 83–93, Oct. 2015, doi: https://doi.org/10.1016/j.cep.2015.08.004.

[262] Y. Xue, S. Zheng, H. Du, Y. Zhang, and W. Jin, "Cr(III)-induced electrochemical advanced oxidation processes for the V_2O_3 dissolution in alkaline media," *Chemical Engineering Journal*, vol. 307, pp. 518–525, Jan. 01, 2017, doi: https://doi.org/10.1016/j.cej.2016.08.115.

[263] C. Modrzynski, J. Z. Bloh, and C. Weidlich, "Kinetic Investigations of the Electrochemically Assisted Leaching of Metals for the Recycling of Photovoltaics," *Journal of The Electrochemical Society*, vol. 169, no. 7, p. 073513, Jul. 27, 2022, doi: https://doi.org/10.1149/1945-7111/ac8021.

[264] Y. Barsukov *et al.*, *2003–2004 Portable Power Design Seminar Text Book*, SLYP085, Texas Instruments, Dallas, TX, pp. 18–19, 2004. [Online]. Available: https://www.ti.com/. [Accessed: May. 10, 2025].

[265] Dirk Uwe Sauer, "SECONDARY BATTERIES–LEAD– ACID SYSTEMS | Lifetime Determining Processes," *Elsevier eBooks*, pp. 805–815, Jan. 2009, doi: https://doi.org/10.1016/b978-044452745-5.00137-4.

[266] A. Pfrang, A. Kriston, V. Ruiz, N. Lebedeva, and F. di Persio, "Safety of Rechargeable Energy Storage Systems with a focus on Li-ion Technology," *Emerging Nanotechnologies in Rechargeable Energy Storage Systems*, pp. 253–290, 2017, doi: https://doi.org/10.1016/b978-0-323-42977-1.00008-x.

[267] J. T. Warner, "Lithium-ion battery operation," *Lithium-Ion Battery Chemistries*, pp. 43–77, 2019, doi: https://doi.org/10.1016/b978-0-12-814778-8.00003-x.

[268] LG Chem, "Product specification: LG ICR18650 B1 rechargeable lithium-ion battery," LRB-PS-CY260, Rev. 5, Seoul, Korea, Apr. 15, 2006. [Online]. Available: https://wp.geekfun.com/wp-content/blogs.dir/26/files/2014/12/LG-ICR18650B1.pdf. [Accessed: May. 02, 2025].

[269] Samsung SDI Co., Ltd., "ICR18650-28A lithium-ion rechargeable cell datasheet," Ver. 1.0, Dec. 01, 2008. [Online]. Available: https://www.dnkpower.com/wp-content/uploads/2018/04/Samsung-ICR18650-28A-Datasheet.pdf. [Accessed: May. 02, 2025].

[270] "Cell Database," *Second Life Storage & Solar*, 2023. [Online]. Available:https://secondlifestorage.com/index.php?pages/cell-database/. [Accessed: May. 02, 2025].

[271] B. A. Johnson and R. E. White, "Characterization of commercially available lithium-ion batteries," *Journal of Power Sources*, vol. 70, no. 1, pp. 48–54, Jan. 30, 1998, doi: https://doi.org/10.1016/s0378-7753(97)02659-1.

[272] D. Kaiser, S. Pavón, and M. Bertau, "Recovery of Al, Co, Cu, Fe, Mn, and Ni from Spent LIBs after Li Selective Separation by the COOL-Process. Part 1: Leaching of Solid Residue from COOL-Process," *Chemie Ingenieur Technik*, vol. 93, no. 11, Aug. 23, 2021, doi: https://doi.org/10.1002/cite.202100098.

[273] B. Makuza, D. Yu, Z. Huang, Q. Tian, and X. Guo, "Dry Grinding - Carbonated Ultrasound-Assisted Water Leaching of Carbothermally Reduced Lithium-Ion Battery Black Mass Towards Enhanced Selective Extraction of Lithium and Recovery of High-Value Metals," *Resources, Conservation & Recycling*, vol. 174, p. 105784, Nov. 2021, doi: https://doi.org/10.1016/j.resconrec.2021.105784.

[274] M. Sommerfeld *et al.,* "A Combined Pyro- and Hydrometallurgical Approach to Recycle Pyrolyzed Lithium-Ion Battery Black Mass Part 1: Production of Lithium Concentrates in an Electric Arc Furnace," *Metals*, vol. 10, no. 8, p. 1069, Aug. 7, 2020, doi: https://doi.org/10.3390/met10081069.

[275] Y. Zhao, Y. Wen, Y. Yang, and S. Xu, "Recovery of fluorine-containing resources from spent lithium-ion batteries as high-value products," *Resources, Conservation & Recycling*, vol. 221, no. 108403, 2025. [Online]. Available: https://doi.org/10.1016/J.RESCONREC.2025.108403.

[276] Mahsa Pourmohammad *et al*., "The Characterization of Black Mass from Spent Lithium-Ion Scooter Batteries Using Multi-Analytical Techniques," *Recycling*, vol. 10, no. 2, pp. 54–54, Apr. 1, 2025, doi: https://doi.org/10.3390/recycling10020054.

[277] H. Shuai *et al.*, "Electrochemically Modulated $LiNi_{1/3}Mn_{1/3}Co_{1/3}O_2$ Cathodes for Lithium-Ion Batteries," *Small Methods*, vol. 3, no. 5, p. 1900065, Mar. 20, 2019, doi: https://doi.org/10.1002/smtd.201900065.

[278] J. Marshall, D. Gastol, R. Sommerville, B. Middleton, V. Goodship, and E. Kendrick, "Disassembly of Li Ion Cells—Characterization and Safety Considerations of a Recycling Scheme," *Metals*, vol. 10, no. 6, p. 773, Jun. 9, 2020, doi: https://doi.org/10.3390/met10060773.

[279] J. Klimko *et al.*, "A Combined Pyro- and Hydrometallurgical Approach to Recycle Pyrolyzed Lithium-Ion Battery Black Mass Part 2: Lithium Recovery from Li Enriched Slag—Thermodynamic Study, Kinetic Study, and Dry Digestion," *Metals*, vol. 10, no. 11, p. 1558, Nov. 23, 2020, doi: https://doi.org/10.3390/met10111558.

[280] M. Aaltonen, C. Peng, B. Wilson, and M. Lundström, "Leaching of Metals from Spent Lithium-Ion Batteries," *Recycling*, vol. 2, no. 4, p. 20, Oct. 31, 2017, doi: https://doi.org/10.3390/recycling2040020.

[281] R. Kumar *et al.*, "Sustainable recovery of high-valued resources from spent lithium-ion batteries: A review of the membrane-integrated hybrid approach," *Chemical Engineering Journal*, vol. 470, p. 144169, Aug. 15, 2023, doi: https://doi.org/10.1016/j.cej.2023.144169.

[282] Whatman, "Filter Papers and Membranes Catalogue," *GE Healthcare UK Limited*, 2006. [Online]. Available: https://www.cytivalifesciences.com. [Accessed: Apr. 15, 2025].

[283] A. Porvali, A. Chernyaev, S. Shukla, and M. Lundström, "Lithium ion battery active material dissolution kinetics in Fe(II)/Fe(III) catalyzed Cu-H_2SO_4 leaching system," *Separation and Purification Technology*, vol. 236, p. 116305, 2020, doi: https://doi.org/10.1016/j.seppur.2019.116305.

[284] J. J. M. M. van de Ven, Y. Yang, and S. T. Abrahami, "A closer look at lithium-ion batteries in E-waste and the potential for a universal hydrometallurgical recycling process," *Scientific Reports*, vol. 14, no. 1, Jul. 19, 2024, doi: https://doi.org/10.1038/s41598-024-67507-7.

Appendix 1 Parameters for the experimental setups of ECL-T-1 and ECL-T-3

Parameter	No BM No Voltage	No BM Voltage Applied	BM added & Voltage through system													ECL-T-1					ECL-T-3				
Sampling No.	1	2	3	4	5	6	7	8	9	10	11	12	13	14	15	16									
Time Total (min)	–	–	0	5	15	30	45	60	75	90	105	120	135	150	165	180									
Time Interval (min)	–	–	0	5	10	15	15	15	15	15	15	15	15	15	15	15									
Current (A)	–	–	0	0.14	0.14	0.14	0.14	0.14	0.14	0.14	0.14	0.14	0.14	0.14	0.14	0.14									
Voltage (V)	–	–	0.1	12.1	10.5	9.7	9.1	8.5	8.3	8.2	8.1	8.1	8.05	7.95	7.95	8									
Temp. H_2SO_4 (°C)	–	–	24	24	24	24	24	24	24	24	24	24	24	24	24	24									
pH of H_2SO_4	–	–	–	–	–	–	–	–	–	–	–	–	–	–	–	–									
Current (A)	0	0.16	0.16	0.16	0.16	0.16	0.16	0.16	0.16	0.16	0.16	0.16	0.16	0.16	0.16	0.16									
Voltage (V)	0	2.4	2.2	2.3	2.3	2.3	2.4	2.4	2.5	2.6	2.8	2.7	2.8	2.8	2.9	2.8									
Temp. H_2SO_4 (°C)	25	25	26	26	26	26	26	26	26	26	26	26	26	26	26	27									
Temp. KOH (°C)	23	23	25	25	25	25	25	25	25	25	25	25	25	25	25	25									
Temp. NaCl (°C)	23	23	23	22	22	22	22	22	22	22	22	22	22	22	22	22									
pH of H_2SO_4	-0.29	-0.44	-0.33	-0.23	-0.23	-0.22	-0.2	-0.19	-0.16	-0.14	-0.12	-0.1	-0.09	-0.07	-0.045	-0.02									
pH of KOH	14.47	14.46	14.45	14.62	14.45	14.45	14.43	14.43	14.43	14.42	14.42	14.4	14.4	14.4	14.39	14.39									
pH of NaCl	7.472	7.497	7.5	7.503	7.504	7.505	7.503	7.507	7.505	7.508	7.506	7.503	7.505	7.51	7.51	7.51									